2016

SYSTEM GENETIC ANALYSIS OF MECHANISMS UNDERLYING EXCESSIVE ALCOHOL CONSUMPTION

Maren L. Smith
Virginia Commonwealth University

SYSTEM GENETIC ANALYSIS OF MECHANISMS UNDERLYING EXCESSIVE ALCOHOL CONSUMPTION

A Dissertation submitted in partial fulfillment of the requirements for the degree of Doctor of Philosophy at Virginia Commonwealth University

By

MAREN LYDIA SMITH
Bachelor of Science, University of Georgia, 2009

Directed by: MICHAEL MILES, MD, PhD
Professor, Department of Pharmacology and Toxicology, Neurology, Human Genetics.

Virginia Commonwealth University
Richmond, Virginia
November, 2016

Acknowledgements

There are several people I would like to thank for their contributions to my academic career. First, I would like to thank my advisor Dr. Michael Miles. I consider myself extremely fortunate to have had the opportunity to work with him at the start of my career. His guidance and patience taught me so much about what it means to be a scientist. I would also like to thank my committee members for their helpful suggestions for both my PhD project and my future career. Additionally, I would like to thank Dr. Rita Shang, whose door was always open, and was always willing to help graduate students in the Department of Human and Molecular Genetics succeed.

I also must express my sincere thanks to all of our collaborators through the INIA Stress Consortium, particularly Drs. Howard Becker, Marcello Lopez, and Kathleen Grant. Their hard work, and willingness to collaborate made my PhD possible. I would also like to thank the National Institute on Alcohol Abuse and Alcoholism and the Virginia Commonwealth University Department of Human and Molecular Genetics for their financial support.

In addition, I would like to thank Drs. Jennifer Wolstenholme and James Bogenpohl for their personal support. I would also like to acknowledge Lorna Macleod, Andrew van der Vaart, Guy Harris, Jessica Jurmain, and Kristin Mignogna for their friendship, and for helping create a positive environment at the Miles laboratory. I would also like to thank former laboratory members Drs. Megan O'Brien and Blair Costin for introducing me to the field of mouse behavioral research, and Drs. Sean Farris and Aaron Wolen for getting the ball rolling on such an interesting project.

Finally, I would like to thank my family and friends for their unconditional love and encouragement, without which I would never have made it to this point in my career and life.

Table of Contents

List of Tables

List of Figures

ABSTRACT

SYSTEMS GENETIC ANALYSIS OF MECHANISMS UNDERLYING EXCESSIVE ALCOHOL CONSUMPTION

By: Maren L. Smith

A Dissertation submitted in partial fulfillment of the requirements for the degree of Doctor of Philosophy at Virginia Commonwealth University

Virginia Commonwealth University 2016

Major Director: Michael Miles, MD, PhD

Professor, Departments of Pharmacology and Toxicology, Neurology, and Human Genetics

Increased alcohol consumption over time is one of the characteristic symptoms of Alcohol Use Disorder (AUD). The molecular mechanisms underlying this escalation in intake is still the subject of study. However, the mesocortical and mesolimbic dopamine pathways, and the extended amygdala, because of their involvement in reward and reinforcement are believed to play key roles in these behavioral changes. Multiple gene expression studies have shown that alcohol affects the expression of thousands of genes in the brain. The studies discussed in this document use the systems biology technique of co-expression network analysis to attempt to find

patterns within genome-wide expression data from two animal models of chronic, high-dose ethanol exposure. These analyses have identified time-dependent and brain-regions specific patterns of expression in C57Bl/6J mice after multiple exposures to intoxicating doses of ethanol and withdrawal. Specifically, they have identified the PFC and HPC as showing long-term ethanol regulation, and identified *Let-7* family miRNAs as potential gene expression regulators of chronic ethanol response. Network analysis also indicates neurotransmitter release and neuroimmune response are very correlated to ethanol intake in chronically exposed mice. Examining gene expression response to chronic ethanol exposure across a variable genetic background revealed that, although gene expression response may show conserved patterns, underlying differences in gene expression influence by genetic background may be what truly underlies voluntary ethanol consumption. Finally, combined network analysis of gene expression in the prefrontal cortex (PFC) of mice and macaques following prolonged ethanol exposure demonstrated that neurotransmission, myelination, transcription, cellular respiration, and, possibly, neurovasculature are affected by chronic ethanol across species. Taken together, these studies generate several new hypothesis and areas of future research into the continued study of druggable targets for AUD

Chapter 1: Introduction

Alcohol Use Disorder (AUD) is a chronic relapsing disorder of problematic alcohol drinking [1]. Symptoms include steadily increasing consumption, tolerance to the intoxicating effects of alcohol, loss of control over alcohol intake; preoccupation with and craving for alcohol; and alcohol seeking to the detriment of other areas of life. Diagnostic symptoms of AUD also include taking part in activities that endanger one's physical safety such as swimming, driving, and operating machinery while intoxicated; continued drinking in spite of negative effects on professional activities and/or personal relationships; and unsuccessful attempts to cut down on or stop drinking [1, 2]. The presence of withdrawal symptoms is also characteristic of AUD and indicates physiological dependence on the drug. Withdrawal symptoms range from psychological, such as anxiety, depression, irritability, and restlessness, to physical symptoms, such as insomnia, heart palpitations, sweating, shortness of breath, diarrhea, nausea and vomiting [1]. Symptoms of severe alcohol withdrawal can be dangerous and even fatal. These include delirium tremens, hallucinations, seizures, stroke, and heart attack [1, 3].

Alcohol drinking is extremely common worldwide. Almost all cultures have a sense of alcohol's potential for abuse. The 2014 National Survey on Drug Use and Health showed that in the United States approximately 87% of adults over the age of 18 reported drinking alcohol in their lifetime [4]. In this survey 24.6% of adults also reported having consumed 5 or more alcoholic drinks on at least one occasion within the past month, and 6.7% reported consuming 5 or more drinks on five or more occasions within the past month [4]. Studies from 2010 to 2015 estimate that excessive alcohol consumption costs the United States 250 billion dollars per year, with an average cost to each American taxpayer of $746 [5]. A 2010 study found 72% of the costs of

excessive alcohol use stem from negative impact on workplace productivity [6]. This study also found 11% of alcohol-related costs attributable to the cost of healthcare to treat the effects of excessive alcohol use, and 9% related to costs associated with criminal offenses committed while under the influence [6]. At the societal level, excessive alcohol use is known to increase incidences of criminal activity, personal injury, traffic accidents and fatalities, vandalism, destruction of property, domestic disputes, and other high risk behaviors [1, 2, 7].

In addition to the socioeconomic costs, excessive alcohol consumption is also considered a major public health issue. In the United States abusive alcohol use has been estimated to be the 3rd to 4th leading cause of preventable death [2, 8]. Using morbidity and mortality data from 11 American states from 2006-2010, the Centers for Disease Control estimates approximately 88,000 alcohol related deaths in the United States every year [8]. Worldwide, that number jumps to 3.3 million deaths, making it the 5th highest cause of death among people between the ages of 15 and 49 [2]. The World Health Organization reports that alcohol consumption has been identified as a causal factor in over 200 disease and injury conditions [2].

One of the most well known alcohol-associated disease conditions is cirrhosis of the liver. AUD is, in fact, considered one of the highest risk factors for liver cirrhosis in the United States [9-11]. Long-term, heavy alcohol use is also associated with increased risk for, or worsening of, pancreatitis [2, 12-17], gastroesophageal reflux disease (GERD) [18, 19], esophageal damage and bleeding [20], gastritis [21, 22], and intestinal malabsorption [23-25]. The impact of chronic alcohol use on the large intestine has not been studied as much as its upper GI effect, though, some studies suggest that alcohol exposure may cause altered bowel motility [18].

In addition, heavy alcohol consumption has been documented to increase risk for several types of cancers including oral, esophageal, gastric, colorectal, liver, pancreatic, and breast cancer [2, 26-35]. A recent review of existing epidemiological data has shown that even light-to-moderate alcohol consumption may increase cancer risk, most specifically breast cancer risk in women [36]. The link between alcohol consumption and cancer risk is so well documented that the International Agency for Research on Cancer declared alcoholic beverages a Class 1 carcinogen in 1988 [37]. Acetaldehyde, the main ethanol metabolite, has also been linked to increased risk for cancers, particularly of the head and neck, and is itself classed as a Class 1 carcinogen [38-40].

Although studies since the mid-20th century have suggested light-to-moderate alcohol consumption may have a cardio-protective effect [41, 42], chronic heavy drinking has repeatedly been associated with significantly increased risk for hypertension [43], heart disease [41, 42], and ischemic stroke [41, 44, 45]. Heavy drinking may also increase risk for the development of type 2 diabetes mellitus [46-48], and be detrimental to disease control and progression in both type 1 and 2 diabetics [2, 49-51]. Heavy alcohol consumption also appears to impair immune system function [52, 53]. AUD is also a risk factor in the development of pneumonia, tuberculosis, and other infectious diseases [2]. Chronic heavy drinking has also been linked to increased risk for complications associated with HIV/AIDS [54, 55].

The most widely studied consequences of excessive alcohol consumption, however, are those associated with the central nervous system. Seizures are a known symptom of alcohol

withdrawal [56]. Indeed, withdrawal seizures have been so frequently described in medical literature that it is a common treatment protocol to prophylactically administer benzodiazepines when individuals known to have a history of alcohol dependence (or risk thereof) are hospitalized, in order to decrease the risk for seizures and other withdrawal symptoms [3, 57]. There is also some evidence to suggest that AUD is associated with an increased risk for epilepsy outside of withdrawal-induced seizures, though the relationship has not been conclusively demonstrated [2, 58]. Heavy alcohol consumption has also been linked to an increased risk for Alzheimer's disease, and other forms of dementia and age-related cognitive decline [2], though some evidence exists that light-to-moderate drinkers may have lower risk for dementia later in life than non-drinkers, suggesting a protective effect [59-61]. One form of dementia frequently observed in individuals with alcohol use disorder is Wernicke–Korsakoff syndrome, resulting from co-morbid severe alcohol abuse and vitamin B1 deficiency [25, 62, 63]. Chronic alcohol abuse has also been associated with the demyelinating disorders Marchiafava–Bignami disease and osmotic demyelinating syndrome [64, 65]. A relationship has also been observed between alcohol use disorder and psychiatric disorders such as anxiety, depression, and bipolar disorder [2, 66]. The association between AUD and psychiatric disorders has long been considered to be a "chicken and egg" relationship with competing hypotheses as to whether individuals with psychiatric conditions are more vulnerable to developing AUD or whether alcohol use may contribute to the development of psychiatric illness, with compelling evidence in support of both ideas [66].

Underlying the myriad negative socioeconomic and health consequences of excessive alcohol consumption is, of course, its addictive nature. Long-term heavy alcohol use leads to behavioral

changes such as increased consumption in order to avoid withdrawal symptoms, and in order to gain the rewarding effects of alcohol after tolerance has developed [67]. In some individuals, this sort of long term alcohol use results in the physiological dependence, and loss over control of intake that are characteristic of AUD [1]. One of the major challenges in the field of alcohol research is identifying strategies for treating AUD. This is due to the fact that treatment options for AUD remain limited. Treatment for AUD may include medically assisted withdrawal in severe cases, but often focuses on behavioral interventions designed to facilitate cognitive restructuring in relation to alcohol use and seeking behavior, and enhancement of coping-skills to deal with the negative effects of cessation of alcohol use [68]. Pharmacotherapeutic treatments include the opioid antagonists naltrexone and nalmefene [69, 70]. These agents are believed to block the rewarding effects of alcohol, and, thus, decrease desire to drink [71] . Another type of treatment is the administration of acetaldehyde dehydrogenases inhibitors, such as disulfiram, which produce a strong sensitivity to alcohol by inhibiting the metabolism of ethanol's first byproduct [72]. Acamprosate is another drug approved for the treatment of alcohol use disorder, though its mechanism of action is uncertain [73, 74]. Another common AUD disorder treatment, often initiated by the individual outside of medical intervention, is the use of self-help and faith-based support groups such as Alcoholics' Anonymous [75]. All of these strategies have shown limited efficacy [76-79], highlighting the need for identification of new therapeutic targets.

The need for new therapeutic targets for the treatment of alcohol use disorder led to the experiments described in this document. The over-arching hypothesis of these studies was that chronic ethanol induced gene expression changes are key to the pathogenesis of alcohol dependent behaviors such as excessive drinking. Furthermore, I propose that network analysis of

gene expression changes, measured genome-wide by DNA microarrays, will identify such molecular underpinnings of AUD and potentially lead to new therapeutic targets for treating this disorder.

Employing C57BL/6J mice (*Mus musculus*) as model organisms we examined the transcriptome-level effect of chronic, high-dose alcohol exposure with the chronic intermittent ethanol (CIE) by vapor chamber paradigm (to be discussed in detail in chapter 2). The gene expression effect of multiple cycles of CIE on five different brain-regions within the mesocorticolimbic system and extended amygdala was studied. The first experiment was a time-course looking at gene expression at four different time-points after multiple cycles of CIE. This experiment provided insight into the short-term and long-term effect of chronic, high-dose ethanol exposure on brain gene expression [80]. The second C57BL/6J mouse experiment combined multiple cycles of vapor chamber CIE with intermittent two-bottle choice drinking. The purpose of combining two means of exposure, involuntary exposure to ethanol vapor and voluntary ethanol drinking, came from previous studies which have demonstrated that repeated cycles of CIE by vapor chamber led to a sustained increase in voluntary two-bottle choice consumption [81]. By examining genome-wide gene expression changes after multiple cycles of CIE, we have attempted to uncover the molecular mechanisms underlying the behavioral effects of chronic, high-dose ethanol exposure.

We also began to explore the influence of genetic background on ethanol responsive gene expression networks in the brain. C57BL/6J mice are an extremely inbred laboratory mouse strain [82]. We, therefore, asked whether gene expression networks identified in C57BL/6J mice

after CIE are present on a more diverse genetic background. To do this we used multiple strains from the BXD recombinant inbred panel. The BXD panel is a cohort of mice bred from two laboratory mouse strains: C57BL/6J and DBA/2J (to be discussed in detail in chapter 2). The resulting panel consists of several mouse strains whose genetic make-up contains alleles originating from progenitor strains in unique proportions and combinations. Multiple strains of BXD mice, as well as C57BL/6J and DBA/2J progenitors, underwent repeated cycles of CIE by vapor chamber with intermittent drinking, and gene expression assessed with Affymetrix microarrays, similar to the study conducted in C56BL/6J mice. Unlike the C57BL/6J, however, the BXD study looked only at prefrontal cortex (PFC). This brain-region is of particular interest because of its involvement in executive function [83] and impulse control [84], suggesting it has significant influence on voluntary alcohol intake [85]. This region has also been shown to be differentially affected by ethanol exposure between C57BL/6J and DBA/2J mice [86].

Our final approach was to study gene expression networks associated with chronic ethanol consumption in two different species. This entailed a co-analysis of gene expression in the PFC of C57BL/6J mice after CIE and intermittent drinking with gene expression in PFC of rhesus macaques (*Macaca mulatta*). Macaques used in this study were exposed to prolonged, voluntary ethanol drinking (to be discussed in detail in chapter 6). This analysis tested the hypothesis that ethanol responsive networks, and highly connected hub genes within these networks, that are present in both species could represent a conserved response to chronic ethanol that may also occur in humans. This cross-species approach could aid in the identification of hub genes that may represent therapeutic targets for the treatment of AUD.

Chapter 2: Background

Molecular Mechanisms of Ethanol Action on Neurons

Ethanol was long considered a nonspecific agent whose pharmacologic and behavioral effects were thought to result from disruption of neural cells through interaction with cellular lipids [87]. During the second half of the 20th century, however, empirical evidence from new studies supported what was known as the "protein hypothesis," which stated that the effects of ethanol were due to direct or indirect interaction between ethanol molecules and cellular proteins [87]. Such studies eventually led to the identification of specific ethanol targets [88]. These include the N-methyl-D-aspartate (NMDA) receptor [89], γ-aminobutyric acid (GABA) receptors [90], neuronal nicotinic acetylcholine receptors (nAChR) [91], 5-HT_3 receptors [92], L-type Ca^{2+} channels [93], and G-protein-activated inwardly rectifying K^+ channels (GIRKs) [88, 94, 95].

$GABA_A$ receptors are pentameric ligand-gated ion channels [96] that act as one of the main inhibitory neurotransmitters in the central nervous system [97]. Ethanol acts as a positive allosteric regulator of $GABA_A$ receptors [98, 99]; meaning ethanol enhances the inhibitory action of GABA binding to $GABA_A$ receptors. Ethanol has been shown by electrophysiology studies in *Xenopus* oocytes to enhance the inhibitory effects of GABA binding, at concentrations as low as 3mM, by binding to the δ subunit of extrasynaptic $GABA_A$ receptors [100]. There is also substantial evidence that genetic alteration of α, β, and γ $GABA_A$ subunits alters ethanol response in animal models [97, 101]. $GABA_A$ receptor subunits have also shown significant brain-region differences in gene and protein level expression, as well as differences compared to matched controls in post-mortem tissue from human alcoholics [102-107]. Genetic differences in the structure or expression of $GABA_A$ receptor genes have also been shown to affect gene expression and behavioral response to ethanol exposure. In human studies SNPs in the GABRA2

gene have been associated with reduced acute alcohol tolerance [108], alcohol dependence [109], and alcohol-related cue induced activation, measured by functional magnetic resonance imaging (fMRI), in medial prefrontal cortex and ventral tegmental area [110]. Multiple single nucleotide polymorphisms (SNPs) in the GABRG3 gene were found to be associated with alcohol dependence [111]. Further studies have shown that a GABBR1 SNP that may be associated with reduced risk for alcoholism [112]. Chronic ethanol exposure has been demonstrated, in rats, to significantly alter $GABA_A$ receptor subunit expression [113]. Behavioral studies in rodents into the effect of GABAergic response to chronic ethanol exposure have mostly focused on withdrawal symptoms, particularly withdrawal seizures [97], however, chronic high-dose ethanol exposure has been shown to produce tolerance to the GABA-mediated effects of ethanol such as sedation, motor impairment, and cognitive impairment [114, 115]. Animal models have also shown that sequence variation and gene expression of several other genes may affect $GABA_A$ receptor subunits in the presence of ethanol, indicating interactions between multiple gene products affect the GABAergic response to ethanol exposure [106, 116, 117].

NMDA receptors are another type of multi-subunit ligand-gated ion channels that bind glutamate and glycine to potentiate excitatory neurotransmission by facilitating the flow of positively charged ions [118]. NMDA receptors are a vital component of the molecular mechanisms underlying synaptic plasticity and learning, as evidenced by their role in the electrophysiological component of memory known as long-term potentiation. Ethanol acts as a negative allosteric modulator, decreasing the excitatory effect of NMDA receptors in neurons [89]. Acute ethanol exposure decreases the excitatory effect of NMDA receptors in cultured neurons [87], as well as slices from rodent hippocampus [119-121], amygdala [122, 123], cingulate cortex [124], dorsal

striatum [125], and nucleus accumbens [126]. The exact site of physical interaction with ethanol molecules and the NMDA receptor is still a subject of study, however, experimental evidence indicates that GluN1 (NR1) receptor subunits are far less sensitive to ethanol's effect compared to GluN2A (NR2A) subunits [127], indicating ethanol's NMDA modulating effects are mediated by interactions with GluN2. In behavioral studies using rodent models, ethanol has been shown to block long-term potentiation in the hippocampus [121, 128, 129] and dorsal striatum at concentrations relevant to intoxication [130, 131]. Further, ethanol impaired performance on short-term memory tests in human subjects [132] indicating ethanol's effect on NMDA-mediated neurotransmission may play a role in ethanol associated cognitive impairment. Pharmacologic and genetic manipulations of NMDA receptor subunits have also indicated a role for NMDA-mediated transmission on behaviors such as sedation [133, 134], sensitization [135], and reward [136, 137]. Due to ethanol's effect on NMDA-mediated long-term potentiation, it has been hypothesized that, in humans, modulation of NMDA-mediated neurotransmission may underlie alcohol-related blackouts [127, 138] and amnesia associated with binge drinking [127, 138]. In contrast to ethanol's acute effect, chronic ethanol exposure has been shown to upregulate NMDA receptor subunit expression [138], most likely representing an adaptive mechanism to compensate for the inhibitory effects of ethanol on NMDA receptor function. There is also evidence for interaction between glutamatergic ethanol response and expression of downstream regulators of neuronal activity and plasticity such as BDNF [139] and DARPP-32 [140]. BDNF, a major of regulator central nervous system development and plasticity related to learning and memory [141], has been shown to be affected by ethanol exposure at the mRNA and protein level in rodents [86, 142] and humans measured by peripheral blood levels [143, 144]. DARPP-32 is a protein phosphatase with an established role in regulation of dopaminergic

neurotransmission [145] in response to NMDA activation. In addition, it has been shown that this gene's expression is regulated by ethanol exposure in rodents [146-148].

The nicotinic acetylcholine receptor (nAChR) is a pentameric ligand gated ion channel that is widely expressed in the central nervous system [149]. Along with the $GABA_A$ receptor, another ethanol target, nAChRs are members of the Cys-loop family of ligand gated ion channels [149]. nAChRs are widely expressed in the mesocorticolimbic system where they respond to acetylcholine binding to allow cation flux into neurons, leading to depolarization, neuronal excitation, and neurotransmitter release [149]. Genetic studies in rodents have shown that knockout of the α4 nAChR subunit decreases acute ethanol consumption in mice [150], and decreases dopamine release in the VTA [151] revealing that nAChR activation modulates the rewarding effects of ethanol, and that ethanol molecules may directly interact with the α4 subunit. However, deletion of other nAChR subunits has also been shown to alter drinking behavior in transgenic mice [152]. Similar findings using pharmacologic manipulation have been demonstrated in rats [153-155]. Some attempts have been made to study the effect of nAChR targeting in human subjects using nAChR antagonists. A few studies found that nAChR antagonist treatment lead to a self-reported reduction in desire to drink alcohol [156, 157] however, findings in these studies are mixed [158] highlighting the complexity of alcohol's effect on the brain, and of humans' motivation to consume alcohol.

5-HT3 receptors, along with nicotinic acetylcholine receptors and $GABA_A$ receptors, are also members of the Cys-loop family of pentameric ligand-gated ion channels [159, 160]. 5-HT3 receptors are expressed the central and peripheral nervous system, particularly in the cortex,

hippocampus, nucleus accumbens, substantia nigra, and ventral tegmental area [160, 161]. When activated by serotonin binding, 5-HT3 receptors allow cations to pass through the channel, leading to cellular depolarization [92]. Ethanol exposure enhances this receptor's excitatory effect [92, 161]. Most studies on the effect of ethanol exposure on 5-HT3 receptors relates to the resulting release of dopamine from neurons that connect the VTA and NAc [161]. Inhibition of 5-HT3 receptors in the presence of ethanol has been shown to decrease dopamine release in the NAc [162], and to decrease ethanol self-administration, conditioned place preference (a model of drug rewarding properties), and locomotor activation in rodent models [161] - thus strongly suggesting ethanol's modulation of neuroexcitation via interaction with the 5-HT3 receptor influences the drug's behavioral effects.

L-type Ca^{2+} channels are voltage-gated ion channels that allow Ca^{2+} cation influx into the cell in response to membrane depolarization [163, 164]. These channels are expressed in cardiac muscle, smooth muscle, skeletal muscle, retinal neurons, hair cells, neuroendocrine cells, and central nervous system neurons [163]. In neurons, L-type Ca^{2+} channels are believed to enhance the neuroexcitatory actions of activation of NMDA receptors by glutamate binding [163]. Acute ethanol acts as a blocker of L-type Ca^{2+} channels [93]. Chronic ethanol exposure has been shown to increase expression of L-type Ca^{2+} channel subunits at the protein level in cultured mouse cortical neurons [165]. Calcium channel antagonists have also been shown to decrease withdrawal seizures in rats exposed to chronic ethanol [166]. Calcium channel antagonists also decrease activity, as measured by electrophysiology, in hippocampal sections from chronic ethanol exposed mice [167]. These finding indicate a role for changes in L-type Ca^{2+} channel

expression in the negative reinforcing effects of ethanol, particularly as related to the occurrence of withdrawal symptoms.

G-protein-activated inwardly rectifying K^+ channels (GIRKs) are ion channels that are activated by ligand binding to a G-protein coupled receptor which, in turn, releases G proteins that bind to GIRKS, and allow K^+ ion flux leading to hyperpolarization of neurons, and inhibition of neuronal activity [168]. Expression of GIRK types vary by brain-region [168]. Functionally, these channel types are involved in neuroplasticity, learning and memory, and motor coordination [168]. Ethanol has been shown to enhance the opening of GIRKs [94, 95]. Human gene association studies have found SNPs in the promoter region of the GIRK2 gene, KCNJ6, to be associated with alcohol dependence in adults, and stress-related alcohol abuse during adolescence [169]. GIRK2 has also been shown to alter ethanol behaviors including analgesia [170], open-field activity [170], locomotor activation [171], taste aversion [172], and conditioned place preference [172] in knockout mice. Animal model studies also indicate a role for GIRK3 in ethanol behavioral response. GIRK3 knockout mice show fewer withdrawal seizures, increased binge-like consumption in a limited access paradigm, reduced neuronal activation in the VTA, and blunted dopamine release in NAc following ethanol administration [173]. A more recent study also demonstrated that *Girk3* null mice show enhanced conditioned place preference following ethanol administration [174], indicating a role for *Girk3* in association-based learning related to the development of addiction. The mouse *Girk3* gene, *Kcnj9*, shows significant differential expression between C57BL/6J and DBA/2J mice [175], two mouse strains with widely divergent behavioral responses to ethanol. *Kcnj9* is also located at the genomic position of a quantitative trait locus (QTL) on chromosome 1 that is associated with withdrawal from

multiple drugs, including ethanol [175], as well as several other ethanol related behaviors in mouse models [168]. Together these findings strongly suggest that ethanol enhances GIRK signaling in neural tissue, and variation in GIRK expression may contribute to the development of AUD.

Ethanol Actions on Non-Neuronal Cells

In addition to primary receptor targets in neurons, ethanol exposure also affects glial cells [176]. Glial cells are the most abundant cell type in the brain [177] and include astrocytes, oligodendrocytes, and microglia. Astrocytes perform a number of functions including structural and metabolic support of neurons aiding in repair of neural injuries, modulation of neurotransmission, and promoting myelination by oligodendrocytes [178]. Astrocytes are particularly important in glutamatergic neurotransmission by regulating concentration of glutamate, glycine, and K+ ions in the extracellular space [178]. Ethanol has been demonstrated to modify astrocyte density in rodent models and human alcoholics with an overall empirical trend toward increased astrocyte density with prolonged ethanol exposure, and decrease with abstinence, though results are mixed [176, 178]. Ethanol may disrupt the function of astrocytes in regulating glutamatergic neurotransmission both by its effect on neuronal NMDA receptors, and by modulating expression of the glutamate transporters GLAST and GLT-1 in astrocytes themselves [176]. Indeed, it has been shown that, in cell culture models, ethanol treatment increases glutamate uptake by glial cells [178]. GLT-1 expression has been shown to be significantly increased in the NAc of drinking rats [176, 179, 180] and pharmacologic and genetic manipulations of GLT-1 and GLAST in mice result in altered ethanol behavioral response [176]. Less research has been done on the influence of astrocytes on GABAergic

neurotransmission, though there is some evidence that GABA receptors are expressed in astrocytes [177, 181]. Further, the role of astrocytes in the neuro-inflammation response may act in ethanol-related neurotoxicity [176]. The effect of both acute and chronic ethanol exposure on astrocytes is an area in need of further study; however, experimental evidence indicates that ethanol-regulated gene expression in astrocytes may affect cell-cell signaling with neurons and other glial cell types, such as oligodendrocytes, possibly contributing the behavioral effects of ethanol [176].

Oligodendrocytes are crucial in nervous system function due to their role in structural and functional support of neurons by myelin ensheathment [178]. Indeed, diseases of reduced myelination often have debilitating clinical effects [178]. There are a few demyelinating diseases in particular that are associated with AUD including Wernicke-Korsakoff syndrome. Wernicke-Korsakoff syndrome is seen in the presence of heavy alcohol consumption and vitamin B1 deficiency, and results in brain atrophy of both white and gray matter in PFC, mammillary bodies, thalamus, hypothalamus, and cerebellum [65]. Marchiafava–Bignami syndrome is also linked to heavy alcohol use, and is characterized by demyelination in corpus callosum, middle cerebellar peduncles, and periventricular white matter [65]. Another disease of demyelination, osmotic demyelinating syndrome is characterized by white matter loss in the pons, basal ganglia, thalamus, and deep cerebral white matter, and is strongly linked to AUD [65]. Outside of clinically defined myelin disease states, decreased volume of the corpus callosum, the major white matter tract of the brain, has been observed in human alcoholics [182]. Human studies also indicate that white matter loss associated with heavy alcohol use may be reversible with prolonged abstinence [183]. There is also a multitude of experimental evidence indicating that

ethanol exposure affects myelination at all developmental stages, and that the PFC, which, in humans, continues to myelinate into early adulthood [184], may be a particularly vulnerable region. Rodent models studies have shown decreased expression of structural constituents of the myelin sheath, and regulators of myelination, with acute [86] and chronic [185, 186] ethanol exposure.

Neurocircuitry Actions of Ethanol

As outlined above, ethanol has widespread effects on the brain; however, the majority of focus in research on AUD is on areas within the mesocorticolimbic system and extended amygdala. The mesocorticolimbic system refers to pathways of dopamine producing neurons in the cerebral cortex originating in the midbrain [187]. Of particular interest are dopaminergic neurons with cell bodies that originate in the ventral tegmental area. These neurons have projections to the amygdala, cingulate gyrus, hippocampus, and olfactory bulb, however the major connections are to the prefrontal cortex, and shell of the nucleus accumbens where dopamine is released in response to a variety of stimuli [187]. The extended amygdala includes the bed nucleus of the stria terminalis, central and medial nuclei of the amygdala, ventral pallidum, and substantia innominata [188]. These pathways are a major part of the limbic system and are involved in reward processing, motivation, learning, and memory [189]. Along with other drugs of addiction, ethanol stimulates the release of dopamine to the NAc and PFC, as well as other brain-regions in this system, from neurons originating in the VTA [65]. This response to acute ethanol exposure is hypothesized to mediate the positive reinforcing effects of ethanol consumption such as euphoria and hedonia [67]. Models of the development of AUD hypothesize that repeated exposure leads to tolerance and increased consumption in order to achieve the same rewarding

effects [67, 190]. Prolonged exposure and increased consumption eventually results in the development of the negative reinforcing properties of ethanol such as preoccupation, craving, and withdrawal causing individuals to continue to drink in order to avoid the negative effects of stopping eventually leading to altered brain function, physiological dependence, and addiction [190]. The extended amygdala's connections to mesocorticolimbic structures is believed to play an important role in the negative reinforcing effects of prolonged exposure [190]. For this reason, brain-regions within these pathways are the focus of the analyses outlined in this dissertation.

Experimental findings over the course of decades of research into the effect of both acute and chronic alcohol exposure have demonstrated that the actions of ethanol on known targets such as $GABA_A$ receptors, NMDA receptors, etc., and interaction between these targets, as well as the effects on downstream signaling cascades are all involved in the way alcohol changes brain activity. Alcohol's effect is brain-region dependent and cell-type dependent. Signaling between cells, both between neurons and glial cells at the synapse, as well as communication between neurons with connections to more distant brain-regions, is disrupted by ethanol exposure. Gene expression studies of chronic alcohol exposure indicate that prolonged ethanol exposure, particularly at high-doses, leads to sustained changes in expression of certain genes. As outlined above, manipulation of the expression of certain genes, such as by knockout mouse models, leads to significant changes in ethanol behaviors. Finally, electrophysiology studies have shown that ethanol alters neuronal activity in the mesocorticolimbic systems and extended amygdala. Taken together, this research supports the hypothesis that ethanol-related behavioral changes observed with prolonged use, such as increased consumption, are the result of synaptic plasticity.

Further, that changes in gene expression mediate synaptic plasticity in response to ethanol exposure. Therefore, changes in gene expression lead to behavioral changes **(Figure 1)**.

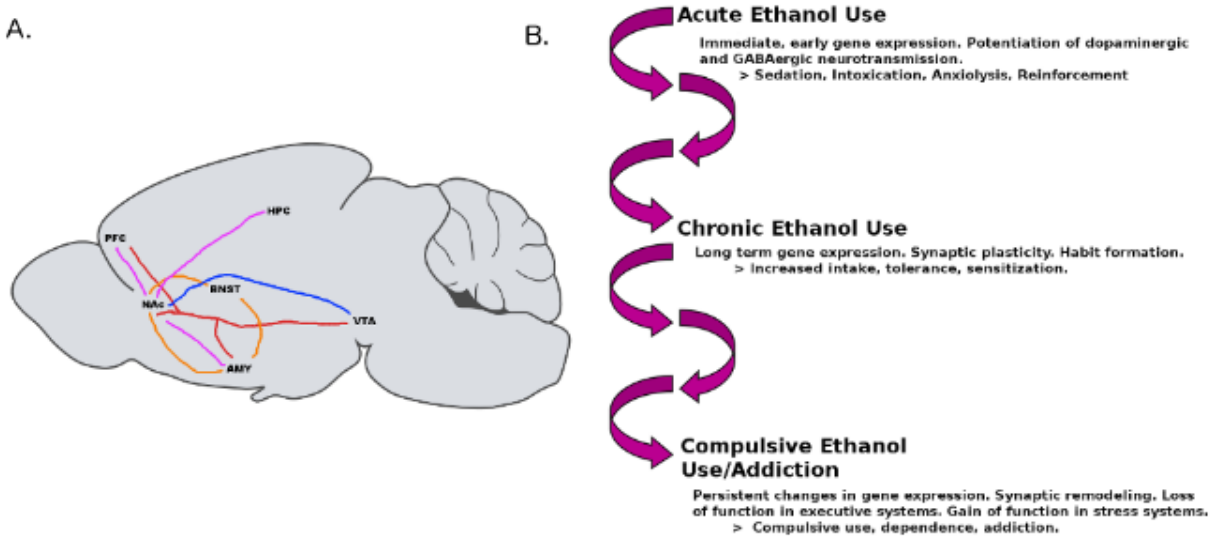

Figure 1: Regions of brain reward system, and neurobiological changes that occur with repeated ethanol exposure. a) Brain-regions of the mesocorticolimbic system and extended amygdala. Ethanol exposure stimulates dopamine release from the VTA to NAc, PFC, and AMY. NAc receives glutamatergic input from PFC, HPC, and AMY. VTA receives GABAergic inhibitory signals from NAc. These signaling pathways are involved in reward and reinforcement. Communication between the centromedial nuclei of the AMY, BNST, and NAc are involved in reward-based processing and learning. PFC=prefrontal cortex, NAc=nucleus accumbens, AMY=amygdala including central nucleus of the amygdala, BNST=bed nucleus of the stria terminalis, VTA=ventral tegmental area, HPC=hippocampus. Red lines=dopamine signaling pathays. blue lines=GABAergic pathways, pink lines=glutamatergic pathways, orange lines=extended amygdala circuit.
b) Beginning with acute ethanol exposure, gene expression in the mesocorticolimbic system and extended amygdala is altered, resulting in behavioral changes. As ethanol exposure continues, lasting changes in gene expression occur, leading to synaptic plasticity. Chronic exposure eventually leads to loss of control over ethanol intake and addiction. Figure adapted from Miles et al. - manuscript in preparation.

Gene Expression

Early research on the effect of ethanol in gene expression began in cultured neural cells. These studies demonstrated that ethanol could directly regulate expression of specific genes such as $GABA_A$ receptor proteins, G-protein coupled receptor subunits, and stress response proteins such

as Hsc70 [113, 191-193]. Completion of the Human Genome Project led to the advent of new research methods, such as gene expression microarrays and RNA-sequencing (RNAseq), that allow for genome-wide RNA quantification. These technologies have proven highly useful in starting to demystify ethanol's effect on the brain. Transcriptome studies using microarrays have demonstrated that ethanol significantly affects gene expression in the central nervous system at the level of hundreds to thousands of genes [86, 194]. Such studies began in cultured cells [195], and expanded to model organisms ranging from *C. elegans* to non-human primates [86, 196-203]. Transcriptome studies have identified specific gene expression patterns in ethanol preferring rats, with both long-term [196] and shorter-term ethanol exposure [204, 205], in genes involved in synaptic transmission and cellular homeostasis. Similar results have been found in mice, and, further indicate that ethanol's effect on gene expression is brain-region specific [206], varies with genetic background [86, 207], and occurs with a single [86] or repeated exposures to ethanol [200, 208]. Similar pathways have been identified in zebrafish [197, 201] suggesting a conserved neurogenomic response to ethanol exposure. This hypothesis is also supported by meta-analyses that integrate gene expression data after ethanol exposure across multiple animal models and human subjects [203, 209].

Gene expression has also been studied directly in humans using brain tissue, collected by autopsy, of individuals diagnosed with AUD [85, 194, 210-212]. These studies have demonstrated that the gene expression patterns of alcoholics can be distinguished from those of non-alcoholics [210], and have identified genes involved in known biological processes such as neuron ensheathment by myelin, synaptic transmission, and regulation of cellular proliferation [194, 210] indicating that ethanol disrupts specific biological processes in the brain. Transcriptome studies in human tissue, however, present a number of difficulties. Brain tissue

from humans is difficult to obtain in large numbers. There is also a lack of ability to control the amount, frequency, and duration of alcohol exposure over an individual's lifetime. Further, information about these factors may be limited, inaccurate due to reliance on self-reported data, or missing entirely. Controlling for other lifestyle factors that may contribute to changes in brain gene expression, such as age at death, presence of co-morbid neuropsychiatric conditions, use of other drugs of abuse, and history of neural injury and disease, is also not possible with human subjects, and may be limited in availability and accuracy [206, 213]. Furthermore, in animal model studies neural tissue is rapidly collected and frozen immediately after death. In human postmortem tissue there is usually considerable variation in the interval between death and harvesting of brain tissue, which may interfere with the accuracy of mRNA quantification [85, 194, 210-212]. For these, and other reasons, gene expression data from model organisms, mainly mice, are used in the analyses described in this dissertation. Microarrays were chosen over RNAseq for these studies because my advisor, Dr. Michael Miles, has extensive experience in the use of microarrays to quantify gene expression, appropriate equipment and protocols for processing large numbers of Affymetrix microarrays were in place at the Miles laboratory at Virginia Commonwealth University and the Medical University of South Carolina Proteomics Core, and arrays were still more cost-effective than RNAseq at the time these experiments were performed. Some of the disadvantages to microarrays over RNAseq include greater reliance on existing genomic sequences, greater background noise, loss of sensitivity in detecting very high or very low expressed genes, and less efficacy in detecting spice variants [214]. Even with these downsides, however, microarrays were the better choice for the purposes of the experiments discussed in this dissertation.

That ethanol exposure has been repeatedly shown to affect expression of hundreds to thousands of genes presents unique challenges to the analysis of ethanol transcriptome studies. Based on the fact that gene expression studies have identified clusters of genes involved in known biological processes whose expression are significantly altered by ethanol exposure [86, 194-196, 198, 200], one may hypothesize that these genes represent several different biological processes, some of which are regulated independently of each other, and some of which show co-regulation between pathways. Network analysis provides tools to identify more biological processes disrupted by ethanol exposure, and to pinpoint important regulators of these processes.

Network Analysis

The field of systems biology provides tools for identification of groups of genes that are coordinately regulated with the hypothesis that clusters of regulated genes represent biological processes that occur within the cell [215]. Systems biology uses mathematical and computational methods to model biological systems, and identify how perturbing factors, such as high dose ethanol exposure, affect those systems [216]. The studies outlined in this thesis extensively utilize one systems biology technique, that of network analysis. Network analysis involves the application of network theory, the analysis of graphs as representations of connections between discrete objects [216, 217]. In the case of transcriptome studies, each mRNA transcript represents a discrete object. Connections between mRNA transcripts can be determined in a variety of ways depending on the relational factor of interest. For the purposes of these studies, correlations in gene expression, measured by Affymetrix microarrays, are the relationship of interest, and are determined using the Weighted Gene Correlated Network Analysis method (WGCNA or Weighted Gene Co-Expression Network Analysis) [218].

WGCNA is an analysis method that builds networks based on scale-free topology [218]. Scale-free topology is theorized to be relevant to biological systems due to a few key observations: i) biological data such as those from proteomic, metabolomic, and transcriptomic studies behave similar to other types of large complex networks in showing high degree of self-organization, and the probability of a single node interacting with a certain number k of other nodes decays as a power law: $P(k) \sim k^{-\gamma}$, indicating a small number of highly connected nodes within the network [219] ii) cellular functions depend on a small number of proteins that have been described as 'master regulators' [217]. Master regulators are highly connected proteins that have been experimentally demonstrated to be necessary for a certain cellular process, usually development, differentiation, or continued metabolic function [220]. Yeast protein-protein interaction networks have shown that the most highly connected nodes are often proteins essential to life [221]. Using a variety of cultured cells, Weintraub et al. identified MyoD as a master regulator gene/protein in muscle differentiation [222], and *in vivo* and *in vitro* manipulation of cancer cell-lines with genetic techniques identified specific genes as master regulators of metastasis [223]. In network analysis with WGCNA master regulators are referred to as "hub genes," and are identified using the property of connectivity [218]. Connectivity is quantified by the sum of correlation to other nodes in the network [224]. This approach hypothesizes that important regulatory genes will be among the most highly connected [218]. (**Figure 2**).

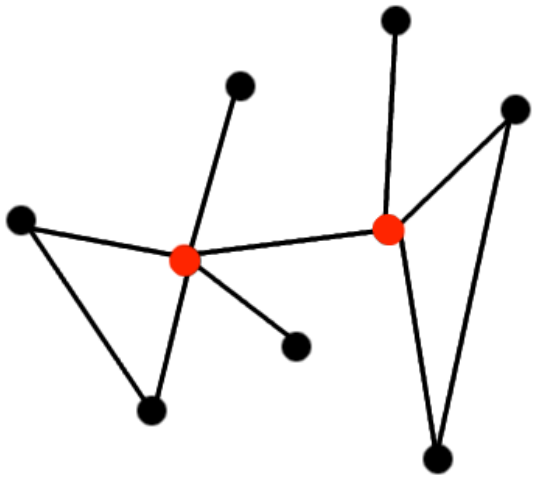

Figure 2: Diagram example of a scale-free network. Black lines=edges representing connectivity between nodes, black circles=nodes representing genes, red circles=highly connected nodes representing hub genes.

WGCNA has been applied to a variety of biological problems, and used to identify networks related to complex traits. Gene expression studies employing WGCNA have ranged from those on diseases such as obesity [225]**,** Alzheimer's disease [226]**,** Amyotrophic Lateral Sclerosis [227], cancer [228, 229]**,** and alcohol use disorder [80, 212, 230]**;** to gene expression similarities and differences between different rodent strains [231], or two closely genetically related species (*Homo sapiens* and *Pan troglodytes*) [232]; to identifying expression networks underlying specific behaviors in rodent models [233]. For the purposes of these studies, WGCNA is used to identify gene expression networks that respond to chronic, high-dose ethanol delivered by vapor chamber. These analyses were performed with the hypothesis that such correlated changes in gene expression underlie ethanol related behaviors, in this case a sustained escalation in drinking; and that the most highly connected hub genes may represent new therapeutic targets.

Chronic Intermittent Ethanol by Vapor Chamber

The chronic intermittent ethanol by vapor chamber paradigm was developed as a rodent model of ethanol dependence [234]. In this model mice, after being given a priming dose of ethanol intraperitoneally, were placed, in their home cages, in a Plexiglass chamber for 16 to nearly 24 hours a day with ethanol delivered in vapor form at a concentration of 10-16 mg/L [234, 235]. In the vapor chambers mice achieved blood ethanol concentrations (BECs) between 1.25 and 3.00 mg/mL. Human blood alcohol concentrations (BACs) are measured in g/dL, making the BECs achieved in the vapor chambers equivalent to human BACs of 0.125 to 0.3. During their time in the vapor chamber mouse BECs were stabilized using the alcohol dehydrogenase inhibitor pyrazole to maintain intoxicating blood ethanol levels at a steady state [234]. The CIE paradigm was first demonstrated to cause withdrawal seizures, establishing it as a model of ethanol dependence. Studies of CIE induced withdrawal seizures demonstrated that longer duration [234] and repeated cycles of vapor chamber exposure interspersed with periods of abstinence [235, 236] resulted in significantly more withdrawal seizures than control groups that received no ethanol vapor exposure in the Plexiglass chambers or only received a single session, or a shorter session [234-236]. In addition to a model of chronic ethanol exposure that demonstrably leads to physiological dependence, CIE by vapor chamber is a powerful model because, when used over multiple cycles, it involves prolonged periods of intoxicating BECs with intermittent periods of abstinence. Our laboratory, and collaborators through the INIA Stress Consortium, selected this model of ethanol exposure because this cyclic pattern of high-dose ethanol followed by abstinence is similar to observations from previous studies of human alcoholics [237] and rat models [238], demonstrating that ethanol self-administration in dependent subjects often occurs in an episodic fashion. In addition, repeated cycles of CIE by vapor chamber have been combined with intermittent voluntary ethanol consumption in order to experimentally explore the

link between ethanol dependence and increased drinking. Exposure to chronic, high-dose ethanol by vapor chamber lead to a significant increase in ethanol intake [239], that, with repeated cycles of CIE, was maintained for several weeks after final vapor chamber session [81, 240]. Additionally, multiple cycles of CIE lead to a reduction in condition taste aversion to ethanol [241]. In addition to the increase in ethanol intake, repeated cycles of CIE have recently been shown to lead to decreased myelination and axon degeneration in multiple regions of the central nervous system [242], and to significantly alter gene expression in a time and brain-region dependent manner in multiple regions of the mesocorticolimbic system and extended amygdala [208, 243]. The analyses outlined in this dissertation build on these previous findings using network analyses techniques to identify patterns in gene expression in the mesocorticolimbic system and extended amygdala in response to multiple cycles of CIE by vapor chamber to identify biological processes disrupted by chronic high-dose ethanol that may underlie increased ethanol consumption.

Chapter 3: Time-course Gene Expression and Network Analysis in C57BL/6J Mice after CIE by Vapor Chamber

Introduction

Alcohol abuse and dependence have significant health and social consequences. Alcohol Use Disorder (AUD) is characterized by chronic excessive alcohol consumption, often alternating with periods of abstinence [237, 244]. Previous studies over the last two decades have suggested that neuroplasticity occurring in the brain's reward and stress pathways contributes to the development of AUDs, and that changes in gene expression may be an important molecular mechanism underlying such neuroadaptations [1, 67, 86, 190, 245].

Genomic approaches involving microarrays or RNAseq, together with scale-free network analyses, have shown that gene networks of highly correlated expression patterns are associated with acute or chronic ethanol exposure in brain tissue derived from animal models and human autopsies [86, 212, 246, 247]. Such networks often have conserved biological functions or regulatory mechanisms [246, 248, 249] providing novel mechanistic information about the neural actions of ethanol and other drugs of abuse [248, 250]. Additionally, network topology analysis allows the identification of highly connected "hub genes" that have been shown to provide key regulatory functions over expression networks [212, 246, 247, 249]. Applying such approaches to animal models of alcohol dependence could thus provide new understanding of mechanisms underlying associated neuroplasticity, and identify new therapeutic targets for intervention in AUDs.

Animal models to more accurately model development of AUDs have recently shown considerable progress in providing predictive validation for new therapeutic targets [187, 212, 250]. One such widely used model is the chronic intermittent ethanol vapor (CIE) paradigm where rodents are exposed intermittently to cycles of ethanol vapor such that they experience repeated cycles of exposure and withdrawal [81, 251, 252], as seen in alcoholics [237, 244]. This model has been shown to produce lasting increases in ethanol consumption as well as neurochemical, physiological and synaptic structural changes [81, 187, 252-254]. Earlier genomic studies of CIE exposure in mice indicated brain regional and time-dependent changes in gene expression that may contribute to the behavioral and physiological plasticity evoked by chronic intermittent ethanol exposure [81, 208]. However, a detailed network level analysis of gene expression adaptations with CIE has not been performed. Such an approach may identify key regulatory hubs that may play a significant role in mediating behavioral and physiological consequences of CIE treatment.

Here we use the Weighted Gene Correlated Network Analysis (WGCNA) scale-free network algorithm to analyze a detailed time-course study of CIE-evoked changes in gene expression across multiple brain regions comprising the mesolimbocortical dopamine and extended amygdala pathways. These neural pathways are thought to have a pivotal role in the development of excessive ethanol consumption associated with dependence [67, 190, 245]. We show that shortly after cessation of ethanol vapor exposure, both conserved and region-specific waves of expression network changes occur across multiple brain regions. However, following prolonged withdrawal (7 days), the hippocampus and the prefrontal cortex show persistent expression network alterations. The functional and network topology analysis of such networks provides

key targets for future studies aimed at elucidating mechanisms of behavioral plasticity occurring with CIE. In particular, we implicate a Bdnf-containing network in prefrontal cortex as a potentially important contributor to the neurobiology of progressive ethanol consumption associated with dependence.

Materials and Methods

Animals and Chronic Intermittent Ethanol (CIE) Exposure

Adult male C57BL/6J mice purchased from Jackson Laboratories (Bar Harbor, ME, USA) were individually housed in an AAALAC-accredited animal facility under a 12-hour light/dark cycle. Mice were given free access to food and water during all experimental procedures. After a 2-week acclimation period, mice (n=48) were exposed to chronic intermittent ethanol vapor or air in inhalation chambers, as previously described [81, 239, 240]. Mice were divided into two groups of 24. One group (CIE) received ethanol vapor exposure for 16 hours/day for 4 days while the other group was similarly handled but received only air exposure in the inhalation chambers (Control; Ctrl). For CIE mice, ethanol was volatilized by passing air through an air stone submerged in 95% ethanol. Chamber ethanol concentrations were monitored daily and air flow was adjusted to maintain ethanol concentrations within a range (10-13 mg/l air) that has been shown to yield stable blood ethanol concentrations (175-225 mg/dl) in C57BL/6J mice [81]. Before each chronic ethanol exposure cycle, intoxication was initiated in the CIE group by administration of ethanol (1.6 g/kg), and blood ethanol concentration was stabilized by injection of the alcohol dehydrogenase inhibitor pyrazole (1 mmol/kg). Both ethanol and pyrazole were administered intraperitoneally (i.p.) in a volume of 0.02 ml/g body weight. Ctrl mice were handled similarly, but administered saline and pyrazole (i.p.) prior to being placed in control

chambers that delivered only air (no ethanol vapor). Thus, all mice received the same number and timing of pyrazole injections prior to final removal from the inhalation chambers. Following 4 days in the inhalation chamber, mice underwent 7 days of complete abstinence from ethanol. At the end of the abstinence period, mice were returned to the inhalation chamber to begin the next cycle of CIE. This pattern of 4 days CIE (or control air) exposure followed by 7 days abstinence was repeated for four complete cycles (**Figure 3**).

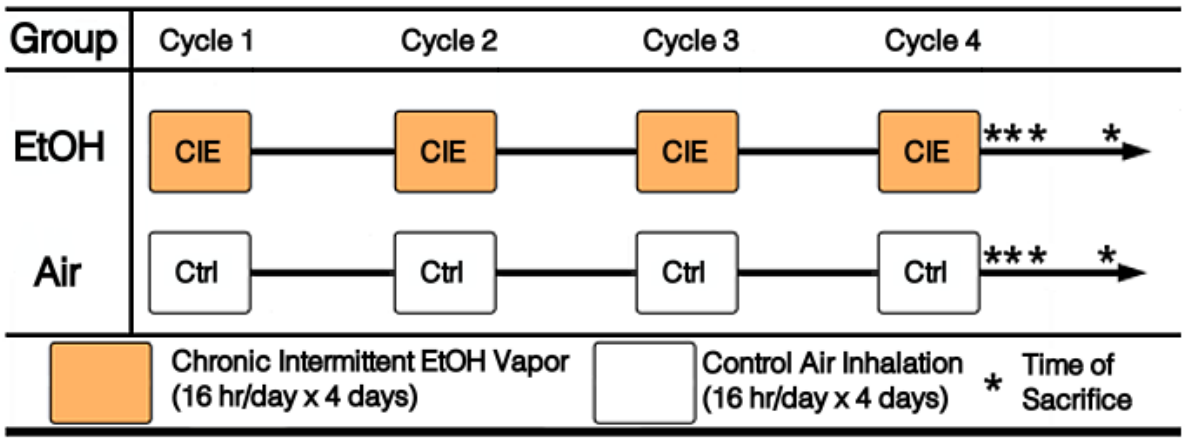

Figure 3: Overview of time-course CIE experiment.

Tissue Harvesting and RNA Isolation

Immediately following the last cycle of air or ethanol exposure as above, mice were removed from the inhalation chambers and euthanized at the appropriate time point by decapitation. Time points collected were 0, 8, and 72 hours (h) and 7 days (d), with n=6 for each treatment/time group (**Figure 3**). Following decapitation, mouse brains were immediately extracted from the skull, chilled on ice and dissected by brain punch microdissection. Tissue samples were frozen on dry ice and stored at -80^{o}C until processed for RNA isolation. Total RNA was isolated using the RNeasy Mini Kit (Qiagen, Valencia, CA) as described previously [208].

Gene Expression Microarrays

The MUSC ProteoGenomics Core Facility processed RNA samples for microarray analysis using standard procedures as described by the manufacturer (Affymetrix, Santa Clara, CA). Samples were processed as a group by brain region with treatment groups and time points randomized to minimize batch effects. Gene expression was quantified with Affymetrix GeneChip® Mouse Genome 430, type 2 arrays. Scanning data was stored in CEL file format using Affymetrix Expression Console software, and these data files were transferred to Virginia Commonwealth University (VCU) for further analysis. Raw data files (CEL files) and RMA normalized expression values for all brain regions have been submitted to the Gene Expression Omnibus (GEO) database under accession number GSE72517.

Microarray Analysis

Affymetrix GeneChip® Mouse Genome 430, type 2 arrays were analyzed using The R Project for Statistical Computing (http://www.r-project.org/). RNA degradation, average background, and percent present probesets were used to assess array quality, and inspect for outlier arrays. Quality of each microarray was also assessed primarily by principal component analysis. Plots of first principal component by second principal component allowed for visual identification of outliers and batch effects between arrays. Background correction and normalization were performed using the affy package for R [255]. Due to batch effects noted in principal component plots, microarrays were separated by RNA hybridization batch for initial normalization. Each batch was background corrected with the Robust Multi-array Average (RMA) technique and normalized by quantile normalization [256]. The second step involved subjecting all microarrays

together to another round of quantile normalization. Finally, ComBat with hybridization group as the batch effect was used to remove any remaining batch effects reflected in the data [257]. The only exception to this procedure was the prefrontal cortex where repeat group was used as only the batch effect correction factor (**Figure 4**).

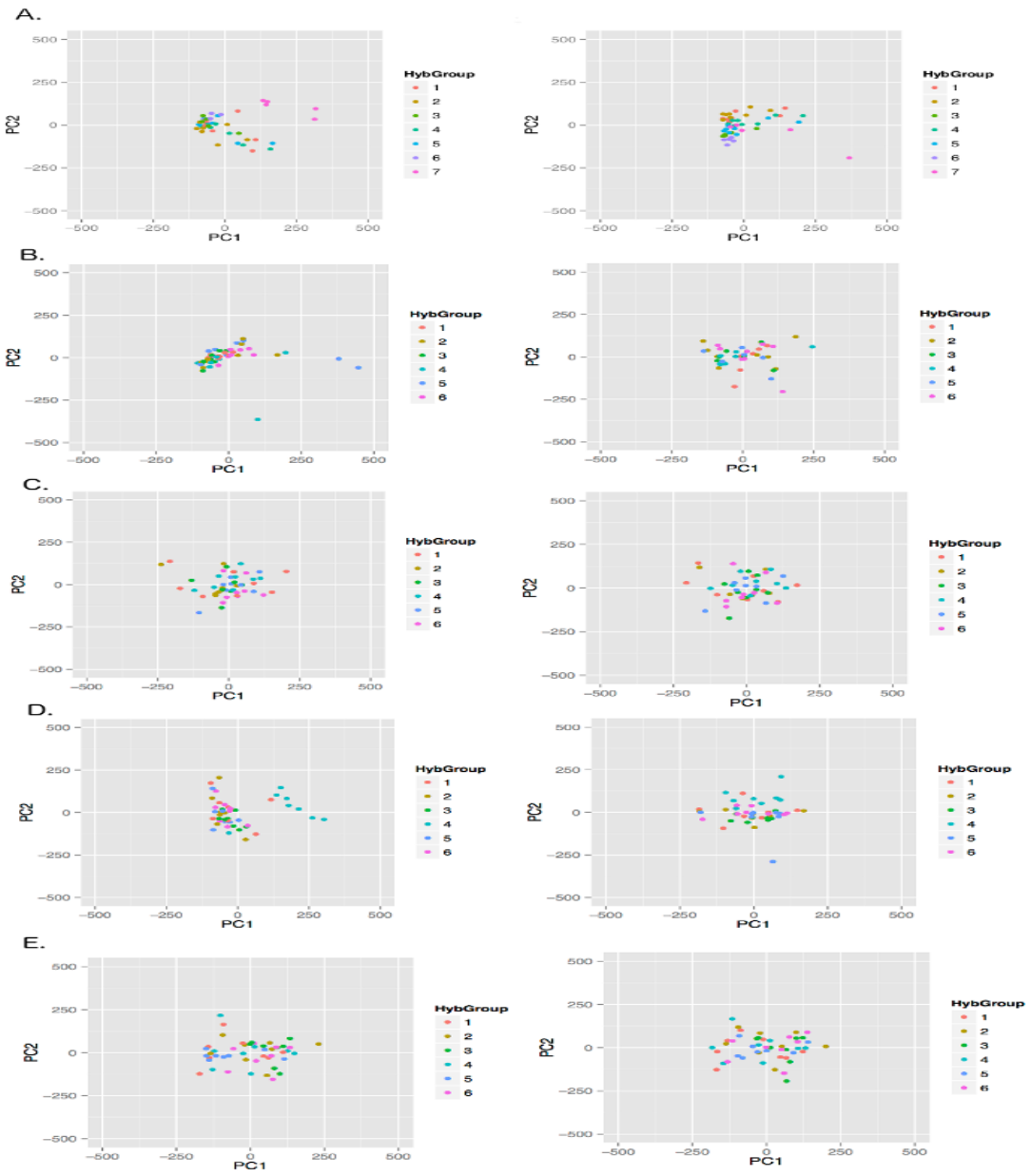

Figure 4: Multidimensional scale plots showing 1st and 2nd principal component of all arrays for each brain-region before (left panel) and after (right panel) quantile normalization and ComBat. A) PFC, B) NAc, C) HPC, D) BNST, E) CeA

CIE Responsive Genes

CIE regulated genes were identified using the limma package for R [258]. Comparisons were made between CIE and Ctrl groups at each time point (0h, 8h, 72h, and 7d), and overall significance was determined by ANOVA. The Benjamini and Hochberg false discovery rate method (FDR) [259], was used to account for multiple testing. For the purposes of these studies, false discovery rates equal to or less than 0.01 were considered indicative of significant differences in gene expression between CIE and Ctrl mice.

Weighted Gene Correlated Network Analysis

Weighted Gene Correlated Network Analysis (WGCNA) was used for scale-free network topology analysis of microarray expression data [246]. WGCNA was performed on each brain region independently with the WGCNA package for R [260]. Probesets were selected for WGCNA based on overall significance by ANOVA (FDRs equal to or less than 0.01). Any probeset found to be significant by ANOVA in any brain region was included, resulting in a total of 10,072 probesets used for WGCNA. Standard WGCNA parameters were used for analysis, with the exceptions of soft-thresholding power and deep split. A soft-thresholding power of 6 was used for all brain regions; this power was selected using methods described by Langfelder and Zhang [260]. WGCNA was performed with deep-split values of 0-3. Deep-split value was selected based on a multi-dimensional scaling (MDS) plot, which displayed first and second principal components. The criterion for deep-split value selection was that no modules showed overlap with each other by the MDS plot. Deep-split values of 3 were selected for all brain regions, except the nucleus accumbens, where a deep-split value of 2 was chosen.

Overlap Analysis

Overlap was determined between WGCNA modules and genes differentially expressed, as indicated by LIMMA FDR values equal to or less than 0.01 at each time-point. Fisher's Exact Test [261] was then used to quantify the significance of overlap. WGCNA modules with Fisher's Exact Test p-values ≤ 0.005 combined with odds ratios greater than 3 were determined to be significantly over-represented for differentially expressed genes at a certain time-point.

To compare differentially expressed genes under CIE to those regulated by acute ethanol exposure, the results of a previous gene expression study at the Miles' Laboratory was used. This study looked at the gene expression response in the prefrontal cortex, nucleus accumbens, and ventral tegmental area in various strains of mice from the BXD recombinant inbred mouse panel after an intraperitoneal injection of 1.8 g/kg ethanol. Gene expression was then measured using Affymetrix GeneChip 430, type 2 arrays. Differential gene expression across the panel was determined using Fisher's Combined Probability Test and S-Scores as previously described [247]. Differentially expressed genes between CIE and control at each time-point in PFC and NAC were compared to genes significantly regulated across the BXD RI panel with acute ethanol exposure within the same brain-regions using Fisher's Exact Test. Similar to overlap between CIE WGCNA modules and LIMMA results for each time-point for the CIE data, odds ratios and p-values were used to determine whether there was significant overlap between genes regulated at each time-point with CIE and genes regulated across the BXD RI panel with acute ethanol.

Bioinformatics

Modules identified by WGCNA were examined for function using publicly available bioinformatics resources. The Functional Annotation Chart tool from DAVID (http://david.abcc.ncifcrf.gov/) [262, 263] was used to identify biological pathways highly represented by genes grouped into each module. GeneMANIA (http://www.genemania.org/) [264] was also utilized for functional analysis through use of constituent genes in each module as query lists for validation in GeneMANIA derived networks driven by previously published biological data sources (microarray, protein-protein interaction and others) [264]. The miRvestigator Framework application (http://mirvestigator.systemsbiology.net/) [265] was then used to identify microRNAs that may regulate modules that significantly overlap with differentially expressed genes at 0h and 7d in the PFC and HPC. The PFC and HPC were chosen for microRNA target analysis because these regions showed an appreciable level of regulation with CIE at 7d. A complete workflow of microarray analysis from tissue collection through bioinformatics is represented in **Figure 5**.

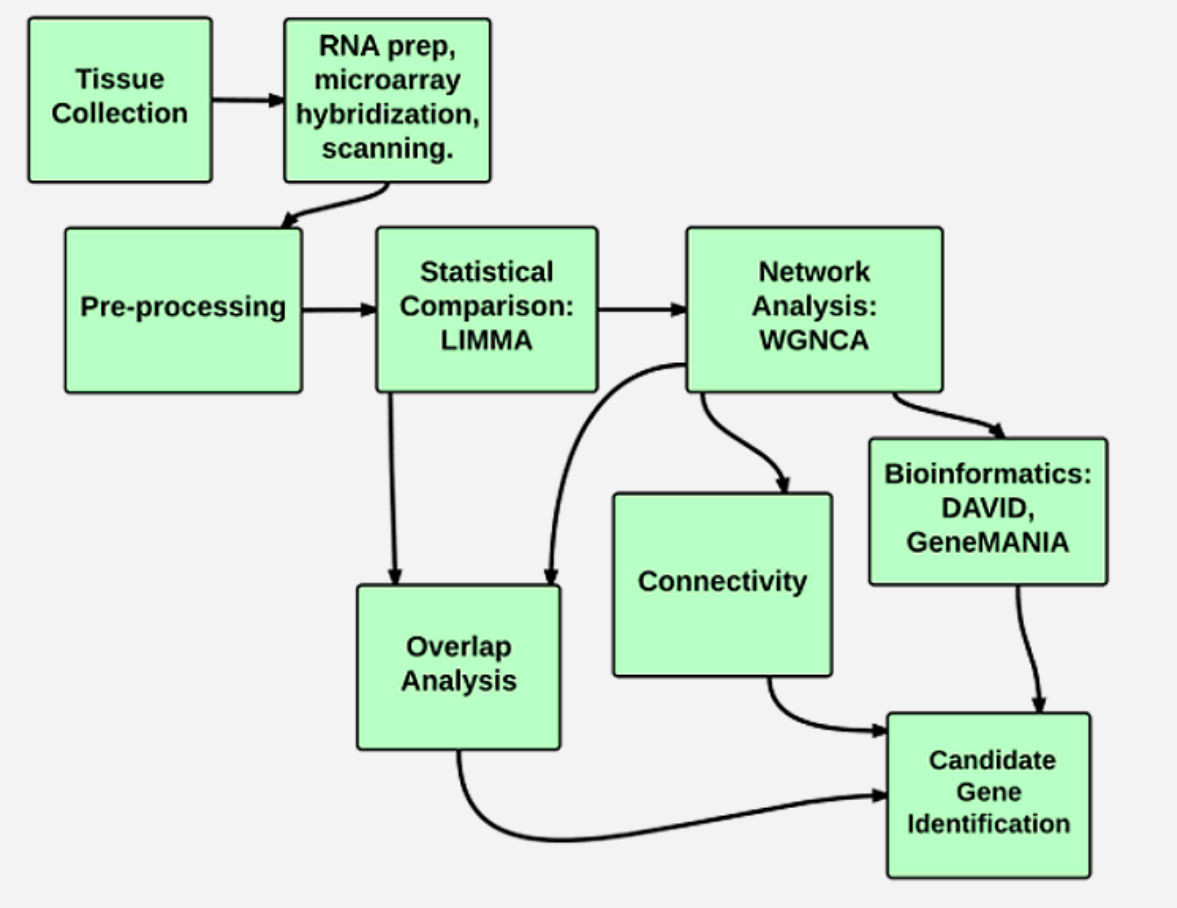

Figure 5: Workflow diagram of all analyses performed on C57BL/6J mice after 4 cycles of CIE by vapor chamber.

Candidate Gene Identification

The prefrontal cortex and hippocampus were chosen for detailed candidate gene characterization because these brain regions showed both immediate and long-term (7d) CIE induced changes in gene regulation (**Table 1**). Previous studies have shown a sustained increase in ethanol consumption at 7d post multiple CIE cycles [81], indicating that expression differences found at this time-point may contribute to the alteration in ethanol consumption. We reasoned that prolonged ethanol exposure-induced changes in gene expression (0h) might induce long-lasting structural or functional components of synaptic plasticity and contribute to elevated ethanol consumption, even if those genes mRNA expression patterns decayed to baseline over the 7d

withdrawal period. Therefore, we restricted our detailed bioinformatics analysis and candidate gene identification to genes that were included in WGCNA, and showed significant differential gene expression by LIMMA at 0h or at 7d (FDRs equal to or less than 0.01). Genes fitting these criteria were then ranked by scaled within module connectivity (kIM) as described by Langfelder and Horvath [260].

Quantitative RT-PCR

To verify the presence of *mmu-let-7c-1* in the B6 mouse, PFC samples from male and female B6 mice that underwent 5 cycles of CIE by vapor chamber and drinking as part of a larger experiment on the effect of CIE with intermittent 2-bottle choice drinking on gene expression in the PFC of BXD recombinant inbred mice and their progenitors. This study will be discussed in greater detail in Chapter 5 of this dissertation. RNA from these samples was extracted using the Qaigen miRNeasy Mini Kit (Qiagen, Valencia, CA), which preserves small RNAs. For this reason, these samples rather than those from the B6 time-course mice, were used because the B6 time-course RNA used for gene expression network analysis was extracted with the mRNeasy Mini Kit (Qiagen, Valencia, CA). This kit does not preserve RNAs shorter than 200nt in length. Primers for *mmu-let-7c-1* were designed using NCBI's Primer BLAST primer design tool (http://www.ncbi.nlm.nih.gov/tools/primer-blast), and supplied by Eurofins Genomics (Eurofins Scientific, Luxembourg). Three primer pairs were tested for efficiency, and the pair with the highest efficiency was chosen: forward primer-GTGCATCCGGGTTGAGGTAG, reverse primer-AGTGTGCTCCAAGGAAAGCTA.

RNA was transcribed into cDNA using the iScript cDNA Synthesis Kit (Bio-Rad, Hercules, CA) according to manufacturer instructions. qRT-PCR was run on a CFX Connect Real-Time PCR

Detection System (Bio-Rad, Hercules, CA) using iQ SYBR Green Supermix (Bio-Rad, Hercules, CA). *Ublcp1* and *Ppp* were used as reference genes. *let-7c-1* expression was calculated relative to both *Ublcp1* and *Ppp* for male and female mice in each treatment group, CIE and Air, and examined for significance using a t-test.

Results

Time-Course Gene Expression with CIE

Gene expression analysis with LIMMA identified significant differential expression between CIE and Ctrl groups. The majority of gene regulation in all brain regions was observed during the first 8h after the final cycle of chronic intermittent ethanol. The prefrontal cortex (PFC) or hippocampus (HPC) showed the greatest number of CIE-regulated genes at any particular time point and they were the only regions to show expression changes at all time points. The contrasting response in PFC and HPC was particularly striking at the 7d time point where they each showed hundreds of post-CIE regulated genes while other brain regions were virtually quiescent **(Table 1, Suppl. Table S1)**. Interestingly, the number of CIE-responsive genes at 7d in PFC and HPC were both greater than the numbers seen at 72h, suggesting a possible late withdrawal response or an unmasking of chronic CIE regulated genes following recovery from acute withdrawal.

Table 1: LIMMA results. Number of significantly differentially expressed probesets at each time-point, LIMMA FDR ≤ 0.01

Brain Region	CIE 0h vs. Air 0h	CIE 8h vs. Air 8h	CIE 72h vs. Air 72h	CIE 7d vs. Air 7d
PFC	3277	1527	238	427
NAC	717	28	0	0
HPC	865	967	3	604
BNST	1079	251	195	0
CEA	62	79	0	1

Comparison of overlaps in CIE-regulated gene sets either across time points within a brain region or across brain regions within a single time point revealed patterns of co-regulation. In all brain-regions, the greatest amount of overlap across time periods was seen between 0h and 8h, but these patterns largely decayed by 72h in most brain regions (**Suppl. Table S2**). Only PFC showed significant temporal overlaps across all time points. In both the PFC and HPC, there were over 100 probesets with overlapping regulation at both 0h and 7d, indicating that many genes responding to CIE showed persistent changes following a prolonged withdrawal period (**Suppl. Table S2**). Across brain regions, there was overlap in gene sets most prominently at the 0 and 8h time points (**Figure 6**). However, across brain-regions at 7d, only three genes overlapped between the PFC and HPC and one gene between PFC and CeA (**Figure 6**). This finding shows long-term gene regulation after CIE was specific to individual brain regions. There was also no overlap seen between the PFC and BNST at 72h, suggesting that gene expression changes during late withdrawal were also brain-region specific (**Figure 6**). Thus, four cycles of CIE induced robust changes in gene expression across multiple brain regions that steadily decreased over a 72h withdrawal period, except for PFC and HPC where region-specific persistent changes were seen.

	PFC		NAC		HPC		BNST		CEA	
PFC-0hr	3277	PFC-0hr								
PFC-8hr	1527	PFC-8hr								
PFC-72hr	238	PFC-72hr								
PFC-7day	427	PFC-7day								
NAC-0hr	176	PFC-0hr	717	NAC-0hr						
NAC-8hr	11	PFC-8hr	28	NAC-8hr						
NAC-72hr	0	PFC-72hr	0	NAC-72hr						
NAC-7day	0	PFC-7day	0	NAC-7day						
HPC-0hr	146	PFC-0hr	127	NAC-0hr	865	HPC-0hr				
HPC-8hr	57	PFC-8hr	20	NAC-8hr	967	HPC-8hr				
HPC-72hr	0	PFC-72hr	0	NAC-72hr	3	HPC-72hr				
HPC-7day	3	PFC-7day	0	NAC-7day	604	HPC-7day				
BNST-0hr	284	PFC-0hr	235	NAC-0hr	158	HPC-0hr	1079	BNST-0hr		
BNST-8hr	39	PFC-8hr	16	NAC-8hr	70	HPC-8hr	251	BNST-8hr		
BNST-72hr	0	PFC-72hr	0	NAC-72hr	0	HPC-72hr	195	BNST-72hr		
BNST-7day	0	PFC-7day	0	NAC-7day	0	HPC-7day	0	BNST-7day		
CEA-0hr	23	PFC-0hr	30	NAC-0hr	33	HPC-0hr	49	BNST-0hr	62	CEA-0hr
CEA-8hr	22	PFC-8hr	10	NAC-8hr	43	HPC-8hr	31	BNST-8hr	79	CEA-8hr
CEA-72hr	0	PFC-72hr	0	NAC-72hr	0	HPC-72hr	0	BNST-72hr	0	CEA-72hr
CEA-7day	1	PFC-7day	0	NAC-7day	0	HPC-7day	0	BNST-7day	1	CEA-7day

Figure 6: Overlap between CIE- regulated probesets at each time-point across brain regions. Table documents number of probesets significantly regulated by CIE (FDR ≤ 0.01) at each time point within individual brain regions (shaded cells) and overlap with same time-points across other brain regions.

In comparing those genes significantly differentially expressed at each time-point in the PFC and NAC to genes significantly regulated by acute ethanol exposure in a previous study of the gene expression effect of a single i.p. injection of 1.8 g/kg ethanol [247], no overlaps were found with sufficiently high odds ratios and p-values ≤ 0.05 (**Suppl. Table S3**).

Weighted Gene Correlated Network Analysis

WGCNA identified expression modules in each of the 5 brain regions studied. Similar to differential gene expression analysis, the PFC (n=31) and HPC (n=27) had the largest number of modules and CeA (n=18) the least (**Figure 7**). Module sizes varied from over 3000 probesets to

less than 35 (**Figure 7**, **Suppl. Table S4**). Of these modules, 31 were significantly over-represented with genes regulated by CIE at 0h, 23 at 8h, 9 at 72h, and 13 at 7d (**Figure 7**, and **Suppl. Table S5**). When genes within modules were summarized as "eigengenes" (first principal component of expression patterns for all genes in the module), a variety of temporal profiles were identified (**Figure 8**, **Suppl. Figures S1-S5**). The topology of kinetic profiles was most diverse in PFC and HPC while other brain regions mainly displayed module eigengene profiles that decayed to control levels by 8 or 72h post withdrawal (**Figure 8**). PFC and HPC were the exception with some modules displaying persistent or de novo expression changes at 7d in CIE-treated animals.

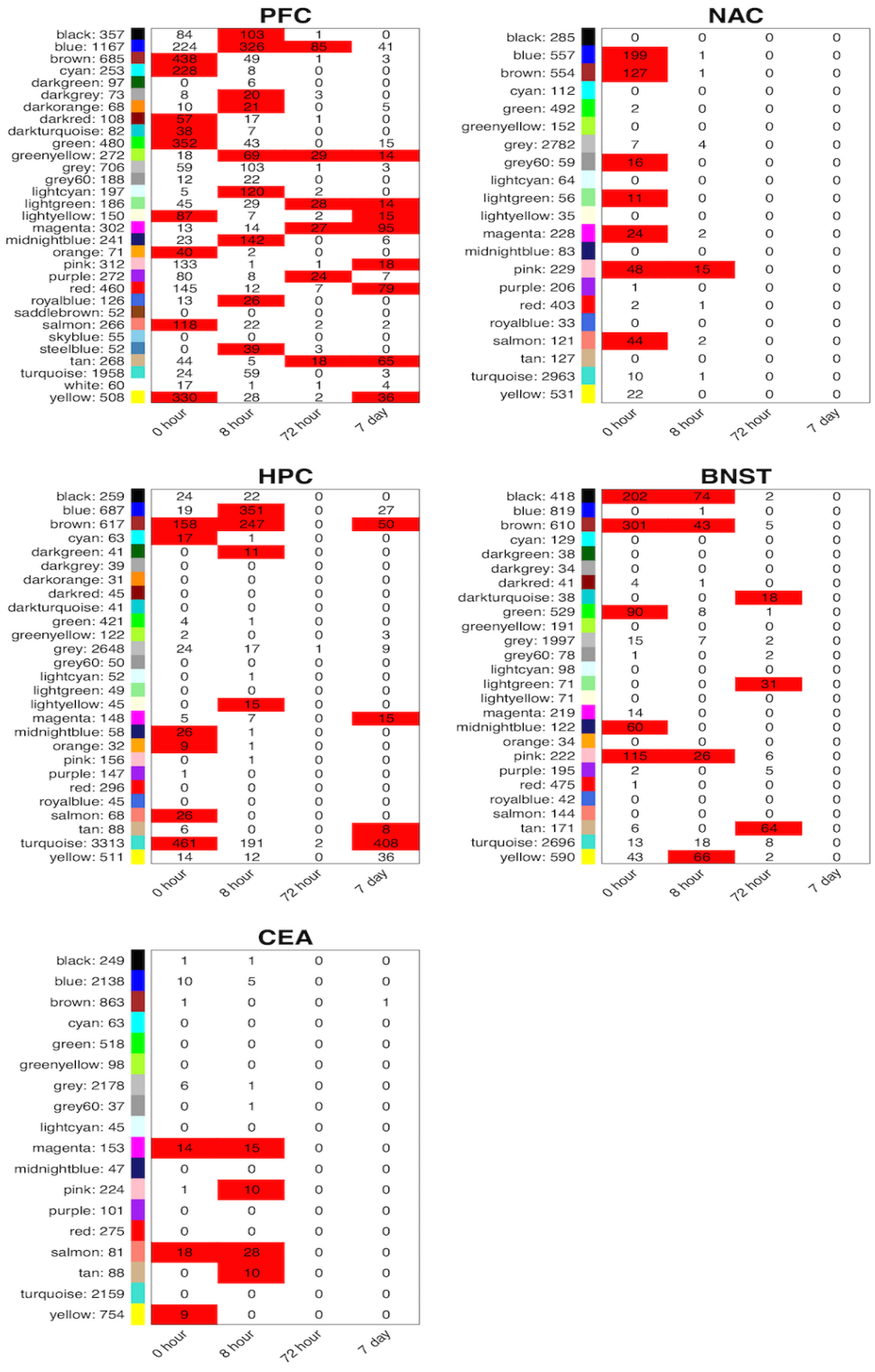

Figure 7: Overlap between CIE-regulated probesets and modules identified by WGCNA. Cell numbers indicate number of overlapping probe-sets, Cell color indicates significant overlap. Significant overlap: p-value ≤ 0.005 and Odds Ratio ≥ 3. Names and number of genes for each module are listed at far left columns within each brain region.

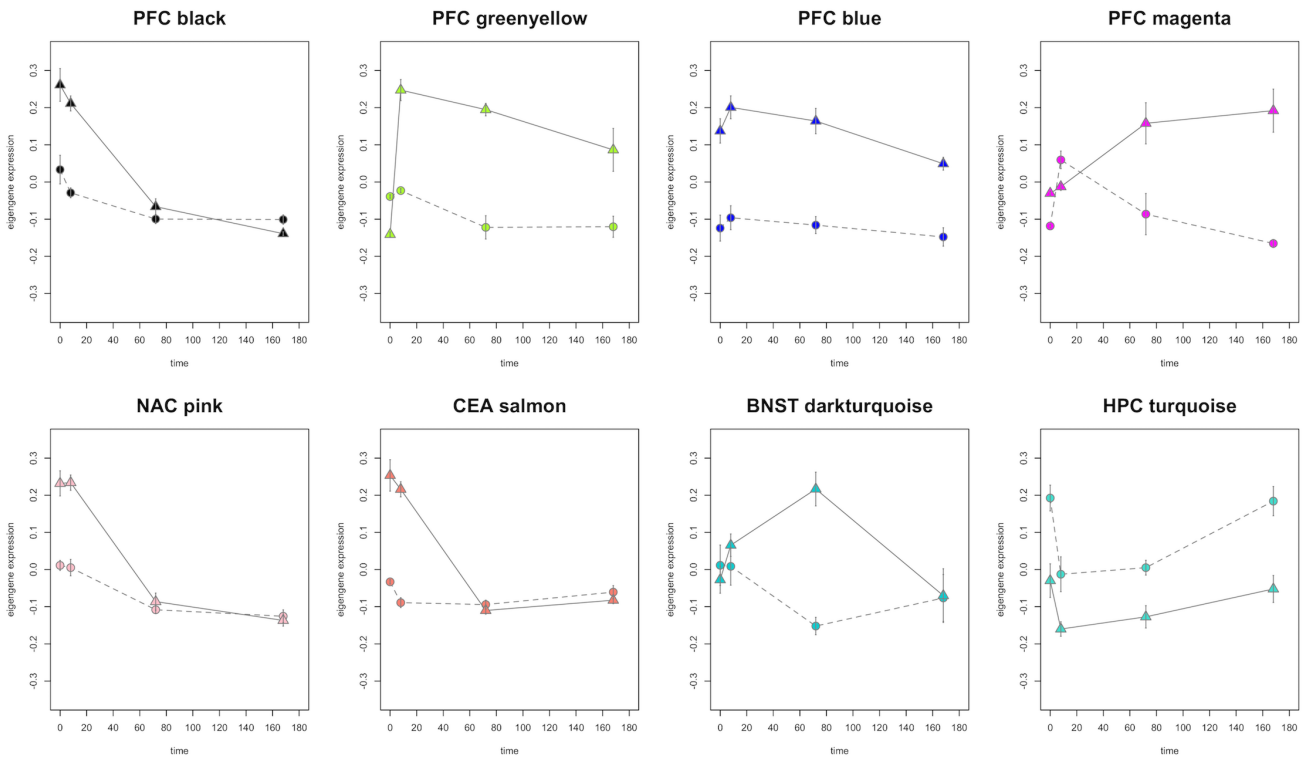

Figure 8: Representative kinetic profiles for module eigengenes. Module eigengene expression vs. time plots (hours) for the black, greenyellow, blue, and magenta modules in PFC, pink module in NAC, salmon module in CEA, darkturquoise module in BNST, and turquoise module in HPC. (Detailed discussion of module functions in Results section). Triangle = CIE, Circle = Air.

Commonly Occurring Biological Processes

Modules that significantly overlapped with differentially expressed genes at the 0h and 7d time points were chosen to discuss further bioinformatics analyses because these time points represent the initial and sustained responses to chronic ethanol exposure (**Figure 7**, **Suppl. Table S4**). However, over-representation analysis of all modules for all brain regions is contained in **Suppl. Tables S6-S10**. At the 0h and 7d time points, a number of gene ontology categories showed significant over-representation ($p \leq 0.05$) across modules in multiple brain regions. This suggests more global functional changes produced by CIE being elicited at those time points. Gene Ontology categories were considered "commonly occurring" if they showed significant overlap

with 10% or more of all WGCNA modules across brain-regions (≥12 modules). 10 GO categories were represented in 12 or more modules, and all of these were represented in all brain-regions studied (**Table 2**, **Suppl. Tables S11**). Functionally, these 10 fell into 4 general categories: RNA processing (GO:0006397~mRNA processing, GO:0008380~RNA splicing), DNA damage response (GO:0006511~ubiquitin-dependent protein catabolic process, GO:0010942~positive regulation of cell death, GO:0006974~cellular response to DNA damage stimulus, GO:0006457~protein folding), development and differentiation (GO:0045596~negative regulation of cell differentiation, GO:0048732~gland development, GO:0051301~cell division), and chromatin (GO:0000785~chromatin) (**Table 2**). Of note, ubiquitination and RNA-splicing were two gene ontology functional categories identified in our earlier global study of CIE-regulated gene expression [208]. The two categories related to RNA processing contained several DEAD box proteins (**Suppl. Tables S6-S10**, and **Suppl. Tables S5**). These proteins are known to function as RNA helicases [266]. Serine/arginine matrix proteins (*Srrm1, Srrm2, Srrm3*) were also represented in these categories. Functionally, serine/arginine matrix proteins are involved in mRNA splicing [264-269]**.** These three genes have also been found to be regulated by ethanol in multiple brain-regions in mice and human alcoholics or correlated with ethanol consumption in previous genomic studies. Many genes were represented within the categories related to DNA damage. *Usp1, Ube2d3,* and *Tecb1* are just a few examples of genes within these categories that have also been found to be regulated by ethanol in cultured cells, mice, and rats [194, 196, 209, 212, 246, 268-270]. These results may in part be indicative of the genotoxic effects seen with high-dose ethanol exposure [271].

Table 2: Top 10 commonly occurring biological processes across time-points and brain-regions.

GO Number	Number Modules	Number Brain-regions
GO:0006397~mRNA processing	17	5
GO:0006457~protein folding	16	5
GO:0008380~RNA splicing	15	5
GO:0000785~chromatin	14	5
GO:0051301~cell division	14	5
GO:0006974~cellular response to DNA damage stimulus	13	5
GO:0010942~positive regulation of cell death	12	5
GO:0048732~gland development	12	5
GO:0006511~ubiquitin-dependent protein catabolic process	12	5
GO:0045596~negative regulation of cell differentiation	12	5

Prefrontal Cortex

Overlap analysis between WGCNA modules and CIE-regulated gene sets revealed 9 modules enriched for genes regulated by chronic intermittent ethanol at 0h in PFC (**Figure 7**). Many of these modules contained genes involved in regulation of the cell cycle and apoptosis (**Suppl. Table S6).** The salmon and green modules showed several GO hits related to neuronal development, differentiation, and neuronal function. Genes within these GO categories included *Bdnf, c-fos, Bcor, Ppp2r3a, Hdac9* (green module), and *Notch1, Sox21, Sema3f, Gata2, Hdac2, Bmpr1a, Mkks* (salmon module) (**Suppl. Tables S4** and **S6**). A highly significant number of genes in the green module contained potential base pairing motifs (68% with 8 base motif; 92% with 6 base-pairing match) for *mmu-let-7c-1* (**Figure 9**). Bdnf occupied a highly interconnected central position in the green module (**Figure 9**), while showing significant expression changes only at the 0h time point (**Figure 9**). The salmon module similarly had 68% of the genes with 8

base-pairing motifs for sequences within the *miR-181* family and the *let-7* family (**Suppl. Table S12**). These motifs were also contained in *miR-543, miR-318*, and *miR-539-3p*.

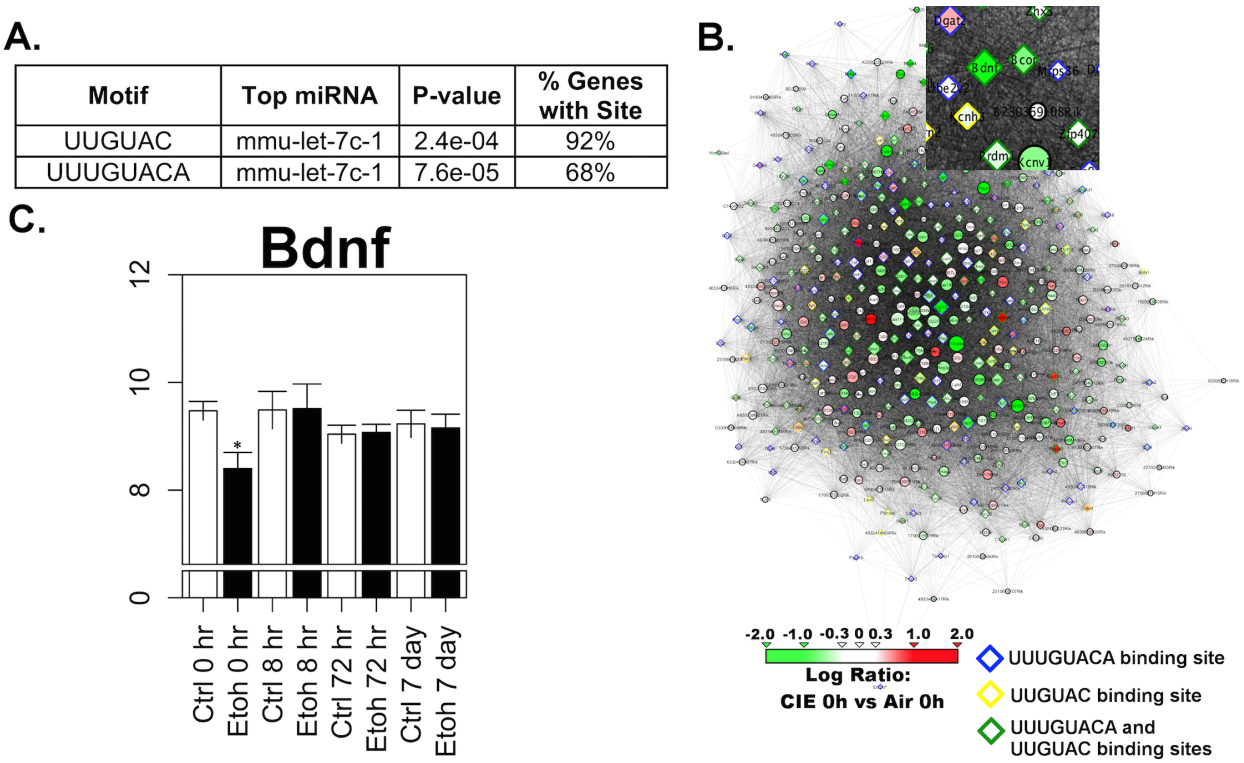

Motif	Top miRNA	P-value	% Genes with Site
UUGUAC	mmu-let-7c-1	2.4e-04	92%
UUUGUACA	mmu-let-7c-1	7.6e-05	68%

Figure 9: Bioinformatic analysis of PFC green module containing *Bdnf*. A) miRvestigator results of top miRNA motifs with complementary binding sequences in the PFC Green module. B) Network representation of the PFC Green module based on adjacency. Edge transparency indicates Pearson correlation coefficient. Node size reflects within-module connectivity determined by WGCNA. Node color indicates log-ratio of gene expression at 5 days CIE vs. Ctrl. Genes with *mmu-let-7c-1* complementary sequences are highlighted. C) Average RMA value (log2 scaled, ±S.E.) expression of *Bdnf* at each time-point and treatment condition in the prefrontal cortex. (* = LIMMA FDR ≤ 0.05)

Mmu-let-7c-1 expression was verified by qPCR, in the PFC of C57BL/6J mice that underwent 5 cycles of CIE by vapor chamber with intermittent 2-bottle choice drinking as part of a gene expression study in BXD recombinant inbred mouse panel. A significant reduction in *mmu-let-7c-1* expression was seen in male C57BL/6J mice after multiple-cycles of CIE (p-value ≤ 0.05). Interestingly, results from female C57BL/6J mice that also underwent multiple-cycles of CIE

suggested an opposite effect. *Mmu-let-7c-1* expression levels in females after multiple-cycles of CIE were higher than those of air controls; however, the difference between treatment groups in females was not significant (**Figure 10**).

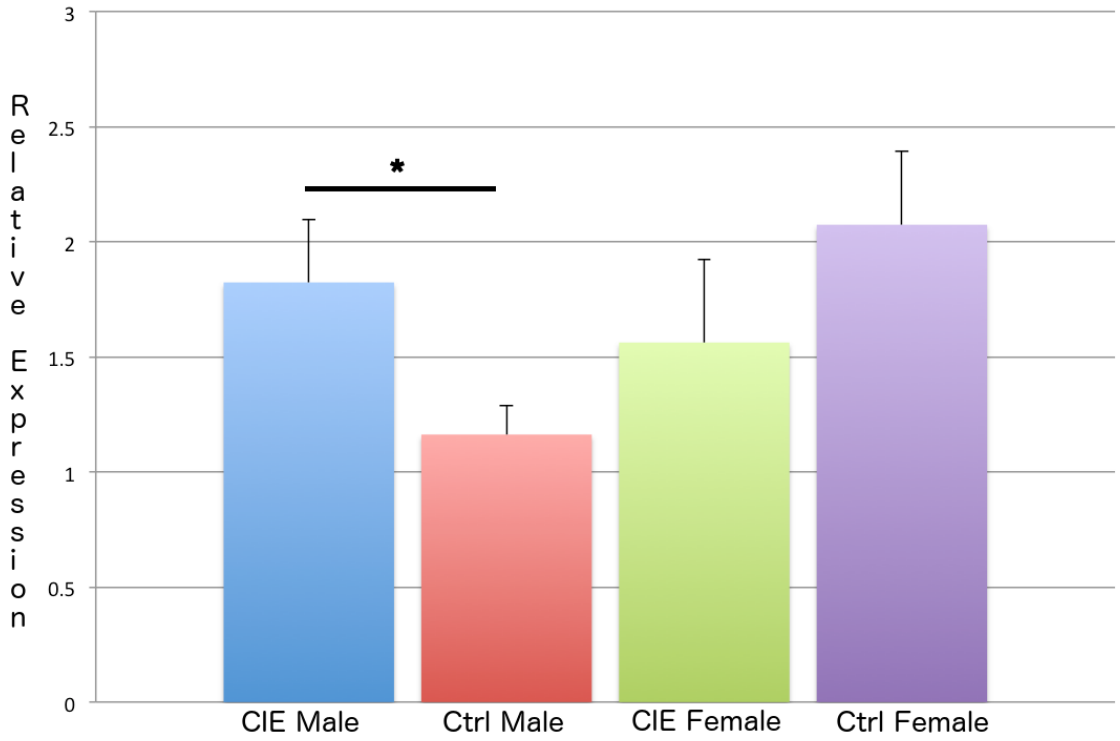

Figure 10: Bar graph of qRT-PCR results *Let-7c-1*. *Let-7c-1* expression quantified (n=4 mice/group) relative to reference gene *Ublcp1,* error bars=standard error. * = p-value ≤ 0.05.

Given the potential role of Bdnf in mediating long-term plasticity underlying increased ethanol consumption after CIE [208, 272, 273], we performed further network analysis of the green module (**Figure 11**). Strikingly, while many genes in the green module show significant changes in expression at the 0h time point, there was also a group of genes that showed changes at 0h and 7d (**Figure 11**). Looking solely at genes within the green module that were significantly regulated at 7d, network connectivity analysis within control vs. CIE samples showed that this group showed a striking increase in connectivity in the CIE samples at 7d versus 0h, or compared to the control samples at 0h or 7d (**Figure 11**). Module eigengene expression values

for the green module genes significantly regulated at 7d reflected the bimodal pattern, with decreased expression in CIE samples versus control at 0h and 7d (**Figure 11**).

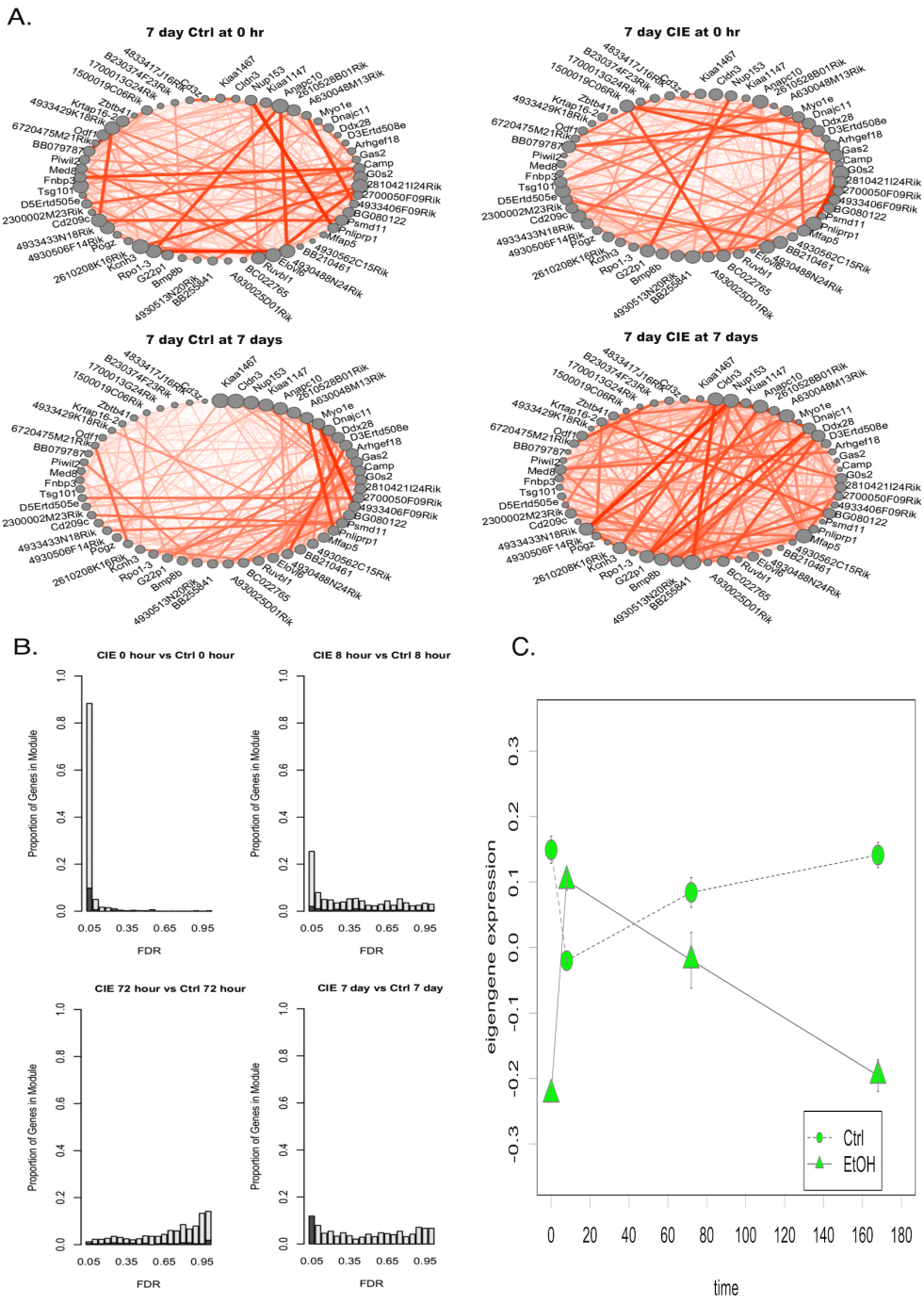

Figure 11: Figure 6: Network level analysis of PFC green module. A) Disruption of co-expression with CIE in genes regulated at 5 days (LIMMA FDR ≤ 0.05). Node size=within module connectivity. Ordered by within module connectivity at 5 days in Ctrl mice. B) Histograms for FDR of genes in PFC Green module at each time point. Dark grey = overlap of genes regulated at 5 days (LIMMA FDR ≤ 0.05). C) Eigengene expression time course for green module genes in control or ethanol (CIE) treated animals.

Two additional modules, lightyellow and yellow, were enriched for genes that showed significant differential expression between CIE and Ctrl at both the 0h and 7d time-points, but not at 8h or 72h (**Figure 7**, **Suppl. Figure S1**). This functional overlap mirrors the overlap between the 0h and 7d time points seen with gene lists by LIMMA analysis (**Figure 6**, **Suppl. Table S2**). Contained in the lightyellow module were genes involved in cell cycle regulation, nerve cell development, and organization of cell projections (**Suppl. Table S6**). The yellow module also included several genes related to cell cycle regulation and vesicular trafficking. The latter group included *Syn2, Syn3, Syt7,* and *Syt11* [270, 273-277]**.** These modules may thus include biological pathways relevant to both immediate and long-term neuroplasticity resulting from CIE exposure, but not the physiological effects of withdrawal, since there was no overlap with genes regulated at the 8h and 72h time points that cover the interval of peak withdrawal [274, 275, 278, 279]. The PFC yellow module also contained a high percentage of genes (70%) with 8 base-pairing motifs for *mmu-let-7c-1-3p*, another *let-7* family microRNA (**Suppl. Table S12**).

A total of 13 modules from PFC were enriched for genes regulated at the peak withdrawal time-points of 8 and 72h post-CIE (**Figure 7**, **Suppl. Table S4**). Only 3 of these modules were enriched for genes significantly regulated both at 8h and 72h. These findings indicate that gene expression functional patterns changed significantly as withdrawal progressed. Those modules enriched for genes regulated at both withdrawal time-points contained genes involved in regulating cell proliferation and cell death (**Suppl. Table S6**). The black module, one of the modules significantly enriched at 8h but not 72h, contained genes involved in stress hormone response and hypothalamic-pituitary-adrenal signaling such as *Sgk1*, *Sgk3*, and *Nfkbia*. These

genes were also regulated by acute ethanol in our prior studies [86, 247]. Three modules, lightgreen, magenta, and tan, were over represented at both the 72h and 7d time-points. The tan and lightgreen modules showed significant overlap (p-value ≤ 0.05) with GO categories related to T-cell mediated immunity (**Suppl. Table S6**), including *Il2, Il4, Igh-6, IGH-VJ558* and *Cebpg*. Regulation of these genes by ethanol has been demonstrated in mice and humans previously [85, 212, 246, 267, 269]. These modules may thus reflect biological processes having longer lasting regulation by withdrawal, or they may represent long-term functional adaptations to chronic ethanol exposure that are only apparent in the absence of ethanol. If the latter is the case, then such immunoregulatory-laden modules could have an important role in long-term behavioral consequences of CIE.

Finally, 8 modules in the PFC were significantly overrepresented for genes differentially regulated only at 7d after the final cycle of CIE (**Figure 7**, **Suppl. Table S4**). All these modules contained genes associated with neurodevelopment or neurotransmitter release (**Suppl. Table S6**). The greenyellow, lightyellow, pink, and red modules also had several gene ontology (GO) hits related to calcium binding, and cytoskeletal organization and control. Similarly, GO hits related to the cell cycle and cell proliferation were identified in the pink, red, tan, and yellow modules. Finally, biological processes related to immune response were identified in the greenyellow and lightgreen modules. The gene co-expression networks identified by WGCNA in PFC and regulated by CIE, therefore appear to represent both the lasting neuroplasticity and neuroinflammatory responses to chronic ethanol exposure.

Nucleus Accumbens

Significant differences in gene expression between CIE and Ctrl mice in NAC were only found immediately after the final cycle of CIE exposure (0h) and during acute withdrawal (8h) (**Table 1**). Seven WGCNA modules were enriched for genes expressed at the 0h time-point (**Figure 7**, **Suppl. Figure S2**). Several of these modules showed overlap with GO categories related to cellular stress response, metabolism, chromatin structure and regulation of gene expression (**Suppl. Table S7**). For example, the salmon module contained genes significantly differentially expressed at 0h in the NAC (**Figure 7**) and was over-represented for functions involved in chromatin structure (**Suppl. Table S7**). Several genes in this general functional group of the salmon module (*Bptf, Mysm1 and Ube2b*) all were previously shown to respond to acute ethanol in mice [86]. The brown module also showed significant expression changes at the 0h time point and had a striking enrichment for genes involved in RNA splicing and processing (**Suppl. Table S7**).

Hippocampus

Hippocampus showed the second greatest amount of differential gene expression between Ctrl and CIE mice. This brain region was also the only one, besides the PFC, to show significant differential gene expression at both 0h and 7d (**Table 1**). Furthermore, the HPC had the largest number of genes showing differential expression at 7d (604) with the vast majority of these residing within the turquoise module (408/604; **Figure 7**). Overall, 27 modules were identified by WGCNA in the HPC, and 5 of these were significantly overrepresented for genes regulated by CIE at 7d (**Figure 7**, **Suppl. Table S4**, **Suppl. Figure S8**). Furthermore, there was a highly significant overlap of genes regulated at 0h or 7d in HPC. The 0h and 7d time points showed 796 and 556 genes, respectively, significantly regulated by CIE at FDR≤ 0.01 (**Figure 7**). These gene

sets showed an overlap of 104 genes ($p \leq 2.2 \times 10\text{-}16$; Fisher's Exact Test), with 89 of these residing in the turquoise module (**Figure 7**, **Suppl. Table S4**).

The turquoise module in HPC was enriched for CIE-regulated genes at both the 0h and 7d time points and contained over 3000 genes, producing a complex bioinformatics analysis. Gene ontology analysis of the entire module showed strong over-representation for several functional groups potentially relevant to long term synaptic plasticity (**Suppl. Table S8**). These included extended groups of genes functioning in chromatin modification (**Figure 12**) such as histone acetylation (including *Baz2a, Brd8, Hdac4, Hdac6, and Myst3*), histone/DNA methylation (*Kdm6b, Kdm5c, Suv38H1, Suv420H1, and Dnmt3a*), chromatin remodeling (*Baz1b, Smarca4, Smarca5, SmarcaL1, SmarcC1, SmarcE1*), and histone/nuclear protein ubiquitination (*Ube2b, Ube2n, Ubn1, Usp16, and Usp22*). Similar results were found on over-representation analysis of only the genes showing CIE regulation ($p \leq 0.05$) at the 7d time point (**Suppl. Table S8**). Network connectivity analysis identified several highly connected hub genes in the HPC turquoise module, as discussed further in the Candidate Gene Identification section below.

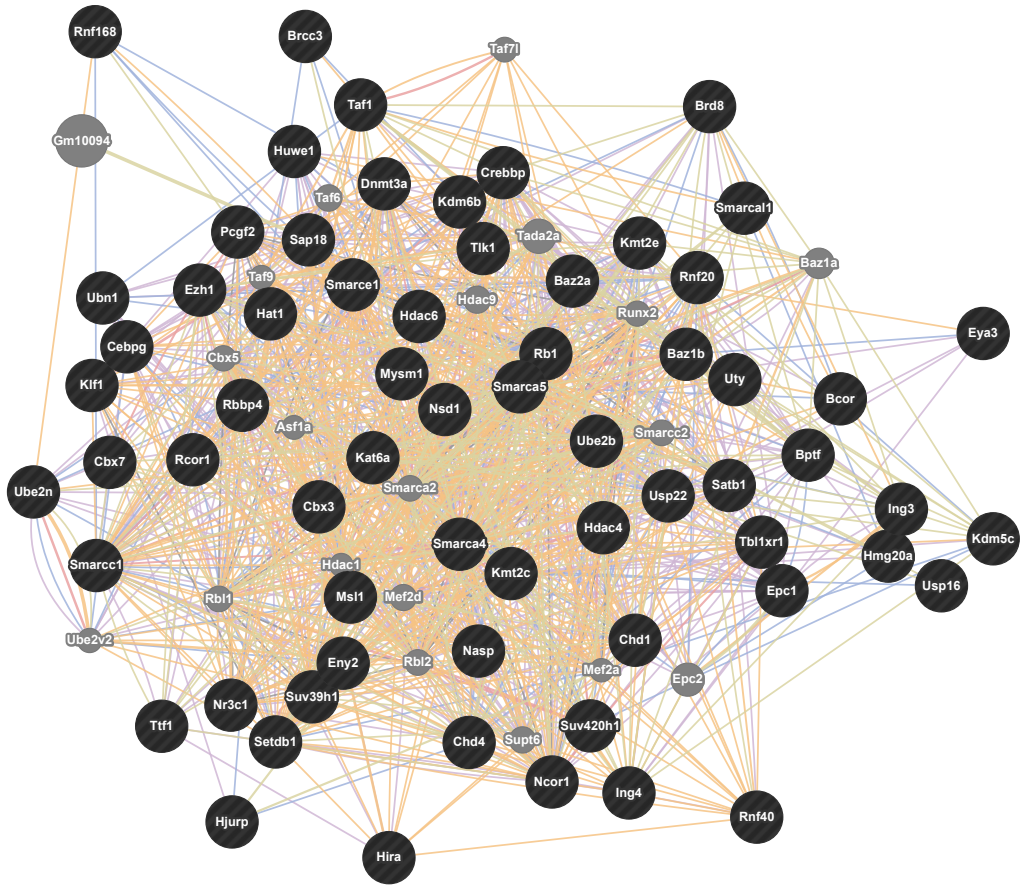

Figure 12: GeneMANIA analysis of genes from HPC turquoise module related to chromatin modification. Chromatin modification genes were identified from Gene Ontology analysis of the HPC turquoise module (Suppl. Table S6) and submitted to the GeneMANIA resource (www.genemania.org) for identification of network interactions using default criteria and databases.

Other HPC modules over-represented for genes regulated by CIE at 7d included the brown module, the only other module containing genes regulated at both 0h and 7d (**Figure 7**). This module contained genes related to immunity and cellular stress responses, including several genes encoding components of the major histocompatibility complex (**Suppl. Table S8**). Three HPC modules, magenta, tan, and yellow, were enriched for genes regulated by CIE at only the 7d time-point. The magenta module contained genes functioning in neurodevelopment, neuroplasticity, and synaptic transmission. These include *Vegfc, Notch1, Ppap2b, Scg2*, and

several *Sox* family genes [276-284]**.** The yellow module also included genes known to be involved synaptic transmission such as glutamate receptors (*Gria1, Grik2*) and the D1 dopamine receptor gene (**Suppl. Table S4** and **Suppl. Table S8**) [190, 281-287].

Of the HPC modules significantly overlapping with genes regulated by CIE only at 0h or 8h, most represented Gene Ontology hits seen in other brain regions such as immunity, cellular stress response, RNA splicing, transcription, and cell proliferation (**Suppl. Table S8**). Of note, preliminary genomic analysis of CIE responses in hippocampus showed very prominent expression changes during acute withdrawal (8h) that included over-representation of genes involved in RNA splicing [208].

Bed Nucleus of the Stria Terminalis

The BNST was the only brain region other than PFC that showed significant gene regulation at 72h post-CIE (**Figure 7**, **Suppl. Figure S9**). Three modules were significantly overrepresented for genes regulated at only the 72h time-point. Two of these modules, tan and lightgreen, contained several genes related to neurodevelopment, and synaptic transmission. These included *Ndrg1*, a myelin-related gene identified as an acute ethanol-responsive gene in our prior studies [86, 247, 288], (**Suppl. Tables S4** and **S9**).

The third 72h module, darkturquoise, contained genes related to the *Ras* GTPase intracellular signaling cascade. An additional 6 modules in the BNST (black, brown, green, midnightblue, pink, and yellow) were overrepresented for genes regulated by CIE at 0h, 8h, or both times (**Figure 7**, **Suppl. Figure S9**). Functionally, these modules contained genes overlapping with

GO categories related to immune response, chromatin organization, transcription regulation, cell cycle control, and development (**Suppl. Table S9**).

Central Nucleus of the Amygdala

The CeA showed the least amount of differential expression between CIE and Ctrl mice at all time-points (**Table 1**) and, subsequently, fewer modules were identified by WGCNA than in the other brain regions (**Figure 7**, **Suppl. Table S4**). The CeA magenta and salmon modules were significantly enriched for genes expressed at both 0h and 8h post-CIE (**Figure 7**, **Suppl. Figure S10**). Bioinformatics analyses revealed that the magenta module contained genes related to immune response, particularly those encoding components of the major histocompatibility complex (**Suppl. Table S10**). Analysis of the salmon module identified several GO hits related to cell proliferation through negative regulation of programmed cell death. NF-κB was also identified as binding partner to multiple genes within the salmon module (**Suppl. Table S10**). Thus, NF-κB represents a possible target for network modulation in the CeA.

The CeA yellow module was overrepresented for genes regulated at the 0h time point only. This module contained multiple genes related to neurodevelopment and synaptic transmission. Individually, only *Kif1b* was significantly regulated by CIE treatment in the CeA, but multiple other yellow module genes (including *Myo5a, Als2, Dlgap1, Egr3, Agtpbp1, Stx4a, Mecp2, Mylk2, Cacnb2, Lin7a, Psen1, Gria2, Trim9, Ssyn2, Chrna7, Ppp3ca, Bdnf, Grm5, Dlg4, Ncs1, Adra1a,* and *Lgi1*) were contained in 4 Gene Ontology categories related to synaptic transmission (**Suppl. Table S10**)**.**

Two modules, pink and tan, were overrepresented for genes regulated by CIE only at the 8h time point, a time of peak withdrawal. The tan module was enriched with genes related to cellular stress response, many of which have been previously been associated with ethanol response in mice and humans (*Hsp5a, Cebpb, Dnajb9, Herpud1, Hes5, Creld2)* [86, 209, 212, 246, 267]. Analysis of the pink module also identified biological pathways representing cellular stress response, and included several genes previously identified as ethanol-responsive in brain, such as *Tsc22d3, Arrdc2, Htra1, Gclm,* and *Mt1* [86, 209, 246, 267] (**Suppl. Tables S4** and **Suppl. Tables S10**).

Candidate Gene Identification

To identify candidate genes for future study as major regulators of CIE-associated increased ethanol consumption, we focused attention on PFC and HPC where CIE-responsive genes (FDR≤0.05) were identified at 7d after removal from the vapor chambers. Furthermore, we identified hub genes having the highest scaled intramodular connectivity (kIM) (**Tables 3** and **4**), to focus on potential major regulators of network function [289].

Table 3: Top 30 Most Highly Connected Genes PFC. Top 30 most highly connected genes significantly differentially expressed at 7 days (LIMMA FDR ≤ 0.01) in the prefrontal cortex. Scaled module connectivity = within module connectivity/maximum number of connections possible as determined by WGNCA.

ProbesetID	Gene Symbol	Within Module Connectivity	FDR CIE 7 days vs. Air 7 days
1439113_at	2410018L13Rik	1	0.002992
1460202_at	Myoz1	1	0.003258
1455946_x_at	Tmsb10	1	0.007169
1422988_at	Sgsh	1	0.009857
1436556_at	A930027H06Rik	1	0.010611
1417711_at	0610012D09Rik	1	0.019986
1418694_at	Kcmf1	1	0.033193
1433996_at	Suv39h2	1	0.033521
1425943_at	Nmur2	1	0.042005
1432306_at	Rapgef5	0.985487792	0.013411
1428006_at	Scfd1	0.978661198	0.043765
1432615_at	Wdr37	0.975757558	0.00092
1421837_at	Rps18	0.971410445	0.000305
1430764_at	1700023F06Rik	0.93092978	0.014083
1431466_at	4930553D19Rik	0.918138893	0.002845
1446239_at	4921522A10Rik	0.907947577	0.001026
1416893_at	Fam107b	0.897669051	0.033433
1422166_at	Clec2i	0.895384084	0.004557
1454088_at	5330411O13Rik	0.89304966	0.000504
1443872_at	March2	0.891815155	0.033597
1445578_at	Elovl6	0.887035261	0.005246
1459149_at	Zfp809	0.880999634	0.012917
1416154_at	Srp54	0.872907354	0.011815
1459941_at	4933402J24Rik	0.870728481	0.016754
1447850_x_at	Tex27	0.866050347	0.001139
1432346_a_at	Cdh23	0.862870513	0.033619
1423618_at	Bin1	0.856808229	0.004701
1441289_at	C1orf54	0.842362396	4.30E-05
1445973_at	C79461	0.838505315	0.000829
1431332_a_at	Terf1	0.83327272	0.038797

Table 4: Top 30 Most Highly Connected Genes HPC. Top 30 most highly connected genes significantly differentially expressed at 7 days (LIMMA FDR ≤ 0.01) in the hippocampus. Scaled module connectivity = within module connectivity/maximum number of connections possible as determined by WGNCA.

ProbesetID	Gene Symbol	Within Module Connectivity	FDR CIE 7 days vs. Air 7 days
1428941_at	Zmym2	1	0.027277
1423065_at	Dnmt3a	1	0.007277
1448940_at	Trim21	1	0.046253
1426964_at	3110003A17Rik	1	0.034399
1416897_at	Parp9	0.991065128	0.005768
1429537_at	Srrp130	0.974022419	0.030291
1420909_at	Vegfa	0.968485508	0.044605
1451941_a_at	Fcgr2b	0.96833963	0.003962
1447903_x_at	Ap1s2	0.967369115	0.026812
1436343_at	Chd4	0.965709803	0.013961
1439300_at	Chic1	0.962065891	0.019558
1445499_at	Zc3h13	0.961427474	0.0158
1460426_at	9430063L05Rik	0.957494576	0.018324
1456316_a_at	Acbd3	0.956078895	0.007682
1438069_a_at	Rbm5	0.954792407	0.018425
1437638_at	Srrm2	0.949510043	0.003749
1440375_at	5730419I09Rik	0.949349871	0.016499
1456110_at	3010027A04Rik	0.947378212	0.018324
1430599_at	Myt1l	0.942990128	0.006486
1434055_at	Galnt9	0.942494306	0.038438
1435477_s_at	Fcgr2b	0.942120391	0.003962
1420402_at	Atp2b2	0.936601271	0.027895
1438929_at	Actr1a	0.934610301	0.009362
1423184_at	Itsn2	0.934589282	0.009606
1451564_at	Parp14	0.934530093	0.041199
1456262_at	Rbm5	0.934320516	0.023106
1427401_at	Chrna5	0.933413798	0.004894
1458147_at	Mamdc1	0.93278567	0.019733
1438476_a_at	Chd4	0.926274574	0.004894
1434020_at	Pdap1	0.924460754	0.010438

Genes regulated by CIE in PFC at 7d and within the top 30 highest kIM scores, included *Myoz1* and *Sgsh* (**Figure 13**), with the former only becoming significantly different from Ctrl at the 72h and 7d time points. This strongly supports a possible role for *Myoz1* in longer term adaptations resulting from CIE. Previous studies from this laboratory have shown *Myoz1* expression

correlates with individual variation in ethanol consumption in C57BL/6 mice [142]. *Myoz1* is most highly expressed in skeletal muscle but brain microarray databases suggest widespread lower expression in brain (www.genenetwork.org). The protein associates with the actin cytoskeleton and may play a role in determining cell shape [290]. *Sgsh* has also been correlated with ethanol behaviors in previous studies [209, 291] and found to have altered expression in alcoholic brain postmortem tissue [212, 246, 267, 288]**.** *Sgsh* is involved in glycosaminoglycan degradation and mutations in the gene cause mucopolysaccharidosis IIIa. As two of the most highly connected genes within their respective modules, *Myoz1* and *Sgsh* may represent important regulatory proteins within a biological pathway induced by chronic ethanol exposure.

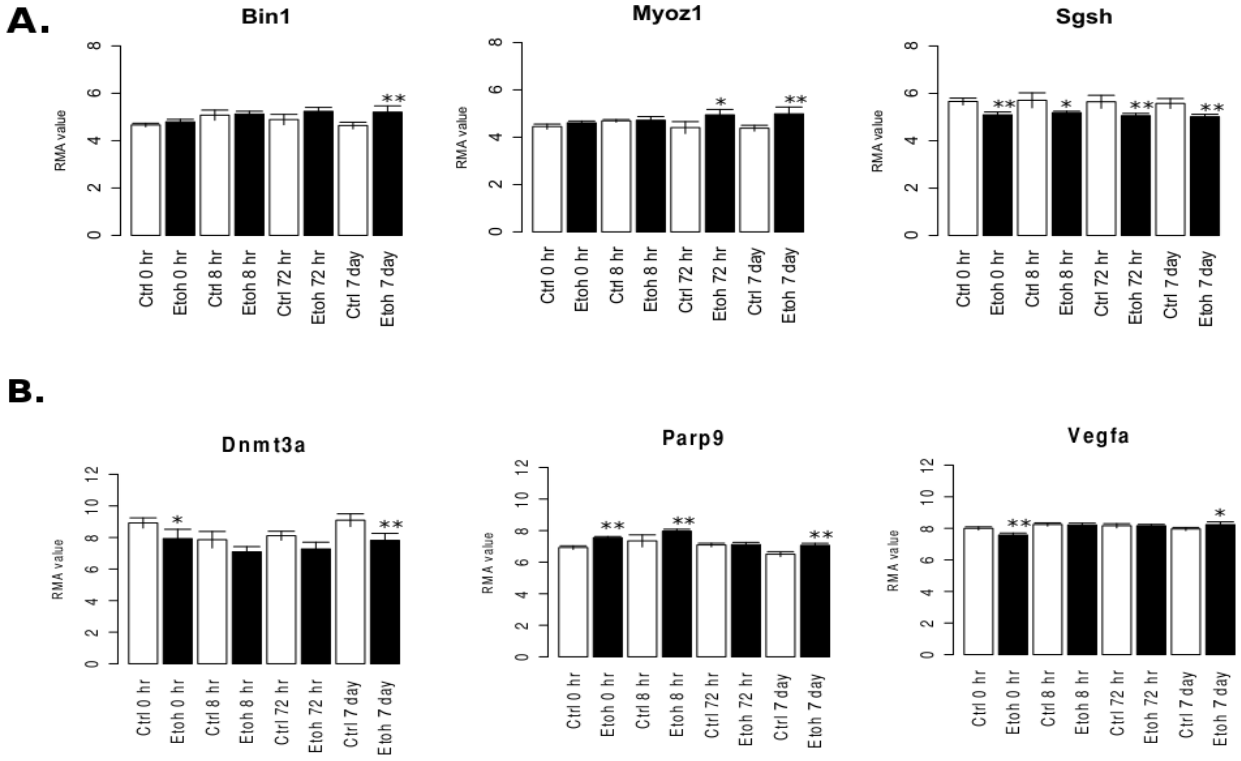

Figure 13: Expression patterns for representative candidate genes. A) Average RMA value (log2 scaled) expression of candidate genes at each time-point and treatment condition in the PFC cortex. (* = LIMMA FDR ≤ 0.05, ** = LIMMA FDR ≤ 0.01) B) Average RMA value (log2 scaled) expression of candidate genes at each time-point and treatment condition in the HPC. (* = LIMMA FDR ≤ 0.05, ** = LIMMA FDR ≤ 0.01).

In the HPC, 1352 of the 10,072 probesets used for WGCNA were regulated by CIE (FDR≤ 0.05) at 7d. Interestingly, 60% (19/30) of the top 30 most highly connected genes in the HPC were within the turquoise module, even when within-module connectivity was scaled by the number of total genes in the module. The highly connected genes in the turquoise module represent a variety of biological functions from DNA processing to vesicle trafficking (**Table 4**, and **Suppl. Table S8**). Among the most highly connected genes in any HPC module were *Vegfa, Parp9*, and *Dnmt3a* (**Table 4**, **Figure 13**). All these genes have previously been associated with ethanol responses in the literature [208, 291, 292]. Perhaps most strikingly regarding the highly interconnected turquoise module was the large subgroup of genes involved in chromatin modification (**Suppl. Table S8**). **Figure 12** illustrates an external validation of this subnetwork, where the chromatin modification-related genes of the turquoise module were analyzed using the GeneMania bioinformatics tool (www.genemania.org) to illustrate connectivity between these genes using external data sources.

Discussion

The investigation described in this manuscript employed a network-centric approach to identify brain region and time specific gene expression regulation by multiple cycles of chronic intermittent ethanol vapor exposure [81, 239, 251, 293]. Prior genomic studies have been conducted using similar vapor exposure models in mice and rats [208, 294]. This study represents a detailed network analysis of the time dependent effects on gene expression with this behavioral model. Network analysis with WGCNA revealed modules of co-expressed genes regulated by CIE that showed robust time and brain-region specific expression patterns, with PFC and HPC showing the most persistent, and largest number of gene expression changes. Functionally, chronic intermittent ethanol exposure and withdrawal caused time- and region-

specific gene expression changes reflecting neuroplasticity, neuroimmunity, and neuroendocrine signaling responses to chronic ethanol. This analysis also suggests that possible mechanisms underlying persistent expression changes following chronic ethanol exposure may involve regulation by miRNAs and chromatin remodeling. Finally, overlap between results from this study and previous experiments exploring gene expression response to acute ethanol indicates that the hypothesis that acute ethanol paradigms are relevant to the brain's biological response to long-term ethanol exposure is only applicable to a small number of genes [230]. All together, these results demonstrate that systems genetic analysis of genomic expression data is an effective means of teasing out the complex molecular and biological responses to chronic ethanol exposure.

The prefrontal cortex and hippocampus, however, were most affected by chronic ethanol, both in terms of number of differentially expressed genes at all 4 time-points, and as indicated by sustained gene expression changes at 7d post-CIE (**Table 1** and **Suppl. Tables S1**). Indeed, it was somewhat surprising that areas such as the BNST, CeA and particularly NAC did not show persistent changes induced by CIE. These regions did show strong responses at 0-8h after removal from the vapor chambers, particularly in regard to stress/inflammation-related functions, and it is certainly possible that these mRNA expression changes evoked long-lasting translational or post-translational alterations that were relevant to long-lasting behaviors, but this hypothesis will require additional study at the protein, structural or functional level. Additionally, the long-term gene expression response in PFC and HPC, and lack of such in other brain-regions, may have implications for system level signaling in the brain. The NAC receives glutamatergic feedback from the PFC and HPC [190]. At 7 days post-CIE gene expression differences are seen

in the PFC and HPC, but not the NAC, indicating that long-term ethanol induced activity in the PFC does not alter activity in the NAC, or any other regions of the extended amygdala such as the CeA or BNST. These results may, in fact, indicate that long-term gene expression changes in the PFC and HPC in response to chronic ethanol do not change gene expression in other brain-regions basally. One might hypothesize, however, that basal changes in gene expression induced by CIE could affect ethanol response in these other brain-regions. This effect may not be seen in the gene expression data presented in this chapter, because, with the exception of the 0 hour group, mice are not exposed to ethanol at the time of sacrifice. A future study in which mice are exposed to repeated cycles of CIE by vapor chamber, withdrawn from ethanol for 7 days, and then re-exposed and sacrificed for gene expression studies while they still have ethanol on board may be performed at a later date to investigate this hypothesis.

The findings presented in this study strongly implicate prefrontal cortex and hippocampus as brain regions most strongly influenced in terms of genomic regulation by CIE exposure, both at immediate time-points (0h) and after long-term abstinence (7d). The long-term changes in gene expression (**Table 1**, **Suppl. Table S1**) were of most interest because these possibly underlie behavioral responses to repeated chronic intermittent ethanol exposure, such as escalation of voluntary consumption observed in previous studies [81, 239]. Chronic heavy, and even moderate, ethanol intake has been shown to impair memory and hippocampal neurogenesis in humans and rodents [85, 293, 295, 296]. The hippocampus has also been implicated in withdrawal seizures, though there are mixed findings about the relationship between hippocampal atrophy with chronic heavy drinking, and onset and severity of withdrawal seizures [296-302]. Gene expression changes in the prefrontal cortex in response to both acute and

chronic ethanol exposure have been demonstrated in mice and humans [86, 209, 212, 230, 247]. The prefrontal cortex's involvement in impulse control is hypothesized to underlie ethanol seeking behaviors, increased consumption, and lack of control over intake associated with alcohol use disorders [85, 303, 304].

In contrast to the long lasting changes noted for PFC and HPC gene expression, chronic ethanol exposure and acute withdrawal, represented by tissue collected at 0-72h, affected all brain regions studied (**Figures 6-7**, **Table 1**). The greatest amount of overlap in differential gene expression, across all brain regions, also occurred at 0 and 8h (**Figure 6**). This pattern of differential gene expression reflects the activation of the mesocorticolimbic system and extended amygdala by ethanol exposure, and ethanol withdrawal [86, 187]. Functional over-representation studies showed, across all brain regions, an over-representation of genes involved in development, cell stress, programmed cell death, and immune responses at the 0h time point (**Suppl. Tables S6-S10**).

As discussed in the Results section, the BNST tan module was enriched for genes differentially regulated between CIE and control mice at 72 hours, and within this module there were genes related to neurodevelopment such as *Ndrg1*. This laboratory has previously showed that *Ndrg1* is regulated by acute ethanol in the prefrontal cortex [86, 288]. In 2013, Farris and Miles [288] published data indicating that *Ndrg1* is co-expressed with a group of myelin genes in the PFC. Recent work at this laboratory has also demonstrated that *Ndrg1* is expressed both in neurons and oligodendrocytes (Park and Miles, publication pending), and cell type enrichment analysis showed that the tan module in the BNST is enriched both for genes expressed in neurons and

those expressed in oligodendrocytes (**Suppl. Table S9**). The data presented in this manuscript indicates that *Ndrg1* is also regulated in the BNST during protracted withdrawal (**Suppl. Table S4**). Together with other genes significantly regulated by CIE in the BNST tan module such as *Kif2a, Dgkg, Syn2, Ppfia2, Grim8, Cpne7, Pnoc, Prkacb* [305], this leads to the hypothesis that CIE driven *Ndrg1* regulation occurs primarily through neurons in the BNST. This hypothesis represented an area of future study that may lead to a greater understanding of the effect of chronic ethanol on the bed nucleus of the stria terminalis, and the role of *Ndrg1* in specific brain regions.

In the CeA, the yellow module contained several genes related to synaptic transmission. However, only one was significantly regulated by CIE (**Suppl. Tables S4,** and **S10**). That these genes are organized into the same module in the CeA indicates correlated mRNA expression, and that their gene products may interact at the molecular levels with gene products of those genes within the module significantly regulated by CIE. Therefore, at the post-translational level, regulation of the expression of a just few genes by chronic ethanol may influence the cellular activity of synaptic transmission within the CeA. *Kif1b* in in particular is a good candidate for influencing post-translational expression of other genes within the CeA yellow module because it is a kinesin family molecular motor involved in the transport of modules from the cell body to axons and dendrites [306]. Further study, is of course, needed to determine at the cellular level how *Kif1b* regulation by CIE influences the gene products of other module genes at the molecular level.

Previous studies at VCU have also shown that activation of the hypothalamic-pituitary-adrenal (HPA) axis with ethanol sensitization leads to regulation of gene expression in the prefrontal cortex [307]. Those NF-κB genes present in the CeA salmon module raise the possibility that ethanol mediated changes in HPA activity may also influence gene expression in the central amygdala through this pathway. Future studies may, therefore, focus on testing the hypothesis that CIE by vapor chamber influences the HPA axis which, through NF-κB signaling, alters gene expression in the central amygdala.

Another CeA module, magenta, showed striking over-representation for genes related to MHC class 1 antigen responses with an over 2-fold up-regulation of H2-K1 and H2-L at 0h (**Suppl. Tables S4** and **S10**). The HPC brown module showed similar results (**Suppl. Table S10**). While many of these responses resolved as withdrawal proceeded to 72h and 7d, both HPC and PFC showed persistent regulation of genes relating to immune responses at 7d. The strong presence of immune response genes across time points and brain regions in this study on CIE is consistent with observations from expression profiling of human autopsy brain material from alcoholics and subsequently validated in animal models [308]. Additionally, multiple recent studies have reported that intermittent ethanol exposure in adolescent animals can induce persistent changes in ethanol behaviors, including in adulthood, and that neuroinflammatory responses are a critical aspect of these responses to ethanol [52, 307]. Together, these studies have suggested that ethanol-evoked activation of brain inflammatory responses may not just be a toxic response to ethanol, but could also play an important role in neuroadaptations leading to compulsive consumption. Neuroimmune responses have previously been implicated in other forms of experience-induced or developmental plasticity [52].

It was assumed, based on previous studies, that CIE would regulate networks of genes related to synaptic function, plasticity or development as part of the molecular events leading to progressive ethanol consumption following CIE. Indeed, gene modules over-represented with such functional groups were detected and showed regulation by CIE particularly at early time points (**Suppl. Tables S6-S10**). The PFC salmon module was significantly enriched for immediate early genes at the 0h time-point and several gene ontology hits related to neurodevelopment (**Suppl. Table S6**). *Notch1, Sox2,* and *Bmpr1a* are among the genes in the PFC salmon module with known roles in neurodevelopment. In particular, these genes have been shown to be important for the process of adult neurogenesis [281, 309-312]. Neurogenesis continues to occur into adulthood in the lateral ventricles and the dentate gyrus of the hippocampus [313-315]. Studies examining adult neurogenesis occurring in other areas of the brain, including the medial prefrontal cortex (mPFC), have had mixed results [315, 316]; but it has been shown that chronic stress and chronic alcohol exposure lead to observable structural and functional changes in the PFC [317-322]. The PFC salmon module in this data set, therefore, may represent the effect of CIE on neurogenesis in the PFC of adult mice.

The PFC green module also contained genes related to neuroplasticity, notably *Bdnf*. *Bdnf* has previously been studied as a potential candidate gene for the genesis of alcohol use disorders. Previous studies have shown that *Bdnf* regulates neurodevelopment [323]**,** synaptic plasticity [324], and is regulated by several drugs of addiction including ethanol [86, 247, 325-328]. In looking more closely at the time-course of *Bdnf* expression in the PFC after CIE, *Bdnf* was significantly down regulated with CIE at 0h, in agreement with several prior studies on either

CIE or intermittent oral ethanol consumption [208, 272, 273]. However, between 8h and 72h, *Bdnf* mRNA levels returned to control levels such that at 7 days, *Bdnf* gene expression was not significantly different between CIE and Ctrl mice (**Figure 9**, **Suppl. Table S1**). This does not exclude the possibility that changes in BDNF protein might persist for more prolonged withdrawal periods. Additionally, we found that a subgroup of genes in the PFC green module (not containing *Bdnf*) did show altered expression at both 0h and 7d post-CIE (**Figure 11**). This subgroup of PFC green module genes also showed network level increases in connectivity at 7d post-CIE (**Figure 11**). This may be further evidence for the role of a *Bdnf*-related gene network in the long-term neuroadaptive events leading to increased ethanol consumption following CIE exposure.

Studies by two separate laboratories using the vapor chamber CIE model in rats [273] or the intermittent ethanol consumption model in B6 mice [272], recently showed that chronic intermittent ethanol down-regulates mPFC *Bdnf* expression via increasing expression of select microRNA species, with resultant increases in ethanol consumption. Using a 7-week ethanol vapor exposure model, Tapocek et al. showed that reduced *Bdnf* expression in mPFC was accompanied by region-selective persistent increases in expression of *miR-206* and that viral vector over-expression of *miR-206* could, in itself, decrease mPFC *Bdnf*, with subsequent increases in ethanol consumption [273]. Darcq et al. showed similar results in a mouse chronic intermittent binge ethanol model, including transient upregulation of *miR-1*. The *miR-1* miRNA family includes *miR-206*. However, Darcq et al. also found involvement of *miR-30a-5p*, including that inhibition of miR-30a-5p action could reverse the increased consumption caused by intermittent ethanol access [272]. In our own analysis of miRNA binding site over-

representation among genes of the PFC green module, binding sites for both *miR-30a* (p=0.003) and *mmu-miR-1a/mmu-miR-206* (p= 0.04) showed nominally significant potential binding motifs among genes in the PFC green module using MiRvestigator Framework (**Suppl. Table S12**) suggesting that these miRNA families may be involved in regulation of green module genes beyond *Bdnf* alone. Future direct studies will be needed to confirm these findings.

Additionally, our studies suggested that the PFC green module was over-represented with binding sites for the *let-7c-1* group of miRNA, with 6 base motifs for *let-7c-1* being found in over 90% of the green module genes (p< 0.00024; **Figure 9**). MiRvestigator Framework web-software also revealed that 12 differentially regulated modules in the PFC and HPC were enriched for potential *let-7* family target genes (**Figure 9**, **Suppl. Tables S12** and **S13)**. qRT-PCR experiments confirm *let-7c-1* expression in the mouse PFC, and show that expression of this miRNA is significantly downregulated by CIE in male B6 mice **(Figure 10)**. *Let-7* was one of the earliest microRNA's discovered, and is highly conserved in function across species [329]. In the brain, in addition to being a key regulator of cell differentiation in early development, previous studies have shown that *let-7* expression is regulated by several types of neurodegenerative processes, from prion disease to ischemic brain injury [330-333]. CIE exposure may, therefore, increase long-term consumption through a miRNA-dependent regulation of the green module genes, including a role for the *let-7* miRNA family, which could impact CIE regulation of other modules as well. This hypothesis complements the prior direct work on *Bdnf* and suggests that mechanisms underlying regulation of the green module by chronic ethanol could be a novel target for future therapeutic approaches in treatment of alcohol use disorders. Confirmation that *let-7c-1* regulates genes of the PFC green module *in vitro* and *in*

vivo, and investigation of the behavioral and gene expression effect of modulating *let-7c-1* expression *in vivo* in the PFC by stereotactic delivery of plasmids to either knockdown or overexpress the miRNA represent an area of potential future studies based on the findings of this network analysis.

Long-term gene expression and behavioral changes resulting from CIE exposure require a mechanism for persistence in the absence of further ethanol vapor exposure. Epigenetic mechanisms have lately been implicated as a causal factor for long-term functional and behavioral changes evoked by ethanol and other drugs of abuse [334, 335]. It is certainly possible that synaptic reorganization caused, for example, by miRNA-driven alterations in *Bdnf* expression, could subsequently produce persistent changes in synaptic function and behaviors. Our time course analysis of expression changes following CIE provided strong preliminary evidence for additional epigenetic mechanisms possibly influencing persistent changes in ethanol consumption following CIE exposure. The striking over-representation for chromatin modification in hippocampal turquoise module genes regulated by ethanol, suggests a mechanism for long-lasting shifts in transcriptional adaptations to CIE in hippocampus. Our candidate gene analysis for hub genes further emphasized the potential importance of these chromatin modification genes in CIE-associated expression network structure (**Figure 13**, **Table 4**). Ongoing studies in our laboratories seek to identify such epigenetic signatures amongst hippocampal networks showing long-lasting expression changes following CIE.

Finally, the small degree of overlap with acute ethanol expression (**Suppl. Table S3**) demonstrates that the principle of initial response to ethanol as a predictor of future behavior

applies to gene expression response only for specific genes [335]. This finding has major implications for the alcohol research field because it indicates that genomic studies of animals exposed to acute ethanol are effective for the identification for some genes regulated with chronic ethanol exposure and, thus, may be useful for the identification of new therapeutic targets in the treatment of alcohol use disorders. However, comparison between chronic and acute ethanol exposure is important to determine whether targetable genes identified through acute ethanol studies also show long-term regulation by ethanol exposure.

In conclusion, differential gene expression and scale-free network analysis has revealed region-specific correlated changes in gene expression with chronic intermittent ethanol exposure in the mesolimbocortical dopamine and extended amygdala pathways. Bioinformatics investigation has shown some conservation of functional groups, both across brain regions and time points, among the differentially regulated networks. In general, neuroinflammatory responses were seen across multiple brain regions at early time points, while genes involved in development, neuroplasticity, and chromatin remodeling were found to be over-represented at 3-7d post ethanol vapor. Notably, PFC and HPC were the only regions of the five surveyed that showed expression changes at 7d after removal from the vapor chamber model of chronic ethanol exposure. Since animals offered oral ethanol intake at that time will show increased consumption, these PFC and HPC networks may have a significant mechanistic role in the neuroplasticity underlying progressive ethanol consumption. The Bdnf-containing green network from PFC is a major target for future confirmatory studies since other investigators have previously implicated a miRNA-directed regulation of *Bdnf* consequent to chronic ethanol exposure in the mechanisms of progressive ethanol consumption. Importantly, however, our studies suggest that members of

the green network other than *Bdnf* may also be involved in the long-lasting molecular mechanisms underlying increased ethanol consumption. Finally, our discovery of a striking subgroup of genes involved in chromatin modification having altered expression in HPC at 7d post ethanol vapor suggest future studies on chromatin structure as an important regulatory event contributing to long-term abusive ethanol consumption patterns as seen in alcoholism. Taken together, these findings provide novel and significant insight to the molecular neurobiology contributing to abusive alcohol consumption, and could thus eventually lead to development of new therapeutic strategies for AUD.

Chapter 4: Network Analysis of C57BL/6J Mice Under CIE with and without Intermittent Drinking

Introduction

One of the most well known symptoms of alcohol use disorder (AUD) is a steady upward trend in the amount of alcohol consumed over time [244]. This progressive increase in consumption has been attributed to the neurobiological adaptations brought on by repeated cycles of high-dose ethanol exposure and ethanol withdrawal [336]. Previous studies of physiological and structural changes in the brain after chronic alcohol exposure have lead to the hypothesis that changes in gene expression are a major molecular mechanism leading to physiological and behavioral changes observed with and leading to AUD [86, 194, 195, 207, 211]**.**

Technologies such as microarrays have allowed for the study of the genome-wide effects of ethanol exposure on mRNA expression [86], and scale-free network analysis provides a means to organize transcriptome data into networks of co-expressed genes representing functional pathways [80, 212, 230, 246, 249]. Further, gene-phenotype correlations allow for the identification of both individual genes and gene networks associated with ethanol consumption. Using these approaches it may be possible to decipher which molecular effects play the most important role in increased drinking seen with chronic ethanol exposure, and to pinpoint candidate genes whose expression correlates with consumption; thus identifying new therapeutic targets for the treatment of AUD.

Recent experimental studies provide substantial evidence for the use of animal models in the discovery of therapeutic targets for the treatment of AUD [187, 273, 288, 337]. Chronic

intermittent ethanol vapor is one such model of long-term intoxicating ethanol exposure. As a part of this paradigm, mice experience repeated cycles of high ethanol exposure followed by withdrawal similar to behavioral patterns seen in alcoholics [237]. The CIE by vapor chamber model has been shown to cause neurochemical and structural changes at the synapse, and, when combined with intermittent 2-bottle choice drinking, leads to significant increases in ethanol consumption [81, 254]. Previous studies of gene expression with CIE in C57BL/6J mice have focused on differential gene expression during early withdrawal [208], or on RNA networks during ethanol exposure and withdrawal associated with cell type-specific gene expression [243]. This study explores the relationship between high-dose ethanol vapor exposure, intermittent drinking, and withdrawal in an attempt to identify mechanisms by which this model leads to progressive increases in ethanol intake.

This chapter includes a detailed analysis of the gene expression changes caused by CIE exposure with or without intermittent oral ethanol consumption, across multiple brain-regions, using Weighted Gene Correlated Network Analysis (WGCNA) [218]. The brain-regions studied have been associated in numerous studies with the development of AUD [67, 187, 190]. We show through these analyses that the gene expression changes elicited by repeated cycles of CIE by vapor chamber, withdrawal, and drinking correlate with increased ethanol consumption. We also show that some of the most strongly correlated genes are those related to synaptic transmission and synaptic plasticity. This study thus supports the hypothesis that changes in gene expression in the brain underlie the behavioral features of AUD via physiological and functional changes at the neuronal synapse.

Materials and Methods

Animals

Adult male C57BL/6J mice were purchased from Jackson Laboratories (Bar Harbor, ME, USA) at 10 weeks of age. Mice were kept under a 12-hour light/dark cycle and given free access to water and standard rodent chow (Harland, Teklad, Madison, WI). Mice were kept on corncob bedding (#7092a and #7902.25 Harland, Teklad, Madison, WI). All studies were conducted in an AALAC-accredited animal facility, and approved by the Institutional Animal Care and Use Committee at Medical University of South Carolina (MUSC). All experimental and animal care procedures met guidelines outlined in the NIH Guide for the Care and Use of Laboratory Animals.

Chronic Intermittent Ethanol (CIE)

Mice were divided into 4 groups: the CIE-Drinking group received inhaled ethanol in the vapor chambers followed by 2-bottle choice drinking, the Air-Drinking group received only air in the vapor chambers and 2-bottle choice drinking, the CIE-NonDrinking group received inhaled ethanol in the vapor chambers but did not drink in between CIE cycles, and the Air-NonDrinking group remained ethanol naïve both in and out of the inhalation chambers. Following a 2-week acclimation period, mice in the CIE-Drinking and Air-Drinking groups underwent 6-weeks of 2-bottle choice drinking to establish baseline drinking levels. Mice were given access to 15% v/v ethanol for 2 hours per day. Ethanol and water intake for each individual mouse was measured daily. Following 6-weeks of baseline drinking, mice were placed in Plexiglass inhalation chambers (60x36x60 cm) 16 hours/day for 4 days. Ethanol was volatilized with an air stone submerged in 95% ethanol. Chamber ethanol concentrations were monitored daily and air flow was adjusted to ethanol concentrations within 10-13 mg/L air. This ethanol vapor concentration has been shown to yield stable blood ethanol concentrations (175-225 mg/dL) in C57BL/6J mice

[234]. Before each vapor chamber session, intoxication was initiated in the CIE group by administration of 1.6 g/kg ethanol and 1 mmol/kg pyrazole intraperitoneally (i.p.) at a volume of 0.02 ml/g body weight. Pyrazole is an alcohol dehydrogenase inhibitor used to stabilize blood ethanol concentrations. All mice received the same number and timing of pyrazole injections prior to final removal from the inhalation chambers with control mice receiving saline and pyrazole (i.p.), also at a volume of 0.02 ml/g body weight, prior to being placed into control vapor chambers. Control vapor chambers delivered only air, no ethanol vapor. After 4 days in the inhalation chambers, mice underwent a 72-hour period of total abstinence from ethanol. Following the abstinence period, mice in the CIE-Drinking and Air-Drinking groups were given 2-bottle choice drinking for 2 hours per day for 5 days. A total of 4 cycles of CIE-abstinence-drinking were performed. After the end of the 4th cycle mice were sacrificed on the 5th drinking day at the time they received ethanol access on all previous drinking days (**Figure 14**).

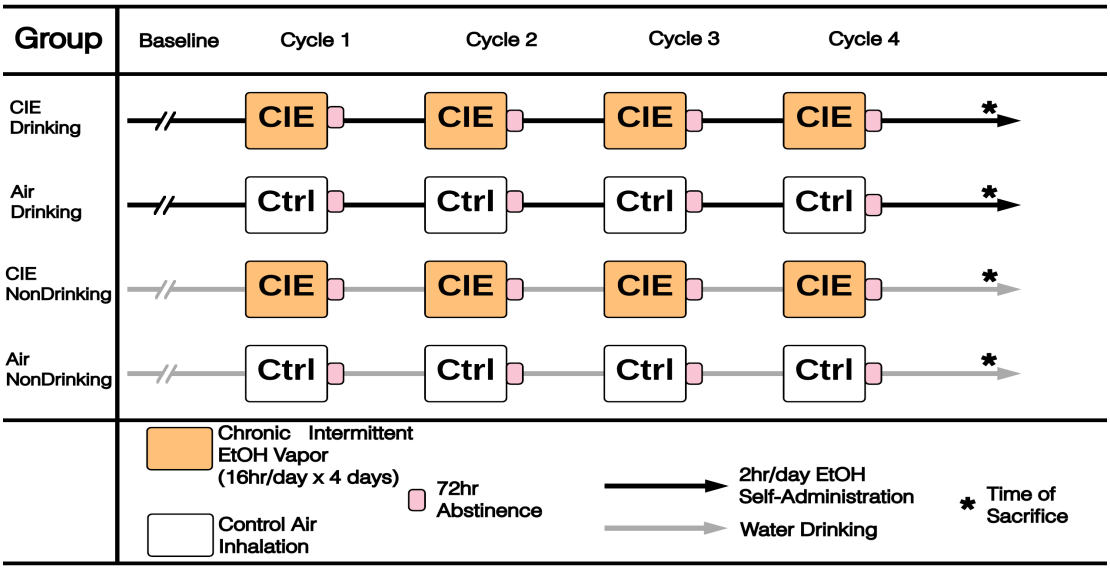

Figure 14: Overview of C57BL/6J CIE by vapor chamber with and without intermittent 2-bottle choice drinking.

Tissue Harvesting, RNA Isolation, and Microarray Hybridization

Mice were sacrificed by decapitation, brains were immediately removed from the skull, and brain-regions dissected as previously described [208]. Tissues were stored at -80°C until RNA isolation. Total RNA was extracted using the RNeasy Mini Kit (Qiagen Valencia, CA). Affymetrix GeneChip® Mouse Genome 430, type 2 arrays were used to measure gene expression. Sample preparation, hybridization, and array scanning were performed at the MUSC ProteoGenomics Core Facility according to procedures optimized by Affymetrix (Santa Clara, CA, USA). Each brain-region was processed separately with treatment groups randomized to minimize batch effects. Array data was stored in CEL file format, and sent to Virginia Commonwealth University (VCU) for analysis.

Microarray Analysis

Affymetrix GeneChip® Mouse Genome 430, type 2 arrays were analyzed with The R Project for Statistical Computing (http://www.r-project.org/). Microarray quality was assessed by RNA degradation, average background, percent present probesets, and multi-dimensional scale plots (first principal component by second principal component). Arrays showing low quality measures, or that appeared to be outliers, were removed from the dataset. Background correction using Robust Multi-array Average (RMA) and quantile normalization was performed using the affy package for R [255, 256]. Each brain-region was normalized separately. ComBat by RNA hybridization batch was used to correct for any batch effects present in the data [257].

CIE and Drinking Responsive Genes

Statistical analysis to identify significantly regulated genes was performed using the limma package for R [258]. Two factor LIMMA looking at treatment and drinking, as well as interaction, was used for initial analysis. However, we also ran LIMMA with each treatment

group as independent. This was done based on the fact that, over the course of the study, each group received a different overall dose of ethanol, number of, and duration of exposure. Each possible comparison between the 4 treatment groups was performed leading to 6 total comparisons labeled 1 through 6. Overall significance was also measured by ANOVA. Multiple testing was adjusted using the Benjamini and Hochberg method, also known as false discovery rate (FDR) [259]. False discovery rates equal to or less than 0.01 were considered significant.

Statistical Analysis of 2-Bottle Choice Drinking

Average ethanol intake (g/kg) was calculated across 5 drinking days of each week during the baseline-drinking period. During the testing cycles, mice also drank for 5 days; therefore average drinking across these 5 days was calculated to represent drinking during each CIE cycle. Differences in drinking were determined by Two Way ANOVA with Repeated Measures using SigmaPlot 12.0 (Systat Software, San Jose, CA, USA).

Weighted Gene Correlated Network Analysis

Weighted Gene Correlated Network Analysis (WGCNA) was used to perform scale-free network topology analysis of microarrays [218]. Scale-free networks have been used previously to identify biological pathways influenced by acute ethanol exposure in mice [230]. WGCNA was performed on each brain-region separately using the WGCNA package for R [260]. Overall significance by one-way ANOVA comparing all groups (FDR equal to or less than 0.01) was used to select probesets to be included in network analysis. A probeset found to be significant by ANOVA in any brain region was included. Standard WGCNA parameters were used for analysis with the exceptions of soft-thresholding power and deep split. Appropriate soft-thresholding powers were selected using previously described methods [338]. A soft-thresholding power of 6

was used for all brain-regions except the PFC for which a soft-thresholding power of 8 was used. WGCNA was performed with deep-split values of 0-3. Deep-split value was selected by multi-dimensional scaling (MDS) plot, which displayed first and second principal components. Deep-split values of 3 were chosen for the prefrontal cortex (PFC), nucleus accumbens (NAC), and central nucleus of the amygdala (CeA). For the hippocampus (HPC) a deep-split of 2 was chosen, and a deep-split of 0 for the bed nucleus of the stria terminals (BNST).

WGCNA-Drinking Correlation

Modules identified by WGCNA were related to drinking data by Spearman Rank correlation using the module eigengene as previously described [339, 340]**.** Individual probesets were also correlated to drinking data with the Spearman Rank method. These correlations were then used to identify modules enriched in genes whose expression showed systemic relationships with drinking behavior across 4 cycles of CIE with 2-bottle choice drinking.

Bioinformatics

Modules identified by WGCNA were examined for function using publicly available bioinformatics resources. The Functional Annotation Chart tool from DAVID (http://david.abcc.ncifcrf.gov/) [262] was used to identify biological pathways highly represented by genes grouped into each module. Gene Ontology terms were then summarized by semantic similarity using REVIGO (http://revigo.irb.hr/). Co-expression modules identified in this dataset were also compared to those identified in corresponding brain-regions in the B6 CIE time-course study (Chapter 3) [80] using WGCNA's userListEnrichment() function. This function uses hypergeometric overlap to determine significance of enrichment [260]. Hypergeometric overlap p-values were adjusted for multiple testing using false discovery rates [259]. Module overlaps

were considered significant at a false discovery rate ≤ 0.05. Since all brain-regions in this study used RNA from whole tissue samples, modules were also examined for enrichment for genes expressed in each specialized cell-type [341] found in brain (neurons, astrocytes, and oligodendrocytes) to demine whether any modules identified represented gene expression changes in a specific cell-type within a brain-region. This analysis was done because previous studies have shown that WGCNA can be used to identify cell-type specific modules [342]. The userListEnrichment() function was also used for cell-type enrichment analysis, Bonferroni corrected p-values ≤ 0.05 were considered significant.

Results

Gene Expression with CIE and Drinking

Statistical analysis with LIMMA found more significant differences in gene expression when each treatment group was treated as an independent group (**Table 5**). Significant differences in gene expression were seen between each of the four treatment groups in the PFC. Other brain regions, however, showed very different patterns of differential gene expression. In the NAC, HPC, BNST, and CeA, significant differences in gene expression were seen only seen with comparisons 1 (CIE-Drinking vs. Air-Drinking), 3 (CIE-Drinking vs. CIE-NonDrinking), and 4 (CIE-Drinking vs. Air-NonDrinking) (**Table 6**). Examining overlap between these comparisons revealed that a substantial number of genes were significant across all 3 comparisons, or between any combination of 2 comparisons in the PFC, BNST, and CeA. However, in the NAC and HPC, the majority of overlap was between CIE-Drinking vs. Air-NonDrinking and CIE-Drinking vs. Air-Drinking (**Figure 15**). Across NAC, HPC, BNST and CeA, the largest number of differentially expressed genes was seen between the CIE-Drinking group and the ethanol naïve Air-NonDrinking group. These four regions, however, showed less differential gene expression

in comparison 1 (CIE-Drinking vs. Air-Drinking), and comparison 3 (CIE-Drinking vs. CIE-NonDrinking) (**Table 6**). This finding indicates an interaction between prolonged exposure to inhaled ethanol and voluntary intermittent drinking. Unique to the PFC, large expression differences were seen across all comparisons but comparison 4 (CIE-Drinking vs. Air-NonDrinking) had the smallest number of changes, in contrast to other brain regions (**Table 6, Suppl. Table S14**).

Table 5: Two factor LIMMA results. Number of significantly differentially expressed probesets by each factor: drinking and treatment group (numbers in parenthesis indicate number of unique genes represented by these probesets), LIMMA FDR ≤ 0.01, and 0.05.

	Treatment	Drinking	Interaction
PFC	569 (528)	629 (574)	1315 (1149)
NAc	0 (0)	0 (0)	0 (0)
HPC	0 (0)	0 (0)	0 (0)
BNST	0 (0)	0 (0)	0 (0)
CeA	0 (0)	0 (0)	0 (0)
FDR = 0.01			
PFC	2339 (1980)	2627 (2288)	3665 (3032)
NAc	9 (9)	1 (1)	0 (0)
HPC	1 (1)	0 (0)	1 (1)
BNST	0 (0)	0 (0)	514 (465)
CeA	0 (0)	0 (0)	0 (0)
FDR = 0.05			

Table 6: LIMMA results. Number of significantly differentially expressed probesets between each comparison of treatment groups (numbers in parenthesis indicate number of unique genes represented by these probesets), LIMMA FDR ≤ 0.01.

	Comparison1	Comparison2	Comparison3	Comparison4	Comparison5	Comparison6
	Drinker CIE vs. Drinker Air	NonDrinker CIE vs. NonDrinker Air	Drinker CIE vs. NonDrinker CIE	Drinker CIE vs. NonDrinker Air	NonDrinker CIE vs. Drinker Air	Drinker Air vs. NonDrinker Air
PFC	840 (775)	569 (527)	843 (764)	325 (306)	759 (705)	629 (573)
NAC	127 (122)	0 (0)	9 (9)	1219 (1069)	1 (1)	0 (0)
HPC	549 (502)	0 (0)	37 (37)	1615 (1395)	0 (0)	0 (0)
BNST	419 (391)	0 (0)	178 (168)	543 (508)	0 (0)	0 (0)
CeA	78 (76)	0 (0)	721 (641)	818 (726)	0 (0)	0 (0)

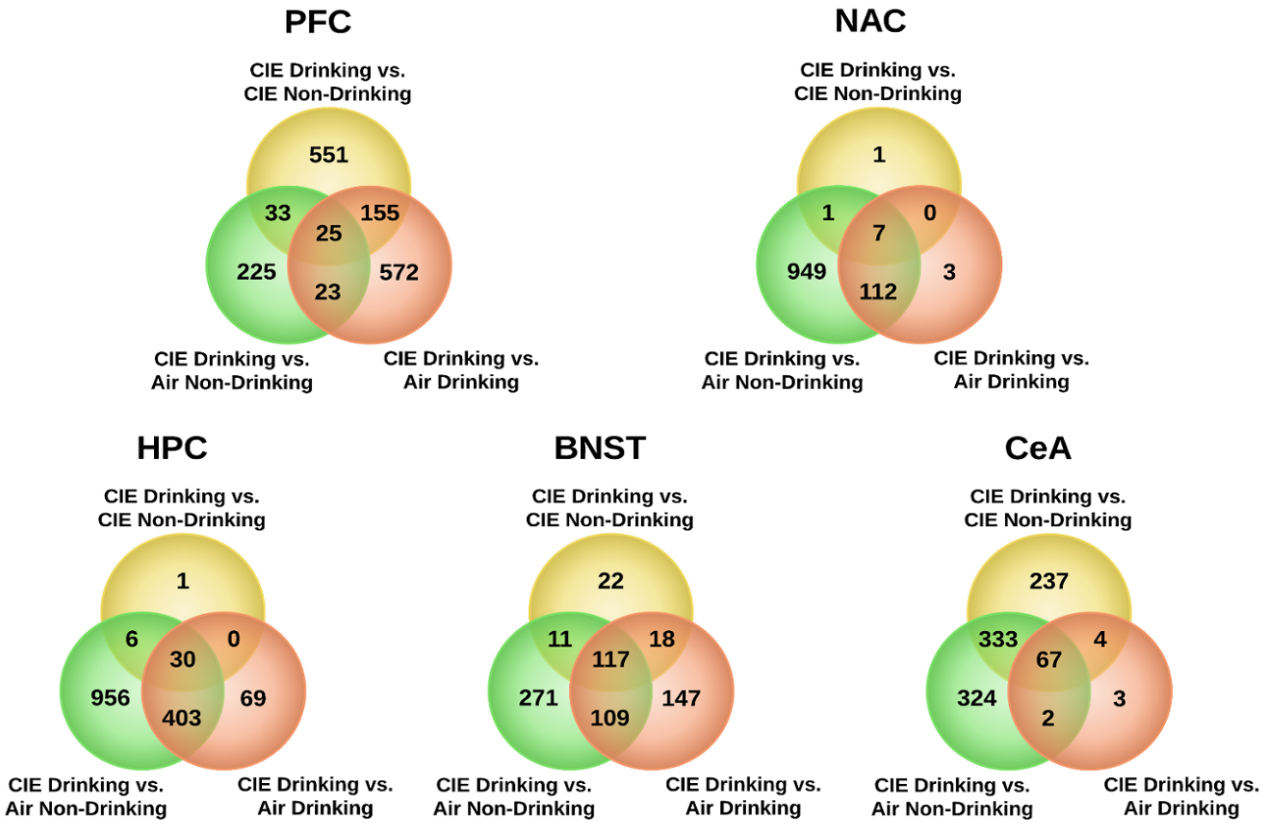

Figure 15: VennDiagrams of 3 treatment/drinking group comparisons in all brain-regions. Overlap between all probesets significantly differentially expressed between CIE Drinking vs. CIE Non-Drinking, CIE Drinking vs. Air Non-Drinking, and CIE Drinking vs. Air Drinking (LIMMA FDR ≤ 0.01.)

2-Bottle Choice Drinking

Consistent with previous behavioral studies of CIE combined with ethanol consumption [81], Two Way ANOVA with Repeated Measures revealed significant differences in ethanol intake ($p\text{-value} \leq 0.05$) between the CIE-Drinking and Air-Drinking groups after the first, third, and fourth vapor chamber session. After the second vapor chamber cycle, the CIE-Drinking group decreased ethanol intake compared to the first vapor chamber cycle, therefore, at this time-point, there was no significant difference in amount of ethanol consumed between CIE-Drinking and Air-Drinking groups. However, after the third and fourth vapor chamber sessions, the CIE-Drinking group drank significantly more ethanol than the Air-Drinking group (**Figure 16**). Interestingly, both the CIE-Drinking and Air-Drinking groups drank significantly more, compared to baseline, after only one session in the vapor chamber (**Figure 16**). This suggests that exposure to the inhalation chambers alone may affect ethanol consumption. However, animals exposed to ethanol vapor during inhalation chamber sessions consumed significantly more ethanol, indicating that prolonged exposure to intoxicating levels of ethanol is the major driver of changes in drinking behavior.

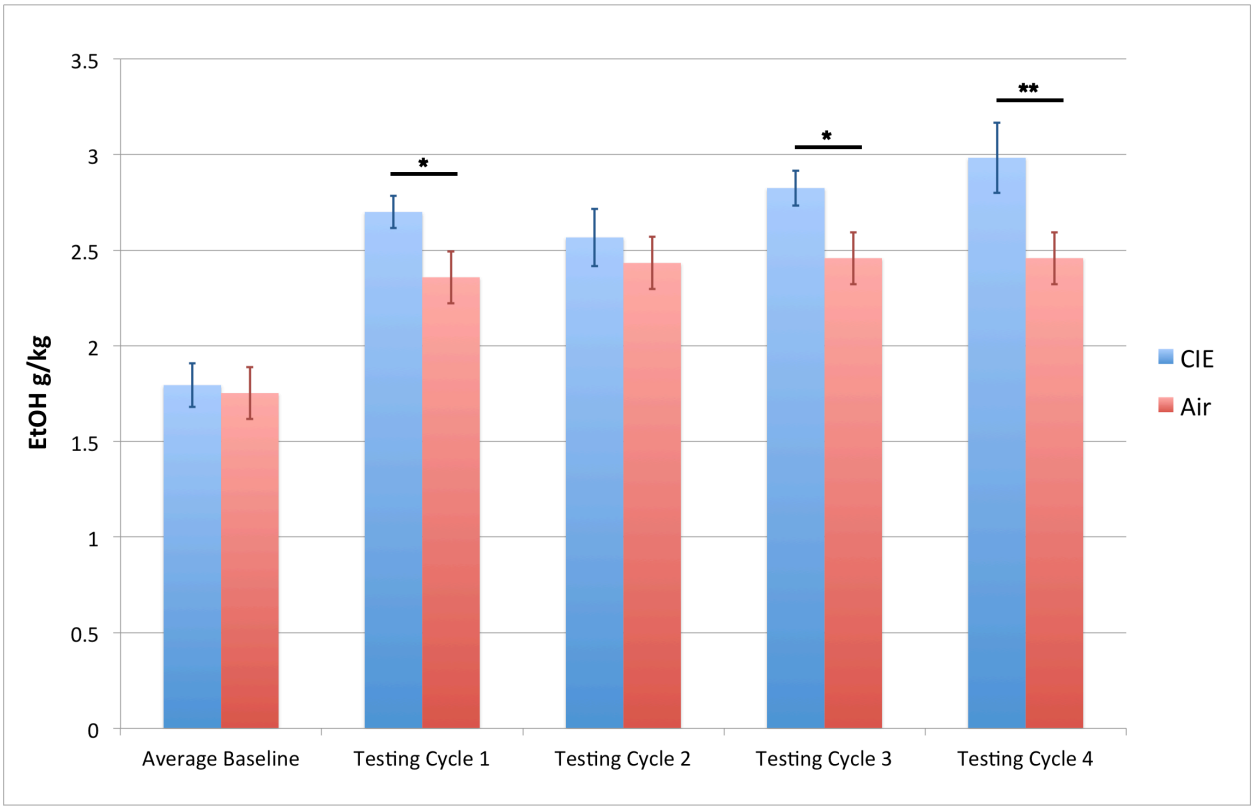

Figure 16: Bar graph of ethanol intake across study. Ethanol intake in g/kg over 6 weeks baseline, and 4 cycles of CIE. Columns = mean ethanol intake in g/kg, bars = standard error of mean. Significance CIE-Drinking vs. Air-Drinking (n=12/group) by RMANOVA: * ≤ 0.05, ** ≤ 0.01.

Weighted Gene Correlated Network Analysis

WGCNA identified modules of co-expressed genes in all brain-regions. Module sizes varied from over 3000 probesets to less than 35 (**Table 6**). Across brain regions, the highest correlation between drinking data and module eigengene expression was seen with ethanol intake after CIE cycle 4, and with change in ethanol intake between baseline and CIE cycle 4. This result is, perhaps, expected given that mice were sacrificed following cycle 4. The PFC and NAC showed the largest number of modules with highly significant correlation to drinking (**Figure 17** and **20**). The HPC, BNST, and CeA did not show as many strong correlations to drinking, but certain modules showed module-phenotype correlations with significant p-values (≤0.05) at specific time-points in the study (**Figure 21-23**).

Table 7: Sizes of WGCNA modules in all brain regions.

Brain Region	Module Color	Module Size	Module Color	Module Size
PFC (n=22)	Black	250	Lightyellow	40
	Blue	1926	Magenta	108
	Brown	1588	Midnightblue	66
	Cyan	71	Pink	192
	Darkred	33	Purple	98
	Green	513	Red	422
	Greenyellow	87	Royalblue	37
	Grey	1828	Salmon	74
	Grey60	49	Tan	81
	Lightcyan	64	Turquoise	1943
	Lightgreen	43	Yellow	771
NAC (n=25)	Black	304	Lightgreen	63
	Blue	1406	Lightyellow	52
	Brown	1369	Magenta	212
	Cyan	103	Midnightblue	97
	Darkgreen	40	Pink	220
	Darkgrey	33	Purple	204
	Darkred	42	Red	490
	Darkturquoise	38	Royalblue	44
	Green	975	Salmon	118
	Greenyellow	192	Tan	127
	Grey	550	Turquoise	2339
	Grey60	66	Yellow	1107
	Lightcyan	96		
HPC (n=16)	Black	276	Midnightblue	45
	Blue	1856	Pink	184
	Brown	1735	Purple	179
	Cyan	54	Red	422
	Green	461	Salmon	93
	Greenyellow	165	Tan	115
	Grey	1451	Turquoise	2415
	Magenta	184	Yellow	630
BNST (n=15)	Black	387	Pink	239
	Blue	1451	Purple	180
	Brown	1087	Red	808
	Cyan	57	Salmon	72
	Green	829	Tan	150
	Greenyellow	174	Turquoise	2653
	Grey	901	Yellow	1080
	Magenta	201		
CeA (n=19)	Black	251	Magenta	187
	Blue	2010	Midnightblue	59
	Brown	1202	Pink	245
	Cyan	70	Purple	125
	Green	931	Red	755
	Greenyellow	96	Salmon	72
	Grey	802	Tan	89
	Grey60	35	Turquoise	2205
	Lightcyan	43	Yellow	1035
	Lightgreen	34		

Prefrontal Cortex

As previously noted, the strongest correlations between ethanol intake and modules in the PFC were seen after the 4th CIE cycle. The strongest correlations between WGCNA modules and all intake measures were between change from baseline drinking after CIE cycle 4 and the turquoise module (r=0.8, p-value = 1e-12), the magenta module (r=0.65, p-value = 6e-7), and the grey60 module (r=-0.72, p-value = 9e-9) **(Figure 17)**. The magenta and turquoise modules showed Gene Ontology (GO) hits related to neuron development and synaptic transmission **(Suppl. Table S17)**. Specific genes within these GO categories include *Ngfr, Ppp1r9a, Fgfr1, Sox1, Slc1a3* (turquoise module), and *Grin2b, Htt, Cacna1a, Ppp3ca, Rims1* (magenta module). All of these genes, individually, show significant correlation with change in drinking between baseline and CIE cycle 4 **(Suppl. Table S16)**. The green module also showed significant correlation to ethanol intake after CIE cycle 4, and to percent change in ethanol intake between CIE cycle 4 and baseline (r=0.49, p-value=6e-4 with ethanol intake, r=0.39, p-value=0.02 with percent change from baseline) (**Suppl. Table S17**). This module also showed significant enrichment for regulation of neurotransmission as indicated by several GO categories (**Figure 18**). In addition, this module was significantly enriched for genes involved in neuron ensheathment by myelin (GO: 0007272, GO: 0008366, GO: 0042552). Myelin genes within this module include *Cd9, Lgi4, Cldn11, Olig2, Gjc3, Gas3st1,* and *Mbp* (**Suppl. Table S17**). Using the myelin-related genes from the green module as an input list, GeneMANIA validated that those genes have shown co-expression, co-localization, or protein-protein interactions in previous published studies (**Figure 18**). The large turquoise module showed a strong GO hit for chromatin modification (GO:0016568). Genes in the turquoise module within this category include many well-known chromatin modification genes such as *Dnmt1, Dnmt3b, Hdac8, Bcor, Crebbp, Ctcf,*

Bptf, Smarca5, and *Smarcc1* [343-348] (**Figure 19**). The grey60 module also showed a significant GO hit for chromatin (GO:0000785). Genes within this category were *H1f0, Tcp1,* and *Klhdc3* (**Suppl. Table S17**). Of these genes, *Hdac8, Bcor, Crebbp, Ctcf, Bptf, Smarca5, Smarcc1, H1f0, Tcp1,* and *Klhdc3* were significantly correlated with change in baseline intake after CIE cycle 4, or with ethanol intake after CIE cycle 4 (**Suppl. Table S17**).

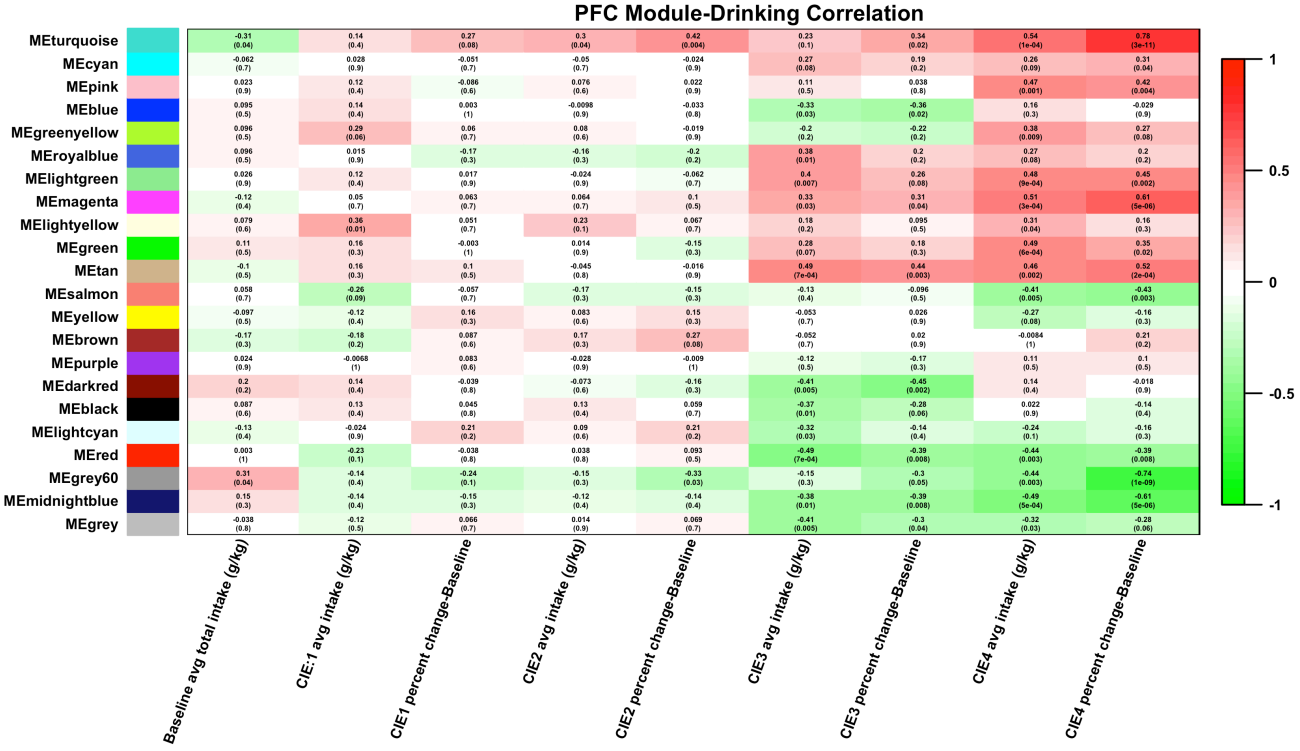

Figure 17: Heatmap of correlations between PFC modules and drinking data. Spearman rank correlation between PFC module eigengenes (1st principal component) and drinking measures during baseline period, and after each CIE cycle.

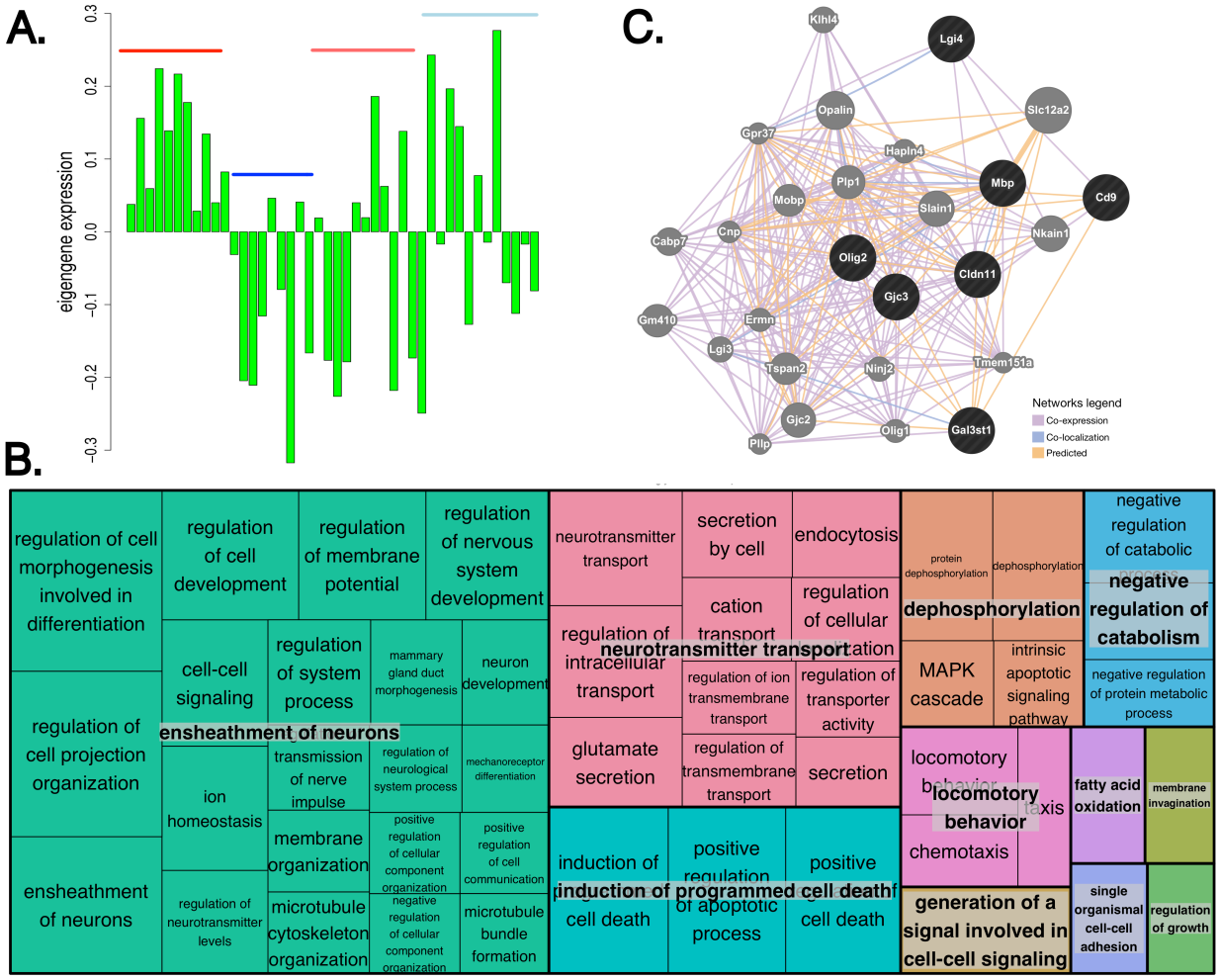

Figure 18: Network level and bioinformatics analysis of PFC green module containing myelin genes. A) Module eigenegene (1st principal component expression of each sample. Colored lines represent each treatment group: red = CIE Drinking, blue = Air Drinking, light red = CIE NonDrinking, light blue = Air NonDrinking. B) Revigo treemap of significant Gene Ontology biological processes. Significance: p-value ≤ 0.05. C) GeneMANIA network build from PFC green module myelin genes.

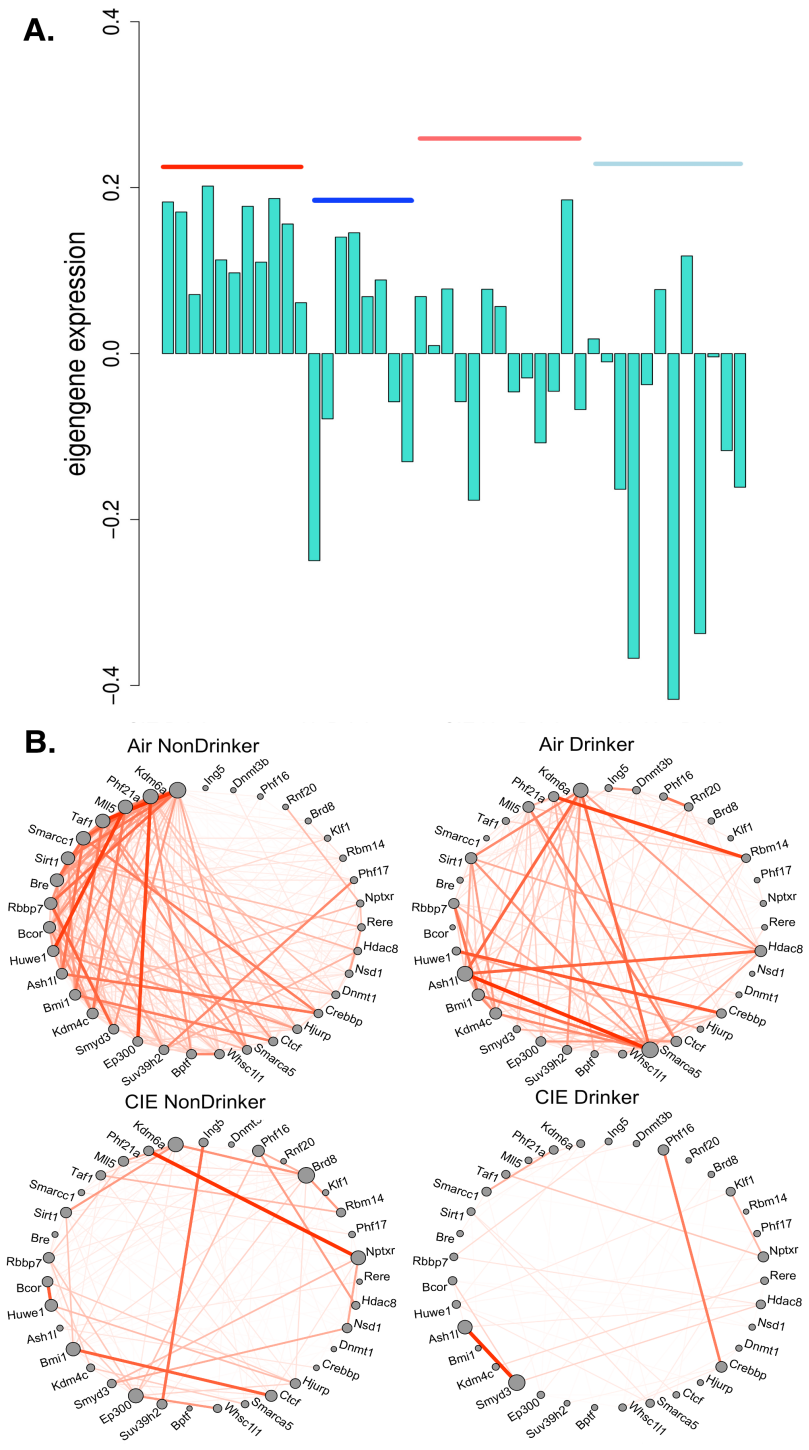

Figure 19: Network level plot of PFC turquoise module and connectivity plot of chromatin genes. A) Module eigenegene (1st principal component) expression of each sample. Colored lines represent each treatment group: red = CIE Drinking, blue = Air Drinking, light red = CIE NonDrinking, light blue = Air NonDrinking. B) Connectivity plots of genes in PFC turquoise module involved in chromatin remodeling. Line thickness and opacity represent pairwise connectivity between genes.

Nucleus Accumbens

Patterns of module-ethanol intake correlations in the NAc were more scattered than those seen in the PFC, but the strongest correlations were still seen with intake after the 4th cycle of CIE **(Figure 20)**. These modules were the royalblue (r=0.74, p-value = 3e-10 with ethanol intake, r=0.67, p-value = 6e-8 with percent change from baseline), and salmon modules (r=-0.79, p-value = 8e-13 with ethanol intake, r=-0.47, p-value = 6e-4 with change in drinking from baseline). The royalblue module contained probesets for several subunits of the ribosomal complex (*Rps7, Rsp10, Rps13, Rps17, Rps26, Rpl12, Rpl28, Rpl32, Rpl35, Rpl36, Rpl37a, Fau*) indicating this module may play a role in regulation of protein synthesis (**Suppl. Table S16** and **Suppl. Table S18)**. Whereas GO hits for cellular metabolic processes, such as glucose, fumarate, glutamate, and aspartate processing, were seen in the salmon module **(Suppl. Table S18)**. The lightyellow and yellow modules repeatedly showed significant correlation with both baseline drinking, and with drinking after each cycle of CIE. In both of these modules, however, this correlation decreased following the 4th CIE cycle. Finally, several modules (blue, lightyellow, tan, magenta, salmon, and yellow) showed very strong correlation to baseline drinking. Of these, the blue, lightyellow, magenta, and yellow showed GO hits related to synaptic transmission or synaptic plasticity **(Suppl. Table S18)**. The magenta and tan modules contained genes related to chromatin modification (Magenta: *Ing4, Ing3, Hdac1, Rbbp4, Kat5*. Tan: *Hdac9, Zbtb16*), and development (Magenta: *Rtn4, Sox9, Bmpr1b*. Tan: *Fgf9, Hdac9, Igfbp3, Zbtb16*) (**Suppl. Table S18)**. Together, these modules indicate that, in addition to alterations in mRNA expression, CIE-induced changes in protein and metabolite populations in the NAC may be involved in the observed increase in ethanol intake **(Figure 16)** [81].

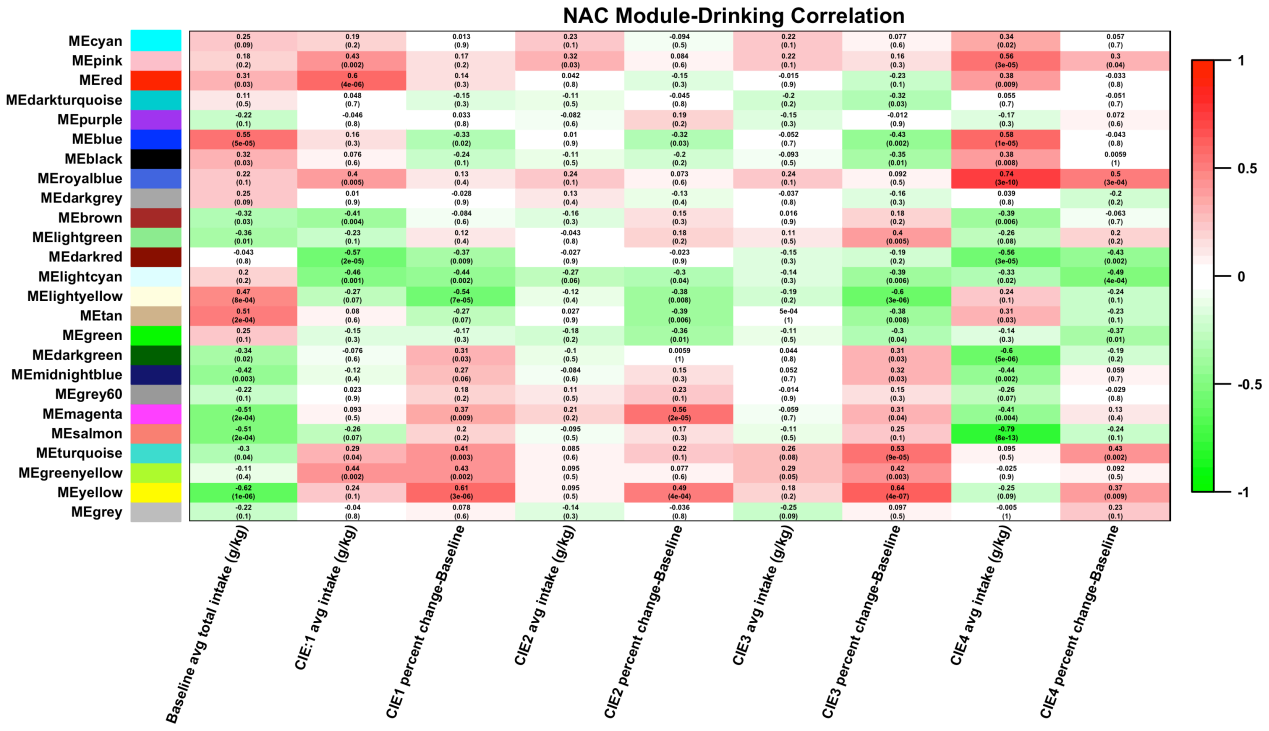

Figure 20: Heatmap of correlations between NAc modules and drinking data. Spearman rank correlation between NAc module eigengenes (1st principal component) and drinking measures during baseline period, and after each CIE cycle.

Hippocampus

In the hippocampus, a noticeable pattern of module-intake correlation was also seen after the 4th cycle of CIE. In the greenyellow, black, purple, and yellow modules significant correlations were seen with change in intake from baseline to CIE cycle 4. All of these modules showed significant overlap with GO categories related to synaptic transmission (black, purple and yellow) or neuron development (purple, greenyellow, and yellow) (**Figure 21**, **Suppl. Table S19**). The pink and magenta modules showed significant correlation to percent change in intake from baseline after CIE cycle 3 (pink module: r=0.4, p-value = 0.009, magenta module: r=0.42, p-value = 0.006). Significant correlations with intake in CIE cycle 1, and percent change from baseline intake were

also seen in a few modules such as the yellow, cyan, and brown. Like the yellow module, the brown and magenta modules showed GO hits specifically for neuron development or synaptic transmission. GO analysis of the pink module showed many hits related to electron transport chain regulation, and cell motility. However, this module also showed significant overlap with two GO categories related to dendrite structure (GO:0043197, GO:0030425) (**Suppl. Table S19).** Genes from the pink module within these categories included *Ppp1r9a, Fbxo2,* and *Gria3. Ppp1r9.* These genes correlated significantly with ethanol intake after CIE cycle 1 and percent change from baseline to CIE cycle 1; and *Fbxo2* and *Gria3* significantly correlated with percent change from baseline to CIE cycle 3 and CIE cycle 4 (**Figure 21**).

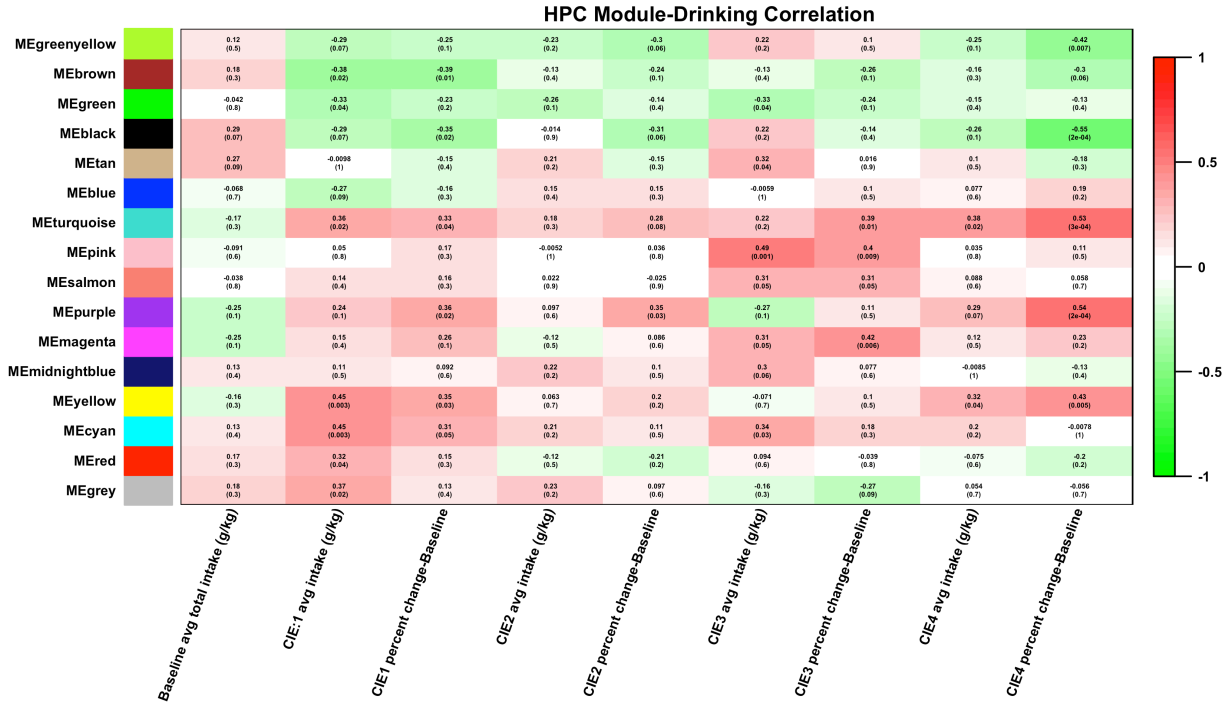

Figure 21: Heatmap of correlations between HPC modules and drinking data. Spearman rank correlation between HPC module eigengenes (1st principal component) and drinking measures during baseline period, and after each CIE cycle.

Bed Nucleus of the Stria Terminals

Fewer compelling intake correlations were seen in the BNST compared to other brain-regions. However, the turquoise and black modules showed very strong correlations to intake after the first cycle of CIE (black module: r=0.57, p-value = 4e-05 with ethanol intake, turquoise module: r=-0.55, p-value = 9e-05 with ethanol intake). Both of these modules showed multiple GO hits for synaptic transmission (**Figure 22, Suppl. Table S20**). The black module also contained 4 gene ontology hits related to myelination (GO:0042552, GO:0008366, GO:0007272, GO: 0019911) (**Suppl. Table S20**). Genes contained within these categories included some of the known myelin building blocks such as myelin basic protein (*Mbp*), myelin-associated oligodendrocyte basic protein (*Mobp*), galactose-3-O sulfotransferase 1 (*Gal3st1*), oligodendrocyte transcription factor (*Olig2*), and Cd9 (*Cd9*) [349, 350]. Although most of these genes correlated with ethanol intake after CIE cycle 1, and with percent change from baseline to CIE cycle 1 (**Suppl. Table S16**), very little change in mRNA expression, with any of the 6 comparisons examined, was seen in the BNST (**Suppl. Table S15**). Compared to other brain-regions, the BNST also showed fewer modules with strong correlations to intake after CIE cycle 4. The red module is a notable exception, with a correlation coefficient of 0.55, and p-value of 7e-05 with change in drinking from baseline. This module also showed significant overlap with several GO categories for synaptic transmission (**Suppl. Table S20**). Similar to the myelin-related genes seen in the black module, however, most of the genes within these GO categories did not show significant differences in mRNA expression between treatment groups (**Suppl. Table S15**). In spite of these relatively level gene expression patterns, certain genes in this module did show significant correlation with ethanol intake after CIE cycle 4 and percent change in drinking from baseline to CIE cycle 4 (**Figure 22**). These genes included ionotropic glutamate

receptor subunits: *Gria4, Grin2b* and *Grin3a*. Metabotropic glutamate receptor 2 (*Grm2*) also correlated significantly with ethanol drinking at CIE cycle 4 and percent change from baseline.

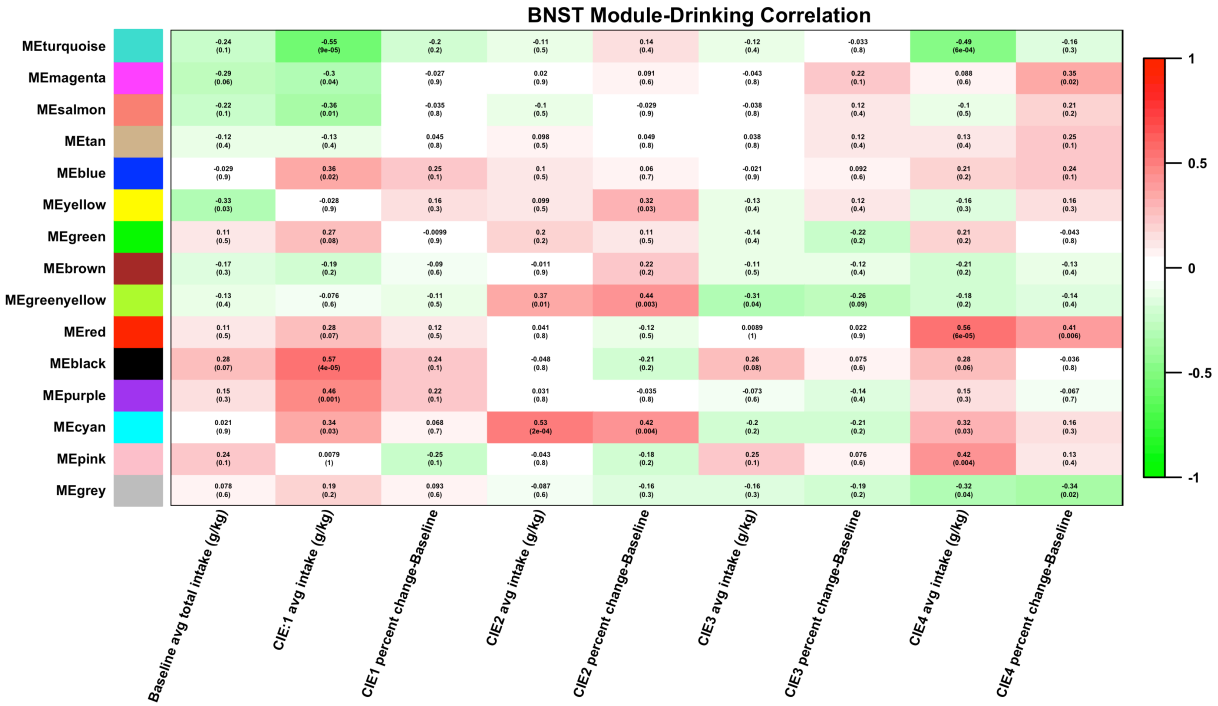

Figure 22: Heatmap of correlations between BNST modules and drinking data. Spearman rank correlation between BNST module eigengenes (1st principal component) and drinking measures during baseline period, and after each CIE cycle.

Central Nucleus of the Amygdala

Module-drinking correlations seen in the CeA were sporadic, with few noticeable trends for correlation to a specific drinking measure. The two strongest correlations observed were correlations between the blue module and percent change from baseline and CIE cycle 4, and the green module with intake with CIE cycle 4 (**Figure 23**). Functionally, the blue module contained several genes related to ion-mediated synaptic transmission such as *Gria4, Grin2b, Grin1, Grid2, Kcnma1, Cacnb4,* and *Cacna1a* (**Suppl. Table S21**). The green module, however, showed many

GO hits related to chromatin modification. Several of the genes in these categories were the same as those seen in the PFC turquoise module such as *Bcor, Smarcc1, Smarca5, Bptf* and *Ctcf.* Other known chromatin remodeling genes present in the CeA green module included *Smarca4, Ncor1, Rcor1,* and *Rbbp4.* All of these genes except *Bptf*, *Rcor1,* and *Rbbp4* strongly correlated with ethanol intake after CIE cycle 4 (**Suppl. Table S21**). This finding is, perhaps, not surprising considering the green module as a whole (as indicated by module eigengene) also significantly correlated to ethanol drinking during the final CIE cycle (**Figure 23**).

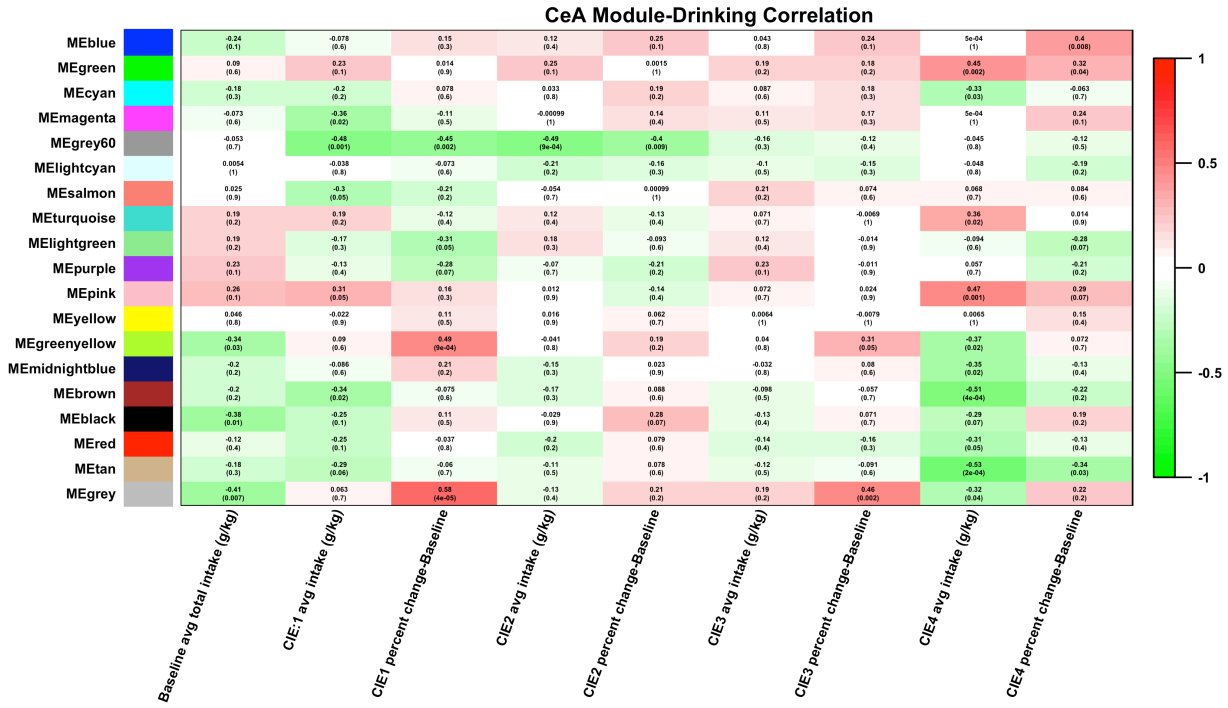

Figure 23: Heatmap of correlations between CeA modules and drinking data. Spearman rank correlation between CeA module eigengenes (1st principal component) and drinking measures during baseline period, and after each CIE cycle.

Cell-type Enrichment Analysis

Cell-type enrichment analysis of WGCNA modules revealed that, across brain-regions, identified modules represented specific populations of central nervous system cells. In PFC, the brown, lightyellow, red, and tan modules were enriched for genes expressed in neurons, and darkred and green modules were enriched for astrocyte genes. The PFC green module was also enriched for oligodendrocyte genes. In NAC, the black, green, greenyellow, grey60, and pink modules were enriched for neuronal genes, and then red module for oligodendrocyte genes. The black, blue, brown, and magenta modules were overrepresented for neuronal genes in the HPC, and the yellow module for both astrocyte and oligodendrocyte genes. The BNST green and tan modules showed enrichment for astrocyte-expressed genes. The BNST green module, as well as the greenyellow, midnightblue, and turquoise modules, were also enriched for neuron genes. One module in the BNST, red, was enriched for oligodendrocyte genes. Finally, in the CEA, the brown, pink, and yellow modules were enriched for gene expressed in neurons. The lightcyan and red modules were overrepresented for oligodendrocyte genes. The CEA red module, and turquoise module, was also over-represented for astrocyte specific genes (**Table 8, Suppl. Table S22**).

Table 8: Cell-type enrichment for all WGCNA modules. Significant overlap, Bonferroni corrected p-values 0.05.

Module	Cell-type	Bonferroni Corrected P-value
PFC		
Green	Oligodendrocyte	1.81e-36
Green	Astrocyte	5.23e-11
Red	Neuron	7.13e-22
Brown	Neuron	1.19e-09
Tan	Neuron	9.15e-04
Darkred	Astrocyte	1.19e-02
Lightyellow	Neuron	2.52e-02
NAc		
Red	Oligodendrocyte	2.73e-66
Green	Neuron	3.71e-46
Greenyellow	Neuron	2.89e-05
Pink	Neuron	5.70-05
Grey60	Neuron	1.75e-04
Black	Neuron	4.58e-02
HPC		
Yellow	Astrocyte	1.42e-50
Yellow	Oligodendrocyte	7.23e-16
Brown	Neuron	2.59e-24
Black	Neuron	1.76e-09
Blue	Neuron	2.75e-06
Magenta	Neuron	4.57e-05
BNST		
Red	Oligodendrocyte	6.99e-37
Turquoise	Neuron	4.84e-16
Green	Neuron	1.17e-10
Green	Astrocyte	3.71e-02
Greenyellow	Neuron	1.21e-10
Tan	Astrocyte	3.58e-09
Midnightblue	Neuron	1.70e-06
CeA		
Red	Oligodendrocyte	4.10e-62
Red	Astrocyte	2.60e-04
Yellow	Neuron	1.37e-48
Turquoise	Astrocyte	4.77e-20
Brown	Neuron	1.96e-14
Lightcyan	Oligodendrocyte	1.00e-11
Pink	Neuron	3.30e-04

Time-course CIE Overlap

WGCNA modules identified in C57BL/6J mice after 4 cycles of CIE with and without drinking were compared for overlap to WGCNA modules identified in corresponding brain-regions of C57BL/6J mice sacrificed at 4 time-points after 4 cycles of CIE without drinking (Chapter 3) [80]. The BNST, NAC, and HPC showed the greatest number of significant overlaps, while the NAC and PFC showed fewer significant overlaps (**Figure 24, Suppl. Table S23**).

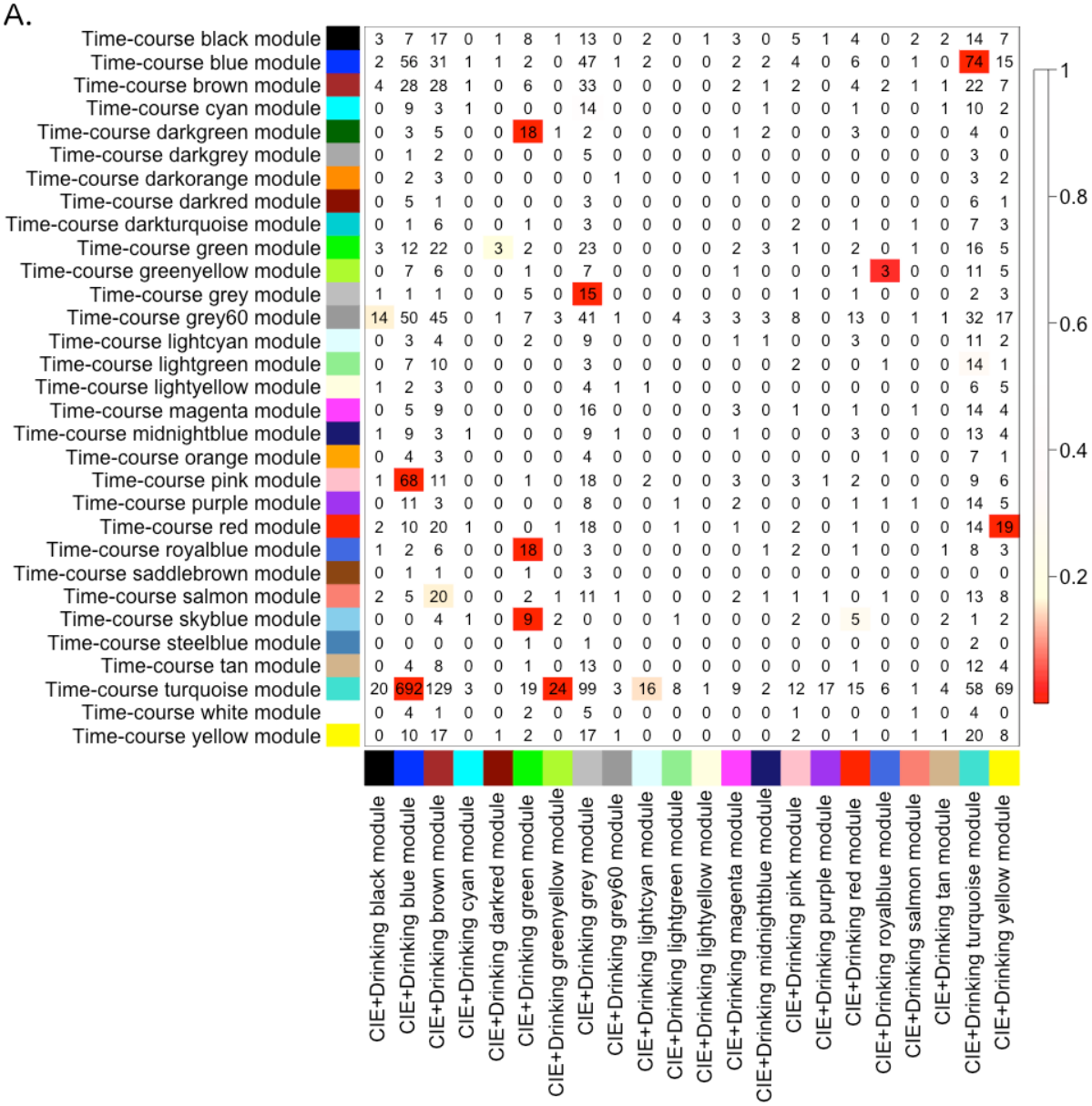
A.
Time-course black module
Time-course blue module
Time-course brown module
Time-course cyan module
Time-course darkgreen module
Time-course darkgrey module
Time-course darkorange module
Time-course darkred module
Time-course darkturquoise module
Time-course green module
Time-course greenyellow module
Time-course grey module
Time-course grey60 module
Time-course lightcyan module
Time-course lightgreen module
Time-course lightyellow module
Time-course magenta module
Time-course midnightblue module
Time-course orange module
Time-course pink module
Time-course purple module
Time-course red module
Time-course royalblue module
Time-course saddlebrown module
Time-course salmon module
Time-course skyblue module
Time-course steelblue module
Time-course tan module
Time-course turquoise module
Time-course white module
Time-course yellow module
CIE+Drinking black module
CIE+Drinking blue module
CIE+Drinking brown module
CIE+Drinking cyan module
CIE+Drinking darkred module
CIE+Drinking green module
CIE+Drinking greenyellow module
CIE+Drinking grey module
CIE+Drinking grey60 module
CIE+Drinking lightcyan module
CIE+Drinking lightgreen module
CIE+Drinking lightyellow module
CIE+Drinking magenta module
CIE+Drinking midnightblue module
CIE+Drinking pink module
CIE+Drinking purple module
CIE+Drinking red module
CIE+Drinking royalblue module
CIE+Drinking salmon module
CIE+Drinking tan module
CIE+Drinking turquoise module
CIE+Drinking yellow module
1
0.8
0.6
0.4
0.2

B.

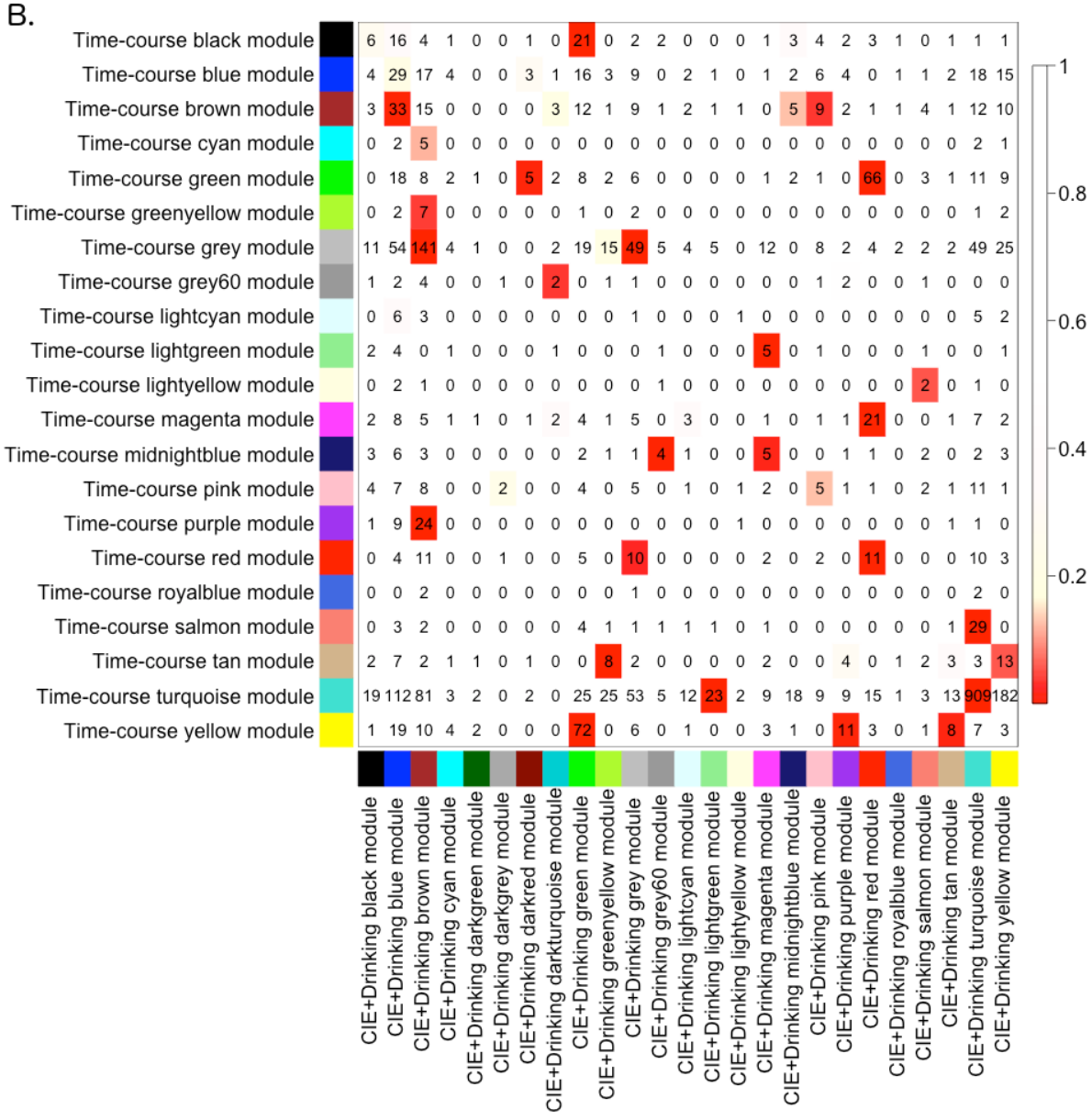
Time-course black module
Time-course blue module
Time-course brown module
Time-course cyan module
Time-course green module
Time-course greenyellow module
Time-course grey module
Time-course grey60 module
Time-course lightcyan module
Time-course lightgreen module
Time-course lightyellow module
Time-course magenta module
Time-course midnightblue module
Time-course pink module
Time-course purple module
Time-course red module
Time-course royalblue module
Time-course salmon module
Time-course tan module
Time-course turquoise module
Time-course yellow module
1
0.8
0.6
0.4
0.2
CIE+Drinking black module
CIE+Drinking blue module
CIE+Drinking brown module
CIE+Drinking cyan module
CIE+Drinking darkgreen module
CIE+Drinking darkgrey module
CIE+Drinking darkred module
CIE+Drinking darkturquoise module
CIE+Drinking green module
CIE+Drinking greenyellow module
CIE+Drinking grey module
CIE+Drinking grey60 module
CIE+Drinking lightcyan module
CIE+Drinking lightgreen module
CIE+Drinking lightyellow module
CIE+Drinking magenta module
CIE+Drinking midnightblue module
CIE+Drinking pink module
CIE+Drinking purple module
CIE+Drinking red module
CIE+Drinking royalblue module
CIE+Drinking salmon module
CIE+Drinking tan module
CIE+Drinking turquoise module
CIE+Drinking yellow module

C.

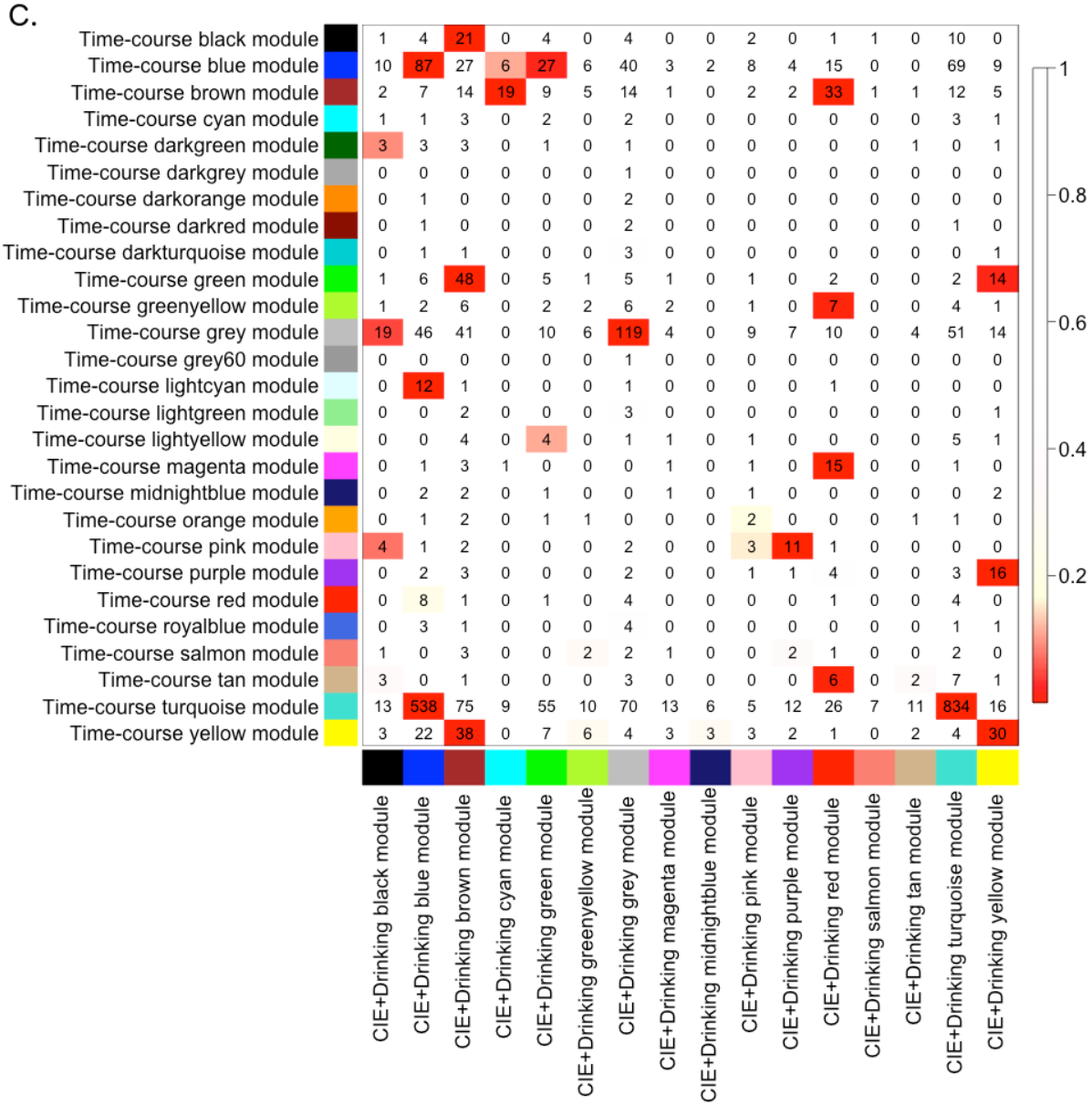
Time-course black module 1 4 21 0 4 0 4 0 0 2 0 1 1 0 10 0
Time-course blue module 10 87 27 6 27 6 40 3 2 8 4 15 0 0 69 9
Time-course brown module 2 7 14 19 9 5 14 1 0 2 2 33 1 1 12 5
Time-course cyan module 1 1 3 0 2 0 2 0 0 0 0 0 0 0 3 1
Time-course darkgreen module 3 3 3 0 1 0 1 0 0 0 0 0 0 1 0 1
Time-course darkgrey module 0 0 0 0 0 0 1 0 0 0 0 0 0 0 0 0
Time-course darkorange module 0 1 0 0 0 0 2 0 0 0 0 0 0 0 0 0
Time-course darkred module 0 1 0 0 0 0 2 0 0 0 0 0 0 0 1 0
Time-course darkturquoise module 0 1 1 0 0 0 3 0 0 0 0 0 0 0 0 1
Time-course green module 1 6 48 0 5 1 5 1 0 1 0 2 0 0 2 14
Time-course greenyellow module 1 2 6 0 2 2 6 2 0 1 0 7 0 0 4 1
Time-course grey module 19 46 41 0 10 6 119 4 0 9 7 10 0 4 51 14
Time-course grey60 module 0 0 0 0 0 0 1 0 0 0 0 0 0 0 0 0
Time-course lightcyan module 0 12 1 0 0 0 1 0 0 0 0 1 0 0 0 0
Time-course lightgreen module 0 0 2 0 0 0 3 0 0 0 0 0 0 0 0 1
Time-course lightyellow module 0 0 4 0 4 0 1 1 0 1 0 0 0 0 5 1
Time-course magenta module 0 1 3 1 0 0 0 1 0 1 0 15 0 0 1 0
Time-course midnightblue module 0 2 2 0 1 0 0 1 0 1 0 0 0 0 0 2
Time-course orange module 0 1 2 0 1 1 0 0 0 2 0 0 0 1 1 0
Time-course pink module 4 1 2 0 0 0 2 0 0 3 11 1 0 0 0 0
Time-course purple module 0 2 3 0 0 0 2 0 0 1 1 4 0 0 3 16
Time-course red module 0 8 1 0 1 0 4 0 0 0 0 1 0 0 4 0
Time-course royalblue module 0 3 1 0 0 0 4 0 0 0 0 0 0 0 1 1
Time-course salmon module 1 0 3 0 0 2 2 1 0 0 2 1 0 0 2 0
Time-course tan module 3 0 1 0 0 0 3 0 0 0 0 6 0 2 7 1
Time-course turquoise module 13 538 75 9 55 10 70 13 6 5 12 26 7 11 834 16
Time-course yellow module 3 22 38 0 7 6 4 3 3 3 2 1 0 2 4 30
CIE+Drinking black module
CIE+Drinking blue module
CIE+Drinking brown module
CIE+Drinking cyan module
CIE+Drinking green module
CIE+Drinking greenyellow module
CIE+Drinking grey module
CIE+Drinking magenta module
CIE+Drinking midnightblue module
CIE+Drinking pink module
CIE+Drinking purple module
CIE+Drinking red module
CIE+Drinking salmon module
CIE+Drinking tan module
CIE+Drinking turquoise module
CIE+Drinking yellow module
1
0.8
0.6
0.4
0.2

D.

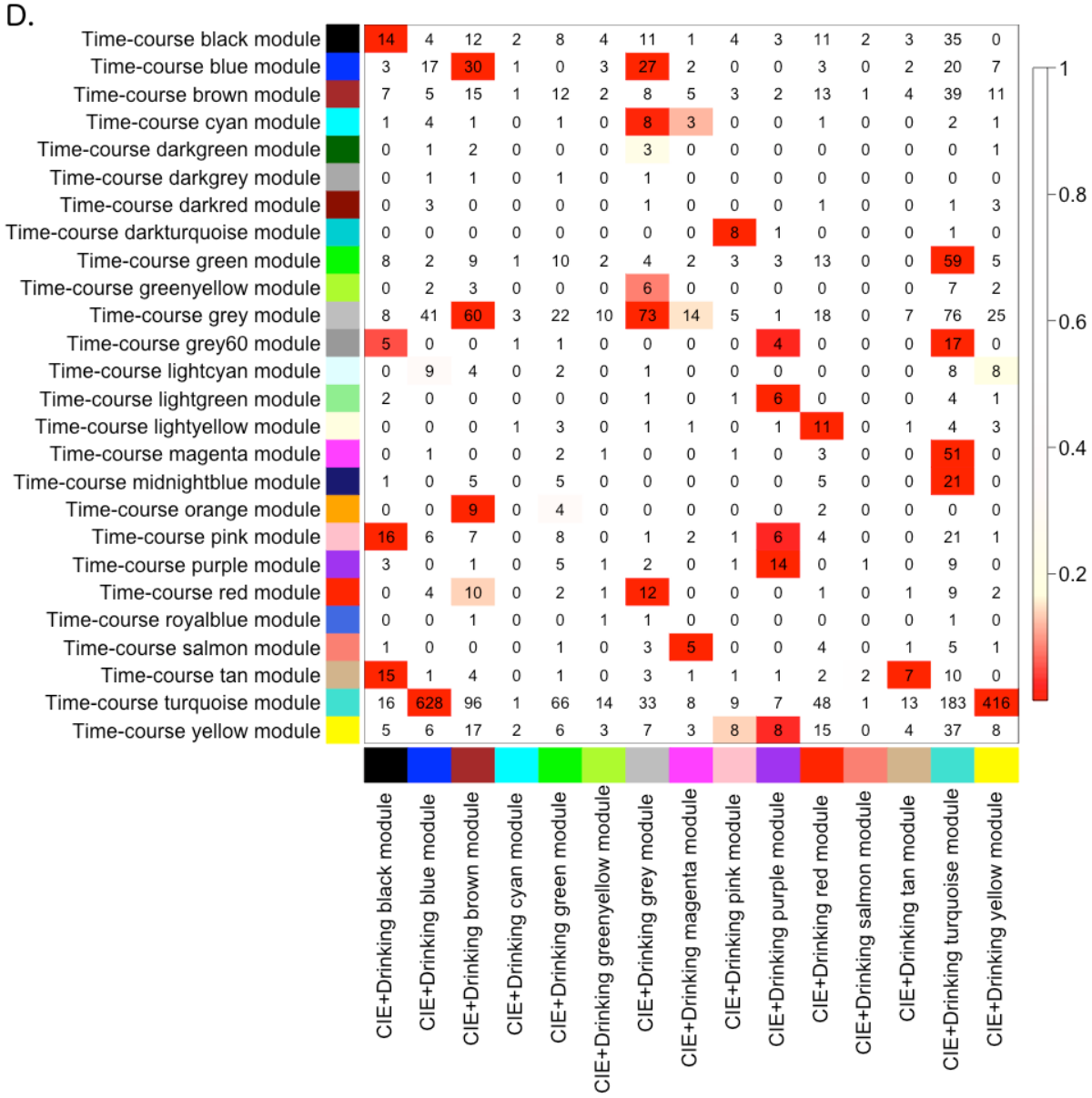
Time-course black module 14 4 12 2 8 4 11 1 4 3 11 2 3 35 0
Time-course blue module 3 17 30 1 0 3 27 2 0 0 3 0 2 20 7
Time-course brown module 7 5 15 1 12 2 8 5 3 2 13 1 4 39 11
Time-course cyan module 1 4 1 0 1 0 8 3 0 0 1 0 0 2 1
Time-course darkgreen module 0 1 2 0 0 0 3 0 0 0 0 0 0 0 1
Time-course darkgrey module 0 1 1 0 1 0 1 0 0 0 0 0 0 0 0
Time-course darkred module 0 3 0 0 0 0 1 0 0 0 1 0 0 1 3
Time-course darkturquoise module 0 0 0 0 0 0 0 0 8 1 0 0 0 1 0
Time-course green module 8 2 9 1 10 2 4 2 3 3 13 0 0 59 5
Time-course greenyellow module 0 2 3 0 0 0 6 0 0 0 0 0 0 7 2
Time-course grey module 8 41 60 3 22 10 73 14 5 1 18 0 7 76 25
Time-course grey60 module 5 0 0 1 1 0 0 0 0 4 0 0 0 17 0
Time-course lightcyan module 0 9 4 0 2 0 1 0 0 0 0 0 0 8 8
Time-course lightgreen module 2 0 0 0 0 0 1 0 1 6 0 0 0 4 1
Time-course lightyellow module 0 0 0 1 3 0 1 1 0 1 11 0 1 4 3
Time-course magenta module 0 1 0 0 2 1 0 0 1 0 3 0 0 51 0
Time-course midnightblue module 1 0 5 0 5 0 0 0 0 0 5 0 0 21 0
Time-course orange module 0 0 9 0 4 0 0 0 0 0 2 0 0 0 0
Time-course pink module 16 6 7 0 8 0 1 2 1 6 4 0 0 21 1
Time-course purple module 3 0 1 0 5 1 2 0 1 14 0 1 0 9 0
Time-course red module 0 4 10 0 2 1 12 0 0 0 1 0 1 9 2
Time-course royalblue module 0 0 1 0 0 1 1 0 0 0 0 0 0 1 0
Time-course salmon module 1 0 0 0 1 0 3 5 0 0 4 0 1 5 1
Time-course tan module 15 1 4 0 1 0 3 1 1 1 2 2 7 10 0
Time-course turquoise module 16 628 96 1 66 14 33 8 9 7 48 1 13 183 416
Time-course yellow module 5 6 17 2 6 3 7 3 8 8 15 0 4 37 8
CIE+Drinking black module
CIE+Drinking blue module
CIE+Drinking brown module
CIE+Drinking cyan module
CIE+Drinking green module
CIE+Drinking greenyellow module
CIE+Drinking grey module
CIE+Drinking magenta module
CIE+Drinking pink module
CIE+Drinking purple module
CIE+Drinking red module
CIE+Drinking salmon module
CIE+Drinking tan module
CIE+Drinking turquoise module
CIE+Drinking yellow module
1
0.8
0.6
0.4
0.2

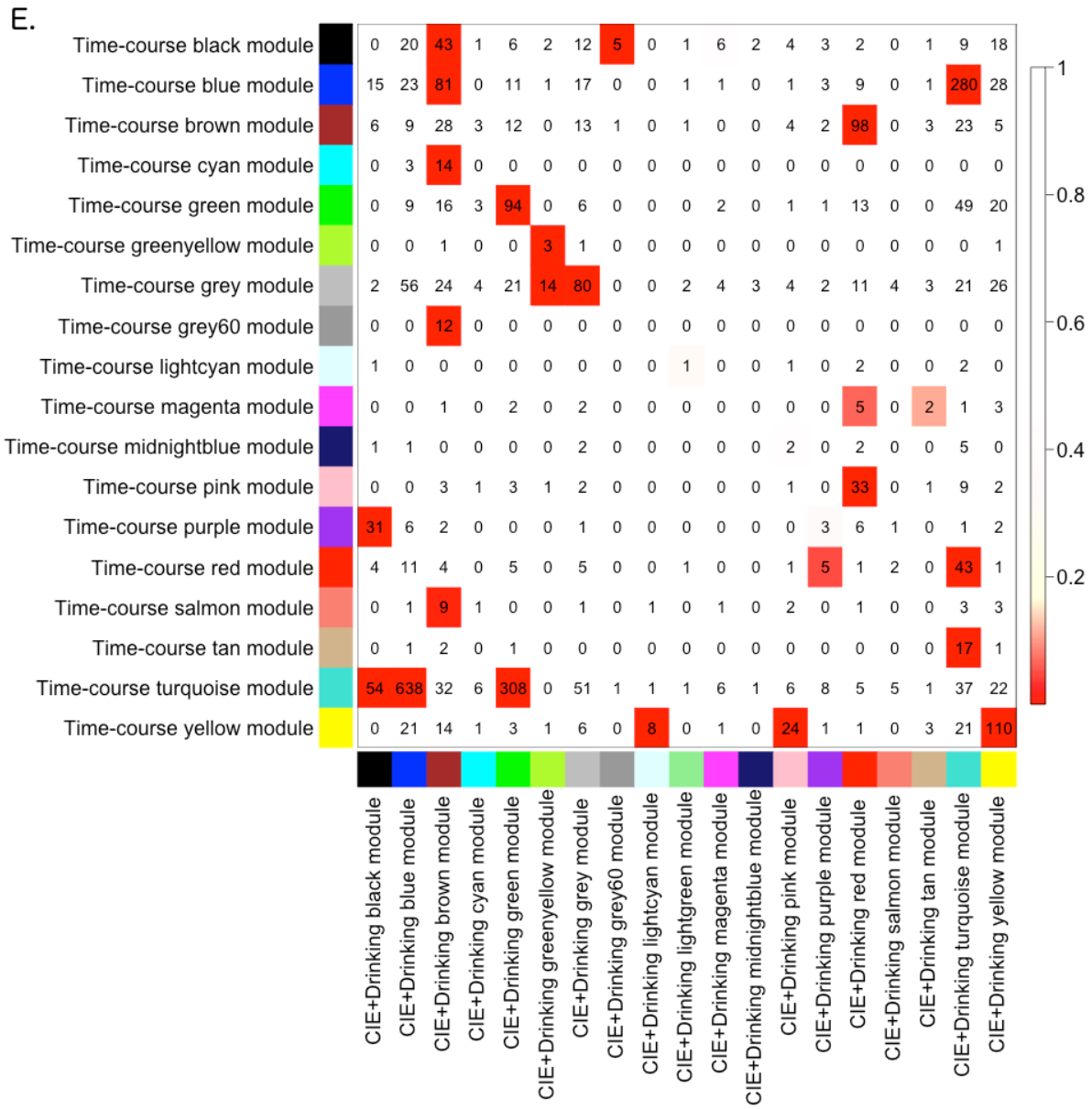

Figure 24: Heatmap of overlap between WGCNA modules of C57BL/6J mice after CIE with and without drinking, and C57BL/6J time-course mice. Numbers indicate number of overlapping probesets. Cell color indicates false discovery rate determined by Fisher's Exact Test. A) PFC, B) NAC, C) HPC, D) BNST. E) CeA.

Discussion

Through a systems biology approach we have characterized the transcriptome level response to chronic intermittent ethanol by vapor chamber with and without 2-bottle choice drinking, and

identified modules of co-expressed genes in 5 regions of the mesocorticolimbic system and extended amygdala. The CIE plus drinking model has been shown, both in this study and in previous ones, to increase ethanol consumption with each successive vapor chamber cycle (**Figure 16**) [81, 239].

Differential expression analysis with LIMMA showed that both CIE and drinking affect gene expression in the PFC. Through overlap analysis between all comparisons of all 4 treatment groups, our results further suggested that gene expression changes in the NAC and HPC are primarily regulated by CIE, whereas in the PFC, BSNT, and CeA an interaction effect between CIE and drinking is seen (**Table 6, Figure 15**). Differences across treatment categories might simply reflect a linear or non-linear response to the total amount of ethanol exposure. However, the nature of the CIE and drinking model also raises the possibility that withdrawal time influences gene expression differences between the 4 treatment groups. The drinking groups, at time of sacrifice, have been abstinent from ethanol for 22 hours, whereas the non-drinking groups have been abstinent for roughly 8 days.

Network analysis with WGCNA revealed specific patterns of correlated gene expression in each brain region used in this study. This network-centric approach also allowed us to correlate both individual genes and modules of co-expressed genes directly to ethanol drinking. The strongest correlations between gene co-expression modules and drinking were seen in the PFC and NAC. These results suggest that these brain regions may have the strongest influence on the increase in drinking seen with CIE (**Figure 15**). The influence of the prefrontal cortex on behaviors associated with alcohol use disorders such as increased ethanol consumption and uncontrolled intake have been associated with this brain region's role in impulse control and compulsivity [85,

304]. The nucleus accumbens, however, has been hypothesized to impact ethanol drinking behavior due to its involvement in reward [351, 352]. Therefore, ethanol-responsive gene expression changes in areas of the brain that control impulsivity and reward are implicated by network analysis in the increase in drinking seen following repeated exposure to intoxicating levels of ethanol.

One particularly striking finding was that those modules most strongly correlated with drinking after CIE exposure were consistently overrepresented for genes involved in synaptic transmission and synaptic plasticity (**Suppl. Tables S17-S21**). This finding is not unexpected, as ethanol exposure has previously been shown to affect synaptic transmission, and synaptic architecture in several of the brain regions studied in these experiments [67, 187, 190, 325, 327]. These findings build on previous investigations into the molecular mechanisms of ethanol response in the brain to suggest that the effect of repeated, prolonged ethanol exposure on synaptic transmission and synaptic architecture may have a direct influence on behavior both in animal models and human alcoholics. Specifically, correlated changes in expression of genes involved in synaptic remodeling in the mesocorticolimbic system and extended amygdala, in response to repeated cycles of CIE by vapor chamber, may underlie the observed increase in voluntary ethanol intake (**Figure 16**). In fact, recent research utilizing neuroimaging technologies have explored the effect of alcohol addiction on brain structure and function, and the relation to drinking behavior in humans [353, 354]. These studies have linked reduced grey matter volume in the medial PFC with increased risk of relapse in people with AUD [355]. SPECT and PET scanning have also shown correlations between decreased basal activity in the medial PFC during alcohol abstinence, as indicated by blood flow and glucose metabolism respectively, with poor AUD treatment outcome [356, 357]. Neuroimaging studies in mouse

models are fewer; however, it is hypothesized based on previous comparative research, including those of the gene expression and behavioral response to ethanol [190, 212], that neuroplastic changes in response to chronic ethanol exposure are highly conserved between species. Indeed, such a hypothesis has been employed in recent work using neuroimaging in rodent models to study the effect of ethanol exposure during gestation on fetal brain structure [358-360]. The results of our microarray analyses, therefore, may help shed light onto the molecular mechanisms underlying both the sustained increase in drinking observed with the CIE model, and, potentially, neuroadaptations observed in the brains of humans. Further study is needed to establish such mechanisms, and will be the topic of future research by this group.

Network analysis also identified modules in both the PFC and BNST enriched for myelin-related genes (**Figure 18, Suppl. Table S17** and **S20**). In the prefrontal cortex, the green module showed significant overlap with 3 GO categories related to myelination. Previous studies at our laboratory, as well as anatomical observations of the brains of human alcoholics, have suggested a role for myelination in the PFC in response to both acute and chronic ethanol exposure [185, 186, 242, 337, 361]. Fewer studies have taken place on myelination in the BNST; however, our analyses identified the BNST black module as one with significant correlations to ethanol intake after the 1st and 2nd CIE cycles. Although the BNST is a lesser-studied brain region in the myelin field, this region has previously been associated with the negative reinforcing properties of alcohol [190, 305]. Our findings suggest that repeated exposures to intoxicating ethanol may also have an effect on myelination in other brain regions that have, up to this point, not been examined as often as other regions more commonly associated with ethanol related demyelination, and that changes in myelin gene expression may be another mechanism underlying increased drinking. Future avenues of study will involve examining the effect of CIE

by vapor chamber on myelination in implicated brain regions, and on the effect of induced demyelination on voluntary ethanol intake with repeated exposures to prolonged levels of intoxicating ethanol.

Bioinformatic analysis also pointed to chromatin remodeling as a potential regulator of the transcriptomic response to CIE. The PFC turquoise module and CEA green module both contained genes involved in both DNA methylation [362] and members of known chromatin remodeling complexes [363-365]. *Smarcc1* has been associated with ethanol response in mouse whole brain meta-analyses [209], and *Smarca5* was found to be associated with alcohol response in network analysis of post-mortem brain tissue from human alcoholics [212]. Indeed, ethanol's effects on epigenetic modifications to chromatin have been an area of intense study, both in humans and rodent models, during recent years [142, 212, 366, 367]. These included a study from Dr. Jennifer Wolstenholme at the Miles laboratory which found that chromatin modification genes correlated with individual variation in ethanol consumption in C57BL/6 mice [142]. Based on our findings in the other brain-regions studied, we hypothesize that this reflects the transcription level response in the brain to chronic ethanol exposure leading to downstream transcriptional regulation such as the observed changes in genes related to synaptic transmission, synaptic plasticity, and myelination.

In summary, differential gene expression and scale-free network analysis of microarray data after multiple cycles of CIE with and without intermittent access drinking has revealed brain region and treatment specific changes. Differential expression in the PFC, CEA, and BNST indicated an interaction effect between CIE and drinking; whereas in the NAC and HPC, the primary effect came from CIE. Analysis of drinking patterns across multiple cycles of CIE showed that both

CIE and air control mice increase their drinking, however, mice exposed to CIE drink significantly more than control. These results are in line with previous studies [81], and indicate that the CIE paradigm consistently produces progressive, lasting increases in voluntary ethanol intake in response to chronic high dose ethanol exposure. Furthermore, we have used the capabilities of network analysis through WGCNA to attempt to bridge the gap between gene expression and behavior by identifying co-expressed networks of genes in each brain region, and then correlating those networks to ethanol drinking. This strategy revealed that the most highly drinking correlated modules were seen in the PFC and NAC. In both brain-regions, as well as those with fewer significant drinking correlations, those modules with the strongest correlations to drinking, particularly after the 4^{th} CIE cycle, were enriched for genes involved in synaptic transmission or synaptic plasticity. Modules from the PFC and BNST also indicated that changes in myelin gene expression also strongly correlate to changes in drinking. These results are of particular interest as previous studies from our group have observed significant changes in myelin gene expression with acute ethanol exposure [86]. Our results also suggest a role for chromatin remodeling, particularly in the PFC and CEA, in the gene expression response to chronic, prolonged ethanol exposure. Future studies will further explore the link between chromatin remodeling and altered synaptic transmission, possibly leading to structural changes in the brain, such as altered myelination. Such changes may be mechanistically important in the drinking behavior response to chronic intermittent ethanol exposure.

Chapter 5: Network Analysis of Prefrontal Cortex Gene Expression after CIE and drinking in BXD Recombinant Inbred Mice

Introduction

AUD is a complex, multifactorial disorder, risk for which has been attributed to both environmental and genetic factors [368]. The tendency of the disorder to run in families has long been observed in biomedical literature [369]. This tendency has seen been explored using family, twin, adoption, and population studies [370-373]. Overviews of these studies have found that about 40-60% of risk can be attributed to genetic factors [368, 374]. Genome wide association studies (GWAS) of human populations have attempted to identify specific genes that influence risk for AUD, however only a few candidate genes have been verified [375-378]. Transcriptome studies using microarrays have found that both acute and chronic alcohol exposure lead to widespread alterations in gene expression in the brain, particularly in prefrontal cortex [80, 86], and previous studies out of the Miles laboratory comparing two different mouse strains indicated that genetic background may play a substantial role in the effect of ethanol exposure on PFC gene expression [86].

Mice are powerful model organisms for genetic research. Their genome has been fully sequenced [379]. Their short lifespan, and ease of husbandry and breeding allows for extensive genetic manipulations that can help uncover the effect of genetic background on gene expression in the PFC, both basally and in response to environmental manipulations such as ethanol exposure. One such mouse genetic resource is the BXD recombinant inbred mouse panel [380]. This panel is a collection of mice strains bred from two inbred mouse strains, C57BL/6J and DBA/2J. After creating an isogenic F1 strain from the two progenitor strains, F1 mice underwent 20+

generations of brother/sister matings leading to several BXD strains of mice, all of which had alleles from C57BL/6J and DBA/2J progenitors in different combinations [380] **(Figure 25)**

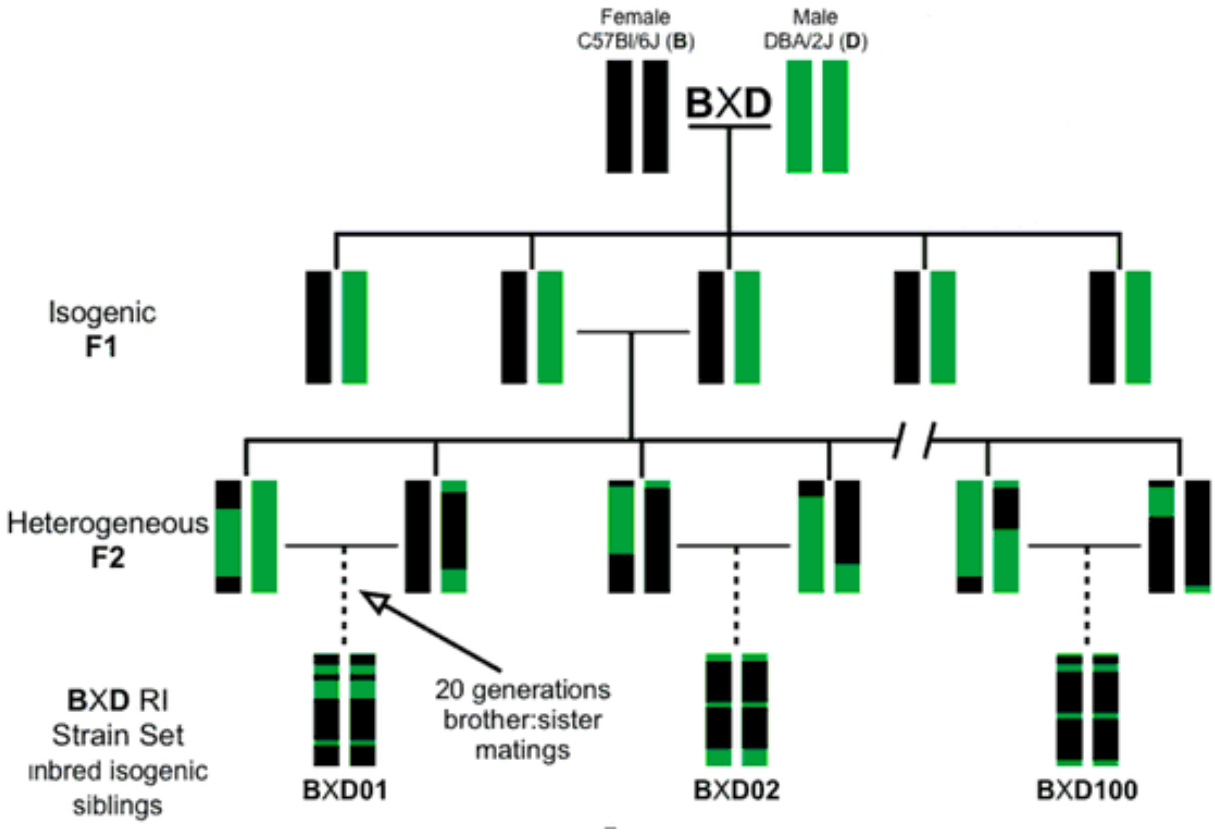

Figure 25: Overview of breeding history of BXD recombinant inbred mice. Figure adapted from Emery et al. [381]

The BXD panel is very useful for alcohol research because C57BL/6J and DBA/2J mice show very different behavioral and gene expression responses to ethanol. For example, C57BL/6J mice will voluntarily consume significantly more ethanol than DBA/2J [382, 383]. Reasons for this are still the subject of investigation [384, 385]. Previous studies have also shown that these two mouse strains show significantly different responses to ethanol's hypnotic and ataxic effects [386]. Additionally, microarray studies found that acute ethanol exposure leads to highly variable gene expression responses across the BXD RI panel in three mesocorticolimbic regions including

PFC [230, 288]. Based on these findings, we undertook this analysis of multiple strains of BXD RI mice with the hypothesis that genetic variation may influence gene expression response to chronic ethanol exposure.

Based on these findings, we collaborated with other members of the INIA Stress Consortium to investigate the effect of genetic background on voluntary ethanol intake, and gene expression response to chronic, high-dose ethanol exposure. Preliminary studies using Affymetrix GeneChip® Mouse Genome 430, type 2 arrays have shown similar gene expression effects in the PFC and NAc of BXD mice after multiple cycles of CIE with intermittent 2-bottle choice drinking (van der Vaart et al. 2016-in press). The analyses described in this chapter represent an expansion of that study to include more individual mice using a newer Affymetrix array type that includes deeper coverage, and probes that span exon junctions, thus allowing for alternative splice analysis.

This chapter outlines an extensive gene-level analysis of a deep-coverage array type across several strains of BXD RI mice, C57BL/6J and DBA/2J progenitors, and F1 generation predecessors after multiple cycles of CIE with intermittent 2-bottle choice drinking. These analyses explore the gene expression response of chronic prolonged ethanol exposure in the PFC using the a well established meta-analysis technique [261], and Weighted Gene Correlated Network Analysis [218]. Using this approach, we show that correlated patterns of gene expression occur across the RI panel in response to chronic ethanol exposure. We also show that WGCNA modules correlate to ethanol intake as well as serum blood levels of endogenous neurosteroids that are known to modulate the known ethanol receptor $GABA_A$. Finally, we have

also found that modules tend to either be enriched for genes that are ethanol responsive across the BXD panel, or correlated to ethanol intake, with almost no overlap between the two.

Materials and Methods

Animals

Male and female BXD recombinant inbred (RI) mice were supplied by the University of Tennessee Health Sciences Center (Memphis, TN, USA) at 12-16 weeks of age. 10 week old male and female C57BL/6 and DBA/2 mice were purchased from Jackson Laboratories (Bar Harbor, ME, USA). All mice were house individually in an AALAC-accredited animal facility. Mice were kept in a 12-hour light/dark cycle (lights on at 0200 hr), and given free access to water and standard rodent chow (Harland, Teklad, Madison, WI.). All studies were approved by the Institutional Animal Care and Use Committee at Medical University of South Carolina (MUSC) and conducted in accordance with the guidelines outlined in the NIH Guide for the Care and Use of Laboratory Animals.

Chronic Intermittent Ethanol (CIE)

All chronic intermittent ethanol (CIE) experiments were performed at Medical University of South Carolina (MUSC) with approval of the Institutional Animal Care and Use Committee. All mice underwent 6 weeks of limited access drinking (2 hr/day) 15% v/v ethanol and water to establish baseline drinking. Mice were then divided into 2 groups: CIE and Control. For each BXD strain, at least one mouse, of the same sex, was assigned to the CIE group and one to the control group. CIE mice received ethanol vapor in Plexiglass inhalation chambers (60x36x60 cm) for 16 hrs/day for 4 days. Control mice were also placed in the inhalation chambers for 16 hrs/day for 4 days, but did not receive ethanol vapor. Mice then underwent 72 hrs of complete

ethanol abstinence, followed by 5 days limited access drinking (2-bottle choice 15% v/v ethanol and water, 2 hr/day) [81]. Ethanol levels in the inhalation chambers were set to produce blood ethanol concentrations of 200-300 mg/dL. Prior to each vapor chamber session, mice were injected intraperitoneally with 1mmol/kg of the alcohol dehydrogenase inhibitor pyrazole to stabilize blood ethanol concentration (BEC). Blood was collected for BEC measurement on the 2nd and 4th inhalation chamber days of each inhalation chamber cycle. Mice surviving at the end of the study were sacrificed at 72 hrs after the 5th inhalation chamber session **(Figure 26)**. A total of 487 male and female BXD RI underwent CIE by vapor chamber **(Suppl. Table S24)**.

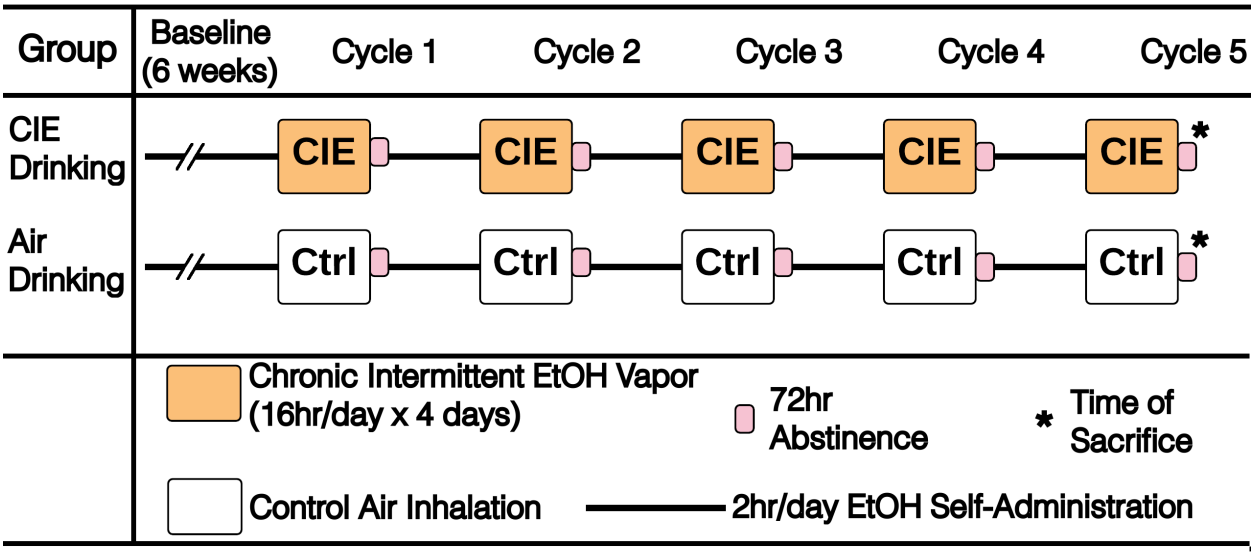

Figure 26: Overview of BXD RI CIE by vapor chamber with intermittent 2-bottle choice drinking.

Tissue Harvesting and RNA Isolation

Brain regions were harvested using brain punch microdissection as previously described [86]. Brain tissues were immediately snap frozen in liquid nitrogen, and stored long-term at -80°C. Simultaneously, trunk blood was collected from mice and time of sacrifice, and sent to collaborators at University of North Carolina Chapel Hill School of Medicine where serum

3α,5α-tetrahydroprogesterone (3α,5α-THP), tetrahydrodeoxycorticosterone (3α,5α-THDOC), and pregnenolone levels were measured as previously described [387]. Neurosteroid data was then shared with the Miles laboratory for correlation to gene expression results.

Prefrontal cortex tissue was homogenized using Stat 60 Extraction Reagent (AMS Biotechnology, Abingdon, UK), and RNA was extracted with the Qiagen miRNeasy Mini Kit. The RNA isolation reagents provided by this kit allowed for efficient isolation of RNA products < 200nt in length, as well as larger size mRNA, tRNA, rRNA. RNA quality was assessed by capillary electrophoresis with the Experion^{TM} Automated Electrophoresis System and RNA HighSens analysis kits (BioRad, Hercules, CA, USA). RNA yield was determined using a NanoDrop 2000 UV spectrophotometer (Thermo Fisher Scientific, Waltham, MA, USA).

Gene Expression Microarrays

Gene expression was measured using Affymetrix GeneChip® Mouse Transcriptome Assay 1.0 (Affymetrix, Santa Clara, CA, USA). Sample preparation was performed according to manufacturer instructions. All samples were randomized before RNA extraction, and then re-randomized before array hybridization using a supervised randomization scheme that minimized dissection cohort, sex, and treatment effects as much as possible (**Suppl. Table S24**). Array hybridization and scanning were carried out with the assistance of the VCU Molecular Diagnostics Laboratory.

Microarray Analysis

Gene expression intensity was quantified by normalization and probe summarization using RMA. RMA values for all arrays were generated using Affymetrix Expression Console software using the Signal Space Transformation (SST) RMA algorithm with GC4 correction, and quantile

normalization (Expression Console User's Guide: http://www.affymetrix.com). A batch effect of cohort was seen, ComBat was used to correct for this effect [257] (**Figure 27**).

Figure 27: Multidimensional scale plot of BXD mice before (left panel) and after (right panel) ComBat to remove the batch effect of cohort. X and Y axes represent 1st and 2nd principal components of the data.

To determine significance of gene expression between CIE and control mice, a method for meta-analysis developed at the Miles laboratory was used [247] (Aaron Wolen PhD Thesis, 2012). Differential gene expression between CIE and control mice was determined using a variant of the S-Score method [388, 389] (Harris and Miles-publication pending) developed at the Miles lab for use with Affymetrix microarrays that do not have PM-MM probes for all probesets. S-Scores were run for all transcript cluster IDs for coding regions (those classed as complex or coding) on each BXD strain separately. For strains with more than one CIE and/or more than one control mouse, S-Scores were determined each CIE mouse was compared to each control mouse, and the

strain mean was then taken. For strains with both male and female mice, CIE males were only compared to control males, and CIE females were only compared to CIE females. In downstream analyses, however, the mean of male and female S-Scores was collapsed to find the strain mean in these initial analyses. Sex effects on gene expression response to CIE may be explored as a future study, but are beyond the scope of this dissertation.

Fisher's Combined Probability test was used to determine whether a gene was significantly differentially expressed across the BXD panel [261]. With this method, we treat each BXD strain as an independent test of the same null hypothesis (that there is no difference in gene expression between CIE and control), and p-values of S-scores are generated based on normal distribution and then compared to a random population of p-values built by randomly permuting S-scores 1000 times to generate empirical p-values. False discovery rate (FDR) was then used to generate empirical q-values to adjust for multiple testing (R Script: Aaron Wolen PhD Thesis, 2012. Appendix A.1). Empirical q-values equal to or less than 0.2 were considered to indicate significant differential expression across the BXD panel.

Weighted Gene Correlated Network Analysis

WGCNA was run at the gene-level on all transcript cluster IDs classed, according to Affymetrix locus ID type, as being within coding regions of the genome. Transcript cluster IDs showing low expression were eliminated from network analysis by filtering out all transcript clusters with average expression less than or equal to an RMA value of 4. WGCNA was run using mostly standard parameters. A soft-thresholding power of 6 was chosen based on the fit of data to scale-free topology. Biweight midcorrelation was used for network analysis due to this method's resilience to outlier samples [390]. Deep-split values of 0-3 were used, and a deep-split value of

3 was chosen based on lack of overlap between modules as assessed by multidimensional scale plots of 1st and 2nd principal components. Modules were then correlated to ethanol intake data provided by collaborators at MUSC, and neurosteroid data provided by collaborators at UNC School of Medicine. Correlations to ethanol intake and neurosteroid levels were done using Spearman rank correlation.

WGCNA-CIE Responsive Gene Overlap

WGCNA modules were compared for overlap to the results of Fisher's Combined S-Scores at a empirical q-values ≤ 0.2 using the userListEnrichment() function in WGCNA [260]. This function uses hypergeometric distribution to measure significance of overlap. Hypergeometric distribution p-values were corrected for multiple testing using Bonferroni correction. Overlaps with corrected p-values ≤ 0.05 were considered significant.

Bioinformatics

CIE responsive genes measured by Fisher's Combined S-Scores, and each module identified by WGCNA were examined for function using DAVID Functional Annotation Chart tool (https://david.ncifcrf.gov/) [262]. Results were filtered to include Gene Ontology (GO) categories which contained between 3 and 1000 genes, and which significantly overlapped with the input list of genes, either those within a WGCNA module or the list of CIE responsive genes, at a p-value ≤ 0.05. Results were curated for semantic similarity using REVIGO (http://revigo.irb.hr/), and visualized using REVIGO's treemap script. In REVIGO a medium (0.7) allowed similarity was used using the SimRel method, and limited to only mouse GO terms.

Results

Gene Expression with CIE and Drinking

1225 transcript cluster IDs, representing 1220 genes, were significantly differentially expressed across the BXD RI panel at an empirical q-value ≤ 0.2 (**Suppl. Table S25**). Functionally, these genes fell into the larger general categories of regulation of Ras signal transduction, cell development, synaptic vesicle transport, antigen processing, protein dephosphorylation, cell-matrix adhesion, cytokinesis, locomotor behavior, regulation of hormone levels, and cell proliferation and activation **(Figure 28)**. These CIE-regulated genes were further explored by overlapping them with co-expression modules identified through WGCNA, and then looking at those biological pathways represented by the modules.

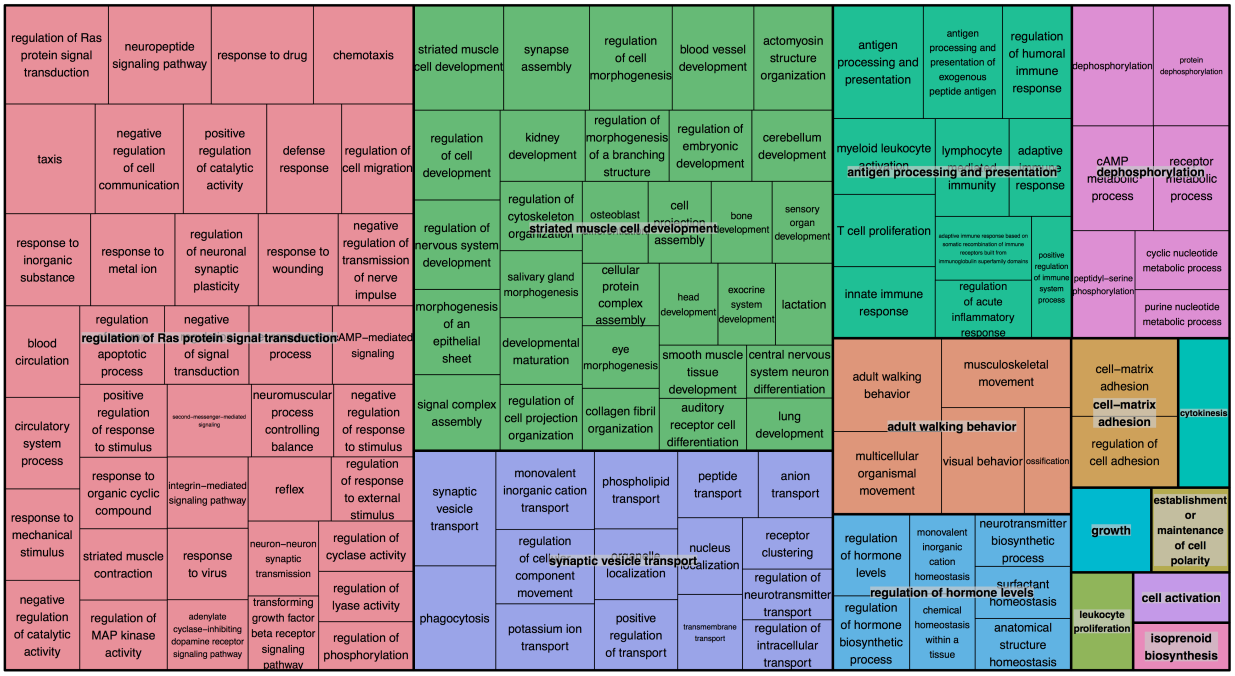

Figure 28: REVIGO Treemap of GO results of significant Fisher's S-Scores. Gene Ontology categories are hierarchically grouped based on semantic similarity. Block size reflects number of GO categories in an overall group.

Weighted Gene Correlated Network Analysis

WGCNA identified 42 modules in the PFC of BXD RI mice after 5 cycles of CIE with intermittent drinking. These modules varied in size between 32 and 3735 transcript clusters

(**Figure 29, Suppl. Table S26**). Of these 10 were significantly enriched for transcript clusters that were CIE responsive across the BXD panel, and around 11 showed highly significant correlation to ethanol intake (**Figure 30**). Correlations to neurosteroid measurements were mixed, with the strongest correlations being those to THDOC (**Figure 31**). Those modules significantly enriched for CIE responsive transcript clusters, or significantly correlated to ethanol intake after CIE exposure, were further explored using bioinformatics resources. Modules significantly correlated to neurosteroid measures were also examined.

Bisque4 33	Black 1424	Blue 3040	Brown 1684	Brown4 34	Cyan 267	Darkgreen 161
Darkgrey 152	Darkmagenta 70	Darkolivegreen 140	Darkorange 131	Darkorange4 41	Darkred 195	Darkslateblue 32
Darkturquoise 161	Floralwhite 43	Green 863	Greenyellow 473	Grey60 218	Lightcyan 227	Lightcyan1 45
Lightgreen 208	Lightsteelblue1 49	Lightyellow 203	Magenta 557	Mediumpurple3 223	Midnightblue 233	Orange 148
Orangered4 58	Paleturquoise 95	Pink 625	Royalblue 195	Salmon 375	Sienna3 66	Skyblue 109
Steelblue 95	Tan 385	Turquoise 3735	Violet 84	White 124	Yellow 920	Yellowgreen 63

Figure 29: BXD RI WGCNA module names and sizes. Highlighted cells indicate modules significantly enriched for genes significantly differentially expressed across the BXD RI panel. Significant = genes with empirical q-values ≤ 0.2 by Fisher's Combined Probability Analysis.

CIE Responsive Modules

The black, brown4, greenyellow, lightcyan, magenta, orangered4, pink, salmon, tan, and yellow modules were significantly enriched for transcript clusters that were significantly CIE responsive across the BXD panel as determined by S-Scores with Fisher's Combined Probability Analysis at q-value ≤ 0.2 (**Figure 29, Suppl. Table S27**). Of these, 9 showed significant enrichment for known biological processes.

The yellow module was highly enriched for several GO processes related to development and differentiation including several neurodevelopment categories **(Suppl. Table S28**). Genes within

this module known to be involved in neurodevelopment included *Fgfr1*, a gene that has also previously been shown to differ in gene expression in whole brain samples of mouse and rat strains that vary in drinking behavior [209, 391]. The yellow module also contained Notch signaling genes (*Notch1* and *Notch2*), and forkhead box (Fox) proteins (*Foxc1, Foxc2, Foxd1, Foxf2*). The role of notch proteins in brain development is well documented [392, 393]. *Notch* was also identified in modules of CIE responsive genes in PFC of C57BL/6J mice only as discussed in Chapter 3 [80]. *Fox* genes have also been shown to be very important in brain development. Further, the yellow module was also enriched for genes within GO categories related to behavior such as response to hypoxia (GO:0001666) and regulation of locomotion (GO:0040012) (**Suppl. Table S28**). One particular gene within the regulation of locomotion category, *Clic4*, was of particular interest because this gene has been found to affect acute ethanol behavioral response in a multi-species analysis [337]. Our findings here suggest that chronic ethanol exposure may affect *Clic4* expression long-term.

Neurodevelopment was a repeatedly observed process among those modules significantly enriched for CIE regulated genes. The black, orangered4, and pink modules also showed significant overlap with GO categories involved in neurodevelopment. The orangered4 module, like the yellow module, was enriched for genes involved blood vessel development and neurodevelopment such as *Mef2c*, *Sema5a*, and *Fgf10* [394-396]. This module also contained some well-known ethanol associated genes such as Dopamine Receptor D1 (*Drd1a*) [397, 398], μ-opiod receptor 1 (*Oprm1*) [397, 399], and two subunits of the nAChR (*Chrna4* and *Chrna5*) [400-403]. The black module significantly overlapped with several GO categories involved in regulation of neurogenesis. Specific genes within these categories include *Sema4f, Psen1, Syngap1* as well as others [404-407]. The pink module also showed significant enrichment for

GO categories related to both neurogenesis and gliogenesis. Genes within this module known to be involved in gliogenesis, specifically of oligodendrocytes include *Sox10*, *Plp1*, *Erbb3*, and *Shh* [408-411]. These results indicate that this module may represent the long-term gene expression effect of chronic ethanol on PFC white matter.

Two modules, greenyellow and tan, showed significant enrichment for chromatin modification genes. These genes included some well-documented chromatin modifying genes such as *Hdac8*, *Nsd1*, *Suv420h1*, *Epc1*, and *Baz1b* in the greenyellow module, and *Dnmt3a*, *Ehmt1, Hdac7*, *Kcnq1ot1*, and *Baz2a* in the tan module. Chromatin remodeling factors have been associated with behavioral and gene expression response to ethanol [142, 367, 412]. Modules enriched for chromatin remodeling processes were also identified in both the CIE time-course, and CIE plus intermittent drinking studies in PFC of C57BL/6J mice as discussed in Chapters 3 and 4 [80]. This adds substantial validation to the finding of chromatin remodeling gene regulation by chronic ethanol exposure, since this functional group was identified across two different experiments conducted several years apart with differing types of microarrays and mouse strains of varied genetic background.

WGCNA-Drinking Correlated Modules

Of those modules significantly correlated to ethanol intake, one of the most functionally striking was the mediumpurple3 module (**Figure 30**). This module significantly overlapped with a GO category titled "behavioral response to ethanol" (GO:0048149) (**Suppl. Table S28**). This is, perhaps, not surprising as this module contained some genes that have been well documented to influence ethanol behavioral response such as dopamine receptor D2 (*Drd2*) and nAChR subunit alpha 7 (*Chrna7*). Repeated ethanol exposure has been shown to downregulate *Drd2* expression

in adolescent rats [413]. *Drd2* expression affects ethanol intake in mice under chronic stress [414, 415]. Network analysis of multiple ethanol exposure models also identified a cluster of genes containing *Drd2* in the prefrontal cortex of chronic intermittent ethanol drinking mice [416]. This finding, in conjunction with findings from our BXD mice, strongly suggests that *Drd2* expression affects PFC gene expression response to chronic ethanol. *Chrna7* expression has also been associated with ethanol intake in knock-down experiments [417], gene association studies [418], and studies of gene expression in certain regions of the mesocorticolimbic system [419]. Relationships between *Chrna7* expression in PFC and ethanol intake are not well documented. However, *Chrna7* expression in PFC has been associated with nicotine preference in rats [420]. A microdeletion in the human chromosome 15 region that includes the CHRNA7 gene has been associated with schizophrenia, and in mouse models has been shown to result in altered brain function in multiple brain-regions including PFC [421, 422]. These findings, together, suggest that *Chrna7* is important in PFC function. As outlined in Chapters 3 and 4, multiple cycles of CIE have widespread effects on PFC gene expression in C57BL/6J mice. *Chrna7* was significantly differentially regulated between control and CIE mice immediately after final exposure in the time-course experiment [80].

The cyan module also significantly correlated to ethanol intake both baseline and after each cycle of CIE (**Figure 30**). Interestingly, this module was enriched for chemokine activity, suggesting that this module may represent a neuroimmune response to chronic ethanol exposure. Indeed, neuroimmune response genes have been shown to alter ethanol consumption, and recovery from the sedative effects of ethanol in a variety of mouse models [361, 423, 424]. The darkgreen module also significantly correlates to ethanol intake both baseline and after each cycle of CIE (**Figure 30**). Functionally, this module showed overlap with some unexpected GO categories:

GO:0007283~spermatogenesis, GO:0048232~male gamete generation, and GO:0007130~synaptonemal complex assembly (**Suppl. Table S28, Suppl. Table S29**). Genes within these categories included the transcriptional activator *Creb3l4* [425]; a member of the tRNA-splicing endonuclease complex *Tsen 34* [426]; *Spata6* which is an important protein the structure of spermatozoa [427]; and *Sycp3* and *Syce1*, genes which are involved synaptonemal complex assembly during meiosis [428-430]. This module also contained genes involved in glycoprotein generation in the Golgi apparatus. Overall, these findings suggest that these genes may have, as of yet, lesser-known roles in neural tissue that also impacts ethanol consumption. Indeed, *Spata6* was differentially regulated in whole brain samples of ethanol preferring vs. non-preferring mice [209], and *Tsen34* in ethanol responsive networks in multiple regions from human brain samples including frontal cortex [212].

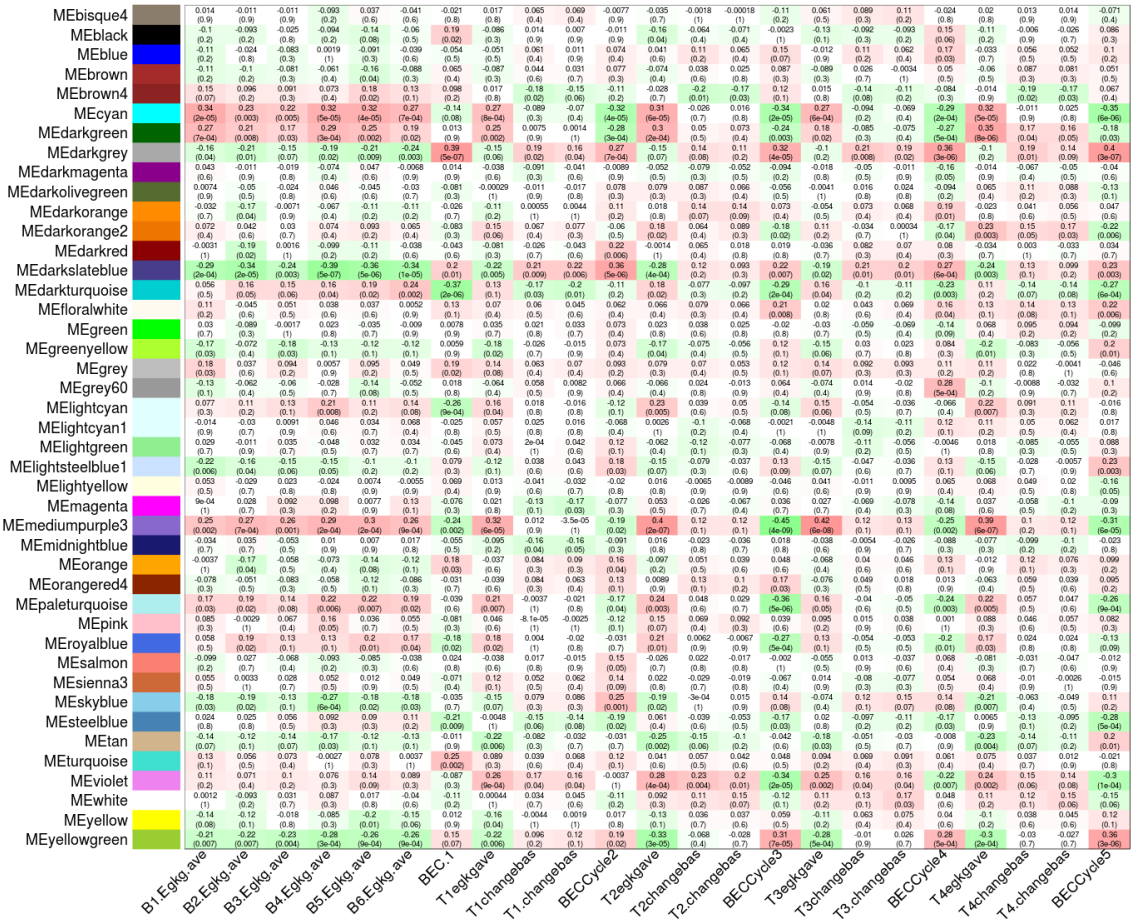

Figure 30: Heatmap of ME correlations to ethanol intake. Module eigengene (1st principal component) correlated to each ethanol intake measure by Spearman rank correlation.

WGCNA-Neurosteroid Correlated Modules

The strongest correlations between WGCNA modules, and neurosteroid measurements were to THDOC (**Figure 31**). Among these was the mediumpurple3 module, which was significantly correlated to baseline and post-CIE ethanol intake, and enriched for genes involved in the behavioral response to ethanol (**Figure 30**). This finding suggests that THDOC levels may regulate the expression of genes whose expression influences ethanol intake. Of the other modules significantly correlated to THDOC expression, the darkgrey, lightyellow, and

midnightblue modules were enriched for genes involved in biosynthetic processes within the cell. The magenta module was enriched for genes involved in the mitogen-activated protein kinase cascade, and inflammatory response (**Suppl. Table S28**).

Several modules also significantly correlated to pregnenolone (**Figure 31**). These included the darkslateblue module, which was enriched for *Serpin* family genes involved in protein processing [431], and the skyblue module, which was also enriched for GO categories involved in biosynthetic processes in the cell. The skyblue module also contained certain genes known to affect neurodevelopment such as *Robo2*, *Sty1*, and *Nmnat1* [432-434] (**Suppl. Table S28, Suppl. Table S29**). Additionally, the yellow module was significantly correlated to serum pregnenolone levels. As discussed, this module was also highly enriched for CIE responsive genes.

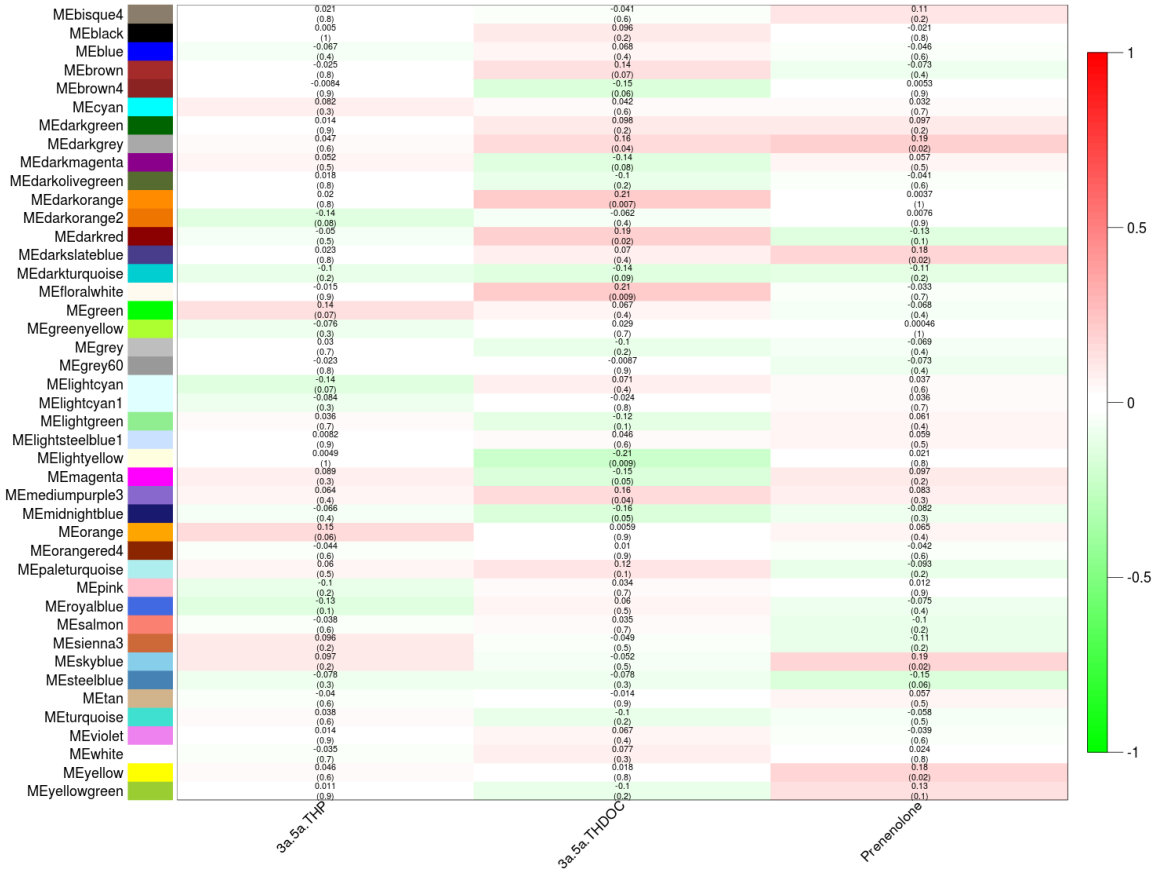

Figure 31: Heatmap of ME correlations to endogenous neurosteriod levels. Module eigengene (1st principal component) correlated to neurosteroid levels by Spearman rank correlation.

Discussion

Through network analysis with WGCNA we have developed an extensive picture of the transcript-level response to repeated cycles of CIE by vapor chamber with intermittent 2-bottle choice drinking across a recombinant inbred mouse panel generated from two progenitor strains that differ widely in their gene expression response to ethanol exposure [86]. The CIE by vapor chamber model has been shown in previously published studies [81, 239], and in chapter 4 of this dissertation, to significantly increase ethanol intake when combined with intermittent 2-bottle choice drinking. The analyses outlined in this chapter revealed the gene expression

response to chronic intermittent ethanol exposure across a panel of genetically variable mice, and identified modules of co-expressed genes that correlated to ethanol intake measures, or to levels of active endogenous neurosteroids in mouse blood after multiple cycles of CIE. Additionally, modules significantly enriched for chronic ethanol responsive genes across the RI panel, revealing that those modules enriched for CIE responsive genes tended not to overlap with those significantly correlated to ethanol intake. This recapitulates findings discussed in Chapter 6 in a co-analysis of C57BL/6J mice and rhesus macaque PFC expression responses to chronic ethanol.

Expression of each individual gene tended to vary considerably across the BXD RI panel, therefore meta-analysis was used to identify genes whose expression was significantly different between CIE and control mice across the panel. At a false discovery rate of 0.2, a little over 1200 genes were significantly regulated by CIE across the BXD panel. Functionally, these genes showed a few overreaching patterns based on bioinformatics analysis. One category highly represented in CIE-regulated genes across the panel was processes involved in Ras signal transduction. Ras has been studied in a variety of fields, particularly cancer cell biology, due to its role in the regulation of cell proliferation and apoptosis [435]. In the brain, however, Ras signaling via the MAPK signaling pathway may play a significant role in synaptic plasticity, and memory formation. Particularly in the hippocampus, pharmacological and genetic manipulation of elements of the Ras signaling pathway have been shown to significantly affect long-term potentiation measured by electrophysiology in rats and mice, and to result in impaired performance on behavioral tests [436, 437] Specifically, deletion of the nucleotide exchange factors RasGRF has led to reduced performance on operant and classical conditioning tasks [436], and, in fact, two RasGRFs (*Rasgrf1* and *Rasgrf2*) were significantly regulated across the BXD panel. *Rasgrf2* has also been found to be highly expressed in heavy drinking mice [438].

Another gene significantly regulated across the panel, *Nf1*, has been shown to affect hippocampal-dependent spatial memory in knock out mice [439]. *Nf1* is a Ras GTPase that is the major Ras signaling inhibitor in dendritic spines [440], and has been found, in mouse forebrain, to be a structural component of the NMDA receptor complex [441]. Although many previous studies on the role of Ras signaling in the brain have focused on the hippocampus, some have also noted that modulation of parts of the Ras signaling cascade in the neocortex results in changes in long-term potentiation [439]. Results from BXD mice indicated that chronic ethanol exposure leads to altered Ras gene expression in the prefrontal cortex, and, based on the role of Ras in other mesocorticolimbic brain-regions, may alter synaptic plasticity in PFC. Further, studies will be needed to determine the behavioral effects, if any, of modulation of Ras gene expression in PFC by chronic ethanol.

Several class I and class II major histocompatibility complex (MHC) genes were also significantly regulated across the BXD panel. MHC genes produce a set of cell-surface proteins that are essential to adaptive immune response [442]. In the central nervous system, however, MHC genes, particularly class I MHC genes, have been shown to be expressed in both the fetal and adult brain [443], and there is considerable evidence that these genes are involved in synaptic plasticity via regulation of neurite outgrowth, and synaptic density [443]. The role of class II MHC genes in the brain is less well known, although there is some evidence that MHC class II gene expression is altered in endothelial cells of the brain's vascular system [444], suggesting that chronic ethanol exposure may have a neuroinflammatory effect on brain vasculature regardless of genetic background.

One of the modules identified by WGCNA also indicates a possible effect of CIE on vasculature in the PFC. The CIE responsive yellow module was enriched for a variety of Gene Ontology pathways related to development and metabolism including several Fox genes, may of which are recorded to play a role in the development and maintenance of the blood-brain barrier. *Foxf2* is expressed in brain pericytes, and has been demonstrated to be important in blood-brain barrier formation during embryonic development [445]. *Foxf2* loss has also been shown to result in blood-brain barrier degradation in conditional knockdown mice [445]. *Foxc1* has been shown to be important in brain development, demonstrated in multiple brain regions [446, 447]. This gene has also been shown to be specifically expressed in pericytes, and essential for blood-brain barrier development [448]. *Fox2c* is known to play a role in cancer progression including gliomas [449], suggesting this gene is important in regulating turnover in glial cells. *Foxd1* has also been shown to regulate glioma development and proliferation via mesenchymal glioma stem cells [450]. Our finding in BXD RI mice provides further evidence that chronic ethanol exposure may affect gene expression in vascular cells in PFC, and, possibly even lead to disruption of the blood-brain barrier. Additionally, *Notch1, Notch2*, and *Bmp*, three other genes within the yellow module, have been shown to be dysregulated in the heart with fetal ethanol exposure [451]. Additionally, angiogenesis factors have been shown to induce *Notch* signaling, and regulate angiogenic sprouting in developing mice [452]. These findings suggest that molecular components of cerebral vasculature may be significantly disrupted by chronic, high-dose ethanol exposure, and could have important implications on the more global impact of chronic ethanol on brain function, as seen with alcoholic dementia [2]. Furthermore, alcoholics are also known to be at increased risk for hemorrhagic stroke [41, 44, 45].

In addition to differential gene expression and ethanol intake, this study also looked at the phenotype of endogenous neurosteroids. Serum 3α,5α-3-hydroxypregnan-20-one (THP) and 3α,5α-3,21-dihydroxypregnan-20-one (THDOC), as well as one precursor steroid pregnenolone, levels after 5 cycles of CIE were correlated to each co-expression module as represented by the module's first principal component. Functionally, very few modules that significantly correlated to neurosteroid measures were significantly enriched for any known biological processes. Of the ones that were, the magenta module, which significantly correlated to THDOC levels, was enriched for genes involved in the mitogen-activated protein kinase cascade, a cellular signaling process that has been implicated in PFC and HPC mediated learning and memory [453]. This suggests the magenta module may represent a group of genes whose expression regulates PFC neuroplasticity modulated by endogenous neurosteroids. No modules significantly correlated to THP expression, however, a few significantly correlated to pregnenolone expression. Pregnenolone is a precursor of THDOC and THP, both of which are allosteric modulators of known ethanol-sensitive receptors, $GABA_A$ and NMDA. Pregnenolone may, therefore, influence ethanol behavioral and molecular responses via THDOC and THP levels [387]. However, lack of overlap between THDOC and pregnenolone correlated modules suggests that gene expression results from CIE exposed BXD mice do not provide sufficient evidence to support this hypothesis. The pregnenolone correlated skyblue module contained known neurodevelopment genes, and the CIE-responsive yellow module also significantly correlated to serum pregnenolone levels. Pregnenolone's sulfate form is a negative allosteric modulator of GABAergic neurotransmission and positive allosteric modulator of glutamatergic neurotransmission [454, 455], suggesting that the effects of pregnenolone sulfate oppose those of ethanol. This finding, therefore, may suggest that pregnenolone levels are altered in response to

chronic ethanol exposure, possibly representing a compensatory mechanism to attempt to return PFC gene expression levels to a more basal state. Future studies, therefore, may involve thoroughly quantifying both serum and brain levels of pregnenolone and pregnenolone sulfate, and investigating, either through transcriptomics or by targeted quantitative RT-PCR of specific genes, the effect of chronic intermittent ethanol by vapor chamber on gene expression in the PFC.

One of the most interesting findings from network analysis of gene expression in the PFC of chronic intermittent ethanol exposed mice across the BXD recombinant inbred panel was that, of those modules significantly correlated to ethanol intake, relatively few were also significantly correlated to percent change from baseline (**Figure 30**). This is a somewhat unexpected finding given that the Becker laboratory has demonstrated that repeated cycles of CIE exposure leads to a significant escalation in ethanol intake [81]. Additionally, none of the modules that were significantly enriched for CIE-responsive genes were also significantly correlated to ethanol intake (**Figure 30**). This is also an unexpected finding given that these analyses were run with the hypothesis that gene expression changes in response to chronic ethanol exposure underlie the escalation in ethanol intake observed with repeated cycles of CIE. These new findings, however, may lead to a new hypothesis: that certain biological pathways are affected at the gene expression level by chronic ethanol exposure, but both basal and escalation of ethanol intake after CIE is regulated more by inborn or stable differences in the expression of genes in other pathways. To further investigate this hypothesis future studies will look at the expression of specific genes within those modules that correlate to ethanol consumption to identify specific candidate genes whose expression also correlates to intake, and look at whether these genes are differentially expressed at the basal level between C57BL/6J and DBA/2J mice. To get a true

measure of basal expression, the confound of vapor chamber exposure, with or without ethanol vapor, will need to be removed. This study may, therefore, be performed as a follow up experiment. Additionally, extensive genotype data from BXD mice available through the University of Tennessee's GeneNetwork resource (http://www.genenetwork.org/webqtl/main.py) will allow for expression QTL (eQTL) mapping to be performed as a follow up study that may identify regions of the mouse genome that are associated with differences in gene expression across the BXD panel. If regions are identified that contain genes significantly correlated to ethanol consumption and show significant cis-eQTL (i.e. the gene is located at the same position as the eQTL, implying cis-regulation by CIE), such genes/regions may be robust candidates for regulators of the amount of ethanol mice will voluntarily consume given the chance.

In conclusion, scale-free network analysis of microarray gene expression data of BXD RI mice revealed that modules of co-expressed genes that were significantly overrepresented for ethanol responsive genes across a genetically varying sample of mice, modules that significantly correlated to ethanol intake over the course of the study, and modules that correlate to endogenous neurosteroid measures. Further, bioinformatics analysis generated the hypothesis that chronic ethanol exposure may disrupt vasculature in prefrontal cortex, suggesting a lesser-studied affect of ethanol-induced neurotoxicity. Correlating the results of network analysis with WGCNA to endogenous neurosteriod levels also suggests that the neurosteriod precursor pregnenolone may have a greater influence on ethanol's long-term modulation of gene expression than previously thought. Differential expression analysis across the recombinant inbred panel revealed biological pathways that appear to be regulated in response to chronic high dose ethanol exposure across diverse genetic backgrounds. These pathways include the Ras signaling cascade, and Notch responsive signaling. Other biological pathways that may be

enriched among genes significantly differentially expressed across the BXD RI panel are neuroimmune response, and neuroplasticity mediated by the major histocompatibility complex. Finally, the finding that ethanol intake-correlated modules tended not to be enriched for ethanol responsive genes across the BXD panel provides support for what is known as the endophenotype hypothesis, which states that intrinsic biological differences, in this case basal gene expression levels, determine behavioral response to chronic ethanol exposure.

Chapter 6: Cross-Species Network Analysis

Introduction

One of ethanol's most well studied actions is activation of the brain's reward system through modulation of GABAergic and glutamatergic signaling. This system might be considered to control more primal behaviors such as pleasure, incentive salience, and positive reinforcement [456]. These neurotransmission pathways, their function, and response to rewarding stimuli such as ethanol are highly conserved across species [456]. It is, therefore, not surprising that patterns of ethanol-regulated gene expression have been shown to involve similar genes and synaptic signaling mechanisms between model species ranging from invertebrates [202, 203], to mammals [86, 200, 209, 212], and even fish [197, 201]. Further, these gene expression patterns may also be seen in humans with alcohol use disorder (AUD) [212].

Based on these observations, we have collaborated with other laboratories through the INIA Stress Consortium to perform a cross-species network analysis of the transcriptome response to prolonged ethanol exposure. Dr. Kathleen Grant at the Oregon National Primate Research Center has used schedule-induced polydipsia (SIP) to establish voluntary ethanol consumption in macaques [457]. Through INIA the Miles laboratory obtained PFC tissue from rhesus macaques that, following SIP induction, voluntarily drank ethanol for a period of 1 year. Microarray gene expression data from these macaques was combined with gene expression data from that of the C57BL/6J mice discussed in Chapter 3. We have used network analysis with WGCNA to identify conserved patterns of chronic ethanol responsive gene expression across mice and nonhuman primates.

As outlined in previous chapters, genomic technologies such as microarrays and scale-free network analysis have identified patterns of correlated gene expression in brain-regions of the mesocorticolimbic system and extended amygdala in response to ethanol exposure [80, 212, 230]. In C57BL/6J mice, modules of co-expressed genes were identified by scale-free network analysis in various brain-regions after four cycles of CIE [80]; and both with and without intermittent drinking, as discussed in Chapters 3 and 4. Both gene expression studies of C57BL/6J mice with CIE looked at five brain-regions, and in both studies the prefrontal cortex (PFC) showed some of the highest numbers of modules, both overall and in terms of enrichment for chronic ethanol responsive genes [80] (Chapters 3 and 4). Additionally, the largest number and strongest correlations to ethanol intake, following CIE treatment, were seen in the PFC (Chapter 4). For this reason, the PFC was chosen as the brain-region in which to perform a cross-species network analysis using Weighted Gene Correlated Network Analysis (WGCNA) [218].

WGCNA is a method for scale-free network analysis that also allows for the identification of modules of co-expressed genes shared between two networks. These types of modules are referred to as consensus modules [339]. Consensus modules are identified by forming networks of correlation matrices for each dataset separately, and grouping genes into modules based on the lower correlation between datasets [339]. This is done to avoid over-inflation of relatedness in gene expression patterns in the event that a group of genes is highly correlated in one dataset, but not the other [339]. The purpose of consensus modules is to identify common gene expression patterns between two datasets. In the case of this analysis, WGCNA was used to identify modules between C57BL/6J mice after CIE with intermittent drinking and chronic ethanol consuming rhesus macaques. Macaques were chosen due to their evolutionary proximity to humans, and because the mode of chronic ethanol exposure used is voluntary, oral, and

prolonged. Additionally, ethanol intake measures before and after chronic ethanol exposure were available for mice. Intake was assessed for baseline, and after chronic ethanol because this ethanol exposure paradigm has been shown to increase drinking with each successive exposure [239]. Ethanol intake and steroid hormone measures across the course of one year were also available for macaques. WGCNA capabilities allow for the correlation of co-expression modules to such phenotype measures.

Gene expression was quantified in the PFC of rhesus macaques and C57BL/6J mice after chronic, prolonged exposure to high dose ethanol using Affymetrix microarrays. Network analysis with WGCNA was used to identify modules of co-expressed genes across species, and across ethanol exposure models. These analyses were performed with the hypothesis that consensus modules represent pathways that show a conserved gene expression response in the PFC to chronic ethanol exposure, and that a network analysis across two species will lead to a deeper understanding of the brain's response to chronic, high-dose ethanol exposure. Network analysis revealed that regulation of neurotransmission and myelination seem to be very conserved ethanol responsive pathways across species. Bioinformatics specifically raise the possibility that Robo-Slit signaling is involved in ethanol responsive plasticity in the PFC, and that genes known to be involved in development and differentiation of neuronal and mesenchymal cells may continue to function in synaptic remodeling in the adult brain. With further study, the identification of biological processes disrupted by chronic ethanol exposure may aid in the identification of new therapeutic targets in the treatment of AUD in humans.

Methods

All cross-species studies in this chapter were done in collaboration with Dr. James Bogenpohl in the Miles laboratory, who was the primary investigator studying gene networks from rhesus microarray studies. In addition, all primate studies were done in collaboration with Dr. Kathleen Grant at Oregon Health and Sciences University. Dr. Grant devised the schedule-induced polydipsia model for obtaining high levels of ethanol intake in macaques [457], performed the behavioral and hormonal studies as well as brain tissue harvesting, and made tissue or RNA samples available to the Miles laboratory as part of a collaborative study within the Interactive Neuroscience Initiative on Alcoholism (INIA-Stress) consortium. The mouse tissue/RNA and microarray data used for these studies are as described in chapter 4 and were made available as part of a collaborative study with Drs. Howard Becker and Marcelo Lopez at Medical University of South Carolina through the INIA Stress Consortium.

Animals and Chronic Ethanol Treatments

Rhesus macaques (*Macaca mulatta*) were individually housed at the Oregon National Primate Research (Hillsboro, Oregon, USA). All housing and experimental protocols were conducted in accordance with the NIH's Guide for the Care and Use of Laboratory Animals and the Oregon Health and Science University's (OHSU) IACUC. 46 Male macaques, ages 5-11 years, were used for gene expression studies. Macaques were conditioned to drink ethanol by schedule-induced polydipsia as previously described [457]. Monkeys were trained to use an operant touch panel, and induced to drink water gradually shifting to ethanol by being given 1g banana-flavored pellets a Fixed-Time 300 sec operant schedule [457]. Scheduled pellet delivery was ceased after 6 months of training and ethanol induction. Monkeys were then given free access to water and 4% (w/v) ethanol for one year; control monkeys were given only water [457]. Ethanol

and water intake were measured using a computerized digital scale system (AV4101C, Ohaus Corporation, Pine Brook, NJ, USA). Blood samples for quantification of blood ethanol concentration were also taken every fifth day from monkeys during from the course of the experiment by voluntary presentation of the leg to allow access to the saphenous vein [457]. Additionally, blood samples were also collected once every week for measurement of the hormones cortisol, adrenocorticotropic hormone (ACTH), testosterone, deoxycorticosterone (DOC), aldosterone, and dehydroepiandrosterone sulfate (DHEA-S).

Adult male C57BL/6 mice were purchased from Jackson Laboratories (Bar Harbor, ME, USA). Mice were acclimated to the animal facility at Medical University of South Carolina (MUSC) for two weeks before undergoing any experiments. All animals were kept under a 12-hour light/dark cycle and given free access to food and water. All studies were conducted in an AALAC-accredited animal facility at MUSC, and approved by the Institutional Animal Care and Use Committee. All experimental and animal care procedures met guidelines outlined in the NIH Guide for the Care and Use of Laboratory Animals. For chronic intermittent ethanol by vapor chamber studies, mice were divided into 4 groups: the CIE Drinking group received inhaled ethanol in the vapor chambers followed by 2-bottle choice drinking, the Air Drinking group received only air in the vapor chambers and 2-bottle choice drinking, the CIE NonDrinking group received inhaled ethanol in the vapor chambers but did not drink in between CIE cycles, and the Air NonDrinking group remained ethanol naïve both in and out of the inhalation chambers. Mice in the CIE Drinking and Air Drinking groups underwent 6-weeks of 2-bottle choice drinking to establish baseline drinking levels. Mice were given ethanol for 2 hours per day. Ethanol and water intake for each individual mouse was measured daily. Following 6-weeks of baseline drinking, mice were placed in Plexiglass inhalation chambers (60x36x60 cm) 16

hours/day for 4 days. After 4 days in the inhalation chambers, mice underwent a 72-hour period of total abstinence from ethanol. Following the abstinence period, mice in the CIE Drinking and Air Drinking groups were given 2-bottle choice drinking for 2 hours per day for 5 days. A total of 4 cycles of CIE-abstinence-drinking were performed. After the end of the fourth cycle mice were sacrificed on the 5th drinking day before receiving ethanol.

Tissue Harvesting and RNA Preparation

Macaques sacrificed and necropsied after one year of open access to ethanol. Four hours after final access to ethanol, monkeys were sedated with 15 mg/kg intramuscular ketamine, prepared for surgery, and anesthetized by 20-35 mg/kg intravenous pentobarbital. Craniotomy was then performed, followed by transcardial perfusion with oxygenated buffer solution. Macaque brains were rapidly removed, brain-regions dissected, and tissue samples flash frozen. Tissue samples were then deposited into the Monkey Alcohol Tissue Research Resource (MATRR; http://matrr.com). Macaques used in this study included those from rhesus cohorts 4, 5, 7a, and 7b with age and treatment information as described above. A detailed diagram of the experimental timeline for each cohort can be found at http://matrr.com. Samples of the monkey anterior cingulate and subgenual cortices (Brodmann areas 24, 25, and 32) were obtained from MATRR. RNA was extracted from brain tissue using either RNeasy Mini Kit (Quiagen, Valencia, CA; cohorts 4 & 5) or the All Prep DNA/RNA/miRNA Universal Kit (Qiagen, Valencia, CA; cohorts 7a & 7b) according to manufacturer protocol. RNA samples were assessed for quality by capillary electrophoresis (Experion Automated Electrophoresis System, BIO-RAD, Hercules, CA-cohorts 4 & 5; or 2100 Bioanalyzer, Agilent Technologies, Palo Alto, CA-cohorts 7a & 7b).

Mice were sacrificed by decapitation on the final drinking day of the 4th CIE cycle at the time they received 2-bottle choice drinking all previous drinking days. Mouse brains were immediately removed from the skull and dissected as previously described [208] and outlined in Chapter 4. Tissues were stored at -80°C until RNA isolation. Total RNA was extracted using the RNeasy Mini Kit (Qiagen, Valencia, CA) at MUSC.

Gene Expression Microarrays

Monkey RNA samples were prepared using standard procedures outlined by Affymetrix. Samples were processed in two groups (cohorts 4 and 5, and cohorts 7a and 7b) consisting of a total of 8 microarray processing batches. Arrays randomized within each array batch by treatment group and cohort to minimize batch effects. Gene expression was measured using Affymetrix GeneChip® Rhesus Macaque Genome Arrays. Arrays were scanned at 2.5 µm pixilation with an Affymetrix GeneChip Scanner 3000 7G. Arrays probes were prepared and hybridized by the VCU Molecular Diagnostics Laboratory.

Affymetrix GeneChip® Mouse Genome 430, type 2 arrays were used to measure gene expression. Sample preparation, hybridization, and array scanning were performed at the MUSC ProteoGenomics Core Facility according to Affymetrix protocols. Each brain-region was processed separately, with treatment groups randomized to minimize batch effects. Array data was transferred to Virginia Commonwealth University (VCU) in .CEL file format for further analysis.

Microarray Analysis

All arrays were analyzed using The R Project for Statistical Computing (http://www.r-project.org/). Dr. James Bogenpohl in the Miles laboratory performed detailed quality control

studies, generated RMA values and performed initial statistical analyses on macaque arrays as described below. Each macaque arrays were assessed for quality based on 3'/5' ratios for the housekeeping genes ACTB and GAPDH, and percent present probes for each probeset on the array. Rhesus arrays were background corrected with the Robust Multi-array Average (RMA) method [256] and quantile normalized using the 'affy' package for R [255]. Principal component analysis was then used to identify any batch effects within the data. Examination of first and second principal components with multi-dimensional scale plots showed evidence of batch effects for array hybridization batch and cohort. These effects were corrected using ComBat for hybridization batch [257], which successfully removed batch effects for both hybridization batch and cohort. Macaque arrays were analyzed for differential gene expression between ethanol-drinking and control animals using Linear Models for Microarrays (LIMMA) [258] with Multi-Experiment Viewer (MeV) software by Dr. James Bogenpohl. Probesets were considered significantly differentially expressed at an FDR ≤ 0.01.

Affymetrix GeneChip® Mouse Genome 430, type 2 arrays were also analyzed with R as described in Chapter 3. Microarray quality was assessed by RNA degradation, average background, percent present probesets, and multi-dimensional scale plots (first principal component by second principal component). Arrays showing low quality measures, or that appeared to be outliers, were removed from the dataset. Background correction using Robust Multi-array Average (RMA) and quantile normalization was performed using the 'affy' package for R. ComBat by hybridization batch was used to correct for any batch effects present in the data [257]. Differential gene expression was determined by LIMMA using the 'limma' package for R. LIMMA comparisons between each possible comparison between the 4 treatment groups

of C57BL/6J mice were made, as well as, one-way ANOVA to compare all groups for any difference was performed. For the purposes of this analysis, results of one-way ANOVA were used FDR ≤ 0.01.

Weight Gene Correlated Network Analysis

Consensus WGCNA was run on mouse and macaque arrays as described in [226]. Probesets from both mouse and macaque arrays were curated to include only those probesets within genes that had recorded homologs in both species. Gene homology data from Ensembl BioMart (http://www.ensembl.org/biomart) and NCBI Homologene (http://www.ncbi.nlm.nih.gov/homologene) were used to identify homologous genes. Multiple probesets were then eliminated based on maximal expression using the collapseRows() function in WGCNA [458]. Arrays were then filtered to exclude probesets with RMA values ≤ 3.75 in at least 80% of macaque samples. Of these, only 1% showed expression values ≤ 3.75 in at least 80% of mouse arrays. These filtering steps lead to a final list of 10,990 genes (**Suppl. Table S30**). Consensus WGCNA was then run on 43 macaque arrays (32 ethanol drinking, 11 control), and 47 mouse arrays (23 CIE, 24 control). To ensure datasets were on a similar scale, the mouse topological overlap matrix was scaled to that of the macaques. A soft-thresholding power of 8 was chosen based on the data fit to scale-free topology as described in [218]. A deep-split value of 3 was chosen using principal component analysis as described in previous chapters. Multidimensional scale plots using first and second principal components were used for the x and y axes. A deep-split where there were no overlaps between modules was then chosen. Consensus modules were the compared for overlap to significantly differentially expressed genes in mice, and in macaques. Overlap was assessed using hypergeometric overlap. The Bonferroni

method was applied to correct for multiple testing. Modules with Bonferroni corrected p-values $\preceq 0.05$ were considered significantly enriched for ethanol responsive genes.

Bioinformatics

Mouse/macaque consensus modules identified by WGCNA were for functional enrichment using the ToppGene Suite's Topp Funn tool (https://toppgene.cchmc.org/) by postdoctoral fellow Dr. James Bogenpohl at the Miles laboratory. Functional enrichment analysis was performed with a p-value cutoff of 0.01 within the ontological categories Molecular Function, Biological Process, Cellular Component, Human Phenotype, Mouse Phenotype, Pathway, Gene Family, and Disease, focusing on ontologies containing between 3 and 1000 genes. ToppFun results were processed to decrease complexity and merge redundant categories using REVIGO (http://revigo.irb.hr/). In REVIGO an output list size of small (0.5) was used. All other settings were left at default.

Cell-type Enrichment Analysis

Dr. James Bogenpohl in the Miles laboratory performed cell-type enrichment analysis on consensus WGCNA modules by hypergeometric overlap using the userListEnrichment() function [260]. Gene expression data was taken from two previous studies of cell types in mouse cortex. One used Affymetrix 430, type 2 arrays to assess gene expression FACS sorted brain-cells [341]. Data from these arrays were filtered to only include only genes with a 3+ fold enrichment in each cell type. The second dataset came from single-cell RNAseq of mouse cortex and hippocampal cells [459]. The Bonferroni correction was used to account for multiple testing. Modules with Bonferroni corrected p-values $\preceq 0.05$ were considered significantly enriched for gene expressed in a certain cell-type.

Results

Chronic Ethanol-Responsive Genes

Two-factor LIMMA was run on the macaque arrays by Dr. James Bogenpohl at the Miles laboratory. 2,294 probesets were determined to be significantly ethanol responsive at FDR ≤ 0.01. On the mouse arrays, one-way ANOVA using the 'limma' package revealed 2787 significantly differentially expressed probesets at FDR ≤ 0.01 (**Suppl. Table S31**). Due to the large number of significant probesets, ethanol responsive genes were used for overlap with consensus WGCNA modules to help determine which modules represented chronic ethanol responsive pathways in PFC.

Consensus Weighted Gene Correlated Network Analysis

15 consensus modules were identified from WGCNA on mouse and macaque arrays as described. Of these, only one module significantly correlated to average ethanol intake in the macaques. Many more consensus modules, however, were significantly correlated to ethanol intake in the mice, particularly after the 4th CIE cycle **(Figure 32)**.

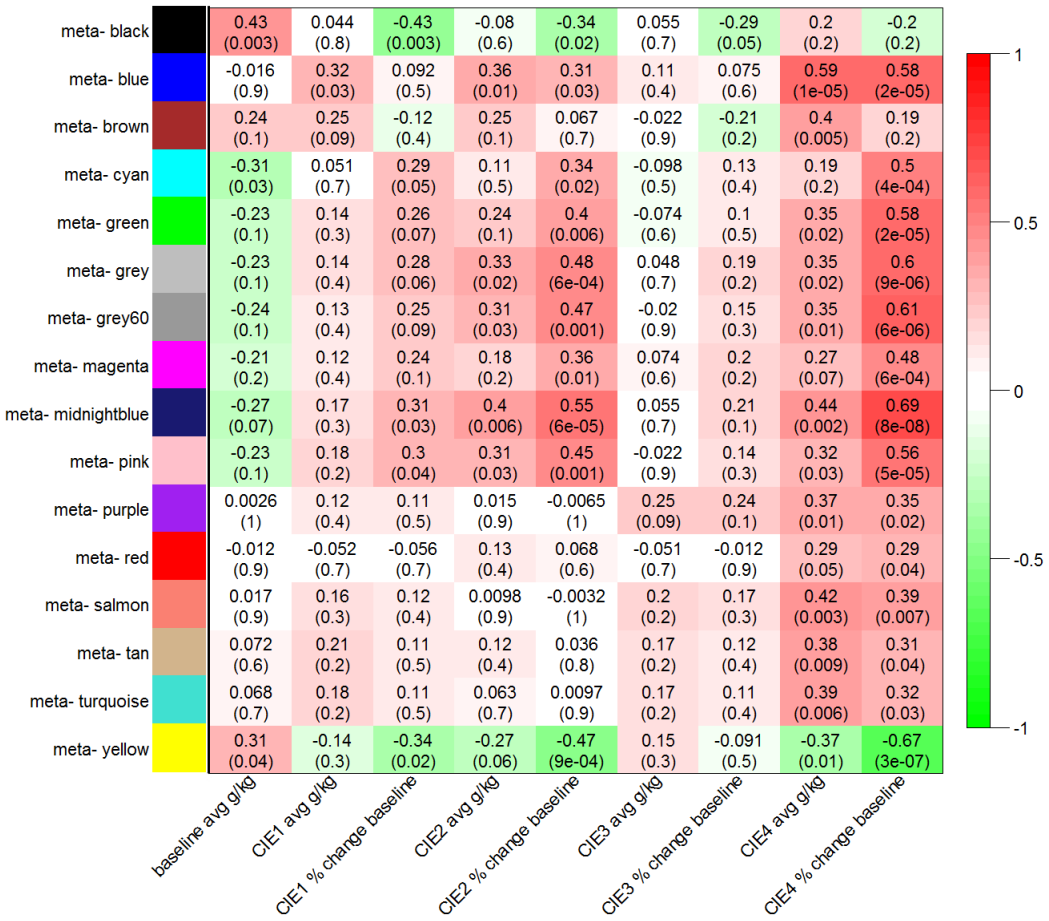

Figure 32: Heatmap of Consensus Module Correlation to Mouse Ethanol Intake. "meta" modules refer to consensus modules. Cell color indicates Spearman rank correlation.

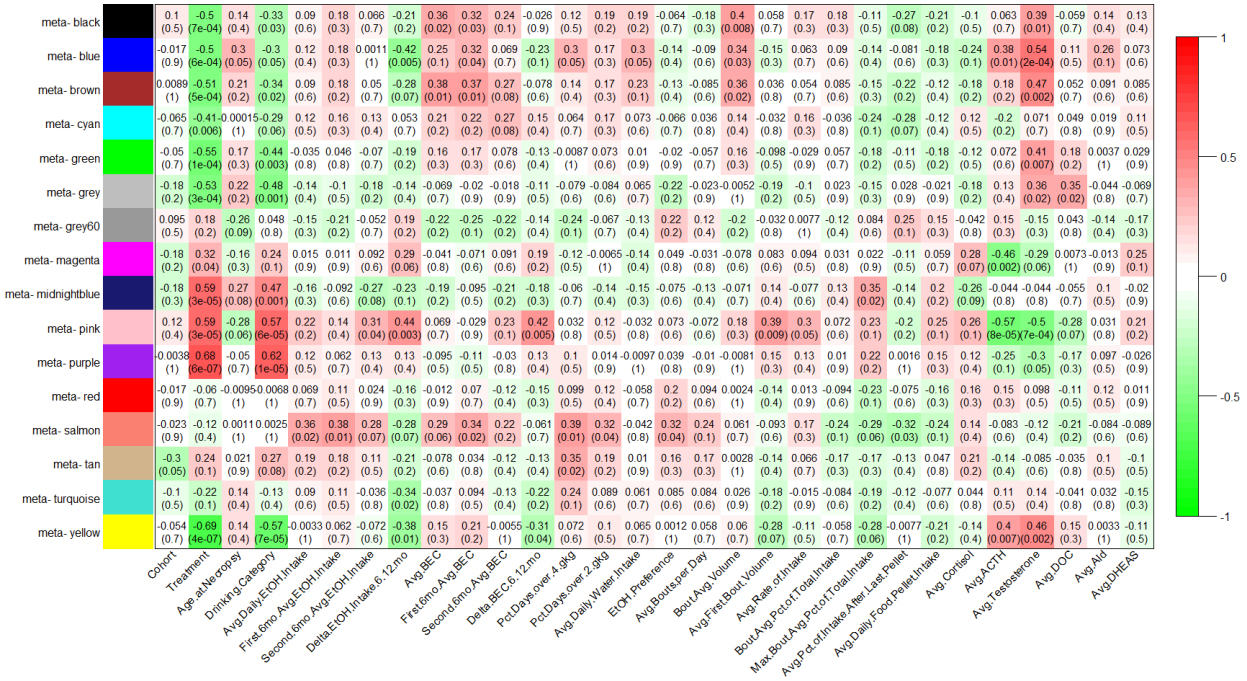

Figure 33: Heatmap of Consensus Module Correlation to Macaque Ethanol Intake. "meta" modules refer to consensus modules. Cell color indicates Spearman rank correlation.

The salmon module was significantly correlated both to macaque average daily ethanol intake (r=0.36, p-value=0.02), and to mouse ethanol intake after the 4th CIE cycle (r=0.42, p-value=0.003) and percent change from baseline (r=0.39, p-value=0.007) (**Figure 32-33**). This module was functionally enriched for genes involved in both GABAergic and glutaminergic signaling (**Suppl. Table S32**). GRIN2B, one of the major subunits of the NMDA receptor, was present in this module [106, 127]. Interestingly, GABRB3 was also present in this module. This gene encodes the beta 3 subunit of the $GABA_A$ receptor. Previous research into any possible link between this subunit and AUD has shown variable results [111, 460, 461]. This module also showed significant overlap with several gene ontology (GO) categories related to female sexual development and regulation of the estrous cycle (**Suppl. Table S32**). Specific genes within these categories that were in the salmon module, UBE3A, SLIT3, and ROBO2, have also been found to regulate neurodevelopment and axon guidance in the forebrain, particularly the olfactory bulb

[462]. Indeed, the salmon module also significantly overlapped with four GO categories related to olfactory bulb development and one related to overall forebrain development **(Figure 34)**.

Figure 34: REVIGO Treemap of Consensus Salmon Module. Gene Ontology categories are hierarchically grouped based on semantic similarity. Block size reflects number of GO categories in an overall group.

The yellow, turquoise, and purple modules were significantly correlated to ethanol intake after the 4th CIE cycle in mice. In macaques the yellow and turquoise modules also showed a significant negative correlation to change in daily ethanol intake during the last 6 months of the study, but not overall average daily intake (**Figure 33**). Functionally, all 3 of these modules showed enrichment for GO categories related to regulation of transcription and translation (**Suppl. Table S32**). Other modules with significant correlation to ethanol intake post 4th CIE cycle and percent change from baseline with similar functional enrichment were blue, grey60, pink, and tan (**Figure 32**). These modules were enriched for genes involved in developmental regulation in the brain including neurogenesis and axonogenesis (**Suppl. Table S32**). Correlations to macaque data was mostly unremarkable, though the blue module showed some

significant positive correlations to BEC, ethanol bout volume, change in ethanol intake from 6 to 12 months, water intake, ACTH levels, and testosterone levels (**Figure 33**). This module also showed significant positive correlation to age at necropsy. The correlations to ethanol and water intake, BEC, and hormone levels may, therefore, be explained by age related variation in hormone production and ethanol metabolism in macaques. Mice, however, were age matched, so further studies will be required to determine if co-expression of genes in this module is driven by variation in macaque age or ethanol response. The grey60 module was also highly enriched for genes involved in neurodevelopment and neuron differentiation. The exact genes within these categories, however, were very interesting as many are also involved in development and differentiation of bone, eye, and connective tissue (COL3A1, BMP7, LUM, OMD, FN1, CRABP2, OGN, ZIC2) [463-467]. The tan module was significantly correlated to mouse ethanol intake during CIE cycle 4 (r=0.38 , p-value=0.009), and percent change from baseline to CIE cycle 4 (r=0.31 , p-value=0.04) (**Figure 32**). Correlation of this module to macaque phenotype data showed only significant correlation to percent days consuming over 4 g/kg ethanol (r=0.35, p-value=0.02) (**Figure 33**). With cell-type analysis, this module showed significant enrichment for genes expressed in both astrocytes and oligodendrocytes, suggesting it is a glial-cell specific module driven mostly by mouse gene expression (**Table 9, Suppl. Table S33**).

Table 9: Cell-type enrichment for consensus modules.

Consensus Module	Cell-type	Bonferroni Corrected P-value
Black	Oligodendrocyte	3.32e-77
Brown	Oligodendrocyte	8.82e-23
Pink	Neuron	7.15e-14
Magenta	Neuron	4.74e-10
Tan	Oligodendrocyte	2.60e-06
Tan	Astrocyte	4.38e-05
Cyan	Astrocyte	1.19e-04
Cyan	Oligodendrocyte	2.73e-03
Brown	Neuron	3.09e-02

The magenta module correlated to percent change in drinking from baseline between CIE cycles 2 (r=0.36 , p-value=0.01) and 4 (r=0.45 , p-value=6e-04) in the mouse. In the monkey, this module significantly correlated to ACTH levels across the study (r= -0.46, p-value=0.002), as well as marginal correlation to change in ethanol intake between 6 and 12 months, cortisol, and testosterone levels **(Figure 33)**. Functionally, this module was enriched for genes involved in neurotransmitter signaling including two subunits of the $GABA_A$ receptor complex (GABRAB1 and GABRA1), a few voltage gated potassium channel genes, and calcium dependent protein phosphatase genes **(Suppl. Table 32)**. Cell-type enrichment analysis showed that this module was significantly overrepresented for genes expressed in neurons, supporting the possibility that this module represents the gene expression effect of chronic ethanol on synaptic signaling genes (**Table 9, Suppl. Table S33**). Additionally, the correlation to ACTH and cortisol levels in monkey suggests that expression of genes in this module may be influenced by stress hormone response, a hypothesis supported by the presence of the corticotropin releasing hormone gene in the magenta module (**Suppl. Table 32**).

Cell-type enrichment analysis showed that the black module was highly enriched for genes expressed in oligodendrocytes (**Table 9. Suppl. Table S33**). Bioinformatics analysis supports this result. This module significantly overlapped with several GO categories related to myelination, demyelinating diseases, and human and mouse phenotypes related to neuron ensheathment (**Suppl. Table S32, Figure 35**). This module contained multiple genes expressed in oligodendrocytes such as MBP, MOG, MAG, MAL, GAL3ST1, FA2H, TF, LPAR1, NDRG1, CD9, ASPA, UGT8, QKI, MYRF, PLP1, CNTN2, and JAM3 [341, 459]. In terms of correlation to phenotypes, this module significantly correlated to monkey BEC, testosterone levels across the study, average bout volume (r=0.4, p-value=0.008) (**Figure 32**). In mice, the black module

correlated most significantly to baseline drinking (r=0.43, p-value=0.003). After CIE exposure this module switched from a positive to negative correlation, and decreased in significance with each successive CIE cycle (**Figure 32**).

Figure 35: REVIGO Treemap of Consensus Black Module. Gene Ontology categories are hierarchically grouped based on semantic similarity. Block size reflects number of GO categories in an overall group.

Overall, the bioinformatics analyses of all identified consensus modules revealed some very specific patterns of functional enrichment. Several modules were enriched for regulation of transcription and translation reflecting the effect of ethanol on brain gene expression. Regulation of neurotransmission and neurodevelopment also appeared as a functional category in multiple modules, indicating that prolonged, high-dose ethanol exposure leads to alteration in synaptic function across species. Cellular respiration, myelination, and blood vessel development also

appeared, suggesting that these cellular processes are significantly affected by chronic ethanol **(Figure 36)**.

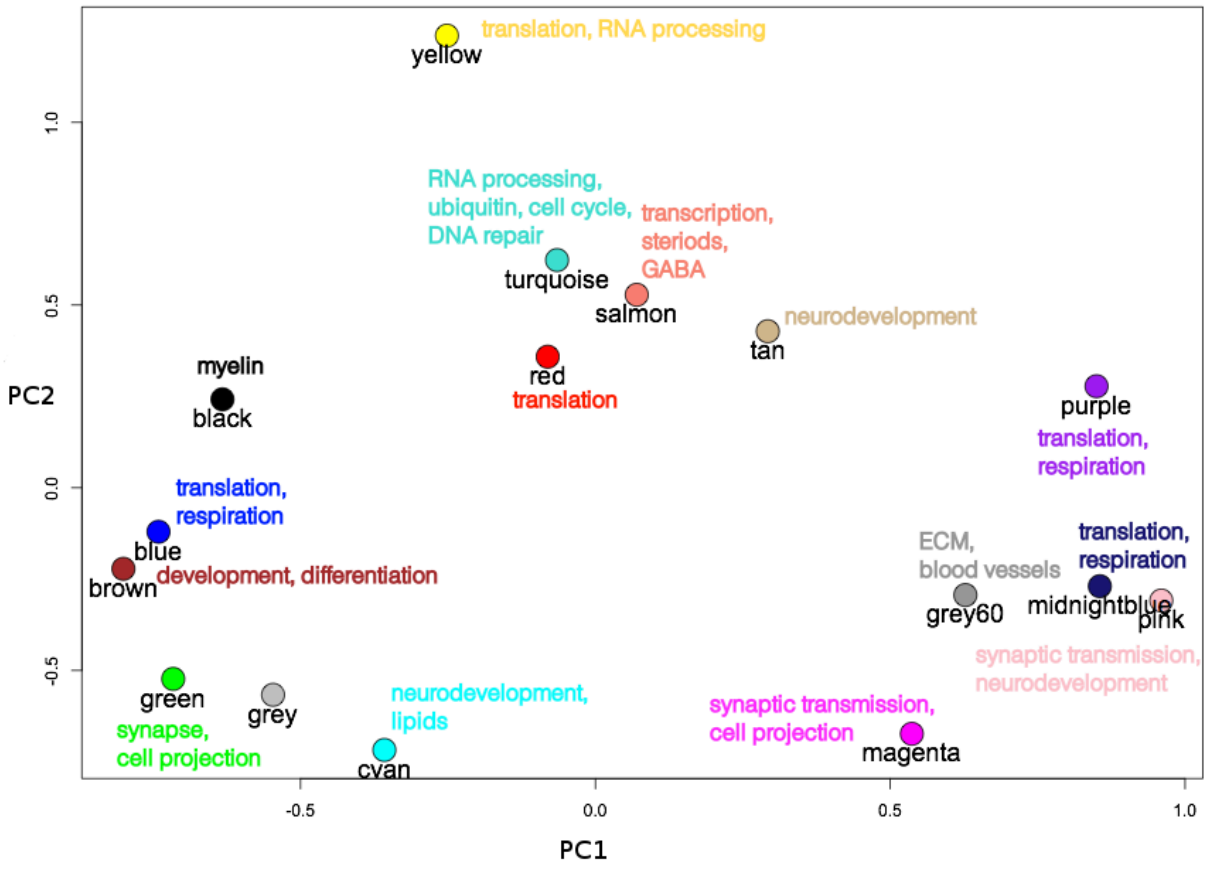

Figure 36: Multidimensional scale plot with summary of bioinformatics results. X and y axes = 1st and 2nd principal components.

WGCNA-Ethanol Responsive Gene Overlap

Consensus modules were compared for overlap to significantly differentially expressed genes in mice, and macaques. The salmon and blue modules were significantly enriched for mouse ethanol responsive genes. In contrast, the brown, turquoise, yellow, blue, green, red, purple, and midnightblue modules were significantly enriched for macaque ethanol responsive genes. This finding, along with the relative lack of correlation to intake in macaques, raises the intriguing possibility that consensus module formation was driven by genes correlated to ethanol intake in

mice, but the macaque contribution was driven more by genes that are significantly ethanol responsive (**Figure 37, Suppl. Table 34**).

Black 113	Blue 215	Brown 204	Cyan 47	Green 123
Grey60 35	Magenta 83	Midnightblue 46	Pink 111	Purple 83
Red 115	Salmon 48	Tan 50	Turquoise 593	Yellow

Figure 37: Table of all consensus modules. Modules enriched for mouse (blue) and macaque (yellow) ethanol response highlighted. Green highlighted cells indicate enrichment for genes significantly differentially expressed in both species.

Discussion

These analyses outline the use of two powerful model organisms for alcohol use disorder research. These module organisms were exposed to high-doses of ethanol over long periods of time using paradigms that have previously been shown to lead to escalations in ethanol intake [81, 457]. Expression at the mRNA transcript level was measured using gene expression microarrays. In addition to standard differential gene expression analysis using LIMMA, network analysis with WGCNA allowed us to identify patterns of correlated gene expression across species. This approached led to the identification of consensus modules, groups of genes with correlated expression in the PFC of both model organism species and ethanol exposure methods. Functionally, these modules tended to represent specific biological processes such as regulation of transcription and translation, neurodevelopment including myelination, regulation of neurotransmission, cellular respiration, and blood vessel development **(Figure 36)**. These findings suggest that these processes reflect the conserved response to prolonged ethanol exposure in neural tissue. More in depth examination of specific genes within these modules helped to identify signaling cascades that may mediate the cellular response to ethanol exposure.

We found that modules overlapped with previously characterized data on gene expression patterns in specific neural cell-types [341, 459], demonstrating that network analysis with WGCNA can identify cell-type specific responses across species even in mixed tissue samples.

The gene content of the only module that correlated with ethanol intake in both mice and macaques (salmon), raises the intriguing possibility that the Robo-Slit signaling pathway is disrupted by prolonged ethanol exposure across species. This pathway has been shown to be important in axon guidance and neurodevelopment in multiple brain-regions including the neocortex [468-470]. This pathway has not been extensively associated with alcohol exposure, although the effect of early alcohol exposure on olfactory bulb development is quite extensively studied in fetal alcohol research [471-475]. This connection is significant because Robo-Slit signaling is important in olfactory bulb development [462]. Findings from this cross-species analysis, therefore, raise the possibility that this signaling pathway in the PFC underlies chronic ethanol behaviors such as increased consumption even in adults.

In this study, a module enriched for some very well known myelin genes including structural components of the CNS myelin sheath was identified across species. This module, the black module, supports findings from previous studies at the Miles laboratory that myelin genes are significantly disrupted by ethanol in the PFC [86]. In mice exposed to chronic ethanol, a coherent network of ethanol responsive myelin genes was identified [86] (van der Vaart et al. – in press, Miles et al. – in preparation). Additionally, network analyses of rhesus gene expression data alone identified a module highly enriched in myelin genes (Bogenpohl & Smith et al. - in preparation). Networks containing a significant number of myelin genes were also identified in the C57BL/6J time-course study (Chapter 3) [80], and in the BXD network analysis discussed in

Chapter 5. Together with previous observations that white matter tracts in certain brain-regions are reduced in human alcoholics, and the fact that specific demyelinating diseases associated with heavy drinking and alcohol use disorder are recorded, these studies all support the hypothesis that cerebral myelination is a biological process disrupted by ethanol exposure and, furthermore, that basal myelin expression may be a "risk factor" influencing initial sensitivity to ethanol and ethanol consumption rates. Further, the *Clic4* gene was also sorted into the black module. *Clic4* is a chloride intracellular channel. The function of this gene's product is still the subject of investigation [476]. However, *Clic4* and its orthologs have been associated with ethanol response in a study of multiple model organisms, and shown to have variable expression in response to ethanol exposure across the BXD mouse panel, and in C57BL/6J and DBA/2J progenitors in PFC [337]. CLIC4 protein was also detected as part of the human and mouse myelinome in a proteomic study of CNS white matter [477]. These results, along with the presence of *Clic4* in the myelin enriched black module provides further evidence for the role of *Clic4* in myelination.

Finally, that more consensus modules significantly overlap with genes differentially regulated by ethanol in the macaque, while more consensus modules were significantly correlated with ethanol intake in mice, may support previous findings. The BXD mouse analysis discussed in Chapter 5 found that co-expression modules in the PFC tend to either be enriched for ethanol responsive genes or significantly correlated with ethanol intake, but not both. This same pattern was seen in network analysis of the Rhesus arrays only with WGCNA performed by Dr. James Bogenpohl (Bogenpohl&Smith et al – in preparation). These results may, therefore, provide further support for the endophenotype hypothesis [478]. This hypothesis states that intrinsic

differences in individual biological function, for example variation in gene expression due to genetic differences, may underlie voluntary ethanol intake more than genes whose expression is altered in the presence of ethanol. Alternatively, one could propose that expression of networks such as the myelin-related black module may influence initial ethanol sensitivity (and therefore consumption), and that perturbation of the expression of other networks could contribute to the mechanisms of excessive consumption, even if the expression of genes in those networks do not ultimately show a correlation with chronic ethanol consumption rates.

Here we have presented a cross-species network analysis that has identified groups of co-expressed genes in the PFC of two mammalian species. We have also produced the first analysis of modules of co-expressed genes correlating to ethanol intake in both species, and explored whether any modules identified were enriched for ethanol responsive genes in either species. The only consensus module correlated to ethanol intake in both species was functionally enriched for genes involved in Robo-Slit signaling; an ethanol correlated pathway also identified in PFC transcriptome data from BXD RI mice (Chapter 5). Most importantly, this analysis demonstrates that neurotransmission, transcription and translation, cellular respiration, and myelination are biological processes that show a conserved response to long-term, high-dose ethanol exposure in both species. Future studies will focus on exploring highly connected hub genes within these modules to identify potential targets that may be manipulated by pharmacologic or genetic techniques. We will then examine the effect of altering hub gene expression in the PFC on both ethanol responsive gene expression, and on voluntary consumption, in order to better determine whether basal differences in expression of hub genes affects the network's ethanol response, and, in turn consumption. Due to their shorter life span and availability, such follow up studies will

most likely be done in mice, however, appropriate model organisms will be determined based on candidate genes selected. This approach will, hopefully, aid in the identification of specific target genes that affect consumption, and may be pharmacologically tractable in humans.

Chapter 7: Final Conclusions and Future Directions

Alcohol use disorder is a chronic, relapsing condition of significant biomedical and socioeconomic consequence. Key to this disorder is the widespread effect on the mesocorticolimbic system and extended amygdala. This system has been shown to be involved in cognitive processes such as reward, reinforcement, incentive salience, and aversion-related cognition [190, 351, 456]. In the context of AUD, alcohol stimulates dopamine release, mediating the positive-reinforcing effects of the substance in the short-term, and, with repeated exposure, long-term changes in dopaminergic neurotransmission occur to compensate for the effects of alcohol exposure [67]. These systems then begin to operate in ways that are aberrant without the effect of alcohol, leading to physical and psychological symptoms known as withdrawal. Individuals, in response, continue to consume alcohol to avoid withdrawal symptoms, in a process known as negative-reinforcement [190]. Over time, alcohol use escalates to where an individual is physiologically dependent on the substance, resulting in the collection of physical and behavioral symptoms that constitute AUD [1, 238].

Research using technologies such as microarrays have demonstrated in model systems from cultured cells to model organisms and human autopsy tissue that the effect of alcohol exposure on neural cells begins at the level of mRNA gene expression. Across several brain-regions within the mesocorticolimbic system and extended amygdala, alcohol has been shown to significantly change the level of expression of hundreds to thousands of genes [86, 194, 195, 208, 210]. Other studies have demonstrated that alcohol affects neurotransmission mediated by GABAergic, glutamatergic, acetylcholine, serotonin, endocannabinoid and calcium dependent signaling in neurons, and that the function of glial cells, which potentiate synaptic signaling by modulating synaptic transmission in the case of astrocytes; and insulating neuron projections in the case of

oligodendrocytes, is also affected by alcohol [176, 187]. Taken together with gene expression findings, these results indicate that alcohol affects multiple biological pathways in the brain. The challenge, therefore, was to tease out these responses, and identify specific pathways that may represent targets for pharmacological intervention in the treatment of AUD.

In this dissertation we have described a series of studies using the systems biology technique of network analysis to explore the gene expression response to chronic ethanol exposure across two model organism species in brain-regions of the mesocorticolimbic system and extended amygdala with special emphasis on the prefrontal cortex. These analyses have revealed that certain cellular signaling processes such as neurotransmission, neuron ensheathment, and regulation of transcription and translation show conserved gene expression response to chronic ethanol exposure in the PFC of both rodents and nonhuman primates, suggesting that these are evolutionarily conserved responses. A multi brain-region study of the time-course gene expression response to repeated cycles of high dose ethanol exposure in C57BL/6J mice revealed that lasting changes in gene expression are seen in the PFC and HPC. Bioinformatics analyses of these gene expression changes have identified patterns of correlated gene expression representing neurotransmission, neurodevelopment, and neuroimmune response. These studies have also helped identify highly connected candidate genes within co-expression modules, and potential microRNA regulators of the genes within these modules. A similar analysis of microarray expression data from C57BL/6J mice under chronic intermittent ethanol by vapor chamber that also received limited access two-bottle choice drinking revealed modules of correlated gene expression that correlate to ethanol intake after chronic high-dose exposure, particularly in the PFC and NAC. This study showed that, across brain-regions, those modules most strongly correlated to ethanol intake tended to be those enriched with genes known to

regulate synaptic transmission. This finding seemed to suggest that long-term gene expression changes in neurotransmission regulation, in response to chronic high-dose ethanol exposure, underlie the escalation in drinking behavior seen in this rodent model, and, potentially, in alcohol abusers. However, this finding was somewhat contradicted by network analysis of gene expression in the PFC of a panel of recombinant mice derived from two inbred mouse lines that vary significantly in their ethanol response. Transcriptome data from the PFC of BXD RI mice revealed that many genes, representing certain biological processes, are significantly regulated by ethanol across a variable genetic background. This study also showed that co-expression modules identified by WGCNA tended to either correlate strongly to ethanol intake, or were significantly overrepresented for ethanol responsive genes across the panel, but not both. This finding raises the interesting possibility that, as observed with cross-species network analysis, those processes whose gene expression is regulated in response to chronic ethanol exposure are conserved. However, this gene expression response may not necessarily regulate ethanol drinking behavior. Instead, ethanol consumption may be largely determined by basal differences in the expression of certain genes. These differences in gene expression are thought to, in turn, lead to variation in certain cellular processes, and that this variation in tissue function is what underlies individual differences in both baseline ethanol consumption, and escalation in drinking observed after multiple cycles of high-dose ethanol exposure and abstinence [239, 244]. This model of the relationship between gene expression and drinking behavior is known as the endophenotype hypothesis [478].

These series of experiments, data generated from them, and network analysis techniques used to discover patterns within these data lead to a number of possible routes for future research. One of the most obvious routes is to utilize the microarray data from BXD RI mice to further explore the

effect of genetic variation on basal and chronic ethanol responsive gene expression. This can be done using the genetical-genomics technique of expression QTL mapping [479]. QTL mapping on the BXD panel has been used previously at the Miles laboratory, in collaboration with other investigators at VCU to identify a polymorphism in the *Chrna7* gene that correlates to nicotine induced conditioned place preference [480]. BXD mice have also been used to identify a cis-QTL on a region of mouse chromosome 12 that correlates to anxiolytic-like response to acute ethanol exposure, and examination of genes within this region lead to the identification of *Ninein* as a candidate gene in ethanol's anxiolytic response [481]. *Ninein* also showed significant differences in expression between C57BL/6J and DBA/2J [481]. Similar analyses, using gene expression as the behavior, and utilizing the extensive SNP data on the BXD RI panel available through the University of Tennessee's GeneNetwork (http://www.genenetwork.org/webqtl/main.py), will likely be the first follow up analysis to accompany the differential gene expression, and network analysis results of CIE exposed BXD mice. This analysis may lead to the identification of genes with polymorphisms that modulate their basal level of expression, and, in turn, influence the amount of ethanol an individual mouse will voluntarily consume. This sort of study would be performed with the hypothesis that such genetic analysis increases the likelihood that a given gene indeed functions in ethanol behaviors such as progressive consumption. Furthermore, polymorphisms in homologous genes in humans may represent risk factors for the development of AUD.

Another needed future study on the BXD mice that underwent CIE would be to expand our gene expression studies with microarrays to other brain-regions. Along with the analyses outlined in Chapters 3-5, previous microarray studies of ethanol responsive gene expression across multiple brain-regions have revealed that ethanol exposure affects different brain-regions in different

ways [247]. The nucleus accumbens and ventral tegmental area are extensively studied in alcohol research because they are central regions in the brain's reward pathway, and alcohol consumption leads to dopamine release in the NAc shell from neurons that originate in the VTA [187]. However, olfactory bulb tissue was also collected from BXD RI mice that underwent 5 cycles of CIE by vapor chamber with 2-bottle choice drinking. WGCNA results from both BXD PFC, and consensus modules in mouse and macaque PFC, contained genes within the Robo-Slit signaling pathway such as *Robo2, Slit3*, and *Ube3a* [469, 482, 483]. The Robo-Slit signaling pathway is known to be involved in axonal guidance, particularly in the olfactory tract [462, 468, 470]. The olfactory bulb and olfactory tract does not directly influence PFC signaling, however, it is believed to receive inputs from multiple areas of the neocortex [484-486]. Olfactory regions of the brain are not as widely studied as mesocorticolimbic regions in alcohol research, however, this brain-region has been studied in relation to the effects of fetal alcohol exposure on sensory perception and ethanol intake later in life [487]. In rodent studies, prenatal and neonatal ethanol exposure resulted in impaired odor discrimination and reduced olfactory bulb size in adulthood [471, 474, 488]. Prenatally exposed rats also consumed significantly more ethanol than matched controls in certain studies [489]. Early alcohol exposure has also been shown to cause altered alcohol odor response in human infants [472]. Fetal alcohol exposure has also been repeatedly documented to increase risk for heavy drinking later in life [489]. The mechanism by which this occurs is still under study, however, alcohol olfactory cues have been shown to increase neural activity, measured by fMRI, in the NAc and VTA [473], and impairs inhibitory control in high drinkers [475]. The influence of olfactory cues on long-term ethanol response, including increased intake, may, therefore, be an important area of future study for the identification of new therapeutic targets.

Another area of potential future study is that of miRNAs as regulators of chronic ethanol responsive co-expression networks. The role of miRNAs in ethanol response, and their link to behaviors is a somewhat recent area of study. In 2008, Pietrzykowski *et al.* showed that alcohol exposure modulates the expression of the BK potassium channel isoforms via miR-9 in culture, and used computer modeling to suggest that this switch in BK isoform population may contribute to increased alcohol tolerance [490]. Since this report, gene expression studies *in vivo* have been used to identify miRNAs with altered expression after ethanol exposure in human alcoholics [491], and rodent models [294, 492]. In 2016, a study of a Mediterranean population identified a polymorphism in the miR-27a sequence that was significantly associated with alcohol consumption [493]. In rats, *miR-206* has been shown to be upregulated in PFC following repeated ethanol exposures, and to increase ethanol self-administration via inhibition of *Bdnf* expression [273]. *miR-30a-5p*, another miRNA with a complementary binding site in the 3' URT of *Bdnf*, was also demonstrated to increase voluntary ethanol intake in mice [272]. These studies suggest that *Bdnf* is a target of miRNA in response to ethanol exposure. As discussed in Chapter 3, our network analysis of gene expression in PFC of C57BL/6J mice after multiple cycles of CIE represents one of the first published studies suggesting that *Let-7* miRNAs may regulate a chronic ethanol responsive co-expression network that includes *Bdnf* as a hub gene [80]. Initial qPCR studies at the Miles laboratory suggest that *Let-7c-1* is significantly regulated by repeated cycles of CIE in male C57BL/6J mice (**Figure 10)**. One potential future study would involve overexpressing *Let-7c-1* in mouse PFC by delivery of an AAV plasmid via stereotactic surgery [337], and then investigating the effect of this modulation on ethanol consumption with/without vapor chamber exposure. The effect of overexpressing *Let-7c-1-3p* on PFC gene expression could then be assessed using microarrays or RNAseq to validate the role of this miRNA in

regulating the Bdnf network. Studies such as these would represent important pre-clinical assessments of the efficacy of *Let-7c-1* as a potential target for the treatment of excessive alcohol consumption.

Using a network-based approach, we have outlined an extensive study of transcriptome networks that are regulated in response to chronic, intoxicating levels of ethanol delivered by vapor chamber. We have explored the time-dependent effect of multiple CIE cycles across multiple brain-regions, and looked extensively at the relationship between long-term gene expression and ethanol intake, in C57BL/6J mice. These analyses where then expanded to account for the effect of genetic background on the gene expression response chronic ethanol in PFC. The conserved gene expression response in the PFC was then determined by identifying co-expression networks preserved in both mice and rhesus macaques that were exposed to prolonged, high-dose ethanol. These studies have led to several new candidate genes, pathways, and even miRNAs as possible regulators the gene expression response to ethanol exposure, and may, in time, open up new areas to study in the field of alcohol research.

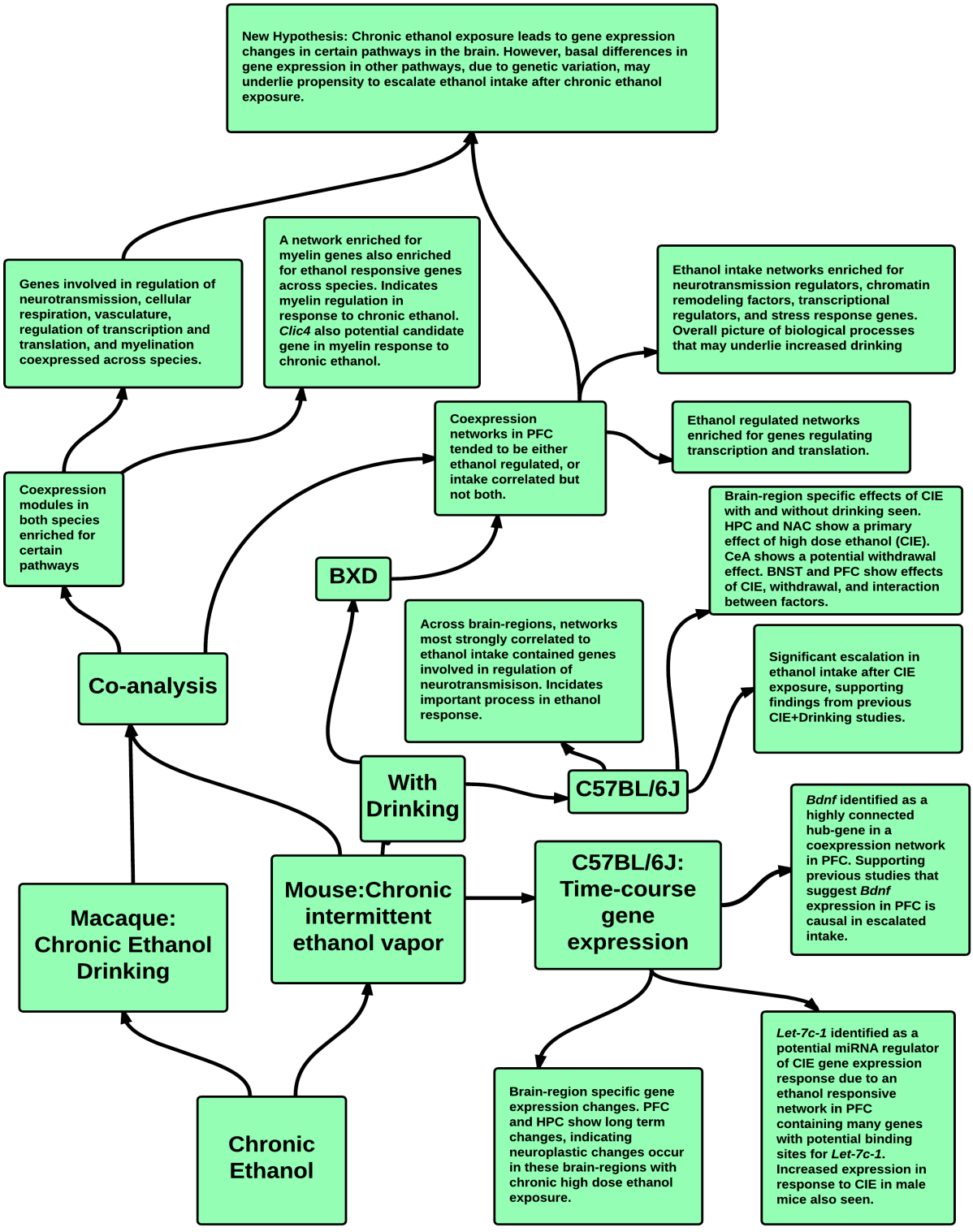

Figure 38: Diagram summarizing findings from all gene expression experiments and conclusions drawn.

Literature Cited

Literature Cited

1. American Psychiatric Association, A.P.A.D.S.M.T.F. *Diagnostic and statistical manual of mental disorders : DSM-5*. 2013; Available from: http://dsm.psychiatryonline.org/book.aspx?bookid=556.
2. WHO, *Global Status Report on Alcohol and Health 2014*. 2014, World Health Organization: Luxembourg.
3. Manasco, A., et al., *Alcohol withdrawal.* South Med J, 2012. **105**(11): p. 607-12.
4. SAMHSA, *Behavioral Health Trends in the United States: Results from the 2014 National Survey on Drug Use and Health*. 2015, Department of Health and Human Services.
5. Sacks, J.J., et al., *2010 National and State Costs of Excessive Alcohol Consumption.* American Journal of Preventive Medicine. **49**(5): p. e73-e79.
6. Bouchery, E.E., et al., *Economic Costs of Excessive Alcohol Consumption in the U.S., 2006.* American Journal of Preventive Medicine. **41**(5): p. 516-524.
7. Gmel, G. and J. Rehm, *Harmful alcohol use.* Alcohol Res Health, 2003. **27**(1): p. 52-62.
8. Gonzales, K., et al., *Alcohol-attributable deaths and years of potential life lost--11 States, 2006-2010.* MMWR Morb Mortal Wkly Rep, 2014. **63**(10): p. 213-6.
9. Bellentani, S., et al., *Drinking habits as cofactors of risk for alcohol induced liver damage.* Gut, 1997. **41**(6): p. 845-850.
10. Klatsky, A.L., M.A. Armstrong, and G.D. Friedman, *Alcohol and mortality.* Ann Intern Med, 1992. **117**(8): p. 646-54.
11. Zakhari, S. and T.K. Li, *Determinants of alcohol use and abuse: Impact of quantity and frequency patterns on liver disease.* Hepatology, 2007. **46**(6): p. 2032-9.
12. Howard, J.M. and E.W. Ehrlich, *The etiology of pancreatitis: a review of clinical experience.* Ann Surg, 1960. **152**: p. 135-46.
13. Irving, H.M., A.V. Samokhvalov, and J. Rehm, *Alcohol as a Risk Factor for Pancreatitis. A Systematic Review and Meta-Analysis.* Jop, 2009. **10**(4): p. 387-392.
14. Kristiansen, L., et al., *Risk of pancreatitis according to alcohol drinking habits: a population-based cohort study.* Am J Epidemiol, 2008. **168**(8): p. 932-7.
15. Talamini, G., et al., *Alcohol and smoking as risk factors in chronic pancreatitis and pancreatic cancer.* Dig Dis Sci, 1999. **44**(7): p. 1303-11.
16. Lin, Y., et al., *Associations of alcohol drinking and nutrient intake with chronic pancreatitis: findings from a case-control study in Japan.* Am J Gastroenterol, 2001. **96**(9): p. 2622-7.
17. Apte, M.V. and J.S. Wilson, *Alcohol-induced pancreatic injury.* Best Pract Res Clin Gastroenterol, 2003. **17**(4): p. 593-612.
18. Bode, C. and J.C. Bode, *Alcohol's role in gastrointestinal tract disorders.* Alcohol Health Res World, 1997. **21**(1): p. 76-83.
19. Bujanda, L., *The effects of alcohol consumption upon the gastrointestinal tract.* Am J Gastroenterol, 2000. **95**(12): p. 3374-82.
20. Michel, L., A. Serrano, and R.A. Malt, *Mallory-Weiss syndrome. Evolution of diagnostic and therapeutic patterns over two decades.* Ann Surg, 1980. **192**(6): p. 716-21.
21. Roberts, D.M., *Chronic gastritis, alcohol, and non-ulcer dyspepsia.* Gut, 1972. **13**(10): p. 768-74.

22. Dinoso, V.P., Jr., et al., *Gastric secretion and gastric mucosal morphology in chronic alcoholics.* Arch Intern Med, 1972. **130**(5): p. 715-9.
23. Pereira, R.S., et al., *Intestinal healing in rats submitted to ethanol ingestion.* Acta Cir Bras, 2012. **27**(3): p. 236-43.
24. Lindenbaum, J. and C.S. Lieber, *Effects of chronic ethanol administration on intestinal absorption in man in the absence of nutritional deficiency.* Ann N Y Acad Sci, 1975. **252**: p. 228-34.
25. Todd, K.G., A.S. Hazell, and R.F. Butterworth, *Alcohol-thiamine interactions: an update on the pathogenesis of Wernicke encephalopathy.* Addict Biol, 1999. **4**(3): p. 261-72.
26. Salaspuro, M.P., *Alcohol consumption and cancer of the gastrointestinal tract.* Best Practice & Research Clinical Gastroenterology, 2003. **17**(4): p. 679-694.
27. Willett, W.C., et al., *Moderate alcohol consumption and the risk of breast cancer.* N Engl J Med, 1987. **316**(19): p. 1174-80.
28. Haas, S.L., W. Ye, and J.M. Lohr, *Alcohol consumption and digestive tract cancer.* Curr Opin Clin Nutr Metab Care, 2012. **15**(5): p. 457-67.
29. Gronbaek, M., et al., *Population based cohort study of the association between alcohol intake and cancer of the upper digestive tract.* Bmj, 1998. **317**(7162): p. 844-7.
30. Bagnardi, V., et al., *Alcohol consumption and the risk of cancer: a meta-analysis.* Alcohol Res Health, 2001. **25**(4): p. 263-70.
31. Al-Sader, H., et al., *Alcohol and breast cancer: the mechanisms explained.* J Clin Med Res, 2009. **1**(3): p. 125-31.
32. Tramacere, I., et al., *Alcohol drinking and pancreatic cancer risk: a meta-analysis of the dose-risk relation.* International Journal of Cancer, 2010. **126**(6): p. 1474-1486.
33. Wang, Y., et al., *A pooled analysis of alcohol intake and colorectal cancer.* Int J Clin Exp Med, 2015. **8**(5): p. 6878-89.
34. Thuler, L.C., R.F. de Menezes, and A. Bergmann, *Cancer cases attributable to alcohol consumption in Brazil.* Alcohol, 2016. **54**: p. 23-6.
35. Connor, J., *Alcohol consumption as a cause of cancer.* Addiction, 2016.
36. Cao, Y., et al., *Light to moderate intake of alcohol, drinking patterns, and risk of cancer: results from two prospective US cohort studies.* Bmj, 2015. **351**: p. h4238.
37. IARC, *Alcohol drinking. IARC Working Group, Lyon, 13-20 October 1987.* IARC Monogr Eval Carcinog Risks Hum, 1988. **44**: p. 1-378.
38. IARC, *Re-evaluation of some organic chemicals, hydrazine and hydrogen peroxide. Proceedings of the IARC Working Group on the Evaluation of Carcinogenic Risks to Humans. Lyon, France, 17-24 February 1998.* IARC Monogr Eval Carcinog Risks Hum, 1999. **71 Pt 1**: p. 1-315.
39. Salaspuro, M., *Acetaldehyde as a common denominator and cumulative carcinogen in digestive tract cancers.* Scand J Gastroenterol, 2009. **44**(8): p. 912-25.
40. Seitz, H.K. and P. Becker, *Alcohol metabolism and cancer risk.* Alcohol Res Health, 2007. **30**(1): p. 38-41, 44-7.
41. Klatsky, A.L., G.D. Friedman, and A.B. Siegelaub, *Alcohol and mortality. A ten-year Kaiser-Permanente experience.* Ann Intern Med, 1981. **95**(2): p. 139-45.
42. Fagrell, B., et al., *The effects of light to moderate drinking on cardiovascular diseases.* J Intern Med, 1999. **246**(4): p. 331-40.
43. Klatsky, A.L., et al., *Alcohol consumption and blood pressure Kaiser-Permanente Multiphasic Health Examination data.* N Engl J Med, 1977. **296**(21): p. 1194-200.

44. Palomaki, H. and M. Kaste, *Regular light-to-moderate intake of alcohol and the risk of ischemic stroke. Is there a beneficial effect?* Stroke, 1993. **24**(12): p. 1828-32.
45. Hansagi, H., et al., *Alcohol consumption and stroke mortality. 20-year follow-up of 15,077 men and women.* Stroke, 1995. **26**(10): p. 1768-73.
46. Carlsson, S., et al., *Alcohol consumption and the incidence of type 2 diabetes: a 20-year follow-up of the Finnish twin cohort study.* Diabetes Care, 2003. **26**(10): p. 2785-90.
47. Knott, C., S. Bell, and A. Britton, *Alcohol Consumption and the Risk of Type 2 Diabetes: A Systematic Review and Dose-Response Meta-analysis of More Than 1.9 Million Individuals From 38 Observational Studies.* Diabetes Care, 2015. **38**(9): p. 1804-12.
48. Baliunas, D.O., et al., *Alcohol as a risk factor for type 2 diabetes: A systematic review and meta-analysis.* Diabetes Care, 2009. **32**(11): p. 2123-32.
49. Engler, P.A., S.E. Ramsey, and R.J. Smith, *Alcohol use of diabetes patients: The need for assessment and intervention.* Acta diabetologica, 2013. **50**(2): p. 93-99.
50. Howard, A.A., J.H. Arnsten, and M.N. Gourevitch, *Effect of alcohol consumption on diabetes mellitus: a systematic review.* Ann Intern Med, 2004. **140**(3): p. 211-9.
51. Ismail, D., et al., *Social consumption of alcohol in adolescents with Type 1 diabetes is associated with increased glucose lability, but not hypoglycaemia.* Diabet Med, 2006. **23**(8): p. 830-3.
52. Barr, T., et al., *Opposing effects of alcohol on the immune system.* Prog Neuropsychopharmacol Biol Psychiatry, 2016. **65**: p. 242-51.
53. Pasala, S., T. Barr, and I. Messaoudi, *Impact of Alcohol Abuse on the Adaptive Immune System.* Alcohol Res, 2015. **37**(2): p. 185-97.
54. Kelso, N.E., D.S. Sheps, and R.L. Cook, *The association between alcohol use and cardiovascular disease among people living with HIV: a systematic review.* Am J Drug Alcohol Abuse, 2015. **41**(6): p. 479-88.
55. Molina, P.E., et al., *Behavioral, Metabolic, and Immune Consequences of Chronic Alcohol or Cannabinoids on HIV/AIDs: Studies in the Non-Human Primate SIV Model.* J Neuroimmune Pharmacol, 2015. **10**(2): p. 217-32.
56. Schmidt, K.J., et al., *Treatment of Severe Alcohol Withdrawal.* Ann Pharmacother, 2016. **50**(5): p. 389-401.
57. Sachdeva, A., M. Choudhary, and M. Chandra, *Alcohol Withdrawal Syndrome: Benzodiazepines and Beyond.* J Clin Diagn Res, 2015. **9**(9): p. Ve01-ve07.
58. Samokhvalov, A.V., et al., *Alcohol consumption, unprovoked seizures, and epilepsy: a systematic review and meta-analysis.* Epilepsia, 2010. **51**(7): p. 1177-84.
59. Perry, C.J., *Cognitive Decline and Recovery in Alcohol Abuse.* J Mol Neurosci, 2016.
60. Kim, J.W., et al., *Alcohol and cognition in the elderly: a review.* Psychiatry Investig, 2012. **9**(1): p. 8-16.
61. Ilomaki, J., et al., *Alcohol Consumption, Dementia and Cognitive Decline: An Overview of Systematic Reviews.* Curr Clin Pharmacol, 2015. **10**(3): p. 204-12.
62. Thomson, A.D. and E.J. Marshall, *The natural history and pathophysiology of Wernicke's Encephalopathy and Korsakoff's Psychosis.* Alcohol Alcohol, 2006. **41**(2): p. 151-8.
63. Vedder, L.C., et al., *Interactions between chronic ethanol consumption and thiamine deficiency on neural plasticity, spatial memory, and cognitive flexibility.* Alcohol Clin Exp Res, 2015. **39**(11): p. 2143-53.
64. Kim, T.E., et al., *Wernicke encephalopathy and ethanol-related syndromes.* Semin Ultrasound CT MR, 2014. **35**(2): p. 85-96.

65. Spampinato, M.V., et al., *Magnetic resonance imaging findings in substance abuse: alcohol and alcoholism and syndromes associated with alcohol abuse.* Top Magn Reson Imaging, 2005. **16**(3): p. 223-30.
66. Modesto-Lowe, V. and H.R. Kranzler, *Diagnosis and treatment of alcohol-dependent patients with comorbid psychiatric disorders.* Alcohol Res Health, 1999. **23**(2): p. 144-9.
67. Koob, G.F. and M. Le Moal, *Drug addiction, dysregulation of reward, and allostasis.* Neuropsychopharmacology, 2001. **24**(2): p. 97-129.
68. Day, E., A. Copello, and M. Hull, *Assessment and management of alcohol use disorders.* Bmj, 2015. **350**: p. h715.
69. Soyka, M., *Nalmefene for the treatment of alcohol use disorders: recent data and clinical potential.* Expert Opin Pharmacother, 2016. **17**(4): p. 619-26.
70. Douaihy, A.B., T.M. Kelly, and C. Sullivan, *Medications for substance use disorders.* Soc Work Public Health, 2013. **28**(3-4): p. 264-78.
71. Sinclair, J.D., *Evidence about the use of naltrexone and for different ways of using it in the treatment of alcoholism.* Alcohol Alcohol, 2001. **36**(1): p. 2-10.
72. Larimer, R.C., *TReatment of alcoholism with antabuse®.* Journal of the American Medical Association, 1952. **150**(2): p. 79-83.
73. Reilly, M.T., et al., *Effects of acamprosate on neuronal receptors and ion channels expressed in Xenopus oocytes.* Alcohol Clin Exp Res, 2008. **32**(2): p. 188-96.
74. Kalk, N.J. and A.R. Lingford-Hughes, *The clinical pharmacology of acamprosate.* Br J Clin Pharmacol, 2014. **77**(2): p. 315-23.
75. Fortney, J., et al., *Controlling for selection bias in the evaluation of Alcoholics Anonymous as aftercare treatment.* J Stud Alcohol, 1998. **59**(6): p. 690-7.
76. Fuller, R.K., et al., *Disulfiram treatment of alcoholism: A veterans administration cooperative study.* JAMA, 1986. **256**(11): p. 1449-1455.
77. Yahn, S.L., L.R. Watterson, and M.F. Olive, *Safety and efficacy of acamprosate for the treatment of alcohol dependence.* Subst Abuse, 2013. **6**: p. 1-12.
78. Humphreys, K., J.C. Blodgett, and T.H. Wagner, *Estimating the efficacy of Alcoholics Anonymous without self-selection bias: an instrumental variables re-analysis of randomized clinical trials.* Alcohol Clin Exp Res, 2014. **38**(11): p. 2688-94.
79. Garbutt, J.C., *Efficacy and tolerability of naltrexone in the management of alcohol dependence.* Curr Pharm Des, 2010. **16**(19): p. 2091-7.
80. Smith, M.L., et al., *Time-Course Analysis of Brain Regional Expression Network Responses to Chronic Intermittent Ethanol and Withdrawal: Implications for Mechanisms Underlying Excessive Ethanol Consumption.* PLoS One, 2016. **11**(1): p. e0146257.
81. Lopez, M.F. and H.C. Becker, *Effect of pattern and number of chronic ethanol exposures on subsequent voluntary ethanol intake in C57BL/6J mice.* Psychopharmacology (Berl), 2005. **181**(4): p. 688-96.
82. Wade, C.M. and M.J. Daly, *Genetic variation in laboratory mice.* Nat Genet, 2005. **37**(11): p. 1175-80.
83. Goldman-Rakic, P.S., *The prefrontal landscape: implications of functional architecture for understanding human mentation and the central executive.* Philos Trans R Soc Lond B Biol Sci, 1996. **351**(1346): p. 1445-53.
84. Miller, E.K. and J.D. Cohen, *An integrative theory of prefrontal cortex function.* Annu Rev Neurosci, 2001. **24**: p. 167-202.

85. Abernathy, K., L.J. Chandler, and J.J. Woodward, *ALCOHOL AND THE PREFRONTAL CORTEX.* International review of neurobiology, 2010. **91**: p. 289-320.
86. Kerns, R.T., et al., *Ethanol-responsive brain region expression networks: implications for behavioral responses to acute ethanol in DBA/2J versus C57BL/6J mice.* J Neurosci, 2005. **25**(9): p. 2255-66.
87. Peoples, R.W., C. Li, and F.F. Weight, *Lipid vs protein theories of alcohol action in the nervous system.* Annu Rev Pharmacol Toxicol, 1996. **36**: p. 185-201.
88. Vengeliene, V., et al., *Neuropharmacology of alcohol addiction.* Br J Pharmacol, 2008. **154**(2): p. 299-315.
89. Lovinger, D.M., G. White, and F.F. Weight, *Ethanol inhibits NMDA-activated ion current in hippocampal neurons.* Science, 1989. **243**(4899): p. 1721-4.
90. Mihic, S.J., et al., *Sites of alcohol and volatile anaesthetic action on GABA(A) and glycine receptors.* Nature, 1997. **389**(6649): p. 385-9.
91. Narahashi, T., et al., *Neuronal nicotinic acetylcholine receptors: a new target site of ethanol.* Neurochem Int, 1999. **35**(2): p. 131-41.
92. Lovinger, D.M., *5-HT3 receptors and the neural actions of alcohols: an increasingly exciting topic.* Neurochem Int, 1999. **35**(2): p. 125-30.
93. Wang, X., et al., *Ethanol directly modulates gating of a dihydropyridine-sensitive Ca2+ channel in neurohypophysial terminals.* J Neurosci, 1994. **14**(9): p. 5453-60.
94. Lewohl, J.M., et al., *G-protein-coupled inwardly rectifying potassium channels are targets of alcohol action.* Nat Neurosci, 1999. **2**(12): p. 1084-90.
95. Kobayashi, T., et al., *Ethanol opens G-protein-activated inwardly rectifying K+ channels.* Nat Neurosci, 1999. **2**(12): p. 1091-7.
96. Miller, P.S. and A.R. Aricescu, *Crystal structure of a human GABAA receptor.* Nature, 2014. **512**(7514): p. 270-5.
97. Kumar, S., et al., *The role of GABA(A) receptors in the acute and chronic effects of ethanol: a decade of progress.* Psychopharmacology (Berl), 2009. **205**(4): p. 529.
98. Suzdak, P.D., et al., *Ethanol stimulates gamma-aminobutyric acid receptor-mediated chloride transport in rat brain synaptoneurosomes.* Proc Natl Acad Sci U S A, 1986. **83**(11): p. 4071-5.
99. Allan, A.M. and R.A. Harris, *Acute and chronic ethanol treatments alter GABA receptor-operated chloride channels.* Pharmacol Biochem Behav, 1987. **27**(4): p. 665-70.
100. Wallner, M., H.J. Hanchar, and R.W. Olsen, *Ethanol enhances alpha 4 beta 3 delta and alpha 6 beta 3 delta gamma-aminobutyric acid type A receptors at low concentrations known to affect humans.* Proc Natl Acad Sci U S A, 2003. **100**(25): p. 15218-23.
101. Boehm Ii, S.L., et al., *γ-Aminobutyric acid A receptor subunit mutant mice: new perspectives on alcohol actions.* Biochemical Pharmacology, 2004. **68**(8): p. 1581-1602.
102. Lewohl, J.M., D.I. Crane, and P.R. Dodd, *Expression of the alpha 1, alpha 2 and alpha 3 isoforms of the GABAA receptor in human alcoholic brain.* Brain Res, 1997. **751**(1): p. 102-12.
103. Buckley, S.T., A.L. Eckert, and P.R. Dodd, *Expression and distribution of GABAA receptor subtypes in human alcoholic cerebral cortex.* Ann N Y Acad Sci, 2000. **914**: p. 58-64.
104. Lewohl, J.M., et al., *GABA(A) receptor alpha-subunit proteins in human chronic alcoholics.* J Neurochem, 2001. **78**(3): p. 424-34.

105. Buckley, S.T. and P.R. Dodd, *GABAA receptor beta subunit mRNA expression in the human alcoholic brain.* Neurochem Int, 2004. **45**(7): p. 1011-20.
106. Buckley, S.T., et al., *GABA(A) receptor beta isoform protein expression in human alcoholic brain: interaction with genotype.* Neurochem Int, 2006. **49**(6): p. 557-67.
107. Bhandage, A.K., et al., *GABA-A and NMDA receptor subunit mRNA expression is altered in the caudate but not the putamen of the postmortem brains of alcoholics.* Front Cell Neurosci, 2014. **8**: p. 415.
108. Kosobud, A.E., et al., *Adaptation of Subjective Responses to Alcohol is Affected by an Interaction of GABRA2 Genotype and Recent Drinking.* Alcohol Clin Exp Res, 2015. **39**(7): p. 1148-57.
109. Edenberg, H.J., et al., *Variations in GABRA2, encoding the alpha 2 subunit of the GABA(A) receptor, are associated with alcohol dependence and with brain oscillations.* Am J Hum Genet, 2004. **74**(4): p. 705-14.
110. Kareken, D.A., et al., *A polymorphism in GABRA2 is associated with the medial frontal response to alcohol cues in an fMRI study.* Alcohol Clin Exp Res, 2010. **34**(12): p. 2169-78.
111. Dick, D.M., et al., *Association of GABRG3 with alcohol dependence.* Alcohol Clin Exp Res, 2004. **28**(1): p. 4-9.
112. Enoch, M.A., et al., *GABBR1 and SLC6A1, Two Genes Involved in Modulation of GABA Synaptic Transmission, Influence Risk for Alcoholism: Results from Three Ethnically Diverse Populations.* Alcohol Clin Exp Res, 2016. **40**(1): p. 93-101.
113. Mhatre, M.C. and M.K. Ticku, *Chronic ethanol administration alters gamma-aminobutyric acidA receptor gene expression.* Mol Pharmacol, 1992. **42**(3): p. 415-22.
114. Le, A.D., et al., *Tolerance to and cross-tolerance among ethanol, pentobarbital and chlordiazepoxide.* Pharmacol Biochem Behav, 1986. **24**(1): p. 93-8.
115. Silvers, J.M., et al., *Chronic intermittent injections of high-dose ethanol during adolescence produce metabolic, hypnotic, and cognitive tolerance in rats.* Alcohol Clin Exp Res, 2003. **27**(10): p. 1606-12.
116. Brunig, I., et al., *BDNF reduces miniature inhibitory postsynaptic currents by rapid downregulation of GABA(A) receptor surface expression.* Eur J Neurosci, 2001. **13**(7): p. 1320-8.
117. Stellwagen, D., et al., *Differential regulation of AMPA receptor and GABA receptor trafficking by tumor necrosis factor-alpha.* J Neurosci, 2005. **25**(12): p. 3219-28.
118. Furukawa, H., et al., *Subunit arrangement and function in NMDA receptors.* Nature, 2005. **438**(7065): p. 185-92.
119. Wright, J.M., R.W. Peoples, and F.F. Weight, *Single-channel and whole-cell analysis of ethanol inhibition of NMDA-activated currents in cultured mouse cortical and hippocampal neurons.* Brain Res, 1996. **738**(2): p. 249-56.
120. Lovinger, D.M., G. White, and F.F. Weight, *NMDA receptor-mediated synaptic excitation selectively inhibited by ethanol in hippocampal slice from adult rat.* J Neurosci, 1990. **10**(4): p. 1372-9.
121. Morrisett, R.A., et al., *Ethanol and magnesium ions inhibit N-methyl-D-aspartate-mediated synaptic potentials in an interactive manner.* Neuropharmacology, 1991. **30**(11): p. 1173-8.

122. Calton, J.L., W.A. Wilson, and S.D. Moore, *Magnesium-dependent inhibition of N-methyl-D-aspartate receptor-mediated synaptic transmission by ethanol.* J Pharmacol Exp Ther, 1998. **287**(3): p. 1015-9.
123. Calton, J.L., W.A. Wilson, and S.D. Moore, *Reduction of voltage-dependent currents by ethanol contributes to inhibition of NMDA receptor-mediated excitatory synaptic transmission.* Brain Res, 1999. **816**(1): p. 142-8.
124. Li, Q., W.A. Wilson, and H.S. Swartzwelder, *Differential effect of ethanol on NMDA EPSCs in pyramidal cells in the posterior cingulate cortex of juvenile and adult rats.* J Neurophysiol, 2002. **87**(2): p. 705-11.
125. Wang, J., et al., *Ethanol induces long-term facilitation of NR2B-NMDA receptor activity in the dorsal striatum: implications for alcohol drinking behavior.* J Neurosci, 2007. **27**(13): p. 3593-602.
126. Nie, Z., S.G. Madamba, and G.R. Siggins, *Ethanol inhibits glutamatergic neurotransmission in nucleus accumbens neurons by multiple mechanisms.* J Pharmacol Exp Ther, 1994. **271**(3): p. 1566-73.
127. Ron, D. and J. Wang, *Frontiers in Neuroscience*
The NMDA Receptor and Alcohol Addiction, in *Biology of the NMDA Receptor*, A.M. Van Dongen, Editor. 2009, CRC Press/Taylor & Francis
Taylor & Francis Group, LLC.: Boca Raton (FL).
128. Morrisett, R.A. and H.S. Swartzwelder, *Attenuation of hippocampal long-term potentiation by ethanol: a patch-clamp analysis of glutamatergic and GABAergic mechanisms.* J Neurosci, 1993. **13**(5): p. 2264-72.
129. Givens, B. and K. McMahon, *Ethanol suppresses the induction of long-term potentiation in vivo.* Brain Res, 1995. **688**(1-2): p. 27-33.
130. Partridge, J.G., K.C. Tang, and D.M. Lovinger, *Regional and postnatal heterogeneity of activity-dependent long-term changes in synaptic efficacy in the dorsal striatum.* J Neurophysiol, 2000. **84**(3): p. 1422-9.
131. Yin, H.H., et al., *Ethanol reverses the direction of long-term synaptic plasticity in the dorsomedial striatum.* Eur J Neurosci, 2007. **25**(11): p. 3226-32.
132. Acheson, S.K., R.M. Stein, and H.S. Swartzwelder, *Impairment of semantic and figural memory by acute ethanol: age-dependent effects.* Alcohol Clin Exp Res, 1998. **22**(7): p. 1437-42.
133. Yaka, R., et al., *Fyn Kinase and NR2B-Containing NMDA Receptors Regulate Acute Ethanol Sensitivity But Not Ethanol Intake or Conditioned Reward.* Alcoholism, clinical and experimental research, 2003. **27**(11): p. 1736-1742.
134. Boyce-Rustay, J.M. and A. Holmes, *Functional roles of NMDA receptor NR2A and NR2B subunits in the acute intoxicating effects of ethanol in mice.* Synapse, 2005. **56**(4): p. 222-5.
135. Broadbent, J., K.M. Kampmueller, and S.A. Koonse, *Expression of behavioral sensitization to ethanol by DBA/2J mice: the role of NMDA and non-NMDA glutamate receptors.* Psychopharmacology (Berl), 2003. **167**(3): p. 225-34.
136. Boyce-Rustay, J.M. and C.L. Cunningham, *The role of NMDA receptor binding sites in ethanol place conditioning.* Behav Neurosci, 2004. **118**(4): p. 822-34.
137. Biala, G. and J. Kotlinska, *Blockade of the acquisition of ethanol-induced conditioned place preference by N-methyl-D-aspartate receptor antagonists.* Alcohol Alcohol, 1999. **34**(2): p. 175-82.

138. Costin, B.N. and M.F. Miles, *Molecular and neurologic responses to chronic alcohol use.* Handb Clin Neurol, 2014. **125**: p. 157-71.
139. Kolb, J.E., J. Trettel, and E.S. Levine, *BDNF enhancement of postsynaptic NMDA receptors is blocked by ethanol.* Synapse, 2005. **55**(1): p. 52-7.
140. Maldve, R.E., et al., *DARPP-32 and regulation of the ethanol sensitivity of NMDA receptors in the nucleus accumbens.* Nat Neurosci, 2002. **5**(7): p. 641-8.
141. Binder, D.K. and H.E. Scharfman, *Brain-derived neurotrophic factor.* Growth Factors, 2004. **22**(3): p. 123-31.
142. Wolstenholme, J.T., et al., *Genomic analysis of individual differences in ethanol drinking: evidence for non-genetic factors in C57BL/6 mice.* PloS one, 2011. **6**(6): p. e21100.
143. Joe, K.H., et al., *Decreased plasma brain-derived neurotrophic factor levels in patients with alcohol dependence.* Alcohol Clin Exp Res, 2007. **31**(11): p. 1833-8.
144. Huang, M.C., et al., *Alterations of serum brain-derived neurotrophic factor levels in early alcohol withdrawal.* Alcohol Alcohol, 2008. **43**(3): p. 241-5.
145. Fienberg, A.A., et al., *DARPP-32: regulator of the efficacy of dopaminergic neurotransmission.* Science, 1998. **281**(5378): p. 838-42.
146. Abrahao, K.P., F.O. Goeldner, and M.L. Souza-Formigoni, *Individual differences in ethanol locomotor sensitization are associated with dopamine D1 receptor intra-cellular signaling of DARPP-32 in the nucleus accumbens.* PLoS One, 2014. **9**(2): p. e98296.
147. Darlington, T.M., et al., *Transcriptome analysis of Inbred Long Sleep and Inbred Short Sleep mice.* Genes Brain Behav, 2013. **12**(2): p. 263-74.
148. Nuutinen, S., K. Kiianmaa, and P. Panula, *DARPP-32 and Akt regulation in ethanol-preferring AA and ethanol-avoiding ANA rats.* Neurosci Lett, 2011. **503**(1): p. 31-6.
149. Rahman, S., E.A. Engleman, and R.L. Bell, *Nicotinic receptor modulation to treat alcohol and drug dependence.* Front Neurosci, 2014. **8**: p. 426.
150. Hendrickson, L.M., et al., *Activation of alpha4* nAChRs is necessary and sufficient for varenicline-induced reduction of alcohol consumption.* J Neurosci, 2010. **30**(30): p. 10169-76.
151. Liu, L., et al., *Nicotinic acetylcholine receptors containing the α4 subunit modulate alcohol reward.* Biol Psychiatry, 2013. **73**(8): p. 738-46.
152. Gallego, X., et al., *Transgenic over expression of nicotinic receptor alpha 5, alpha 3, and beta 4 subunit genes reduces ethanol intake in mice.* Alcohol, 2012. **46**(3): p. 205-215.
153. Blomqvist, O., et al., *Voluntary ethanol intake in the rat: effects of nicotinic acetylcholine receptor blockade or subchronic nicotine treatment.* Eur J Pharmacol, 1996. **314**(3): p. 257-67.
154. Ericson, M., et al., *Voluntary ethanol intake in the rat and the associated accumbal dopamine overflow are blocked by ventral tegmental mecamylamine.* Eur J Pharmacol, 1998. **358**(3): p. 189-96.
155. Kuzmin, A., et al., *Effects of subunit selective nACh receptors on operant ethanol self-administration and relapse-like ethanol-drinking behavior.* Psychopharmacology (Berl), 2009. **203**(1): p. 99-108.
156. Chi, H. and H. de Wit, *Mecamylamine attenuates the subjective stimulant-like effects of alcohol in social drinkers.* Alcohol Clin Exp Res, 2003. **27**(5): p. 780-6.
157. Mitchell, J.M., et al., *Varenicline decreases alcohol consumption in heavy-drinking smokers.* Psychopharmacology (Berl), 2012. **223**(3): p. 299-306.

158. Young, E.M., et al., *Mecamylamine and Ethanol Preference in Healthy Volunteers.* Alcoholism: Clinical and Experimental Research, 2005. **29**(1): p. 58-65.
159. Maricq, A.V., et al., *Primary structure and functional expression of the 5HT3 receptor, a serotonin-gated ion channel.* Science, 1991. **254**(5030): p. 432-7.
160. Thompson, A.J. and S.C. Lummis, *5-HT3 receptors.* Curr Pharm Des, 2006. **12**(28): p. 3615-30.
161. Engleman, E.A., et al., *The role of 5-HT3 receptors in drug abuse and as a target for pharmacotherapy.* CNS Neurol Disord Drug Targets, 2008. **7**(5): p. 454-67.
162. Campbell, A.D. and W.J. McBride, *Serotonin-3 receptor and ethanol-stimulated dopamine release in the nucleus accumbens.* Pharmacol Biochem Behav, 1995. **51**(4): p. 835-42.
163. Striessnig, J., et al., *Role of voltage-gated L-type Ca2+ channel isoforms for brain function.* Biochem Soc Trans, 2006. **34**(Pt 5): p. 903-9.
164. Catterall, W.A., et al., *International Union of Pharmacology. XLVIII. Nomenclature and Structure-Function Relationships of Voltage-Gated Calcium Channels.* Pharmacological Reviews, 2005. **57**(4): p. 411.
165. Katsura, M., et al., *Increase in Expression of α1 and α2/δ1 Subunits of L-Type High Voltage-Gated Calcium Channels After Sustained Ethanol Exposure in Cerebral Cortical Neurons.* Journal of Pharmacological Sciences, 2006. **102**(2): p. 221-230.
166. Little, H.J., S.J. Dolin, and M.J. Halsey, *Calcium channel antagonists decrease the ethanol withdrawal syndrome.* Life Sciences, 1986. **39**(22): p. 2059-2065.
167. Whittington, M.A. and H.J. Little, *A calcium channel antagonist stereoselectively decreases ethanol withdrawal hyperexcitability but not that due to bicuculline, in hippocampal slices.* Br J Pharmacol, 1991. **103**(2): p. 1313-20.
168. Mayfield, J., Y.A. Blednov, and R.A. Harris, *Behavioral and Genetic Evidence for GIRK Channels in the CNS: Role in Physiology, Pathophysiology, and Drug Addiction.* Int Rev Neurobiol, 2015. **123**: p. 279-313.
169. Clarke, T.-K., et al., *KCNJ6 is Associated with Adult Alcohol Dependence and Involved in Gene × Early Life Stress Interactions in Adolescent Alcohol Drinking.* Neuropsychopharmacology, 2011. **36**(6): p. 1142-1148.
170. Blednov, Y.A., et al., *Potassium channels as targets for ethanol: studies of G-protein-coupled inwardly rectifying potassium channel 2 (GIRK2) null mutant mice.* J Pharmacol Exp Ther, 2001. **298**(2): p. 521-30.
171. Blednov, Y.A., et al., *Hyperactivity and dopamine D1 receptor activation in mice lacking girk2 channels.* Psychopharmacology (Berl), 2002. **159**(4): p. 370-8.
172. Hill, K.G., et al., *Reduced ethanol-induced conditioned taste aversion and conditioned place preference in GIRK2 null mutant mice.* Psychopharmacology (Berl), 2003. **169**(1): p. 108-14.
173. Herman, M.A., et al., *GIRK3 gates activation of the mesolimbic dopaminergic pathway by ethanol.* Proc Natl Acad Sci U S A, 2015. **112**(22): p. 7091-6.
174. Tipps, M.E., et al., *G Protein-Gated Inwardly Rectifying Potassium Channel Subunit 3 Knock-Out Mice Show Enhanced Ethanol Reward.* Alcohol Clin Exp Res, 2016. **40**(4): p. 857-64.
175. Kozell, L.B., et al., *Mapping a barbiturate withdrawal locus to a 0.44 Mb interval and analysis of a novel null mutant identifies a role for Kcnj9 (GIRK3) in withdrawal from*

pentobarbital, zolpidem and ethanol. The Journal of neuroscience : the official journal of the Society for Neuroscience, 2009. **29**(37): p. 11662.
176. Adermark, L. and M.S. Bowers, *Disentangling the Role of Astrocytes in Alcohol Use Disorder.* Alcohol Clin Exp Res, 2016. **40**(9): p. 1802-16.
177. Ayers-Ringler, J.R., et al., *Role of astrocytic glutamate transporter in alcohol use disorder.* World J Psychiatry, 2016. **6**(1): p. 31-42.
178. Hansson, E. and L. Ronnback, *Glial neuronal signaling in the central nervous system.* Faseb j, 2003. **17**(3): p. 341-8.
179. Alhaddad, H., et al., *Effects of MS-153 on chronic ethanol consumption and GLT1 modulation of glutamate levels in male alcohol-preferring rats.* Front Behav Neurosci, 2014. **8**: p. 366.
180. Das, S.C., et al., *Ceftriaxone attenuates ethanol drinking and restores extracellular glutamate concentration through normalization of GLT-1 in nucleus accumbens of male alcohol-preferring rats.* Neuropharmacology, 2015. **97**: p. 67-74.
181. Lee, M., C. Schwab, and P.L. McGeer, *Astrocytes are GABAergic cells that modulate microglial activity.* Glia, 2011. **59**(1): p. 152-65.
182. Arnone, D., M.T. Abou-Saleh, and T.R. Barrick, *Diffusion tensor imaging of the corpus callosum in addiction.* Neuropsychobiology, 2006. **54**(2): p. 107-13.
183. Shear, P.K., T.L. Jernigan, and N. Butters, *Volumetric magnetic resonance imaging quantification of longitudinal brain changes in abstinent alcoholics.* Alcohol Clin Exp Res, 1994. **18**(1): p. 172-6.
184. Fields, R.D., *Change in the Brain's White Matter: The role of the brain's white matter in active learning and memory may be underestimated.* Science (New York, N.Y.), 2010. **330**(6005): p. 768-769.
185. Vargas, W.M., et al., *Alcohol binge drinking during adolescence or dependence during adulthood reduces prefrontal myelin in male rats.* J Neurosci, 2014. **34**(44): p. 14777-82.
186. Navarro, A.I. and C.D. Mandyam, *Protracted abstinence from chronic ethanol exposure alters the structure of neurons and expression of oligodendrocytes and myelin in the medial prefrontal cortex.* Neuroscience, 2015. **293**: p. 35-44.
187. Spanagel, R., *Alcoholism: a systems approach from molecular physiology to addictive behavior.* Physiol Rev, 2009. **89**(2): p. 649-705.
188. de Olmos, J.S. and L. Heimer, *The concepts of the ventral striatopallidal system and extended amygdala.* Ann N Y Acad Sci, 1999. **877**: p. 1-32.
189. Morgane, P.J., J.R. Galler, and D.J. Mokler, *A review of systems and networks of the limbic forebrain/limbic midbrain.* Progress in Neurobiology, 2005. **75**(2): p. 143-160.
190. Koob, G.F. and N.D. Volkow, *Neurocircuitry of addiction.* Neuropsychopharmacology, 2010. **35**(1): p. 217-38.
191. Mochly-Rosen, D., et al., *Chronic ethanol causes heterologous desensitization of receptors by reducing alpha s messenger RNA.* Nature, 1988. **333**(6176): p. 848-50.
192. Montpied, P., et al., *Prolonged ethanol inhalation decreases gamma-aminobutyric acidA receptor alpha subunit mRNAs in the rat cerebral cortex.* Mol Pharmacol, 1991. **39**(2): p. 157-63.
193. Miles, M.F., et al., *Ethanol-responsive genes in neural cells include the 78-kilodalton glucose-regulated protein (GRP78) and 94-kilodalton glucose-regulated protein (GRP94) molecular chaperones.* Mol Pharmacol, 1994. **46**(5): p. 873-9.

194. Lewohl, J.M., et al., *Gene expression in human alcoholism: microarray analysis of frontal cortex.* Alcohol Clin Exp Res, 2000. **24**(12): p. 1873-82.
195. Thibault, C., et al., *Expression profiling of neural cells reveals specific patterns of ethanol-responsive gene expression.* Mol Pharmacol, 2000. **58**(6): p. 1593-600.
196. Saito, M., et al., *Microarray analysis of gene expression in rat hippocampus after chronic ethanol treatment.* Neurochem Res, 2002. **27**(10): p. 1221-9.
197. Kily, L.J., et al., *Gene expression changes in a zebrafish model of drug dependency suggest conservation of neuro-adaptation pathways.* J Exp Biol, 2008. **211**(Pt 10): p. 1623-34.
198. Treadwell, J.A. and S.M. Singh, *Microarray analysis of mouse brain gene expression following acute ethanol treatment.* Neurochem Res, 2004. **29**(2): p. 357-69.
199. Walker, S.J., et al., *Long versus short oligonucleotide microarrays for the study of gene expression in nonhuman primates.* J Neurosci Methods, 2006. **152**(1-2): p. 179-89.
200. Mulligan, M.K., et al., *Molecular profiles of drinking alcohol to intoxication in C57BL/6J mice.* Alcohol Clin Exp Res, 2011. **35**(4): p. 659-70.
201. Pan, Y., et al., *Chronic alcohol exposure induced gene expression changes in the zebrafish brain.* Behav Brain Res, 2011. **216**(1): p. 66-76.
202. Patananan, A.N., et al., *Ethanol-induced differential gene expression and acetyl-CoA metabolism in a longevity model of the nematode Caenorhabditis elegans.* Exp Gerontol, 2015. **61**: p. 20-30.
203. Zhao, Z., et al., *Multi-species data integration and gene ranking enrich significant results in an alcoholism genome-wide association study.* BMC Genomics, 2012. **13 Suppl 8**: p. S16.
204. Bell, R.L., et al., *Gene expression changes in the nucleus accumbens of alcohol-preferring rats following chronic ethanol consumption.* Pharmacol Biochem Behav, 2009. **94**(1): p. 131-47.
205. Rodd, Z.A., et al., *Differential gene expression in the nucleus accumbens with ethanol self-administration in inbred alcohol-preferring rats.* Pharmacol Biochem Behav, 2008. **89**(4): p. 481-98.
206. Mayfield, R.D., et al., *Methods for the identification of differentially expressed genes in human post-mortem brain.* Methods, 2003. **31**(4): p. 301-5.
207. Mulligan, M.K., et al., *Alcohol trait and transcriptional genomic analysis of C57BL/6 substrains.* Genes Brain Behav, 2008. **7**(6): p. 677-89.
208. Melendez, R.I., et al., *Brain region-specific gene expression changes after chronic intermittent ethanol exposure and early withdrawal in C57BL/6J mice.* Addict Biol, 2012. **17**(2): p. 351-64.
209. Mulligan, M.K., et al., *Toward understanding the genetics of alcohol drinking through transcriptome meta-analysis.* Proc Natl Acad Sci U S A, 2006. **103**(16): p. 6368-73.
210. Liu, J., et al., *Patterns of gene expression in the frontal cortex discriminate alcoholic from nonalcoholic individuals.* Neuropsychopharmacology, 2006. **31**(7): p. 1574-82.
211. Mayfield, R.D., et al., *Patterns of gene expression are altered in the frontal and motor cortices of human alcoholics.* J Neurochem, 2002. **81**(4): p. 802-13.
212. Ponomarev, I., et al., *Gene coexpression networks in human brain identify epigenetic modifications in alcohol dependence.* J Neurosci, 2012. **32**(5): p. 1884-97.
213. Hoffman, P.L., et al., *Gene expression in brain: a window on ethanol dependence, neuroadaptation, and preference.* Alcohol Clin Exp Res, 2003. **27**(2): p. 155-68.

214. Wang, Z., M. Gerstein, and M. Snyder, *RNA-Seq: a revolutionary tool for transcriptomics.* Nature reviews. Genetics, 2009. **10**(1): p. 57-63.
215. Lukashin, A.V., M.E. Lukashev, and R. Fuchs, *Topology of gene expression networks as revealed by data mining and modeling.* Bioinformatics, 2003. **19**(15): p. 1909-16.
216. Baitaluk, M., *System Biology of Gene Regulation*, in *Biomedical Informatics*, V. Astakhov, Editor. 2009, Humana Press: Totowa, NJ. p. 55-87.
217. Barabasi, A.L. and Z.N. Oltvai, *Network biology: understanding the cell's functional organization.* Nat Rev Genet, 2004. **5**(2): p. 101-13.
218. Zhang, B. and S. Horvath, *A general framework for weighted gene co-expression network analysis.* Stat Appl Genet Mol Biol, 2005. **4**: p. Article17.
219. Barabasi, A.L. and R. Albert, *Emergence of scaling in random networks.* Science, 1999. **286**(5439): p. 509-12.
220. Zhu, X., M. Gerstein, and M. Snyder, *Getting connected: analysis and principles of biological networks.* Genes Dev, 2007. **21**(9): p. 1010-24.
221. Borneman, A.R., et al., *Target hub proteins serve as master regulators of development in yeast.* Genes Dev, 2006. **20**(4): p. 435-48.
222. Weintraub, H., et al., *Activation of muscle-specific genes in pigment, nerve, fat, liver, and fibroblast cell lines by forced expression of MyoD.* Proc Natl Acad Sci U S A, 1989. **86**(14): p. 5434-8.
223. Yang, J., et al., *Twist, a master regulator of morphogenesis, plays an essential role in tumor metastasis.* Cell, 2004. **117**(7): p. 927-39.
224. Langfelder, P., et al., *Is my network module preserved and reproducible?* PLoS Comput Biol, 2011. **7**(1): p. e1001057.
225. Ghazalpour, A., et al., *Integrating genetic and network analysis to characterize genes related to mouse weight.* PLoS Genet, 2006. **2**(8): p. e130.
226. Miller, J.A., M.C. Oldham, and D.H. Geschwind, *A systems level analysis of transcriptional changes in Alzheimer's disease and normal aging.* J Neurosci, 2008. **28**(6): p. 1410-20.
227. Saris, C.G., et al., *Weighted gene co-expression network analysis of the peripheral blood from Amyotrophic Lateral Sclerosis patients.* BMC Genomics, 2009. **10**: p. 405.
228. Horvath, S., et al., *Analysis of oncogenic signaling networks in glioblastoma identifies ASPM as a molecular target.* Proc Natl Acad Sci U S A, 2006. **103**(46): p. 17402-7.
229. Presson, A.P., et al., *Protein expression based multimarker analysis of breast cancer samples.* BMC Cancer, 2011. **11**: p. 230.
230. Wolen, A.R. and M.F. Miles, *Identifying gene networks underlying the neurobiology of ethanol and alcoholism.* Alcohol Res, 2012. **34**(3): p. 306-17.
231. de Jong, S., et al., *Gene expression profiling in C57BL/6J and A/J mouse inbred strains reveals gene networks specific for brain regions independent of genetic background.* BMC Genomics, 2010. **11**: p. 20.
232. Oldham, M.C., S. Horvath, and D.H. Geschwind, *Conservation and evolution of gene coexpression networks in human and chimpanzee brains.* Proc Natl Acad Sci U S A, 2006. **103**(47): p. 17973-8.
233. Park, C.C., et al., *Gene networks associated with conditional fear in mice identified using a systems genetics approach.* BMC Syst Biol, 2011. **5**: p. 43.
234. Goldstein, D.B., *Relationship of alcohol dose to intensity of withdrawal signs in mice.* J Pharmacol Exp Ther, 1972. **180**(2): p. 203-15.

235. Becker, H.C., *Positive relationship between the number of prior ethanol withdrawal episodes and the severity of subsequent withdrawal seizures.* Psychopharmacology (Berl), 1994. **116**(1): p. 26-32.
236. Becker, H.C., J.L. Diaz-Granados, and R.T. Weathersby, *Repeated ethanol withdrawal experience increases the severity and duration of subsequent withdrawal seizures in mice.* Alcohol, 1997. **14**(4): p. 319-326.
237. Mello, N.K. and J.H. Mendelson, *Drinking patterns during work-contingent and noncontingent alcohol acquisition.* Psychosom Med, 1972. **34**(2): p. 139-64.
238. Roberts, A.J., et al., *Excessive ethanol drinking following a history of dependence: animal model of allostasis.* Neuropsychopharmacology, 2000. **22**(6): p. 581-94.
239. Becker, H.C. and M.F. Lopez, *Increased ethanol drinking after repeated chronic ethanol exposure and withdrawal experience in C57BL/6 mice.* Alcohol Clin Exp Res, 2004. **28**(12): p. 1829-38.
240. Griffin, W.C., 3rd, M.F. Lopez, and H.C. Becker, *Intensity and duration of chronic ethanol exposure is critical for subsequent escalation of voluntary ethanol drinking in mice.* Alcohol Clin Exp Res, 2009. **33**(11): p. 1893-900.
241. Lopez, M.F., et al., *Repeated cycles of chronic intermittent ethanol exposure leads to the development of tolerance to aversive effects of ethanol in C57BL/6J mice.* Alcohol Clin Exp Res, 2012. **36**(7): p. 1180-7.
242. Samantaray, S., et al., *Chronic intermittent ethanol induced axon and myelin degeneration is attenuated by calpain inhibition.* Brain research, 2015. **1622**: p. 7-21.
243. Osterndorff-Kahanek, E.A., et al., *Chronic ethanol exposure produces time- and brain region-dependent changes in gene coexpression networks.* PLoS One, 2015. **10**(3): p. e0121522.
244. McMahon, R.C., D. Gersh, and R.S. Davidson, *Personality and symptom characteristics of continuous vs. episodic drinkers.* J Clin Psychol, 1989. **45**(1): p. 161-8.
245. Schuckit, M.A., *Low level of response to alcohol as a predictor of future alcoholism.* Am J Psychiatry, 1994. **151**(2): p. 184-9.
246. Schadt, E.E., et al., *An integrative genomics approach to infer causal associations between gene expression and disease.* Nature genetics, 2005. **37**(7): p. 710-717.
247. Wolen, A.R., et al., *Genetic dissection of acute ethanol responsive gene networks in prefrontal cortex: functional and mechanistic implications.* PLoS One, 2012. **7**(4): p. e33575.
248. Piechota, M., et al., *The dissection of transcriptional modules regulated by various drugs of abuse in the mouse striatum.* Genome Biol, 2010. **11**(5): p. R48.
249. Schadt, E.E., et al., *Genetics of gene expression surveyed in maize, mouse and man.* Nature, 2003. **422**(6929): p. 297-302.
250. Barkley-Levenson, A.M. and J.C. Crabbe, *Bridging Animal and Human Models: Translating From (and to) Animal Genetics.* Alcohol Res, 2012. **34**(3): p. 325-35.
251. Becker, H.C., *Animal models of excessive alcohol consumption in rodents.* Curr Top Behav Neurosci, 2013. **13**: p. 355-77.
252. O'Dell, L.E., et al., *Enhanced alcohol self-administration after intermittent versus continuous alcohol vapor exposure.* Alcohol Clin Exp Res, 2004. **28**(11): p. 1676-82.
253. Griffin, W.C., 3rd, et al., *Increased extracellular glutamate in the nucleus accumbens promotes excessive ethanol drinking in ethanol dependent mice.* Neuropsychopharmacology, 2014. **39**(3): p. 707-17.

254. Kroener, S., et al., *Chronic alcohol exposure alters behavioral and synaptic plasticity of the rodent prefrontal cortex.* PLoS One, 2012. **7**(5): p. e37541.
255. Gautier, L., et al., *affy--analysis of Affymetrix GeneChip data at the probe level.* Bioinformatics, 2004. **20**(3): p. 307-15.
256. Irizarry, R.A., et al., *Exploration, normalization, and summaries of high density oligonucleotide array probe level data.* Biostatistics, 2003. **4**(2): p. 249-64.
257. Johnson, W.E., C. Li, and A. Rabinovic, *Adjusting batch effects in microarray expression data using empirical Bayes methods.* Biostatistics, 2007. **8**(1): p. 118-27.
258. Smyth, G.K., *Linear models and empirical bayes methods for assessing differential expression in microarray experiments.* Stat Appl Genet Mol Biol, 2004. **3**: p. Article3.
259. Benjamini, Y. and Y. Hochberg, *Controlling the False Discovery Rate - a Practical and Powerful Approach to Multiple Testing.* Journal of the Royal Statistical Society Series B-Methodological, 1995. **57**(1): p. 289-300.
260. Langfelder, P. and S. Horvath, *WGCNA: an R package for weighted correlation network analysis.* BMC Bioinformatics, 2008. **9**: p. 559.
261. Fisher, R.A., *On the Interpretation of χ2 from Contingency Tables, and the Calculation of P.* Journal of the Royal Statistical Society, 1922. **85**(1): p. 87-94.
262. Huang da, W., B.T. Sherman, and R.A. Lempicki, *Systematic and integrative analysis of large gene lists using DAVID bioinformatics resources.* Nat Protoc, 2009. **4**(1): p. 44-57.
263. Huang da, W., B.T. Sherman, and R.A. Lempicki, *Bioinformatics enrichment tools: paths toward the comprehensive functional analysis of large gene lists.* Nucleic Acids Res, 2009. **37**(1): p. 1-13.
264. Warde-Farley, D., et al., *The GeneMANIA prediction server: biological network integration for gene prioritization and predicting gene function.* Nucleic Acids Res, 2010. **38**(Web Server issue): p. W214-20.
265. Plaisier, C.L., J.C. Bare, and N.S. Baliga, *miRvestigator: web application to identify miRNAs responsible for co-regulated gene expression patterns discovered through transcriptome profiling.* Nucleic Acids Res, 2011. **39**(Web Server issue): p. W125-31.
266. Gustafson, E.A. and G.M. Wessel, *DEAD-box Helicases: Posttranslational Regulation and Function.* Biochemical and biophysical research communications, 2010. **395**(1): p. 1-6.
267. Blencowe, B.J., et al., *The SRm160/300 splicing coactivator subunits.* Rna, 2000. **6**(1): p. 111-20.
268. Blencowe, B.J., et al., *A coactivator of pre-mRNA splicing.* Genes Dev, 1998. **12**(7): p. 996-1009.
269. Sawada, Y., et al., *Cloning and characterization of a novel RNA-binding protein SRL300 with RS domains.* Biochim Biophys Acta, 2000. **1492**(1): p. 191-5.
270. Wang, J., et al., *Regulation of platelet-derived growth factor signaling pathway by ethanol, nicotine, or both in mouse cortical neurons.* Alcohol Clin Exp Res, 2007. **31**(3): p. 357-75.
271. Kruman, I.I., G.I. Henderson, and S.E. Bergeson, *DNA damage and neurotoxicity of chronic alcohol abuse.* Experimental biology and medicine (Maywood, N.J.), 2012. **237**(7): p. 740-747.
272. Darcq, E., et al., *MicroRNA-30a-5p in the prefrontal cortex controls the transition from moderate to excessive alcohol consumption.* Mol Psychiatry, 2015. **20**(10): p. 1219-31.

273. Tapocik, J.D., et al., *microRNA-206 in Rat Medial Prefrontal Cortex Regulates BDNF Expression and Alcohol Drinking.* The Journal of Neuroscience, 2014. **34**(13): p. 4581-4588.
274. Greengard, P., et al., *Synaptic vesicle phosphoproteins and regulation of synaptic function.* Science, 1993. **259**(5096): p. 780-5.
275. Mizutani, A., et al., *SYNCRIP, a cytoplasmic counterpart of heterogeneous nuclear ribonucleoprotein R, interacts with ubiquitous synaptotagmin isoforms.* J Biol Chem, 2000. **275**(13): p. 9823-31.
276. Orenbuch, A., et al., *Synapsin selectively controls the mobility of resting pool vesicles at hippocampal terminals.* J Neurosci, 2012. **32**(12): p. 3969-80.
277. Thiel, G., *Synapsin I, synapsin II, and synaptophysin: marker proteins of synaptic vesicles.* Brain Pathol, 1993. **3**(1): p. 87-95.
278. Chen, G., et al., *Differential activation of limbic circuitry associated with chronic ethanol withdrawal in DBA/2J and C57BL/6J mice.* Alcohol, 2009. **43**(6): p. 411-420.
279. Daniels, G.M. and K.J. Buck, *Expression profiling identifies strain-specific changes associated with ethanol withdrawal in mice.* Genes, Brain and Behavior, 2002. **1**(1): p. 35-45.
280. Ables, J.L., et al., *Notch1 is required for maintenance of the reservoir of adult hippocampal stem cells.* J Neurosci, 2010. **30**(31): p. 10484-92.
281. Alberi, L., et al., *Activity-induced Notch signaling in neurons requires Arc/Arg3.1 and is essential for synaptic plasticity in hippocampal networks.* Neuron, 2011. **69**(3): p. 437-44.
282. Iwase, K., et al., *The secretogranin II gene is a signal integrator of glutamate and dopamine inputs.* J Neurochem, 2014. **128**(2): p. 233-45.
283. Licht, T., et al., *Reversible modulations of neuronal plasticity by VEGF.* Proceedings of the National Academy of Sciences, 2011. **108**(12): p. 5081-5086.
284. Tillo, M., C. Ruhrberg, and F. Mackenzie, *Emerging roles for semaphorins and VEGFs in synaptogenesis and synaptic plasticity.* Cell Adhesion & Migration, 2012. **6**(6): p. 541-546.
285. Batel, P., et al., *A haplotype of the DRD1 gene is associated with alcohol dependence.* Alcohol Clin Exp Res, 2008. **32**(4): p. 567-72.
286. Kim, D.J., et al., *5′ UTR polymorphism of dopamine receptor D1 (DRD1) associated with severity and temperament of alcoholism.* Biochem Biophys Res Commun, 2007. **357**(4): p. 1135-41.
287. Lacey, M.G., N.B. Mercuri, and R.A. North, *Dopamine acts on D2 receptors to increase potassium conductance in neurones of the rat substantia nigra zona compacta.* J Physiol, 1987. **392**: p. 397-416.
288. Farris, S.P. and M.F. Miles, *Fyn-dependent gene networks in acute ethanol sensitivity.* PLoS One, 2013. **8**(11): p. e82435.
289. Lum, P.Y., et al., *Elucidating the murine brain transcriptional network in a segregating mouse population to identify core functional modules for obesity and diabetes.* J Neurochem, 2006. **97 Suppl 1**: p. 50-62.
290. Takada, F., et al., *Myozenin: an alpha-actinin- and gamma-filamin-binding protein of skeletal muscle Z lines.* Proc Natl Acad Sci U S A, 2001. **98**(4): p. 1595-600.
291. Philip, V.M., et al., *High-throughput behavioral phenotyping in the expanded panel of BXD recombinant inbred strains.* Genes Brain Behav, 2010. **9**(2): p. 129-59.

292. Klugmann, M., et al., *A novel role of circadian transcription factor DBP in hippocampal plasticity.* Molecular and Cellular Neuroscience, 2006. **31**(2): p. 303-314.
293. Becker, H.C., *Alcohol Dependence, Withdrawal, and Relapse.* Alcohol Res Health, 2008. **31**(4): p. 348-61.
294. Tapocik, J.D., et al., *Coordinated dysregulation of mRNAs and microRNAs in the rat medial prefrontal cortex following a history of alcohol dependence.* The pharmacogenomics journal, 2013. **13**(3): p. 286-296.
295. Anderson, M.L., et al., *Moderate drinking? Alcohol consumption significantly decreases neurogenesis in the adult hippocampus.* Neuroscience, 2012. **224**(0): p. 202-209.
296. Beresford, T.P., et al., *Hypercortisolism in alcohol dependence and its relation to hippocampal volume loss.* J Stud Alcohol, 2006. **67**(6): p. 861-7.
297. Bleich, S., et al., *Lack of association between hippocampal volume reduction and first-onset alcohol withdrawal seizure. A volumetric MRI study.* Alcohol Alcohol, 2003. **38**(1): p. 40-4.
298. Chan, A.W., *Alcoholism and epilepsy.* Epilepsia, 1985. **26**(4): p. 323-33.
299. Grant, K.A., et al., *Ethanol withdrawal seizures and the NMDA receptor complex.* Eur J Pharmacol, 1990. **176**(3): p. 289-96.
300. Hauser, W.A., S.K. Ng, and J.C. Brust, *Alcohol, seizures, and epilepsy.* Epilepsia, 1988. **29 Suppl 2**: p. S66-78.
301. Ng, S.K., et al., *Alcohol consumption and withdrawal in new-onset seizures.* N Engl J Med, 1988. **319**(11): p. 666-73.
302. Stepanyan, T.D., et al., *Alcohol withdrawal-induced hippocampal neurotoxicity in vitro and seizures in vivo are both reduced by memantine.* Alcohol Clin Exp Res, 2008. **32**(12): p. 2128-35.
303. Nakamura-Palacios, E.M., et al., *Gray matter volume in left rostral middle frontal and left cerebellar cortices predicts frontal executive performance in alcoholic subjects.* Alcohol Clin Exp Res, 2014. **38**(4): p. 1126-33.
304. Weitlauf, C. and J.J. Woodward, *Ethanol selectively attenuates NMDAR-mediated synaptic transmission in the prefrontal cortex.* Alcohol Clin Exp Res, 2008. **32**(4): p. 690-8.
305. Avery, S.N., J.A. Clauss, and J.U. Blackford, *The Human BNST: Functional Role in Anxiety and Addiction.* Neuropsychopharmacology, 2016. **41**(1): p. 126-41.
306. Okun, E., K.J. Griffioen, and M.P. Mattson, *Toll-like receptor signaling in neural plasticity and disease.* Trends Neurosci, 2011. **34**(5): p. 269-81.
307. Costin, B.N., et al., *Role of adrenal glucocorticoid signaling in prefrontal cortex gene expression and acute behavioral responses to ethanol.* Alcohol Clin Exp Res, 2013. **37**(1): p. 57-66.
308. Robinson, G., et al., *Neuroimmune pathways in alcohol consumption: evidence from behavioral and genetic studies in rodents and humans.* Int Rev Neurobiol, 2014. **118**: p. 13-39.
309. Eriksson, P.S., et al., *Neurogenesis in the adult human hippocampus.* Nat Med, 1998. **4**(11): p. 1313-7.
310. Favaro, R., et al., *Hippocampal development and neural stem cell maintenance require Sox2-dependent regulation of Shh.* Nat Neurosci, 2009. **12**(10): p. 1248-56.
311. Ferri, A.L., et al., *Sox2 deficiency causes neurodegeneration and impaired neurogenesis in the adult mouse brain.* Development, 2004. **131**(15): p. 3805-19.

312. Mira, H., et al., *Signaling through BMPR-IA regulates quiescence and long-term activity of neural stem cells in the adult hippocampus.* Cell Stem Cell, 2010. **7**(1): p. 78-89.
313. Altman, J., *Autoradiographic investigation of cell proliferation in the brains of rats and cats.* Anat Rec, 1963. **145**: p. 573-91.
314. Soumier, A., et al., *Region- and phase-dependent effects of 5-HT(1A) and 5-HT(2C) receptor activation on adult neurogenesis.* Eur Neuropsychopharmacol, 2010. **20**(5): p. 336-45.
315. Staffend, N.A., et al., *A decrease in the addition of new cells in the nucleus accumbens and prefrontal cortex between puberty and adulthood in male rats.* Dev Neurobiol, 2014. **74**(6): p. 633-42.
316. Gould, E., et al., *Neurogenesis in the neocortex of adult primates.* Science, 1999. **286**(5439): p. 548-52.
317. Banasr, M., et al., *Chronic unpredictable stress decreases cell proliferation in the cerebral cortex of the adult rat.* Biol Psychiatry, 2007. **62**(5): p. 496-504.
318. Czeh, B., et al., *Chronic social stress inhibits cell proliferation in the adult medial prefrontal cortex: hemispheric asymmetry and reversal by fluoxetine treatment.* Neuropsychopharmacology, 2007. **32**(7): p. 1490-503.
319. Czeh, B., et al., *Chronic stress-induced cellular changes in the medial prefrontal cortex and their potential clinical implications: does hemisphere location matter?* Behav Brain Res, 2008. **190**(1): p. 1-13.
320. Herrera, D.G., et al., *Selective impairment of hippocampal neurogenesis by chronic alcoholism: protective effects of an antioxidant.* Proc Natl Acad Sci U S A, 2003. **100**(13): p. 7919-24.
321. Nixon, K., et al., *Roles of neural stem cells and adult neurogenesis in adolescent alcohol use disorders.* Alcohol, 2010. **44**(1): p. 39-56.
322. Wang, H.D., et al., *Effects of antipsychotic drugs on neurogenesis in the forebrain of the adult rat.* Neuropsychopharmacology, 2004. **29**(7): p. 1230-8.
323. Klein, R., *Role of neurotrophins in mouse neuronal development.* Faseb j, 1994. **8**(10): p. 738-44.
324. Pang, P.T. and B. Lu, *Regulation of late-phase LTP and long-term memory in normal and aging hippocampus: role of secreted proteins tPA and BDNF.* Ageing Res Rev, 2004. **3**(4): p. 407-30.
325. Bolanos, C.A. and E.J. Nestler, *Neurotrophic mechanisms in drug addiction.* Neuromolecular Med, 2004. **5**(1): p. 69-83.
326. Miller, R., et al., *The effects of chronic ethanol consumption on neurotrophins and their receptors in the rat hippocampus and basal forebrain.* Brain Res, 2002. **950**(1-2): p. 137-47.
327. Russo, S.J., et al., *Neurotrophic factors and structural plasticity in addiction.* Neuropharmacology, 2009. **56 Suppl 1**: p. 73-82.
328. Tapia-Arancibia, L., et al., *Effects of alcohol on brain-derived neurotrophic factor mRNA expression in discrete regions of the rat hippocampus and hypothalamus.* J Neurosci Res, 2001. **63**(2): p. 200-8.
329. Pasquinelli, A.E., et al., *Conservation of the sequence and temporal expression of let-7 heterochronic regulatory RNA.* Nature, 2000. **408**(6808): p. 86-9.

330. Jeyaseelan, K., K.Y. Lim, and A. Armugam, *MicroRNA expression in the blood and brain of rats subjected to transient focal ischemia by middle cerebral artery occlusion.* Stroke, 2008. **39**(3): p. 959-66.
331. Saba, R., et al., *A miRNA signature of prion induced neurodegeneration.* PLoS One, 2008. **3**(11): p. e3652.
332. Wulczyn, F.G., et al., *Post-transcriptional regulation of the let-7 microRNA during neural cell specification.* Faseb j, 2007. **21**(2): p. 415-26.
333. Zhao, C., et al., *MicroRNA let-7b regulates neural stem cell proliferation and differentiation by targeting nuclear receptor TLX signaling.* Proc Natl Acad Sci U S A, 2010. **107**(5): p. 1876-81.
334. Moonat, S., et al., *Aberrant histone deacetylase2-mediated histone modifications and synaptic plasticity in the amygdala predisposes to anxiety and alcoholism.* Biol Psychiatry, 2013. **73**(8): p. 763-73.
335. Robison, A.J. and E.J. Nestler, *Transcriptional and epigenetic mechanisms of addiction.* Nat Rev Neurosci, 2011. **12**(11): p. 623-37.
336. Schmidt, W. and R.E. Popham, *Heavy alcohol consumption and physical health problems: a review of the epidemiological evidence.* Drug Alcohol Depend, 1975. **1**(1): p. 27-50.
337. Bhandari, P., et al., *Chloride intracellular channels modulate acute ethanol behaviors in Drosophila, Caenorhabditis elegans and mice.* Genes Brain Behav, 2012. **11**(4): p. 387-97.
338. Langfelder, P., B. Zhang, and S. Horvath, *Defining clusters from a hierarchical cluster tree: the Dynamic Tree Cut package for R.* Bioinformatics, 2008. **24**(5): p. 719-20.
339. Langfelder, P. and S. Horvath, *Eigengene networks for studying the relationships between co-expression modules.* BMC Syst Biol, 2007. **1**: p. 54.
340. Spearman, C., *The Proof and Measurement of Association between Two Things.* The American Journal of Psychology, 1904. **15**(1): p. 72-101.
341. Cahoy, J.D., et al., *A transcriptome database for astrocytes, neurons, and oligodendrocytes: a new resource for understanding brain development and function.* J Neurosci, 2008. **28**(1): p. 264-78.
342. Miller, J.A., et al., *Genes and pathways underlying regional and cell type changes in Alzheimer's disease.* Genome Med, 2013. **5**(5): p. 48.
343. Papamichos-Chronakis, M. and C.L. Peterson, *Chromatin and the genome integrity network.* Nature reviews. Genetics, 2013. **14**(1): p. 62-75.
344. Robertson, K.D., et al., *The human DNA methyltransferases (DNMTs) 1, 3a and 3b: coordinate mRNA expression in normal tissues and overexpression in tumors.* Nucleic Acids Research, 1999. **27**(11): p. 2291-2298.
345. Schneider, A., et al., *Acetyltransferases (HATs) as Targets for Neurological Therapeutics.* Neurotherapeutics, 2013. **10**(4): p. 568-588.
346. Simon, J.A. and R.E. Kingston, *Occupying chromatin: Polycomb mechanisms for getting to genomic targets, stopping transcriptional traffic, and staying put.* Molecular cell, 2013. **49**(5): p. 808-824.
347. Wolfson, N.A., C.A. Pitcairn, and C.A. Fierke, *HDAC8 Substrates: Histones and Beyond.* Biopolymers, 2013. **99**(2): p. 112-126.

348. Yoder, J.A., et al., *DNA (cytosine-5)-methyltransferases in mouse cells and tissues. studies with a mechanism-based probe1.* Journal of Molecular Biology, 1997. **270**(3): p. 385-395.
349. Kaushansky, N., et al., *The myelin-associated oligodendrocytic basic protein (MOBP) as a relevant primary target autoantigen in multiple sclerosis.* Autoimmunity Reviews, 2010. **9**(4): p. 233-236.
350. Nakamura, Y., R. Iwamoto, and E. Mekada, *Expression and distribution of CD9 in myelin of the central and peripheral nervous systems.* The American Journal of Pathology, 1996. **149**(2): p. 575-583.
351. Engel, J.A. and E. Jerlhag, *Chapter 9 - Alcohol: mechanisms along the mesolimbic dopamine system*, in *Progress in Brain Research*, G.D.C. Marco Diana and S. Pierfranco, Editors. 2014, Elsevier. p. 201-233.
352. Koob, G.F., P.P. Sanna, and F.E. Bloom, *Neuroscience of Addiction.* Neuron, 1998. **21**(3): p. 467-476.
353. Fein, G. and V.A. Cardenas, *Neuroplasticity in Human Alcoholism: Studies of Extended Abstinence with Potential Treatment Implications.* Alcohol Res, 2015. **37**(1): p. 125-41.
354. Seo, D. and R. Sinha, *Neuroplasticity and Predictors of Alcohol Recovery.* Alcohol Res, 2015. **37**(1): p. 143-52.
355. Durazzo, T.C., et al., *Cortical thickness, surface area, and volume of the brain reward system in alcohol dependence: relationships to relapse and extended abstinence.* Alcohol Clin Exp Res, 2011. **35**(6): p. 1187-200.
356. Grusser, S.M., et al., *Cue-induced activation of the striatum and medial prefrontal cortex is associated with subsequent relapse in abstinent alcoholics.* Psychopharmacology (Berl), 2004. **175**(3): p. 296-302.
357. Noel, X., et al., *Contribution of frontal cerebral blood flow measured by (99m)Tc-Bicisate spect and executive function deficits to predicting treatment outcome in alcohol-dependent patients.* Alcohol Alcohol, 2002. **37**(4): p. 347-54.
358. O'Leary-Moore, S.K., et al., *Magnetic resonance-based imaging in animal models of fetal alcohol spectrum disorder.* Neuropsychol Rev, 2011. **21**(2): p. 167-85.
359. Parnell, S.E., et al., *Magnetic resonance microscopy-based analyses of the neuroanatomical effects of gestational day 9 ethanol exposure in mice.* Neurotoxicol Teratol, 2013. **39**: p. 77-83.
360. Wang, X. and C.D. Kroenke, *Utilization of Magnetic Resonance Imaging in Research Involving Animal Models of Fetal Alcohol Spectrum Disorders.* Alcohol Res, 2015. **37**(1): p. 39-51.
361. Montesinos, J., S. Alfonso-Loeches, and C. Guerri, *Impact of the Innate Immune Response in the Actions of Ethanol on the Central Nervous System.* Alcohol Clin Exp Res, 2016.
362. Jeltsch, A. and R.Z. Jurkowska, *New concepts in DNA methylation.* Trends in Biochemical Sciences, 2014. **39**(7): p. 310-318.
363. Aihara, T., et al., *Cloning and mapping of SMARCA5 encoding hSNF2H, a novel human homologue of Drosophila ISWI.* Cytogenet Cell Genet, 1998. **81**(3-4): p. 191-3.
364. LeRoy, G., et al., *Purification and characterization of a human factor that assembles and remodels chromatin.* J Biol Chem, 2000. **275**(20): p. 14787-90.
365. Wang, W., et al., *Diversity and specialization of mammalian SWI/SNF complexes.* Genes Dev, 1996. **10**(17): p. 2117-30.

366. Krishnan, H.R., et al., *Chapter Three - The Epigenetic Landscape of Alcoholism*, in *International Review of Neurobiology*, C.P. Subhash, Editor. 2014, Academic Press. p. 75-116.
367. Kyzar, E.J., et al., *Adolescent Alcohol Exposure: Burden of Epigenetic Reprogramming, Synaptic Remodeling, and Adult Psychopathology.* Front Neurosci, 2016. **10**: p. 222.
368. Schuckit, M.A., *An overview of genetic influences in alcoholism.* J Subst Abuse Treat, 2009. **36**(1): p. S5-14.
369. Cotton, N.S., *The familial incidence of alcoholism: a review.* J Stud Alcohol, 1979. **40**(1): p. 89-116.
370. Cloninger, C.R., M. Bohman, and S. Sigvardsson, *Inheritance of alcohol abuse. Cross-fostering analysis of adopted men.* Arch Gen Psychiatry, 1981. **38**(8): p. 861-8.
371. Goodwin, D.W., et al., *Psychopathology in adopted and nonadopted daughters of alcoholics.* Arch Gen Psychiatry, 1977. **34**(9): p. 1005-9.
372. Goodwin, D.W., et al., *Drinking problems in adopted and nonadopted sons of alcoholics.* Arch Gen Psychiatry, 1974. **31**(2): p. 164-9.
373. Kendler, K.S., et al., *A population-based twin study of alcoholism in women.* Jama, 1992. **268**(14): p. 1877-82.
374. Schuckit, M.A., *New findings in the genetics of alcoholism.* Jama, 1999. **281**(20): p. 1875-6.
375. Biernacka, J.M., et al., *Replication of genome wide association studies of alcohol dependence: support for association with variation in ADH1C.* PLoS One, 2013. **8**(3): p. e58798.
376. Bierut, L.J., et al., *A genome-wide association study of alcohol dependence.* Proc Natl Acad Sci U S A, 2010. **107**(11): p. 5082-7.
377. Edenberg, H.J., et al., *Genome-wide association study of alcohol dependence implicates a region on chromosome 11.* Alcohol Clin Exp Res, 2010. **34**(5): p. 840-52.
378. Zuo, L., et al., *A novel, functional and replicable risk gene region for alcohol dependence identified by genome-wide association study.* PLoS One, 2011. **6**(11): p. e26726.
379. Eppig, J.T., et al., *The Mouse Genome Database (MGD): facilitating mouse as a model for human biology and disease.* Nucleic Acids Res, 2015. **43**(Database issue): p. D726-36.
380. Wang, X., et al., *Joint mouse-human phenome-wide association to test gene function and disease risk.* Nat Commun, 2016. **7**: p. 10464.
381. Emery, F.D., et al., *Genetic control of weight loss during pneumonic Burkholderia pseudomallei infection.* Pathog Dis, 2014. **71**(2): p. 249-64.
382. Gill, K., Y. Liu, and R.A. Deitrich, *Voluntary alcohol consumption in BXD recombinant inbred mice: relationship to alcohol metabolism.* Alcohol Clin Exp Res, 1996. **20**(1): p. 185-90.
383. McCool, B.A. and A.M. Chappell, *Chronic intermittent ethanol inhalation increases ethanol self-administration in both C57BL/6J and DBA/2J mice.* Alcohol, 2015. **49**(2): p. 111-20.
384. Ford, M.M., et al., *The relationship between adjunctive drinking, blood ethanol concentration and plasma corticosterone across fixed-time intervals of food delivery in two inbred mouse strains.* Psychoneuroendocrinology, 2013. **38**(11): p. 2598-610.

385. Moore, E.M., R.D.t. Forrest, and S.L. Boehm, 2nd, *Genotype modulates age-related alterations in sensitivity to the aversive effects of ethanol: an eight inbred strain analysis of conditioned taste aversion.* Genes Brain Behav, 2013. **12**(1): p. 70-7.
386. Linsenbardt, D.N., et al., *Sensitivity and tolerance to the hypnotic and ataxic effects of ethanol in adolescent and adult C57BL/6J and DBA/2J mice.* Alcohol Clin Exp Res, 2009. **33**(3): p. 464-76.
387. Porcu, P., et al., *Simultaneous quantification of GABAergic 3alpha,5alpha/3alpha,5beta neuroactive steroids in human and rat serum.* Steroids, 2009. **74**(4-5): p. 463-73.
388. Kennedy, R.E., K.J. Archer, and M.F. Miles, *Empirical validation of the S-Score algorithm in the analysis of gene expression data.* BMC Bioinformatics, 2006. **7**: p. 154.
389. Zhang, L., et al., *A new algorithm for analysis of oligonucleotide arrays: application to expression profiling in mouse brain regions.* J Mol Biol, 2002. **317**(2): p. 225-35.
390. Song, L., P. Langfelder, and S. Horvath, *Comparison of co-expression measures: mutual information, correlation, and model based indices.* BMC Bioinformatics, 2012. **13**: p. 328.
391. Kimpel, M.W., et al., *Functional gene expression differences between inbred alcohol-preferring and -non-preferring rats in five brain regions.* Alcohol, 2007. **41**(2): p. 95-132.
392. Aguirre, A., M.E. Rubio, and V. Gallo, *Notch and EGFR pathway interaction regulates neural stem cell number and self-renewal.* Nature, 2010. **467**(7313): p. 323-327.
393. Gaiano, N. and G. Fishell, *The role of notch in promoting glial and neural stem cell fates.* Annu Rev Neurosci, 2002. **25**: p. 471-90.
394. Leifer, D., et al., *MEF2C, a MADS/MEF2-family transcription factor expressed in a laminar distribution in cerebral cortex.* Proceedings of the National Academy of Sciences of the United States of America, 1993. **90**(4): p. 1546-1550.
395. Adams, R.H., H. Betz, and A.W. Puschel, *A novel class of murine semaphorins with homology to thrombospondin is differentially expressed during early embryogenesis.* Mech Dev, 1996. **57**(1): p. 33-45.
396. Itoh, N. and H. Ohta, *Fgf10: a paracrine-signaling molecule in development, disease, and regenerative medicine.* Curr Mol Med, 2014. **14**(4): p. 504-9.
397. Ragia, G., et al., *Association study of DRD2 A2/A1, DRD3 Ser9Gly, DbetaH -1021C>T, OPRM1 A118G and GRIK1 rs2832407C>A polymorphisms with alcohol dependence.* Drug Metab Pers Ther, 2016. **31**(3): p. 143-50.
398. Kurokawa, K., K. Mizuno, and S. Ohkuma, *Dopamine D1 receptor signaling system regulates ryanodine receptor expression in ethanol physical dependence.* Alcohol Clin Exp Res, 2013. **37**(5): p. 771-83.
399. Courtney, K.E., D.G. Ghahremani, and L.A. Ray, *The effect of alcohol priming on neural markers of alcohol cue-reactivity.* Am J Drug Alcohol Abuse, 2015. **41**(4): p. 300-8.
400. Butt, C.M., et al., *Interaction of the nicotinic cholinergic system with ethanol withdrawal.* J Pharmacol Exp Ther, 2004. **308**(2): p. 591-9.
401. Coon, H., et al., *Association of the CHRNA4 neuronal nicotinic receptor subunit gene with frequency of binge drinking in young adults.* Alcohol Clin Exp Res, 2014. **38**(4): p. 930-7.
402. Landgren, S., et al., *Association of nAChR gene haplotypes with heavy alcohol use and body mass.* Brain Res, 2009. **1305 Suppl**: p. S72-9.

403. Haller, G., et al., *Rare missense variants in CHRNB3 and CHRNA3 are associated with risk of alcohol and cocaine dependence.* Hum Mol Genet, 2014. **23**(3): p. 810-9.
404. De Strooper, B., et al., *A presenilin-1-dependent gamma-secretase-like protease mediates release of Notch intracellular domain.* Nature, 1999. **398**(6727): p. 518-22.
405. Armendariz, B.G., et al., *Expression of Semaphorin 4F in neurons and brain oligodendrocytes and the regulation of oligodendrocyte precursor migration in the optic nerve.* Mol Cell Neurosci, 2012. **49**(1): p. 54-67.
406. Struhl, G. and I. Greenwald, *Presenilin is required for activity and nuclear access of Notch in Drosophila.* Nature, 1999. **398**(6727): p. 522-5.
407. Clement, J.P., et al., *Pathogenic SYNGAP1 mutations impair cognitive development by disrupting maturation of dendritic spine synapses.* Cell, 2012. **151**(4): p. 709-23.
408. Kuhlbrodt, K., et al., *Sox10, a novel transcriptional modulator in glial cells.* J Neurosci, 1998. **18**(1): p. 237-50.
409. Stolt, C.C., et al., *Terminal differentiation of myelin-forming oligodendrocytes depends on the transcription factor Sox10.* Genes Dev, 2002. **16**(2): p. 165-70.
410. Schmucker, J., et al., *erbB3 is dispensable for oligodendrocyte development in vitro and in vivo.* Glia, 2003. **44**(1): p. 67-75.
411. Edwards, A.M., et al., *Interaction of myelin basic protein and proteolipid protein.* J Neurosci Res, 1989. **22**(1): p. 97-102.
412. Starkman, B.G., A.J. Sakharkar, and S.C. Pandey, *Epigenetics-beyond the genome in alcoholism.* Alcohol Res, 2012. **34**(3): p. 293-305.
413. Pascual, M., et al., *Repeated alcohol administration during adolescence causes changes in the mesolimbic dopaminergic and glutamatergic systems and promotes alcohol intake in the adult rat.* J Neurochem, 2009. **108**(4): p. 920-31.
414. Delis, F., et al., *Regulation of ethanol intake under chronic mild stress: roles of dopamine receptors and transporters.* Front Behav Neurosci, 2015. **9**: p. 118.
415. Delis, F., et al., *Chronic mild stress increases alcohol intake in mice with low dopamine D2 receptor levels.* Behav Neurosci, 2013. **127**(1): p. 95-105.
416. Osterndorff-Kahanek, E., et al., *Gene expression in brain and liver produced by three different regimens of alcohol consumption in mice: comparison with immune activation.* PLoS One, 2013. **8**(3): p. e59870.
417. Kamens, H.M., J. Andersen, and M.R. Picciotto, *Modulation of ethanol consumption by genetic and pharmacological manipulation of nicotinic acetylcholine receptors in mice.* Psychopharmacology (Berl), 2010. **208**(4): p. 613-26.
418. Symons, M.N., et al., *Delineation of the role of nicotinic acetylcholine receptor genes in alcohol preference in mice.* Behav Genet, 2010. **40**(5): p. 660-71.
419. Melis, M., et al., *PPARalpha regulates cholinergic-driven activity of midbrain dopamine neurons via a novel mechanism involving alpha7 nicotinic acetylcholine receptors.* J Neurosci, 2013. **33**(14): p. 6203-11.
420. Gozen, O., et al., *Nicotinic cholinergic and dopaminergic receptor mRNA expression in male and female rats with high or low preference for nicotine.* Am J Drug Alcohol Abuse, 2016. **42**(5): p. 556-566.
421. Gass, N., et al., *An acetylcholine alpha7 positive allosteric modulator rescues a schizophrenia-associated brain endophenotype in the 15q13.3 microdeletion, encompassing CHRNA7.* Eur Neuropsychopharmacol, 2016. **26**(7): p. 1150-60.

422. Nilsson, S.R., et al., *A mouse model of the 15q13.3 microdeletion syndrome shows prefrontal neurophysiological dysfunctions and attentional impairment.* Psychopharmacology (Berl), 2016. **233**(11): p. 2151-63.
423. Blednov, Y.A., et al., *Perturbation of chemokine networks by gene deletion alters the reinforcing actions of ethanol.* Behav Brain Res, 2005. **165**(1): p. 110-25.
424. Wu, Y., et al., *Inhibiting the TLR4-MyD88 signalling cascade by genetic or pharmacological strategies reduces acute alcohol-induced sedation and motor impairment in mice.* Br J Pharmacol, 2012. **165**(5): p. 1319-29.
425. Cao, G., et al., *Molecular cloning and characterization of a novel human cAMP response element-binding (CREB) gene (CREB4).* J Hum Genet, 2002. **47**(7): p. 373-6.
426. Paushkin, S.V., et al., *Identification of a human endonuclease complex reveals a link between tRNA splicing and pre-mRNA 3′ end formation.* Cell, 2004. **117**(3): p. 311-21.
427. Yamano, Y., et al., *A novel spermatogenesis-related factor-1 gene expressed in maturing rat testis.* Biochem Biophys Res Commun, 2001. **289**(4): p. 888-93.
428. Miyamoto, T., et al., *Azoospermia in patients heterozygous for a mutation in SYCP3.* Lancet, 2003. **362**(9397): p. 1714-9.
429. Yuan, L., et al., *The murine SCP3 gene is required for synaptonemal complex assembly, chromosome synapsis, and male fertility.* Mol Cell, 2000. **5**(1): p. 73-83.
430. Bolcun-Filas, E., et al., *Mutation of the mouse Syce1 gene disrupts synapsis and suggests a link between synaptonemal complex structural components and DNA repair.* PLoS Genet, 2009. **5**(2): p. e1000393.
431. Law, R.H.P., et al., *An overview of the serpin superfamily.* Genome Biology, 2006. **7**(5): p. 216-216.
432. Kim, M., et al., *Robo1 and Robo2 have distinct roles in pioneer longitudinal axon guidance.* Developmental biology, 2011. **358**(1): p. 181-188.
433. Zhai, R.G., et al., *Drosophila NMNAT maintains neural integrity independent of its NAD synthesis activity.* PLoS Biol, 2006. **4**(12): p. e416.
434. Kochubey, O., N. Babai, and R. Schneggenburger, *A Synaptotagmin Isoform Switch during the Development of an Identified CNS Synapse.* Neuron, 2016. **90**(5): p. 984-99.
435. Wennerberg, K., K.L. Rossman, and C.J. Der, *The Ras superfamily at a glance.* J Cell Sci, 2005. **118**(Pt 5): p. 843-6.
436. Mazzucchelli, C. and R. Brambilla, *Ras-related and MAPK signalling in neuronal plasticity and memory formation.* Cell Mol Life Sci, 2000. **57**(4): p. 604-11.
437. Shilyansky, C., Y.S. Lee, and A.J. Silva, *Molecular and cellular mechanisms of learning disabilities: a focus on NF1.* Annu Rev Neurosci, 2010. **33**: p. 221-43.
438. Ron, D. and S. Barak, *Molecular mechanisms underlying alcohol-drinking behaviours.* Nat Rev Neurosci, 2016. **17**(9): p. 576-91.
439. Ye, X. and T.J. Carew, *Small G-protein Signaling in Neuronal Plasticity and Memory Formation: the Specific Role of Ras Family Proteins.* Neuron, 2010. **68**(3): p. 340-361.
440. Oliveira, A.F. and R. Yasuda, *Neurofibromin is the major ras inactivator in dendritic spines.* J Neurosci, 2014. **34**(3): p. 776-83.
441. Husi, H., et al., *Proteomic analysis of NMDA receptor-adhesion protein signaling complexes.* Nat Neurosci, 2000. **3**(7): p. 661-9.
442. Rock, K.L., E. Reits, and J. Neefjes, *Present Yourself! By MHC Class I and MHC Class II Molecules.* Trends Immunol, 2016.

443. Elmer, B.M. and A.K. McAllister, *Major histocompatibility complex class I proteins in brain development and plasticity.* Trends Neurosci, 2012. **35**(11): p. 660-70.
444. Etienne, S., et al., *MHC class II engagement in brain endothelial cells induces protein kinase A-dependent IL-6 secretion and phosphorylation of cAMP response element-binding protein.* J Immunol, 1999. **163**(7): p. 3636-41.
445. Reyahi, A., et al., *Foxf2 Is Required for Brain Pericyte Differentiation and Development and Maintenance of the Blood-Brain Barrier.* Dev Cell, 2015. **34**(1): p. 19-32.
446. Haliburton, G.D., G.L. McKinsey, and K.S. Pollard, *Disruptions in a cluster of computationally identified enhancers near FOXC1 and GMDS may influence brain development.* Neurogenetics, 2016. **17**(1): p. 1-9.
447. Prasitsak, T., et al., *Foxc1 is required for early stage telencephalic vascular development.* Dev Dyn, 2015. **244**(5): p. 703-11.
448. Siegenthaler, J.A., et al., *Foxc1 is required by pericytes during fetal brain angiogenesis.* Biol Open, 2013. **2**(7): p. 647-59.
449. Wang, Y.W., et al., *High expression of forkhead box protein C2 is related to poor prognosis in human gliomas.* Asian Pac J Cancer Prev, 2014. **15**(24): p. 10621-5.
450. Cheng, P., et al., *FOXD1-ALDH1A3 signaling is a determinant for the self-renewal and tumorigenicity of mesenchymal glioma stem cells.* Cancer Res, 2016.
451. Sarmah, S., P. Muralidharan, and J.A. Marrs, *Embryonic Ethanol Exposure Dysregulates BMP and Notch Signaling, Leading to Persistent Atrio-Ventricular Valve Defects in Zebrafish.* PLoS One, 2016. **11**(8): p. e0161205.
452. Tammela, T., et al., *VEGFR-3 controls tip to stalk conversion at vessel fusion sites by reinforcing Notch signalling.* Nat Cell Biol, 2011. **13**(10): p. 1202-13.
453. Swart, P.C., et al., *Early ethanol exposure and vinpocetine treatment alter learning- and memory-related proteins in the rat hippocampus and prefrontal cortex.* J Neurosci Res, 2016.
454. Majewska, M.D., J.M. Mienville, and S. Vicini, *Neurosteroid pregnenolone sulfate antagonizes electrophysiological responses to GABA in neurons.* Neurosci Lett, 1988. **90**(3): p. 279-84.
455. Wu, F.S., T.T. Gibbs, and D.H. Farb, *Pregnenolone sulfate: a positive allosteric modulator at the N-methyl-D-aspartate receptor.* Mol Pharmacol, 1991. **40**(3): p. 333-6.
456. Schultz, W., *Neuronal Reward and Decision Signals: From Theories to Data.* Physiol Rev, 2015. **95**(3): p. 853-951.
457. Grant, K.A., et al., *Drinking typography established by scheduled induction predicts chronic heavy drinking in a monkey model of ethanol self-administration.* Alcohol Clin Exp Res, 2008. **32**(10): p. 1824-38.
458. Miller, J.A., et al., *Strategies for aggregating gene expression data: the collapseRows R function.* BMC Bioinformatics, 2011. **12**: p. 322.
459. Zeisel, A., et al., *Brain structure. Cell types in the mouse cortex and hippocampus revealed by single-cell RNA-seq.* Science, 2015. **347**(6226): p. 1138-42.
460. Noble, E.P., et al., *D2 dopamine receptor and GABA(A) receptor beta3 subunit genes and alcoholism.* Psychiatry Res, 1998. **81**(2): p. 133-47.
461. Young, R.M., et al., *Alcohol-related expectancies are associated with the D2 dopamine receptor and GABAA receptor beta3 subunit genes.* Psychiatry Res, 2004. **127**(3): p. 171-83.

462. Cho, J.H., et al., *Requirement for Slit-1 and Robo-2 in zonal segregation of olfactory sensory neuron axons in the main olfactory bulb.* J Neurosci, 2007. **27**(34): p. 9094-104.
463. Sternberg, H., et al., *Seven diverse human embryonic stem cell-derived chondrogenic clonal embryonic progenitor cell lines display site-specific cell fates.* Regen Med, 2013. **8**(2): p. 125-44.
464. Pankov, R. and K.M. Yamada, *Fibronectin at a glance.* J Cell Sci, 2002. **115**(Pt 20): p. 3861-3.
465. Tashima, T., et al., *Osteomodulin regulates diameter and alters shape of collagen fibrils.* Biochem Biophys Res Commun, 2015. **463**(3): p. 292-6.
466. Astrom, A., et al., *Molecular cloning of two human cellular retinoic acid-binding proteins (CRABP). Retinoic acid-induced expression of CRABP-II but not CRABP-I in adult human skin in vivo and in skin fibroblasts in vitro.* J Biol Chem, 1991. **266**(26): p. 17662-6.
467. Iozzo, R.V. and L. Schaefer, *Proteoglycan form and function: A comprehensive nomenclature of proteoglycans.* Matrix Biol, 2015. **42**: p. 11-55.
468. Nguyen Ba-Charvet, K.T., et al., *Diversity and specificity of actions of Slit2 proteolytic fragments in axon guidance.* J Neurosci, 2001. **21**(12): p. 4281-9.
469. Nguyen-Ba-Charvet, K.T. and A. Chedotal, *Role of Slit proteins in the vertebrate brain.* J Physiol Paris, 2002. **96**(1-2): p. 91-8.
470. Shu, T., et al., *Slit2 guides both precrossing and postcrossing callosal axons at the midline in vivo.* J Neurosci, 2003. **23**(22): p. 8176-84.
471. Akers, K.G., et al., *Fetal alcohol exposure leads to abnormal olfactory bulb development and impaired odor discrimination in adult mice.* Mol Brain, 2011. **4**: p. 29.
472. Faas, A.E., et al., *Differential responsiveness to alcohol odor in human neonates: effects of maternal consumption during gestation.* Alcohol, 2000. **22**(1): p. 7-17.
473. Kareken, D.A., et al., *Alcohol-related olfactory cues activate the nucleus accumbens and ventral tegmental area in high-risk drinkers: preliminary findings.* Alcohol Clin Exp Res, 2004. **28**(4): p. 550-7.
474. Marjonen, H., et al., *Early maternal alcohol consumption alters hippocampal DNA methylation, gene expression and volume in a mouse model.* PLoS One, 2015. **10**(5): p. e0124931.
475. Monk, R.L., et al., *Smells like inhibition: The effects of olfactory and visual alcohol cues on inhibitory control.* Psychopharmacology (Berl), 2016. **233**(8): p. 1331-7.
476. Suginta, W., et al., *Chloride intracellular channel protein CLIC4 (p64H1) binds directly to brain dynamin I in a complex containing actin, tubulin and 14-3-3 isoforms.* Biochem J, 2001. **359**(Pt 1): p. 55-64.
477. Ishii, A., et al., *Human myelin proteome and comparative analysis with mouse myelin.* Proc Natl Acad Sci U S A, 2009. **106**(34): p. 14605-10.
478. Salvatore, J.E., Gottesman, II, and D.M. Dick, *Endophenotypes for Alcohol Use Disorder: An Update on the Field.* Curr Addict Rep, 2015. **2**(1): p. 76-90.
479. Michaelson, J.J., S. Loguercio, and A. Beyer, *Detection and interpretation of expression quantitative trait loci (eQTL).* Methods, 2009. **48**(3): p. 265-76.
480. Harenza, J.L., et al., *Genetic variation within the Chrna7 gene modulates nicotine reward-like phenotypes in mice.* Genes Brain Behav, 2014. **13**(2): p. 213-25.

481. Putman, A.H., et al., *Identification of quantitative trait loci and candidate genes for an anxiolytic-like response to ethanol in BXD recombinant inbred strains.* Genes Brain Behav, 2016. **15**(4): p. 367-81.
482. Kidd, T., et al., *Roundabout controls axon crossing of the CNS midline and defines a novel subfamily of evolutionarily conserved guidance receptors.* Cell, 1998. **92**(2): p. 205-15.
483. Yuan, W., et al., *The mouse SLIT family: secreted ligands for ROBO expressed in patterns that suggest a role in morphogenesis and axon guidance.* Dev Biol, 1999. **212**(2): p. 290-306.
484. Carmichael, S.T., M.C. Clugnet, and J.L. Price, *Central olfactory connections in the macaque monkey.* J Comp Neurol, 1994. **346**(3): p. 403-34.
485. Howard, J.D., T. Kahnt, and J.A. Gottfried, *Converging prefrontal pathways support associative and perceptual features of conditioned stimuli.* Nat Commun, 2016. **7**: p. 11546.
486. Scott, J.W., et al., *Functional organization of the main olfactory bulb.* Microsc Res Tech, 1993. **24**(2): p. 142-56.
487. Middleton, F.A., et al., *Gestational ethanol exposure alters the behavioral response to ethanol odor and the expression of neurotransmission genes in the olfactory bulb of adolescent rats.* Brain Res, 2009. **1252**: p. 105-16.
488. Youngentob, S.L., et al., *Experience-induced fetal plasticity: the effect of gestational ethanol exposure on the behavioral and neurophysiologic olfactory response to ethanol odor in early postnatal and adult rats.* Behav Neurosci, 2007. **121**(6): p. 1293-305.
489. Spear, N.E. and J.C. Molina, *Fetal or infantile exposure to ethanol promotes ethanol ingestion in adolescence and adulthood: a theoretical review.* Alcohol Clin Exp Res, 2005. **29**(6): p. 909-29.
490. Pietrzykowski, A.Z., et al., *Post-transcriptional regulation of BK channel splice variant stability by miR-9 underlies neuroadaptation to alcohol.* Neuron, 2008. **59**(2): p. 274-287.
491. Lewohl, J.M., et al., *Up-regulation of microRNAs in brain of human alcoholics.* Alcohol Clin Exp Res, 2011. **35**(11): p. 1928-37.
492. Li, J., et al., *MicroRNA expression profile and functional analysis reveal that miR-382 is a critical novel gene of alcohol addiction.* EMBO Mol Med, 2013. **5**(9): p. 1402-14.
493. Barragán, R., et al., *MicroRNAs and Drinking: Association between the Pre-miR-27a rs895819 Polymorphism and Alcohol Consumption in a Mediterranean Population.* International Journal of Molecular Sciences, 2016. **17**(8): p. 1338

VITA

Maren Lydia Smith was born in Jacksonville, Florida on September 16th, 1986. She graduated December 2009 from the University of Georgia in Athens, Georgia, with a Bachelor of Science with Honors in Biology. She began graduate school at Virginia Commonwealth University in Richmond, Virginia in August 2011 and joined the laboratory of Dr. Michael Miles in 2012. Upon acceptance of this dissertation, she will be awarded a Doctorate of Philosophy in Human Genetics. While attending graduate school at VCU Maren received the Charles C. Clayton Award for outstanding academic and research performance in 2014, and the Phi Kappa Phi Scholar Award in 2015. For most her graduate studies (May 2014-November 2016) she was supported by a Ruth L. Kirschstein National Research Service Award for Individual Predoctoral Fellows (F31 AA023134) from the National Institute of Alcohol Abuse and Alcoholism.